NAZARBAYEV UNIVERSITY

Application of deep eutectic solvents (DES) in bacterial growth and microbial electron activity enhancement

By

Neda Eghtesadi

Submitted In Partial Fulfillment of the Requirements for the Degree of Doctor of Philosophy in Chemical Engineering

School of Engineering and Digital Sciences
Nazarbayev University

August 2024

Application of deep eutectic solvents (DES) in bacterial growth and microbial electron activity enhancement

By

Neda Eghtesadi

Submitted In Partial Fulfillment of the Requirements for the Degree of Doctor of Philosophy in Science, Engineering and Technology

School of Engineering and Digital Sciences
Nazarbayev University

Supervised by
Prof. Yanwei Wang
Prof. Tri Pham
Prof. Enrico Marsili
Prof. Elena Ferapontova

August 2024

Declaration

I, Neda Eghtesadi, declare that the research contained in this thesis unless otherwise formally indicated within the text, is original. The thesis has not been previously submitted to this or any other university for a degree and does not incorporate any material already submitted for a degree.

---------- 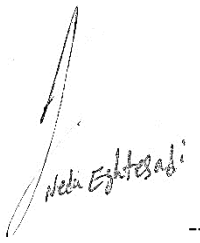 ----------

Signed

Dated: **08/06/2024**

Abstract

Bacillus subtilis, a Gram-positive, spore-forming bacterium, exhibits a versatile metabolism and biofilm-forming ability, making it a promising candidate for the production of industrially relevant metabolites. Under anoxic or nutrient-limited conditions, *B. subtilis* can engage in extracellular electron transfer (EET), a mechanism by which bacteria exchange electrons with charged surfaces or minerals through redox mediators. This process can contribute to the bacterium's energy metabolism and has been associated with enhanced production of primary and secondary metabolites in various electroactive microorganisms. However, *B. subtilis* is considered a weak electricigen, and its electroactivity must be enhanced to optimize its biotechnological potential.

This study investigates two key hypotheses regarding the enhancement of *B. subtilis* electroactivity through biocompatible nutrient additives. The first hypothesis posits that incorporating deep eutectic solvents (DESs), particularly choline chloride (ChCl)-based DESs, into the growth medium at subtoxic concentrations can improve *B. subtilis* electroactivity by acting as both nutritional supplements and osmoprotectant. The second hypothesis explores the role of osmotic stress regulators, specifically the combination of inorganic salts and ChCl-containing DESs, in promoting biofilm formation and enhancing EET in *B. subtilis* under static anoxic conditions.

To evaluate the first hypothesis, Chapter 4 demonstrates that the addition of ChCl-based DESs (ChCl:glycerol, 1:2 mol/mol) significantly enhances the current output and biofilm formation of *B. subtilis* at subtoxic concentrations (55–500 mM). This effect is attributed to the nutritional and osmoprotective properties of ChCl, which acts as a precursor to the compatible solute glycine betaine. Electrochemical analyses and high-performance liquid chromatography (HPLC) further reveal that the enhanced electroactivity is linked to increased riboflavin production, a known redox mediator secreted by *B. subtilis*. The results indicate that low concentrations of DES promote planktonic growth without altering the growth pattern, while higher concentrations induce pseudo-diauxic growth due to the metabolization of choline chloride. Moreover, ChCl at concentrations above 36 mM independently enhances biofilm biomass, whereas glycerol has a minimal impact.

The second hypothesis is addressed in Chapter 5, where a low-carbon tryptone-yeast extract medium supplemented with inorganic salts (NaH2PO4 and KH2PO4) is used to induce salt stress. The combination of salts with D-sorbitol/ChCl DES (1:1 mol/mol) mitigates osmotic stress, enhances biofilm formation, and stimulates electroactivity. The results indicate that ChCl acts as both an osmoprotectant precursor and a stimulant of electroactive exopolymeric substances within the biofilm matrix, while sorbitol serves as a secondary carbon source and a carbon pool for exopolysaccharide (EPS) synthesis. Bioelectrochemical experiments reveal that ChCl has a small positive effect on charge output in the presence of salts but does not alleviate osmotic stress on planktonic growth at higher concentrations.

Overall, this research highlights the potential of ChCl-based DESs as cost-effective and biocompatible nutrient additives to improve *B. subtilis* electroactivity and biofilm formation. The findings suggest that the combination of osmotic stress regulators and DESs can optimize bioelectrochemical processes, such as electrofermentation, particularly in media with high ionic strength. The outcomes of this work provide an optimistic approach to enhancing *B. subtilis* electroactivity and bioproduction of its high-added-value metabolites under EF conditions.

Acknowledgments

"Tell your heart that the fear of suffering is worse than the suffering itself. And that no heart has ever suffered when it goes in search of its dreams because every second of the search is a second's encounter with God and with eternity. Alchemist- Paulo Coelho"

My Ph.D. journey has finally come to an end, and I cannot attribute this achievement only to myself. It goes without saying that some doors were easier to open with the support behind my back.

First and foremost, I express my gratitude to my supervisory team. To my lead supervisor, Prof. Yanwei Wang, thank you for all your great help and guidance during my Ph.D. program, for the opportunity to work under your supervision, to learn from you and through you, and for trusting me. You are supportive beyond my expectations.

To my External supervisor, Prof. Enrico Marsili, with whom my PhD journey started. He supported me throughout my PhD studies, and I appreciate all the time he has invested in it. To my internal co-advisor, Prof. Tri Pham, I would like to express my sincere gratitude for your support throughout my PhD study, especially with microscopy experiments.

I am grateful to the government of Kazakhstan and NU management, as well as Prof Nurxat Nuraje, the director of the PhD programs in the Chemical Engineering Department, for his immeasurable support and timely and constructive feedback. I also express my deepest gratitude to Professor Dana Akilbekova for her invaluable advice and guidance during my research.

I would like to thank Prof. Azza Hashim Abbas for her invaluable guidance and support. Our discussion sessions, accompanied by tea and homemade sweets, created a warm and welcoming environment and made the challenging moments of my research much more enjoyable.

My sincere thanks to Prof. Luis Rojas and Prof. Matteo Rubagotti for their endless support during the gloomy moments of my PhD journey. Your patience and supportive manner inspire me.

I sincerely thank Prof. Elena Ferapontova for her work as an External and host supervisor at the iNANO Centre of Aarhus University. Her support and the unbelievably versatile possibilities she offered me as a Ph.D. student opened new research doors and were a turning point in my developing valuable new skills.

I am grateful to the School of Engineering and Digital Science at Nazarbayev University and the Chemical Engineering department for supporting me throughout my PhD and helping me focus only on my research.

I must also thank my colleagues and friends, Dr. Kayode Olaifa, Dr. Obinna Ajunwa, Alua, Altynay, Malika, Anar, and all the people in the Biofilm Laboratory. Thank you all for your support and the excellent and memorable moments in the lab.

Thanks to my friends and colleagues in Chemical Engineering—Cohort 2020, Lunara Zhazira, Mirat, Guldana, Yerbolat, and Almaz, for their friendship and support throughout this program. I wish you all the best of luck in your PhD path and life.

Finally, I want to express my heartfelt gratitude to my family, especially my parents, for their unwavering belief in me and their continuous support throughout every phase of my education. Your love, patience, and understanding have been invaluable. I also want to thank my best friend, Mahdi, for his incredible support and for becoming a family member during this challenging yet rewarding journey.

Neda Eghtesadi

August 2024

Contents

List of Figures

List of tables

outputs

Publications

Eghtesadi, N., Olaifa, K., Perna, F. M., Capriati, V., Trotta, M., Ajunwa, O., & Marsili, E. (2022). Electroactivity of weak electricigen Bacillus subtilis biofilms in solution containing deep eutectic solvent components. Bioelectrochemistry, 147, 108207. **(Scopus Percentile: 88%, Q1)**

https://doi.org/10.1016/j.bioelechem.2022.108207

Adilkhanova, A., Ormantayeva, A., Kaziullayeva, A., Olaifa, K., **Eghtesadi, N**., Abbas, A. H., Calvio, C., Pham, T.T., Ajunwa, O.M., & Marsili, E. (2024). Electrofermentation increases concentration of poly γ-glutamic acid in Bacillus subtilis biofilms. Microbial Biotechnology, 17(3), e14426. **(Scopus Percentile: 90%, Q1)**

https://doi.org/10.1111/1751-7915.14426

Vitasovic, Toni, Giada Caniglia, **Neda Eghtesadi**, Marcel Ceccato, Espen Drath Bojesen, Ulrich Gosewinkel, Gregor Neusser et al. "**Antibacterial Action of Zn2+ Ions Driven by the In Vivo Formed ZnO Nanoparticles.**" ACS Applied Materials & Interfaces (2024).. **(Scopus Percentile: 95%, Q1)**

https://doi.org/10.1021/acsami.4c04682

Eghtesadi, N., Olaifa, K., Pham, T. T., Capriati, V., Ajunwa, O. M., & Marsili, E. (2024). Osmoregulation by choline-based deep eutectic solvent induces electroactivity in Bacillus subtilis biofilms. Enzyme and Microbial Technology, 180, 110485. **(Scopus Percentile: 79%, Q1)**

https://doi.org/10.1016/j.enzmictec.2024.110485

Chapter 1. Introduction

1.1 Background of study and problem statements

The chemical industry plays a vital role in providing fundamental products for human life. However, the current reliance on non-renewable fossil fuels for chemical manufacturing is becoming increasingly problematic due to the rapid depletion of these finite resources (Obileke et al. 2021).

Additionally, the production processes linked to these fuels have profound environmental impacts, including contributions to climate change, generation of waste, toxic by-products, and end products that pose challenges in terms of degradation and recycling(Wright et al. 2020).

Consequently, there is a pressing need for alternative production technologies that are environmentally friendly and based on non-fossil fuel feedstocks. Considering this perspective, industrial biotechnology has great potential to be a key technology for a sustainable future(Verma et al. 2021)(Obileke et al. 2021).

Biotechnology enables the biocatalytic production of chemicals, materials, and fuels using renewable biomass and organic and inorganic recyclable wastes(Eric M Conners, Rengasamy, and Bose 2022)(Maria Perna et al. 2021).

Electrofermentation is an innovative biotechnological process that integrates electrochemical techniques with traditional fermentation. Unlike conventional fermentation, which relies solely on microbial metabolism to convert substrates into desired products, electrofermentation employs an external electrical input to influence microbial activity and metabolic pathways. This integration allows for enhanced control over the redox environment, potentially improving yields, reducing by-products, and enabling the use of a wider range of substrates. Economic efficiency in biotechnological processes is still crucial due to the context of the electrofermentation process(Gong et al. 2020)(Schievano et al. 2016). The production yield of the desired product could decrease due to the synthesis of unwanted organic acids as the inherent microbial strategy aims to maintain cellular redox balance.

Microbial electrochemical technology (MET), as an emerging interdisciplinary area, provides beneficial tools for stabilizing microbial redox and energy states. METs allow microorganisms to use anode or cathode as external electron sources in a bioelectrochemical system (BES) to enhance the production of the target compounds (Marsili et al. 2008a)(Méhes et al. 2020).

Bioelectrochemical systems focus on the study of electron transfer processes that occur in biological systems, particularly at the interface between biological molecules (such as enzymes, proteins, and cells) and electrode surfaces. It investigates how biological entities can participate in or influence electrochemical reactions and how these reactions can be harnessed for various applications, including sensors, energy conversion, and bioelectronic devices.

BES works based on the microbial electron transfer (ET) mechanism and is a promising technology in producing electrically driven industrially relevant chemicals. Extracellular electron transfer (EET) refers to the transfer of electrons between microorganisms and charged surfaces or minerals. Microorganisms with this property are called "Electroactive microorganisms," and their electron transfer mechanisms have been investigated for bioenergy production and biosensors. While strong electroactive produces relatively high current at strong oxidizing potentials (~1-10 A/m2), most microorganisms show much lower current output under the same conditions (~0.1 A/m2) and thus are termed weak electricians(Doyle and Marsili 2018a). Further, only a small subset of weak electroactive produce a current output under native conditions, while others require exogenous electron transfer agents that facilitate EET(Viti et al. 2014).

Bacillus subtilis is a Gram-positive, spore-forming bacterium with a versatile and adaptable metabolism, which makes it a viable cell factory for microbial production. *B. subtilis* classifies as a weak electroactive microorganism with various applications in industrial bioprocesses (e.g., enzymes, biopolymers, biosurfactants, antimicrobial peptides, etc.). Electroactivity enhancement can potentially affect the metabolic activity of *B. subtilis* and improve the production of its high-added-value metabolites, such as alkaline proteases, biopolymers, biosurfactants, and antimicrobial peptides under electrofermentative conditions(Boch, Kempf, and Bremer 1994)(Su et al. 2020)(L. Chen et al. 2019)

It has been recently reported that weak electricigens' metabolic pathways and activity are affected by the electrochemical potential and current they are exposed to. However, the electroactivity of weak electricians must be enhanced to achieve significant results. Different approaches for improving EET in bacteria have been adopted, ranging from redox mediator-based inducements to genetic and metabolic re-wiring of electrical circuits in these bacteria. Despite these improvements, there are still challenges with the cost of these approaches (e.g., for genetic enhancements) and potential toxicity or product alteration attributed to redox mediators.

Deep eutectic solvents (DESs) are a new emerging class of green solvents(Perna, Vitale, and Capriati 2020). Many DES compositions with various applications are available due to their feasibility for customized design. High biodegradability, non-toxicity, low cost, low volatility, and eco-friendliness, besides several other characteristics, make them an attractive candidate to replace them with conventional ionic solvents(Pandey et al. 2017)(Karimi, Mohammadi, and Hooshyari 2020)(Hansen et al. 2021). Further, DESs enable heterogeneous catalytic processes(Belviso et al. 2021)(Maria Perna et al. 2021). It is hypothesized that they can also be functional in whole bacterial cell interactions and biosynthetic processes and can be extensively involved in redox activities in enzyme or bacterial systems. Thus, DESs can be potentially applied to enhance the electroactivity of bacteria.

In most microorganisms, the respiratory system is embedded in the cytoplasmic matrix, where the most significant percentage of the available oxygen is used up as a terminal electron acceptor in the ETC(Schievano et al. 2016)(Esar et al. 2009). Hence, monitoring and estimating the electron transport to oxygen or another electron acceptor of similar physicochemical properties directly reflects microbial respiration and their cellular activity(Kato 2016)(Choi, Kim, and Chang 2018). This is more adaptable to biofilms as their electron transport can easily be intercepted on the solid surface (electrodes, as in the case of laboratory conditions) upon which their cells are growing.

Electroactivity is enhanced in the presence of biofilm, where the short distance between the electron donor and acceptor and the high microbial concentration enhances the EET rate. Thus, stimulating biofilm production would likely increase electroactivity and,

consequently, the biosynthesis rate of key high-added value metabolites in the so-called electrofermentation process(Schievano et al. 2016).

Biofilms are aggregations of microorganisms that adhere to a surface and are enveloped within a self-produced matrix (EPS)(Paquete et al. 2022a). Formation of the biofilm is an important parameter affecting the electron transfer between the bacterial cells and the anode and, therefore, the electricity generation. The intensity of bacterial electroactivity can be correlated with biofilm characteristics.(Chai et al. 2018)(Xiao and Zhao 2017).

B. subtilis biofilm is capable of producing membrane-bound cytochrome- c and flavin, which both play a crucial role in the extracellular Electron Transfer process (EET) by facilitating electron transfer reactions that generate a proton gradient for ATP synthesis(Bruce E. Logan et al. 2019a) (Yin et al. 2019).

Microbial electrochemical systems (MES) work based on the ability of naturally- or artificially induced electrochemically active microorganisms to generate/consume and transfer to/from polarized electrodes(Méhes et al. 2020) (Schröder, Harnisch, and Angenent 2015). These systems are easy to set up and implement and are relatively cheap. A three-electrode system is a conventional set-up consisting of a working electrode (WE) where the biofilm attachment and growth take place, the counter/auxiliary electrode (CE) to maintain charge balance, and the reference electrode(RE)(Aiyer and Doyle 2022). However, in recent years, there has been an increasing interest in using printed electrodes (SPEs) as disposable, portable, simple-to-use, low-cost, and extremely sensitive biosensing devices for the analysis, detection, and characterization of various microbes. Moreover, SPEs show versatility and amenability characteristics for specific modifications (Alonso-Lomillo, Domínguez-Renedo, and Arcos-Martínez 2010).

1.2 Hypothesis

There is a correlation between electroactivity and the production of key metabolites in many microorganisms. Stimulating biofilm production is expected to increase EET and, consequently, the biosynthesis rate of high-value metabolites in electro-fermentation (EF) processes (Xiao and Zhao 2017) (Viti et al. 2014).Thus, enhancing biofilm-based

bioprocesses through electrical current or potential is an interesting and industrially applicable subject(Viti et al. 2014).

Enhanced electroactivity can be achieved through several strategies, including genetic modifications or induction of redox mediators and metabolic re-wiring of the EET chain(Chiranjeevi and Patil 2020) (Gong et al. 2020). However, some of these techniques are expensive, time-consuming, and may result in product alteration. Alternatively, media optimization and process intensification can be considered as a simple and cost-effective method for EET enhancements in weak electricigen. With these bases, we hypothesized that the addition of selected deep eutectic solvents (DESs) to the bacteria growth medium formulation in sub-toxic percentage could boost biofilm formation in *B. subtilis*, electrical properties, and redox processes associated with microbial activity.

1.3 Aim and specific objective

This work is focused on the use of DES in order to boost the electroactive performance of *Bacillus Subtilis* biofilms, referenced as a weakly electricigen bacterium. The aim of the experiments was to define the most effective DES as well as its conditions of use, then to identify the parameters explaining the improvement in electroactive performance. Thus, planktonic growth, biofilm concentration, charge output, and redox profiles were measured and compared at different solvent concentrations as well as for variations in solvent component concentrations.

To achieve this aim, the following specific objectives were formulated:

1) To evaluate the effect of various DESs on the planktonic growth of *B. subtilis* to find out the promising DES composition and concentrations for bacterial planktonic growth
2) To assess the boosting of *B. subtilis* biofilm biomass in the presence of selected DESs and their components
3) To Determine the effect of selected DES and their components on EET of *B. subtilis* through electrochemical, biochemical, and microscopy methods
4) To Propose a mechanism for the effect of DESs on the redox process in biofilms.

1.4 Significance and Novelty

The findings of this study represent a significant advancement in the field of bioelectrochemistry by introducing deep eutectic solvents (DESs) as novel, biocompatible nutrient additives to enhance the electroactivity of *Bacillus subtilis***.** To the best of our knowledge, this is the first study to systematically evaluate the role of DESs in promoting extracellular electron transfer (EET) and biofilm formation in ***B. subtilis***, a weak electricigen with significant potential for industrial applications.

The novelty of this research lies in the demonstration that choline chloride (ChCl)--based DESs can act as electroactivity-enhancing agents at sub-toxic concentrations. Previous studies have primarily focused on genetically engineered bacteria or exogenous redox mediators to improve EET, both of which present cost and scalability challenges. By contrast, the use of DESs, which are inexpensive, biodegradable, and readily available, provides a more sustainable and versatile approach to bioelectrochemical enhancement.

this could open doors for future research into the non-genetic enhancement of electroactivity in weak electricige**ns**, potentially broadening the range of microorganisms that can be applied in bioelectrochemical technologies.

Another key novel finding of this work is that specific DES compositions (such as ChCl: glycerol (1:2) and D-sorbitol: ChCl (1:1)**)** DESs not only enhance electroactivity but also mitigate osmotic stress, likely by acting as precursors to osmoprotectant like glycine betaine. This dual functionality—both as electroactivity enhancers and osmoprotectants—makes DESs particularly attractive for applications involving high-ionic-strength media, which are common in industrial bioelectrochemical processes. Furthermore, the investigation of DESs under salt-induced osmotic stress conditions represents an additional layer of novelty. The use of D-sorbitol/ChCl (1:1 mol/mol) DES in combination with salt stress not only improved biofilm formation but also mitigated the detrimental effects of high ionic strength environments—a common challenge in microbial biotechnology. This finding highlights the potential of DESs as multifunctional additives that can both enhance

microbial electroactivity and improve microbial tolerance to osmotic stress. The observed improvement in biofilm formation and electroactivity suggests that DESs could be used to engineer more robust microbial communities for sustainable bioprocessing in saline and high-electrolyte environments.

1.5 Structure/overview of the thesis

Chapter One presents the fundamental aspects of the thesis topic, offering essential background information on bioelectroactive microorganisms, Deep eutectic solvents, their potential role in electroactivity enhancement, and the mechanism of electron transfer in electroactive microorganisms in bioelectrochemistry. Also, the inter-relatedness and how these concepts evolved into what is today referred to as microbial electrochemistry or Electromicrobiology is highlighted. The study hypothesis and aims are also described in this chapter.

In **chapter two**, an up-to-date review of existing literature on the subject of my work is presented. This includes the historical perspective, current studies, and future outlook on the fundamental concept related to this subject. The state of the electrochemical techniques and their mechanisms, the challenges with existing methodologies, and the gaps in knowledge on bioelectrochemical mechanisms at the molecular level are presented in this chapter.

Chapter three outlines the fundamental principles underlying the experimental techniques employed in this PhD research.

Chapter four focused on studying the electroactivity of *Bacillus subtilis* biofilms in a solution containing deep eutectic solvent components. In this work, we investigated and compared several DESs to find the most effective DES and its conditions of use that improve the electroactivity performance of *B. subtilis*. This work was published as an article in the Journal of Bioelectrochemistry.

Chapter five focused on studying the combined effects of selected deep eutectic solvents and salts on biofilm formation and electroactivity of *Bacillus subtilis.* This study demonstrated that the addition of a ChCl-containing DES mitigated the inhibitory effect of

inorganic salts while enhancing biofilm formation and electroactivity of *B. subtilis*. Further, DES components mitigate the osmotic stress in the presence of the salts NaH2PO4 and KH2PO4 at sub-inhibiting concentrations. These findings could contribute to developing more effective MET processes for producing high-value metabolites in *B. subtilis*.

In chapter Six, I have described part of the project I contributed at Aarhus University. The work investigated peroxidase-zinc oxide biohybrids for sustainable bio electrocatalysis and provides evidence pf HRP's activity when coupled with ZnO NPs. The biocidal experiment in this project was done by me and included as chapter six.

Finally, in **chapter seven**, concluding remarks and suggestions for future research were provided.

Chapter 2. Literature review

2.1 Electroactive biofilms: What they are and their difference from conventional biofilms

Although the word "biofilm "traditionally evokes adverse effects related to human health (Jiang et al. 2021)(Mukhi 2022) or industrial processes(Alvarez-Ordóñez et al. 2019)(Park et al. 2023), the discovery of "Electroactive biofilms "in the early 2000s has garnered increasing attention due to the unique ability of electroactive biofilms in generating, transferring, and harnessing electrical currents. This opened doors to interdisciplinary areas of research involving topics dominated by Chemical engineering, Microbiology, and bioelectrochemistry(Godbole et al. 2023)(Erable et al. 2010)(Reimers et al. 2001).

Electroactive biofilms (EABs), called electrochemically active biofilms, can exchange electrons with conductive solid surfaces such as electrodes (You et al. 2023)

(Eric M. Conners, Rengasamy, and Bose 2022).

It becomes evident that electroactive biofilms have the potential to revolutionize various industries and address critical environmental challenges, including green chemistry (Eric M. Conners et al. 2022) and sustainable energy development (Saratale et al. 2017), bioengineering and bioproduction(Godbole et al. 2023), corrosion control(Saleem Khan et

al. 2019), bioelectronics, bioelectrosynthesis, and nanomaterials production(Seker et al. 2017).

Electroactive biofilms play a central role in facilitating the conversion of organic waste into green energy and byproducts within MFCs (Zhou et al. 2022)(Reimers et al. 2001)(Seker et al. 2017). The application of MFCs in waste treatment has been reported in many literatures (Wei, Liang, and Huang 2011)(Vijay, Sonawane, and Ghosh 2022)(Saratale et al. 2017).

Recent studies indicate the potential application of electroactive biofilms in the bioremediation of heavy metals bioremediation(Jasu and Ray 2021). The structure and quantity of biofilm could significantly change when exposed to different metal contaminants; this consequently increases the pollution tolerance ability(Jasu and Ray 2021)(de Araújo and de Oliveira 2020).

Electroactive biofilms can help control MIC by competing with corrosive microorganisms for nutrients and space on metal surfaces. Pyocyanin isolated from *Pseudomonas aeruginosa* TBH2 is an electroactive microorganism that can form a massive electroactive biofilm. The anticorrosion role of pyocyanin as a cheap and eco-friendly biofilm inhibitor towards the control of MIC on Cu metal surface in a cooling water system was reported in a study by Narenkumar et al, (Narenkumar et al. 2017).

The word biofilm' was initially introduced by Costerton et al. in 1978 (Costerton, Geesey, and Cheng 1978)(Joo and Otto 2012). Biofilms are defined as aggregations of microorganisms (such as bacteria, fungi, and algae) that adhere to a surface or interface and are enveloped within a self-produced matrix (EPS)(Jiang et al. 2021)(Yin et al. 2019). The EPS layer is the major product of the biofilm structure composed of polysaccharides, proteins, nucleic acids, lipids, and other substances generated by the microbial community (You et al. 2023)(Flemming and Wingender 2010)EPS not only shields the cells from the surrounding environment but also serves as a carbon and energy source for biofilm and promotes its chance of survival. Also, extracellular polymeric substances (EPS) secreted from the cell immobilize the biofilm and make it intact(Limoli, Jones, and Wozniak 2015)(Xiao and Zhao 2017).

Biofilms provide structural stability, protection, and a platform for interactions among the enclosed microbial cells. These features make them resistant to environmental stresses, including antibiotics and immunological reactions.

Biofilm formation is a complex and dynamic developmental process that typically results in the irreversible adhesion of a microbial community encapsulated within a self-produced extracellular polymeric substance (EPS) onto a living/non-living surface (Aliane and Meliani 2021). This multi-step process initially starts with weak and reversible attachment of microbial cells to the proper surface, followed by proliferation and subsequent synthesis and accumulation of polymeric extracellular matrix, which consists of various molecules/compounds (e.g., lipids, proteins, polysaccharides, and nucleic acids) in varying proportions (Achinas, Charalampogiannis, and Euverink 2019)(Ghosh, Jayaraman, and Chatterji 2020). This "cement" structure will make a more robust contact and irreversible attachment of the cells to the surface that firmly anchors the cells to the substrate (Winkelströter et al. 2014). The third step is called maturation, in which microbial cells grow and form microcolonies (Winkelströter et al. 2014)(Ghosh et al. 2020). The maturation process is influenced by quorum sensing (QS) signaling and the release of extracellular polymer materials (Paquete et al. 2022b), which trigger the recruitment of planktonic cells from the surrounding liquid to join the growing biofilm (Jiang et al. 2021)(Saratale et al. 2017)(Mukhi 2022). The biofilm develops a matured three-dimensional (3D) structure as more cells accumulate. Finally, the dispersal stage involves the detachment of microbial cells from the matured biofilm. This dispersion can result in the release of planktonic cells back into the surrounding environment, allowing them to colonize new surfaces and initiate the formation of new biofilms, leading to recurrent biofilm growth cycles(Meireles et al. 2015).

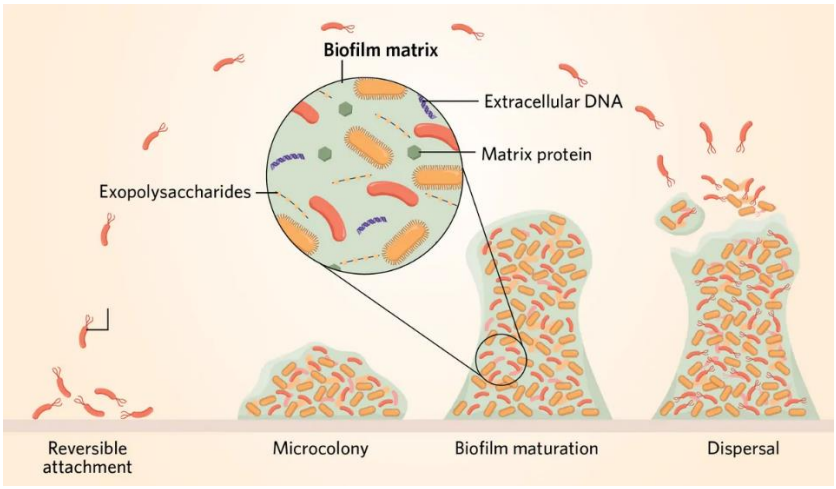

Figure 2.1 Stages of biofilm formation. (Reprinted from Holly Barker, Infographic: Stages of Biofilm Formation).

Although the biofilm concept is generally consistent and centered around main elements including microorganisms; suitable surface, and an extracellular polymeric matrix simply called 'cement'(Flemming and Wingender 2010)(Limoli et al. 2015), a specific subset of biofilms called "electroactive biofilms" attracted particular interest due to their versatile biotechnological and environmental application(Dulon et al. 2007)(Godbole et al. 2023)(Babauta et al. 2012).

Identification of Electroactive biofilms (EABs) caused significant advancements in an emerging field of research known as "electro-Microbiology"(Godbole et al. 2023).This field has experienced considerable advancement due to the extensive research in diverse bio-electrochemical systems (BESs)(Godbole et al. 2023).

The distinguishing feature of Electroactive biofilms (EABs) is their unique electrochemical capabilities. Electroactive biofilms (EABs) matrix composed of electrochemically active microorganisms that are capable of transferring electrons to/or from electrodes, which allows them to participate in electrochemical reactions(Godbole et al. 2023)(Jasu and Ray 2021).

2.2 Anodic and Cathodic Biofilms

The EABs can be categorized into anodic and cathodic biofilms based on their function and location within an electrochemical system(Wei et al. 2011)(Godbole et al. 2023).

In anodic biofilms, electroactive microorganisms interact with the anode (the electrode where oxidation reactions occur) and donate electrons to it as part of their metabolic processes.

Microbial Fuel Cells (MFCs) are one of the main applications of anodic biofilms, which harness gram-negative exo-electrician bacteria such as *Shewanella* and *Geobacter* to form anodic biofilm and generate electrical current (Marsili et al. 2008b) (Lovley 2012)(Marsili, Sun, and Bond 2010).

Organisms that reside on the anodes of microbial fuel cells (MFCs) generate power by using acetate or various types of wastes, such as aqueous wastes (Nevin et al. 2008). *Geobacter sulfurreducens* species are capable of inducing acetate oxidation within the anode. They can form a thick layer of biofilm on the surface of a carbon anode (Von Canstein et al. 2008). *Geobacter metallireducens* species can cause the oxidation of various types of aromatic compounds present within the wastes (Marsili et al. 2010)(Yi et al. 2009). These *Geobacter* sp. have multiheme-c-type cytochromes on their outer membranes, as well as conductive cell surface appendages, that associate with the extracellular electron transfer process (Richter et al. 2009).

In cathodic biofilms, on the other hand, electroactive microorganisms interact with the cathode (the electrode where reduction reactions occur) and accept electrons from it as part of their metabolic processes (Borole et al. 2011)(Babauta et al. 2012). The number of studies performed in the field of cathodic biofilm is much fewer in comparison to the anodic counterparts(Lahiri et al. 2022).

Sulfate—and nitrate-reducing anaerobic bacterial species naturally present in the environment can facilitate the formation and growth of electroactive biofilms (EAB) on the cathode. (Lefebvre, Al-Mamun, and Ng 2008). Bacterial species frequently associated with the cathode include *Brevundimonas diminuta, S. putrefaciens, P. aeruginosa, P. fluorescens, Shigella flexneri*, etc. (Rosenbaum, Aulenta, Villano, & Angenent,

2011)(Cournet et al. 2010).The acceptance of electrons by these species from the cathode can reduce terminal electron acceptors like sulfate, nitrate, metal ions, carbon dioxide, organic compounds, oxygen, and protons(Song, Zhu, and Li 2019)(Ucar, Zhang, and Angelidaki 2017).

Microbial electrosynthesis (MES) and the production of biochemicals from carbon dioxide(CO2) is an emerging application of cathodic biofilms in which microorganisms facilitate the reduction of various compounds (Aryal et al. 2017)(Rabaey et al. 2008). The utilization of a cathode in catalyzing the reduction of oxygen within MFCs has been studied in several investigations (Behera, Jana, and Ghangrekar 2009) (Aryal et al. 2017)(Rabaey et al. 2008).

2.3 Electron transfer mechanism in EABs

As previously noted, electroactive bacteria (EABs) are recognized for their ability to transfer electrons to the electrode surface. Biofilm-embedded electroactive microorganisms (EAMs) transmit electrons from the quinone pool to the electron acceptor substrate (i.e., anode electrode) through conductive elements across the cell membrane (You et al. 2023). Extracellular Electron transfer (EET) mechanism can occur via two pathways: (i) a direct pathway, which refers to the direct physical contact between cell and electron acceptor and involves direct transfer to the electrode through multiheme cytochromes or pili, filaments, and conductive nanowires(T.-H. Lan et al. 2018)(Lahiri et al. 2022). (ii) an indirect pathway, which occurs through the redox mediators which can carry electrons between EAMs and electrodes. Redox mediators can be either soluble (such as flavin, phenazine, hydrogen, formic acid, etc.) or membrane-bound(Godbole et al. 2023).

Redox mediators are crucial in facilitating electron transfer within the biofilm, and protein mediators should be chosen based on the microorganism species and characteristics(Pankratova et al. 2019)(Godbole et al. 2023).

In bacteria, type IV pili also play a crucial function in biofilm formation. Pili is responsible for establishing a structural network, which is essential for arranging the cytochromes within the biofilm and thus enhancing electron transfer efficiency. Type IV pili comprise two isomers named short and long PilA, respectively. According to the literature, short pili is responsible for the bacterial biofilm's conductivity. However, the absence of long PilA in some bacterial strains could result in reduced attachment to the electrode surface during biofilm formation, highlighting the critical role of long PilA in the biofilm formation/development process(Li et al. 2022)(Vijay et al. 2022)(You et al. 2023).

For example, in *Shewanella oneidensis*, Flavins, riboflavin, and cytochrome **MtrF** heme network are responsible for the electron transport process(Xu et al. 2018).

In *G. sulfurreducens*, the outer membrane c-type cytochromes (c-Cyts) and conductive type IV pili (pilA) play significant roles in biofilm formation. Type IV pili, c-type cytochrome gene encoded by gene **OmcZ**, **Omp B**, **Pgc A** are responsible for transferring electrons to electrode and oxidation-reduction process (Saratale et al. 2017)(Borole et al. 2011)(You et al. 2023).

If the expression of the **omcZ** gene (responsible for c-type cytochrome Z) and the pilA gene (responsible for type IV pili) in *G. sulfurreducens* are suppressed, then biofilm formation could be inhibited completely(T.-H. Lan et al. 2018)(Lovley 2012)(Marsili et al. 2010).

In *Shewanella putrefaciens*, c-type cytochromes (MtrC and OmcA), as well as the FAD transporter and the cytochrome **MtrF** heme network, not only play a crucial role in electron transport but also contribute significantly to the formation of biofilms (Saratale et al. 2017)(Xu et al. 2018).

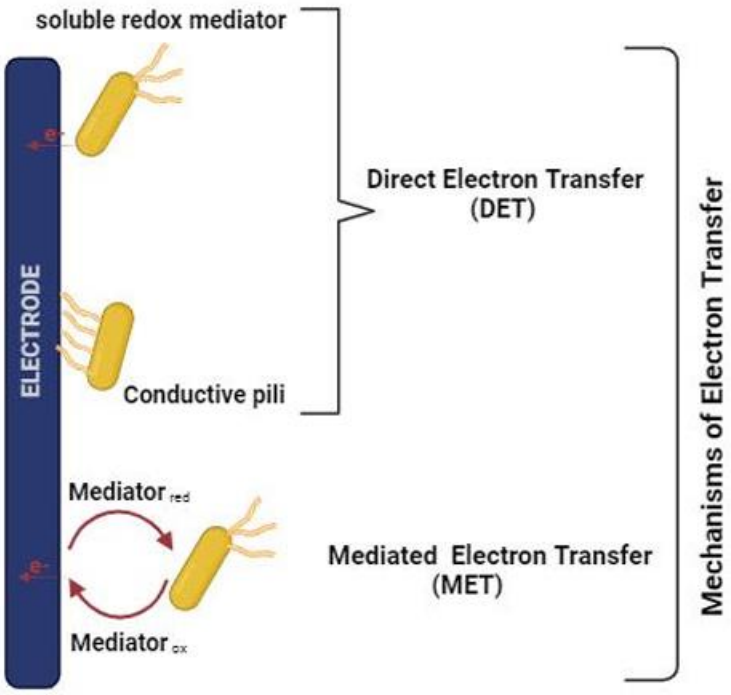

Figure 2.2 Schematic of Electron transfer mechanism in an electroactive Bacterium Created with BioRender.com by Neda Eghtesadi.

2.4 Factors Affecting Electroactive Biofilm Formation

The rate of EAB enrichment is a complex and dynamic process that can be directly influenced by many factors, including the bacterial species, the intrinsic metabolic pathway of microorganisms, and the material utilized for electrode constructions. Electrode surface characteristics like biocompatibility, hydrophobicity, conductivity, and porosity can regulate EAB development (Wei et al. 2011)(Rabaey et al. 2005). Electrode surface modification using chemical catalysts such as surfactants can also boost EAB formation(Song et al. 2015).

The effective parameters on EAB growths generally can be categorized into (1) biological parameters (2) system design parameters (3) operating parameters (Vijay et al. 2022)(Borole et al. 2011)(Saratale et al. 2017).

This thesis focused mainly on boosting the electroactivity performance of *B. subtilis* by addition of Deep Eutectic Solvents (DESs) at optimum concentration into the medium source. This involves altering the composition or characteristics of the system, typically categorized as a modification of the system design parameters in this case, the medium source, to improve its electroactivity.

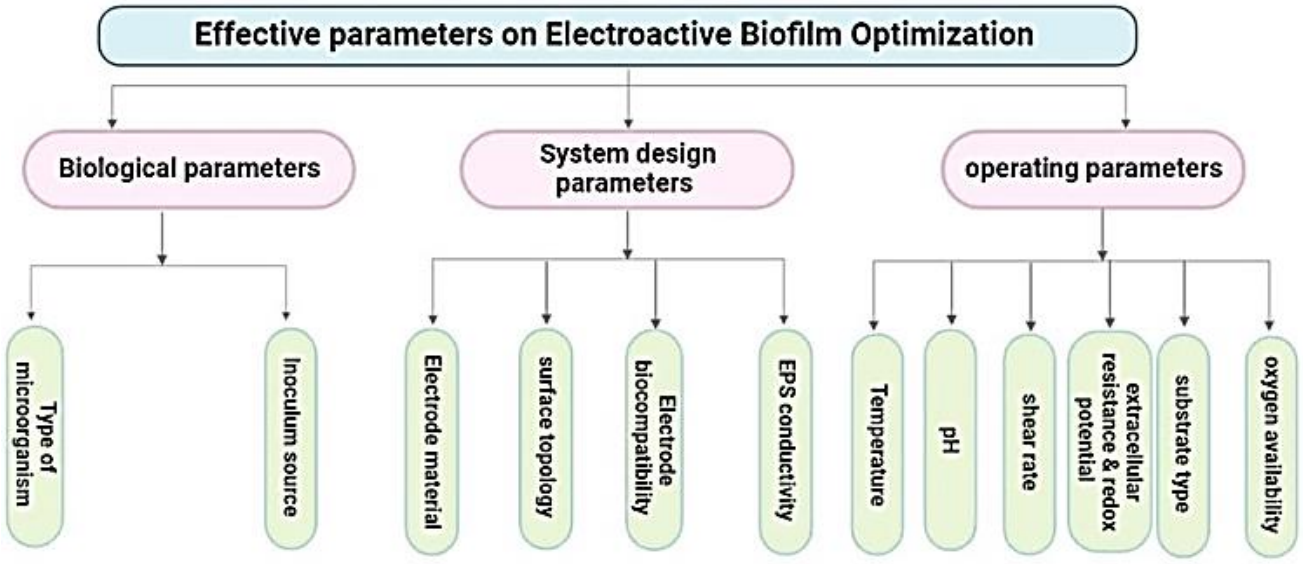

Figure 2.3 An overview of effective parameters on Electroactive Biofilms (EABs) formation, created by BioRender.

2.5 Deep Eutectic Solvents (DESs)

2.5.1 What are DESs

Green technology has become essential to consider in recent years regarding its positive effect on various industrial processing and, finally its long and short-term impact on an ecosystem (Wikene et al. 2017)

Deep Eutectic Solvents (DES) are species of green solvents that are prepared by mixing two or more safe and usually inexpensive Solid components in specific molar ratios physically interact, often through mechanisms such as hydrogen bonding, to form a eutectic mixture that remains liquid at temperatures significantly lower than the melting points of the individual compounds, and even below room temperature (Maria Perna et al. 2021)(Liu et al. 2019).

DESs are biodegradable and recyclable; also they show low vapor pressure, low costs, and low toxicity, which makes them a good candidate as a reaction media in comparison to traditional solvents(Socas-Rodríguez et al. 2021). Moreover, deep eutectic solvents can serve as reaction media for catalysis, enabling efficient and selective chemical transformations (Kim et al. 2016).

2.5.2 Bondings in deep Eutectic Solvents structure

DESs are formed by hydrogen bonding acceptors (HBAs) and hydrogen bonding donors (HBDs), making them liquid eutectic solvents(Wang et al. 2016). Hydrogen Bond Acceptor (HBA) is often a quaternary ammonium salt or a metal chloride, serving as the Lewis acid in the solvent system. A Hydrogen Bond Donor (HBD) component is usually a hydrogen bond donor, such as a carboxylic acid, an amide, or an alcohol which acts as the Lewis base in the solvent system(Abbasi, Farooq, and Anderson 2022).

In a hydrogen bond, the donor is typically a highly electronegative atom like N, O, or F covalently bonded to hydrogen, while the acceptor is an electronegative atom with a lone pair from a neighboring molecule or ion that engages in the bond(Maria Perna et al. 2021).

Hydrogen bonding in Deep Eutectic Solvents (DES) can be crucial for boosting Electron Transfer (EET) in electrochemical systems, even at low concentrations. In DES, hydrogen bonding may assist in facilitating the movement of protons (H^+) within the solvent medium. In redox reactions, transportation of protons can frequently occur with electron transfer. In DES, the formation and breaking of hydrogen bonds may generate ways for protons to travel, thereby contributing to the overall electron transfer process(Sun et al. 2022).

Additionally, due to their hydrogen bonding capability, DES could solubilize a wide range of electroactive species, including ions and redox-active molecules. DES can effectively dissolve and stabilize electroactive substances at low concentrations, providing their availability for electron transfer processes(Pandey et al. 2017).

The hydrogen bonding networks in DES can also affect ion mobility inside the solvent. The enhanced flow of ions across hydrogen-bonded networks can improve the efficiency of electron transfer processes. This is particularly relevant for ionic species that engage in electrochemical reactions(Pandey et al. 2017).

Hydrogen bonding in DES may also alter the physical and chemical properties of the solvent, affecting the dielectric constant and viscosity. Hydrogen bonding interactions between DES and electrode surfaces, on the other hand, may help to stabilize the electrochemical interfaces(Monhemi et al. 2014). At low concentrations, DES may form a thin, stable layer on the electrode surface via hydrogen bonding, improving effective electron transport between the electrode and the electroactive species in solution. The dielectric constant and viscosity of DES may also be influenced by hydrogen bonding. The redox potentials of electroactive species can also be influenced by the hydrogen bonding environment in DES(Hansen et al. 2021).

It can be concluded that the hydrogen bonding characteristics of DES help to improve Electron transfer (EET) in electrochemical processes(Karimi et al. 2020). The potential of DES to improve proton transfer, solubilize electroactive species, increase ion mobility, stabilize surfaces, regulate solution characteristics, and impact redox potentials all work collaboratively to promote effective electron transport even at low concentrations(Torregrosa-Crespo et al. 2020).

2.6 Role of Extracellular Polymeric Substances (EPS) in EABFs

Extracellular polymeric substances (EPS) surround the majority of microbial cells in nature and determine the physiochemical features of a biofilm(Xiao and Zhao 2017). In addition to housing the electroactive elements of the biofilm matrix, such as nanowires and c-type cytochromes, the EPS encloses the biofilm cells in the matrix and keeps them in close contact with the electrode(Markraphael Ajunwa et al. 2021). From the electrochemical

point of view, the EPS features of conductivity and redox ability highlight the critical roles of EPS in microbial extracellular electron transfer (EET). So, basic information regarding EPS structure and components will provide a better understanding of the EET mechanism in bioactive biofilms(Flemming and Wingender 2010)(Vijay et al. 2022)(Esar et al. 2009).

2.6.1 EPS composition in Electroactive biofilms

EPS was described as "biologically derived extracellular polymeric substances that contribute to the formation of microbial aggregates." With the continuous discovery of additional EPS roles, this definition expanded to any adhesive materials found at or outside the cell surface regardless of their origin(You et al. 2023)(Tuck et al. 2021).

The localization and composition of Extracellular Polymeric Substances (EPS) in electroactive biofilms can vary depending on the specific microbial species, environmental conditions, and the particular biofilm's characteristics. The ratio of these components can also vary as it is a consequence of multiple processes, including active secretion, shedding of cell surface material, cell lysis, and adsorption from the environment. Polysaccharides are usually considered the primary constituents of EPS (Paquete et al. 2022b)(Saleem Khan et al. 2019).

They serve as the biofilm's structural framework. Within the biofilm, polysaccharides can potentially act as an electron-conductive network. Moreover, cytochromes, as well as other redox-active proteins, play a role in extracellular electron transport(Aliane and Meliani 2021).

Extracellular DNA (eDNA) participates in charge transfer pathways and helps to maintain biofilm stability(You et al. 2023). EPSs may also contain lipids, which can influence the hydrophobicity of the biofilm and its contact with electrode surfaces (Kouzuma et al. 2010).

Electroactive biofilms may also contain ions and metals, which can be involved in electron transfer processes and biofilm growth. Certain biofilms produce and release small molecules like flavins or other quinones, which act as electron shuttles to facilitate extracellular electron transfer. Some electroactive biofilms, such as those produced by *Geobacter sulfurreducens*, contain conductive nanowires that could facilitate long-distance electron transport (Bond and Lovley 2003).

Although the composition of EABF has scarcely been studied, it is almost certain that there is no biofilm without an EPS matrix. Moreover, studies on EABF grown on different substrates using chemical methods and FTIR spectroscopy prove that EPS composition is almost similar and substrate composition and shape do not have any significant effect on it (Borole et al. 2011).

2.6.2 EPS role in electroactive biofilms

EPS's main role in traditional biofilms is providing structural stability, which is mainly attributed to the Polysaccharides component in EPS(S. Chen et al. 2019). The specific part of polysaccharides in the EABFs is not certainly understood, as different investigations have proposed different ideas. For instance, a study on the mutant strain of *S. oneidensis* MR-1, which had a genetic alteration in a gene related to cell surface polysaccharide biosynthesis, exhibited several favorable characteristics, including increased cell surface hydrophobicity, enhanced attachment to graphite anodes, and higher current generation (Kouzuma et al. 2010).

On the other hand, Tapia et al. used a combination of SEM and TEM techniques to study bacterial adherence to carbon surfaces with the participation of EPS(Tapia et al. 2011). They discovered that an EPS matrix covers the superficial carbon defects following intense cell adhesion, implying that the bacteria may transport electrons through this EPS matrix.

Given the inherently low conductivity of polysaccharides, Ter Heijne et al. suggested that precipitates and deposits of exopolysaccharides (EPSs) may have partially obstructed the electrode surface (ter Heijne et al. 2021). Considering various studies, it can be concluded that EPS components as conductive biofilm matrix play a crucial part in ET, and EPS composition may be impacted by the availability of electrode surface area for electron donation (design parameter) and the system's ability to deliver substrate (operation factors such as loading, flow rate, and so on)(Zhou et al. 2022)(Kohlstedt et al. 2014)(Aelterman et al. 2008).

2.6.3 EPS conductivity properties in an EABF

As discussed earlier, EPS structure includes glycoproteins, polysaccharides, proteins, glycolipids, humic substances, and extracellular DNA. According to several studies, nucleic acids, humic substances, flavins, and protein substances with the EPS structure

show redox-active or semiconductive properties(Li et al. 2016)(Xiao and Zhao 2017). Moreover, it was found that hydrated or ionized polysaccharides are considered biobased electroactive polymers (Finkenstadt 2005).

Chapter 3. Materials and Methods

This chapter compiles the materials, experimental designs, and setups employed throughout this thesis and provides a comprehensive description of the analytical techniques and methods used for result interpretation.

3.1 Inoculum and cell culture

3.1.1 Inoculum

The inoculum used in this study was *B. subtilis* strain ATCC 6051 (Bacillus Marburg strain). The *Bacillus subtilis* Marburg strain is a widely studied variant of *Bacillus subtilis*, extensively utilized in scientific research owing to its fully sequenced genome and significance in various industrial applications. *Bacillus subtilis* is a Gram-positive, spore-forming microorganism typically found in soil and has wide-ranging uses in biotechnology.

3.1.2 Materials and Reagents

Pipette tips in the range of 20 to 1000 µl Eppendorf®, Sterile Petri dishes 100 x 15 mm 500/cs (Fisher Scientific), Sterile 15 and 50ml falcon tube (Fisher Scientific), Inoculating Loop (Sigma-Aldrich), Drigalski spatula (3bscientific, model: 1010258), Growth Conditions based on Product Sheet Bacillus subtilis (Ehrenberg) Cohn 6051 , Medium: Nutrient agar and nutrient broth , Tryptone yeast extract broth (TY) Temperature: 30°C, Atmosphere: Aerobic, Nutrient Agar (Sigma-Aldrich), Glycerol (Sigma-Aldrich), DES1: ChCl/U (1:2 mol mol-1); DES2: ChCl/LA (1:2 mol mol-1); and DES3: ChCl/Gly (1:2 mol mol-1).

3.1.3 Equipment

Erlenmeyer flask (Fisher Scientific), Pipettor (Gilson), Orbital Shaker (Thermo Fisher Scientific), Refrigerated incubator (Thermo Fisher Scientific, Thermo ScientificTM, model: HerathermTM General Protocol Microbiological Incubators), Freezers (-20 °C; So-Low Environmental Equipment), Fiber Optic Light Source (Carl Zeiss Stemi), Vortex (Sigma-Aldrich)

3.1.4 Procedure

3.1.4.1 Bacillus subtilis glycerol stock preparation

(i) A loop (10 µl) from the glycerol stock culture of *B. subtilis* strain will be inserted on an LB agar plate, the inoculum streaks, and then incubated at 37 °C while maintaining axenic working conditions.

Note: LB agar plates with bacteria can be kept at 4 °C up to three weeks. However, they should be cryopreserved in cultures with 25% glycerol for long-term storage. The addition of Glycerol can stabilize frozen bacteria, protecting cell membranes from deterioration and maintaining cell viability. Up to several years of stable storage at -80 °C are possible for the cryopreserved Bacillus. To recover microorganisms from the glycerol stock, the glycerol stock bacteria first need to be thawed. Then, a small drop should be put on the top of the agar plate using a sterile loop or pipette tip, and the surface should be scrapped. The glycerol bacterial stock should be kept on ice during the procedure. The main benefit of working with spores is their stability over time. Also, thermal shock is imposed on the bacteria during the glycerol stock preparation process.

(Keeping bacterium for 15 min at 80°C) will decrease the possibility of microbial contamination.

(ii) Fill a sterile 15 mm falcon tube with 5 mL of sterile NB broth. Inoculate the medium with one colony developed as described in the previous stage.

(iii) Incubate the culture for 48 h at 37 °C with shaking (150 rpm).

(iv) To calculate the bacterial cellular yield (number of cells, or colony-forming units (CFU), per ml), several sequential dilutions of the grown culture are required. The most diluted culture should then be plated on the LB agar plate and incubated for 24 h at 37 °C before CFU counting.

3.1.4.2 Serial dilutions' preparation

100 µl of the cell suspension should be taken, 900 µl of deionized sterile water must be added to it and vortexed. This suspension is labeled as “10-1”. Before the sample settles, 100 µl of the abovementioned cell suspension should be taken with a pipette and transferred into 900 µl deionized sterile water. The sample should be Vortex and labeled as “10-2”.

This dilution step usually repeats seven times, with the addition of 100 µl of the previous suspension and 900 µl-deionized sterile water to reach the appropriate dilution. The last dilution is labeled as “10-7.”

100 µl of the dilutions 10-5 to 10-7 will be spread out on the surface of the LB agar plates and incubated for 24 h at 37 °C in triplicate.

The concentration of colony-forming units (CFU) per milliliter is determined using the following formula:

$$\mathrm{CFU/mL} = (\mathrm{N/V}) \times \mathrm{DF}$$

Where:

CFU/mL: Colony-forming units per milliliter (the desired concentration).

N: The number of colonies counted on a Petri dish or agar plate.

V: The volume of the original sample plated (usually in milliliters).

DF: The Dilution Factor: If the sample was diluted before plating, it is equal to the final volume divided by the aliquot volume.

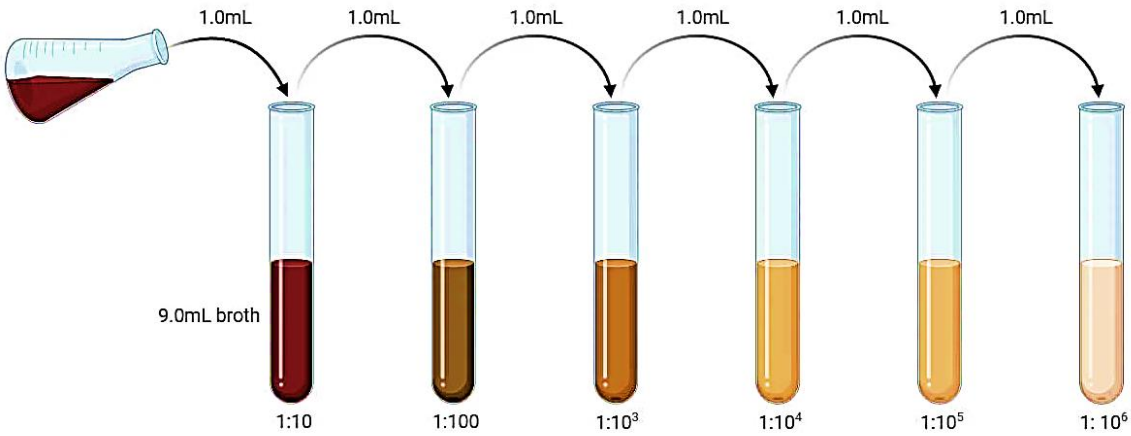

Figure 3.1 Principle of dilution method. Reprinted from *https://microbenotes.com/serial-dilution/*

3.1.4.3 Preparation of *B. subtilis* culture for experiments

100 mL of NB broth will be prepared based on the instructions provided by the manufacturer in a glass flask and autoclave at 121 °C for 15 minutes, then cool down afterward. The amount of 8 x 105 C.F.U./ml of a *B. subtilis* strain grown as indicated in the previous Procedure will be prepared and incubated at 37 °C with shaking (140 rpm) for 14-16 hours to reach the mid-log (O.D. = 0.5). The obtained culture can be used in the experiments immediately.

3.2 Electrochemical experiments

3.2.1 Chronoamperometry

Chronoamperometry (CA) is a highly sensitive method widely used in electrochemistry analysis(Baluta et al. 2022). It has been extensively used in various research studies, independently or in conjunction with other electrochemical methods like cyclic voltammetry (CV)(Rafiee et al. 2024). Moreover, chronoamperometry offers the advantage of providing direct, real-time insights into electroactivity. This technique has the capacity to provide valuable physiological information about the metabolic status of cells within biofilms. It is especially useful for distinguishing between live and dead cells, a crucial capability absent in conventional gold standard methods. Chronoamperometry is a time-

based electrochemical method that involves the application of step potential to the working electrode(Baluta et al. 2022). The current flows through the electrode and is recorded over time, as a function of time, and fluctuates according to the diffusion of an analyte from the bulk solution toward the sensor surface(Trivinho-Strixino, Santos, and Souza Sikora 2017). This technique enables the investigation of how current varies with time, particularly in the context of diffusion-controlled processes at the electrode, which is influenced by the concentration of the analyte(Khater, El-khatib, and Hassan 2018).

3.2.2 Differential pulse voltammetry (DPV)

Differential Pulse Voltammetry (DPV) is a highly sensitive technique used for both qualitative and quantitative analysis of redox species. The method exploits the differing decay rates of charging and faradic currents when a potential pulse is applied. During the procedure, a series of short voltage pulses are applied to the electrode, and the resulting current is recorded at the start and end of each pulse. This generates a peak-shaped voltammogram. DPV is particularly useful for examining the concentration and behavior of electroactive redox species, such as membrane-bound FAD molecules, over time, offering critical insights into their role in electron transfer processes. (Khan et al. 2013) (S. S. Kumar, Kumar, and Basu 2019).

Marsili et al. (2008) used the DPV technique in their study on *Shewanella,* and they found out flavin plays an essential role in the electron transfer mechanism of multilayered, old biofilms(Marsili et al. 2008c).

Choi et al. acquired the DPV technique to detect and characterize the extracellular electron transfer in *S. oneidensis* MR-1 biofilms. Their finding indicated that the initial electron transfer is via a direct pathway using cytochrome due to the direct contact of microbial biofilm with the electrode. After several days and by the growth of biofilm and its thickening, flavin-like mediators were found to be more actively involved in facilitating the ET mechanism (Choi et al. 2018).

Even though electrochemical techniques such as DPV and visual methods can stand alone, merging the advantages of these techniques creates an excellent and powerful tool for understanding and gaining more details on the nature of electro-active biofilms (Y. Kumar et al. 2019).

Differential Pulse Voltammetry (DPV) is a pulse electrochemical technique used to determine the concentration of specific compounds in a sample solution. It is particularly useful for the selective and sensitive analysis of electroactive species, such as ions or molecules that undergo redox reactions (oxidation or reduction) at an electrode surface.

Differential pulse voltammetry is preferred due to its differential nature and low-capacity current, which help minimize the effect of background charging current during analysis and make it a precise and efficient technique for distinguishing analytes that exhibit similar oxidation potentials.

DPV involves applying varying voltage levels across electrodes and measuring the resultant current flow through the electrolytes. This technique investigates the relation of voltage potentials (E), current (i), and time (t) over a specific duration of time for the collected samples.

Differential pulse voltammetry (DPV) is a variation of linear sweep voltammetry where a series of voltage pulses are applied to the electrode with an incrementally increasing baseline. The current is measured just before the application of each subsequent pulse. The DPV setup consists of a working electrode (WE), a counter electrode (CE), and a reference electrode (RE) that regulates the CE's voltage. The CE transmits the voltage pulses, while the WE measure the resulting current. Pulse durations typically range from 10 ms to 100 ms, with increments between 10 and 100 mV. After each pulse, a 1–2 second idle period allows only Faradaic current to be detected, minimizing interference from the charging current.

In differential pulse voltammetry (DPV), current is measured at two distinct points: before the pulse is applied (I1) and at the end of the pulse (I2). This enables the recharging of the redox pool at the electrode interface. The initial current (I1) corresponds to the direct

current ramp, while the difference between the two measurements ($\Delta I = I2 - I1$) represents the current response due to the potential pulse. The DPV signal is thus the difference between the current just before and at the end of the pulse. The peak potential (Ep) approximates the half-wave potential (E1/2), meaning the peak potential in DPV corresponds to the half-wave potential for the redox reaction (oxidation or reduction). The resulting DPV curve, known as a differential pulse voltammogram, plots the difference in current against applied potential. The peak current height is directly proportional to the analyte concentration.(Furst and Francis 2019).

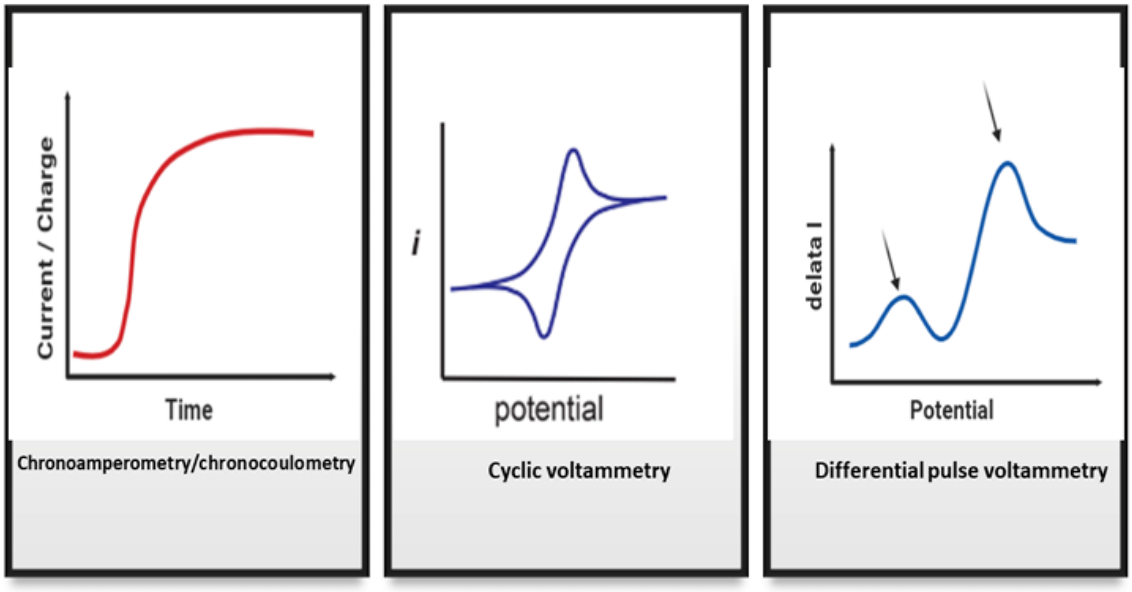

Figure 3.2 Representative plots of selected electrochemical techniques. Reprinted from(Haslett 2012)

3.2.3 The potentiostat

A potentiostat is an electronic amplifier system that regulates the potential difference between the working electrode (WE) and the counter electrode (CE).A potentiostat measures the current based on the potential difference at WE–RE. Depending on the

electrochemical experiment's specific requirements, a potentiostat can operate with either a two-electrode or a three-electrode configuration.

. A two-electrode system comprises the WE and the CE only, while a three-electrode system also has a reference electrode (RE). (Sánchez et al., 2020).

The three-electrode system is preferred over the two-electrode system due to the precise control of the potential difference at WE-RE, which results in higher sensitivity and repeatability of the electrochemical analysis.

In a standard three-electrode system, an "uncompensated resistance" arises between the reference electrode (RE) and the working electrode (WE). This affects the system functionality due to the ohmic potential drop, especially at higher currents.

Unfortunately, the resistance between the RE and WE is due to its inability to incorporate it into its feedback loop. However, this issue can be resolved by reducing the distance between the WE and RE. In some situations, a small glass capillary, known as a Luggin capillary, may be employed to alleviate the uncompensated resistance. It's worth noting that this capillary may become clogged, especially during long-term experiments, leading to instability characterized by voltage fluctuations and consequently resulting in poor electrochemical performance (Zhang 2011).

Furthermore, the characteristics of the various components that make up the electrochemical system, including electrodes, electrolytes, and microorganisms, tend to change over time. This may lead to unstable current flow and complicate the assessment of individual components. While the potentiostat is engineered to maintain control over the potential at the WE by compensating for resistance between the RE and CE (as illustrated in Fig. 2.2), this capability is contingent upon the compliance voltage range of the device. This range is determined by the limitations of the potential control amplifier (as shown in Fig. 2.2). However applying a larger WE can result in an uneven distribution of potential, which could lead to non-uniform biofilm growth and reduced electrochemical system efficiency(Hernández-Fernández et al. 2015)(Oliot et al. 2017) (Hernández-Fernández et

al., 2015; Oliot et al., 2017). Therefore, electrodes with smaller surface areas prove more advantageous for sensing and analytical applications (Sánchez et al., 2020).

One of the challenges with traditional potentiostats (e.g., Fig. 2.2(B)) is that they are relatively bulky, expensive and unsuitable for use in remote locations (Sánchez et al. 2020). Fortunately, technological advancements have led to the creation of portable potentiostats, which are not only cost-effective but also user-friendly(Huang et al. 2018)Additionally, conventional laboratory setups involving two—and three-electrode systems necessitate the purchase, preparation, and upkeep of separate electrodes (RE, CE, and WE). This will increase both the cost and the need for specialized labor in conducting experiments, rendering them less adaptable for biosensing and bio-analytical applications.

Screen-printed electrodes (SPEs) are considered a good solution for the abovementioned limitations. They integrated three electrodes in a compact, cost-effective, versatile, and user-friendly structure. Screen-printed electrode SPEs offer simplicity and adaptability for handling, which makes them a good choice for various electroanalytical techniques (Popescu 2016)(García et al. 2021)(Munteanu et al. 2018).

While concerns exist, especially regarding the potential replacement of conventional methods, the prospects offered by SPEs are immense, and their applications, particularly in the fields of biosensing and clinical diagnosis, are increasingly being explored.

3.2.4 Screen-printed electrodes (SPEs)

A typical SPE resembles a conventional three-electrode cell, with WE, RE, and CE combined into a single arrangement. The CE is often formed of carbon, platinum, or even gold, whereas the RE is typically made of silver or silver/silver chloride layer (Ag or Ag/AgCl). Carbon is primarily utilized for WE due to its affordability, ease of access, strong functionalization potential, and superior electrochemical characteristics, such as low background current, a broad potential range, chemical inertness, and good compatibility with other materials and molecules.

the representative of a typical SPE structure is presented in **Figure 3.3.**

The procedure generally follows a similar pattern. It involves (1) designing electrodes and configuration and manufacturing via ink-printing on sequential layers of ceramic or plastic materials, depending on the final intended application. The application of SPE in bioelectrochemical systems has attracted considerable attention as it seems a promising alternative to conventional systems setups with three electrodes.

This method has been effectively utilized in quality control evaluations of food and beverage samples, environmental pollution monitoring and analysis, forensic investigations, cancer biomarker detection, and the study of key biomolecules. It has also been applied in fundamental microbial research to identify and characterize microbial pathogens and their metabolites.(García et al. 2021)

SPEs can be preferred over conventional three-electrode systems due to their simplicity of use and portability, which makes them suitable for fieldwork. They are also user-friendly; no specific training is needed to assemble them. SPEs are also known for their low background noise, which can lead to improved signal-to-noise ratios in electrochemical measurements. Three-electrode systems generally have higher background noise levels. SPEs also have a broad application range compared to three-electrode systems. They are applicable in many areas, including environmental monitoring, clinical diagnostics, food safety, and biosensing.(Alonso-Lomillo et al. 2010)(García et al. 2021).

It should be considered that despite the numerous advantages of SPEs, traditional three-electrode systems may still be preferred in some cases for specialized research or when certain features are necessary.

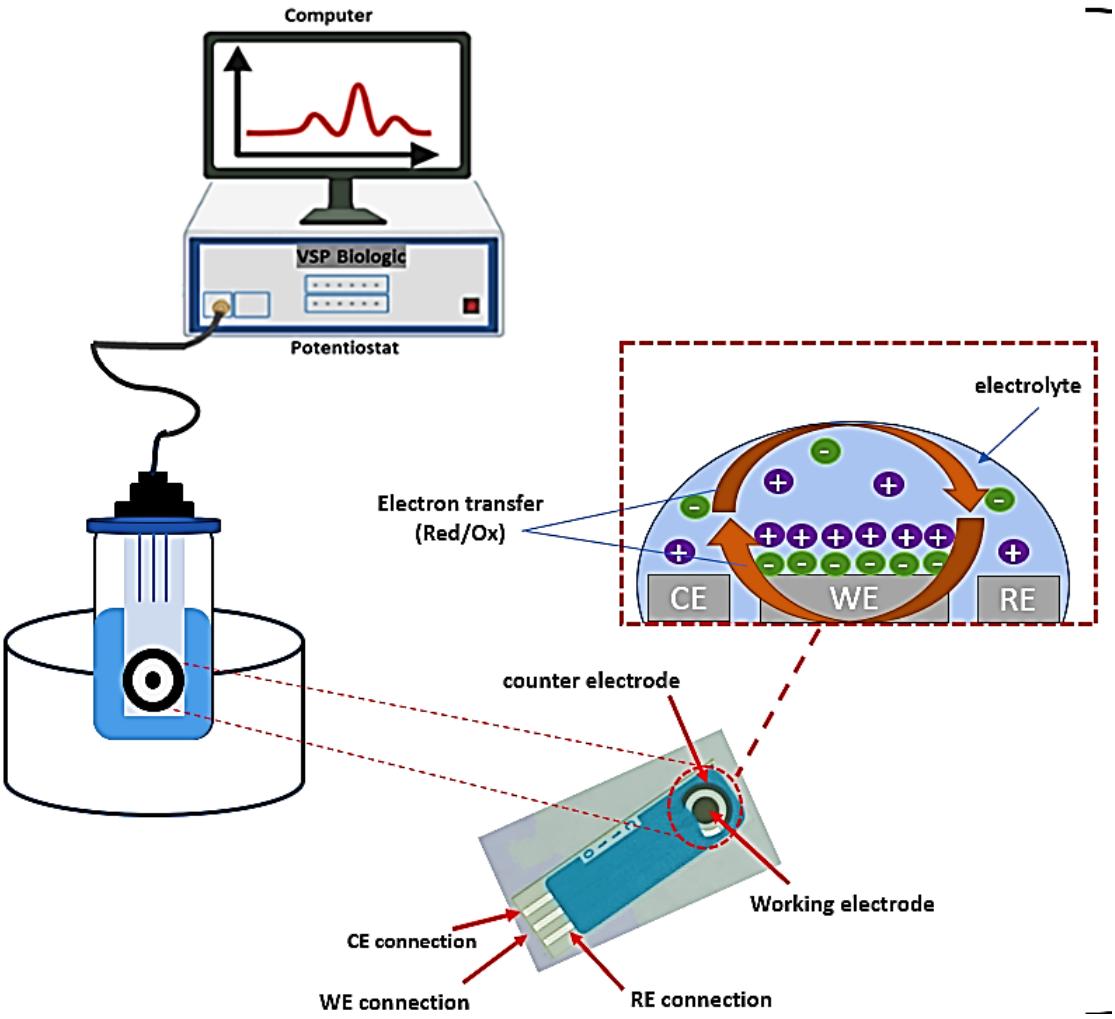

Figure 3.3 Graphical representation of the electrochemical setup, created using Biorender

3.3 Crystal Violet Staining (CV) for Quantitative Biofilm Analysis

Crystal Violet staining is a quantitative technique used to assess and quantify the amount of biofilm formed on walls and surfaces. The microtiter plate assay's ease of use, flexibility, and low cost have made it a critical tool for quantifying biofilms.

Biofilms are complex communities of microorganisms that adhere to surfaces (e.g., microtiter dishes). The microtiter dish assay is an essential tool for studying the early stages of biofilm formation and can be applied primarily to any type of biofilm, including fungal and bacterial biofilms.

Crystal violet staining uses static conditions of the growing batch and does not work with flow cell systems. However, the biofilms grown in microtiter dishes develop some properties of mature biofilms, which are good representatives of mature biofilms.

A simple microtiter dish assay allows biofilm formation on the wall surfaces and/or bottom of a microtiter dish. The assay's simple nature makes it applicable for quantification of biofilm formation for a wide variety of microbes, including but not limited to *B. subtilis* (the bacteria this work is focused on).

The protocol measures the extent of biofilm formation using crystal violet dye (CV). In this work, this assay was used to study B. subtilis biofilm formation.

Biofilm quantification assay using crystal violet has several steps:

1. Growing biofilm: biofilm formation is a dynamic and cyclic process, and it takes 24 up to 48 hours for the initial biofilm to attach and grow on the wall and surfaces of microtiter plate wells

2. Biofilm Staining Procedure: Following incubation, the microtiter plates were inverted and the liquid was gently removed by shaking. The plates were then carefully submerged in a water bath, shaken to remove unattached cells and media components, and this rinsing process was repeated twice. The plates were subsequently air-dried at room temperature for 20 minutes. A 1000 μL aliquot of 0.1% crystal violet solution in water was added to each well of the 48-well microtiter plates, followed by an incubation at room temperature for 10-15 minutes.

3. Biofilm Quantification: To assess biofilm formation, 1000 μL of 30% acetic acid in water was added to each microtiter plate well to solubilize the crystal violet (CV). The plates were then incubated at room temperature for 10-15 minutes. The solubilized CV was subsequently transferred to a new flat-bottomed microtiter plate, and the absorbance was measured at 570 nm (OD570) using a Gen5TM Microplate Reader and Imager Software (BioTek Instruments). Each experimental condition was analyzed with four independent biological replicates, and a solution of 30% acetic acid in water was used as a blank for absorbance measurement at 570 nm.

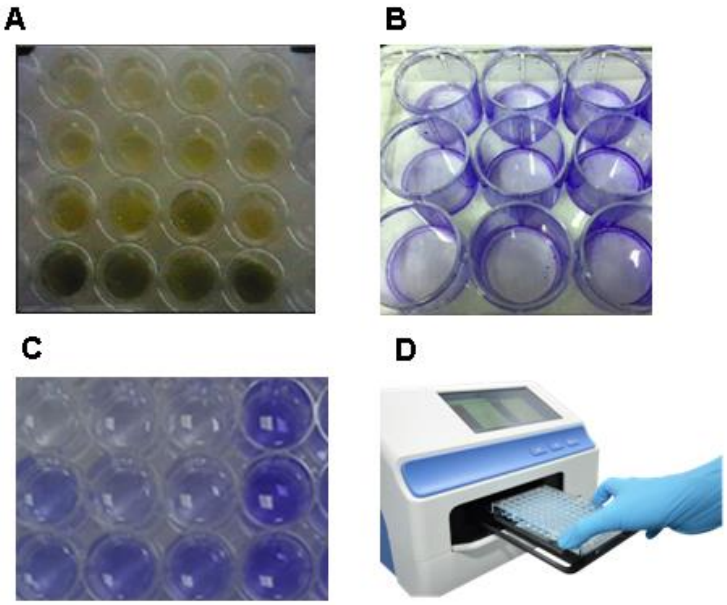

Figure 3.4 Diagram of Crystal Violet Assay for Biofilm Formation in a Microtiter Plate. (A) Biofilm formed in 48 well microtiter plate after 48h. (B) crystal violet absorbed by biofilm (C) CV suspension in acetic acid 30% transferred to the new plates (D)OD measurement using a microtiter plate reader

3.4 Confocal microscopy

An upright Zeiss of Axio Zoom.V16, Carl Zeiss confocal microscope was used to image the crystal violet stained biofilms formed on the surface of the SPE electrodes. Electrodes were collected after a 48h electrochemical experiment and immersed in the 0.1% crystal violet for almost 30 minutes; the extra CV was then washed off the electrode by gently immersing the electrode into the distilled water. The electrodes dried after that for about an hour, and then the stained biofilm on the surface of the electrode was observed using Zeiss of Axio Zoom.V16, Carl Zeiss confocal microscope, the result was recorded by ZEN software, and later the biofilm quantification calculation was done by a MATLAB code.

Confocal microscopy is an advanced bioimaging technique that captures detailed images from various depths within a sample. Its optical system collects light from a thin, defined region known as the focal plane. By selecting a specific depth for analysis, the microscope filters out light from surrounding areas, allowing only the light from the designated focal plane to reach the detector, thereby enhancing image clarity and resolution. (Kuehn et al.

1998) Z-scan involves capturing a series of images at different focal planes, which allows for the reconstruction of a three-dimensional (3D) representation of the sample, particularly biofilm (Xavier and Bassler 2003)(Popescu 2016). To keep the accuracy of the result compared to what was collected from the electrodes, samples for confocal microscopy were immediately prepared after disassembling the potentiostat setup. This was due to the fact that the membrane of bacterial cells could lose its intact structure while removed from the initial experiment condition. Samples were stained using a Crystal Violet Kit and based on the protocol for CV biofilm staining. The confocal microscope was configured with three distinct channels: the first channel, represented in green, for detecting live cells; the second channel, visualizing propidium iodide (PI) in red, to identify dead cells; and the third channel, visualized in blue, to capture the reflectance of optically opaque graphite fibers. A comprehensive overview of the confocal microscopy channels and their settings is provided in Table 3.1.

The staining protocol consisted of preparing the 0.1% crystal violet solution (by dissolving 1 gram of crystal violet powder dye into the 10 mL of 95% ethanol and addition of water to reach 100 mL volume). After completing the staining process and removing the excess dye, the samples were placed on coverslips and positioned on the microscope stage. Since the microscope used a reversed lens, the lens was positioned beneath the coverslip. A magnification of ×25 was utilized for imaging, allowing the entire area of the working electrode to be captured. Three different replicates were selected for each condition, and all quantitative analyses were averaged from these three replicates.

ZEN blue software was employed to determine the threshold for each channel in the images, allowing for the exclusion of background noise. The biofilm coverage on the electrode was quantified for the designated region of the working electrodes using Image J software. To verify the accuracy of the analysis and eliminate the potential impact of noise, a bare electrode rinsed with ethanol served as a negative control.

Table 3.1 The setting of the confocal microscopy

Channel Color	Mode	Excitation	Emission	Targeted object
Red	Fluorescence	590 nm	635nm	Biofilm

3.5 HPLC

High-performance liquid chromatography (HPLC) is an advanced analytical method designed for separating, identifying, and quantifying individual components within a mixture. It represents a significantly enhanced version of traditional column chromatography. The principle of liquid chromatography is based on dissolving a sample mixture in a proper liquid solvent and passing it through a chromatographic column. Within the column, the sample components interact with a stationary phase, which may be a solid material or a bonded phase on the column's inner surface.

HPLC analysis typically includes several steps:

1) A small volume of the sample is injected into the HPLC system. This is mostly an automated process using an injector.

2) A liquid solvent, known as the mobile phase, is pumped through the chromatographic column. The mobile phase carries the sample through the column.

3) Inside the column, the sample components interact with the stationary phase. Components with different chemical properties will interact differently with the stationary phase and, as a result, separate from each other.

4) As the separated components exit the column, they pass through a detector that measures their concentration. Standard detectors include UV-*visible* spectrophotometers, fluorescence detectors, and refractive index detectors.

5) The detector's collected data will be analyzed to determine the identity and concentration of the sample components.

HPLC can be used in various fields, including chemistry, pharmaceuticals, biochemistry, environmental science, and food analysis. It allows for high-resolution separation of complex mixtures and is known for its accuracy and precision in quantifying analytes. Different HPLC methods, such as reverse-phase HPLC, size-exclusion chromatography, and ion-exchange chromatography, are employed based on the specific separation requirements of the analysis.

The HPLC technique allows the separation of complex mixtures with high resolution and is highly accurate in quantifying analytes. It can be used in various fields, including chemistry, pharmaceuticals, biochemistry, environmental science, and food analysis. Various HPLC methods, such as reversed-phase HPLC, size exclusion chromatography, and ion exchange chromatography, are used based on specific separation requirements.

B. subtilis (under-study bacteria in this work) has the capability of secreting riboflavin (vitamin B2) extracellularly and into the medium environment.

B. subtilis can secrete compounds such as menadione and riboflavin, most probably due to metabolic activity. Change in the riboflavin secretion pattern could be due to the influence of the availability of electron donors/ acceptors.

Many studies have investigated the riboflavin secretion by *B. subtilis* to optimize its production and understand the metabolic pathways involved in this process.

This work investigated the presence of Riboflavin (vitamin B2) and menadione (vitamin K) in the supernatant secreted from B. subtilis treated with different conditions using the HPLC technique. *B. subtilis* is a water-soluble compound that can secrete riboflavin (vitamin B2) into its surrounding environment.

The bacterium may secrete riboflavin due to metabolic activity, which could be influenced by the availability of electron donors and acceptors. Changes in riboflavin secretion patterns might indicate variations in metabolic activity, potentially related to EET.

3.6 Ultraviolent-visible spectrophotometry

3.6.1 What is UV-vis technique

Ultraviolet-visible (UV-Vis) spectrophotometry, also known as Ultraviolet-Visible spectrophotometry, is a widely used analytical technique in many areas of science ranging from chemistry and biochemistry to bacterial culture and drug identification. This technique measures the absorption of ultraviolet (UV) and visible (Vis) light by a substance. UV-*Vis* can also be employed to determine the concentration of a particular substance in a solution and to gather information about the chemical properties of a compound.

UV-Vis spectroscopy operates by measuring the specific wavelengths of ultraviolet or visible light absorbed or transmitted by a sample, compared to a reference or blank sample, using light as its primary tool. This property can provide information on the sample composition and concentration.

Light has a certain amount of energy, inversely proportional to its wavelength. Thus, shorter wavelengths of light carry more energy, and longer wavelengths carry less energy.

Absorption refers to the energy required to excite electrons in a substance to a higher energy level. Electrons in distinct bonding environments within a substance require specific amounts of energy for this excitation, leading to absorption at different wavelengths for different substances. This variation in absorption explains why different substances absorb light at different wavelengths. Humans perceive visible light across a spectrum ranging from approximately 380 nm (violet) to 780 nm (red). Ultraviolet (UV) light has shorter wavelengths, down to about 100 nm. In UV-Vis spectroscopy, light is characterized by its wavelength, which helps identify or analyze substances by pinpointing the wavelengths corresponding to their maximum absorbance.

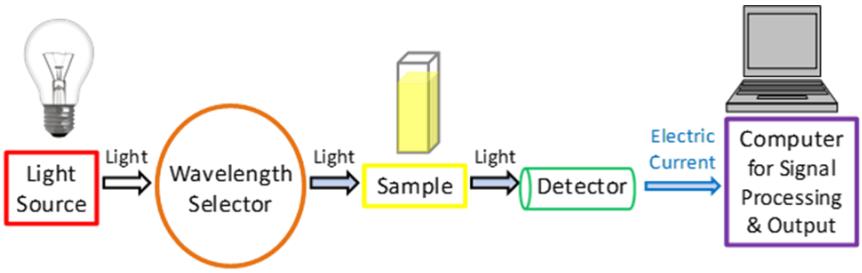

Figure 3.5 A simplified diagram of the key components of a UV-Vis spectrophotometer. Credit: Dr. Justin Tom. Adapted from https://www.technologynetworks.com/analysis/articles/uv-vis-spectroscopy-principle-strengths-and-limitations-and-applications-349865

3.6.2 Light source

UV-vis is a light-based technique, and it requires a steady source that can emit light across a wide range of wavelengths.

UV -vis spectrophotometers are categorized into (i) single xenon lamps and (ii) two tungsten or halogen lamps. Singel Xenon lamps are applicable for both UV and visible ranges, while equipment employing two lamps is mainly used for visible lights.

3.6.3 Sample analysis

Wavelength selection is a very important step in UV-vis analysis. The appropriate wavelengths of light are chosen based on the sample type, and specific analytes must be selected from the wide range of wavelengths emitted by the light source for detection. Once the wavelength is selected, the light passes through the sample. For all analyses, it is essential to measure a reference, commonly referred to as a "blank sample," such as a cuvette containing the same solvent used to prepare the sample.

The sterile culture media is used as a reference when examining bacterial cultures. The instrument later automatically uses the reference sample signal to help obtain the true absorbance values of the analytes.

It is essential to be aware of optimizing the materials and conditions used in *UV-Vis* spectroscopy experiments. Quartz sample holders are the best cuvettes for UV examination compared to plastic and glass ones, as quartz is transparent to most UV light. A special and more expensive setup is usually required for measurements with wavelengths shorter than 200 nm.

3.6.4 Detection

Once light passes through the sample, a sensor converts the light into a readable electronic signal. Typically, photoelectric coatings or semiconductor materials are used for such purposes.

3.6.5 UV-Vis spectroscopy analysis, absorption spectrum, and absorbance units

UV-*Vis* spectroscopy data is generally presented as a plot showing absorbance, optical density, or transmittance as a function of wavelength. Typically, wavelength is plotted on the x-axis, while absorbance is shown on the y-axis, producing an absorption spectrum. Absorbance (A) is calculated as the logarithm of the ratio between the initial light intensity (I_o) and the light intensity after passing through the sample (I). The ratio of I to Io is termed transmittance (T), representing the proportion of light that successfully passes through the sample.

$$A = \varepsilon Lc = Log_{10}\left(\frac{I_0}{I}\right) = Log_{10}\left(\frac{1}{T}\right) = -Log_{10}(T)$$

UV-*Vis* spectrophotometry operates according to Beer's Law, which establishes a direct linear correlation between the solute concentration in a solution and the amount of light absorbed by the solute.:

$$A = \varepsilon * c * I$$

A is the absorbance of the sample.

ε (epsilon) is the molar absorptivity (also known as the molar extinction coefficient), a constant specific to the substance and the wavelength of light being used.

c is the concentration of the analyte in the solution.

l is the path length of the cuvette or cell through which the light passes.

Building a calibration curve depends on the purpose of analysis, and it requires some data analysis.

This technique is a very precise way to accurately obtain a particular substance's concentration in a sample based on absorbance measurements.

However, the calibration curve is not required for OD measurements for bacterial culture, collecting absorbance ratios at specific wavelengths to detect the purity of nucleic acids, or identifying specific medications in a solution.

3.6.6 Strengths and limitations of UV-*Vis* spectroscopy

- The method is non-destructive; the sample can be utilized again for further analysis.
- Measurements can be made quickly, allowing easy integration into experimental protocols.
- Instruments are user-friendly, requiring little user training before use.
- Data analysis generally requires minimal processing
- The instrument is generally inexpensive, making it accessible for many laboratories.

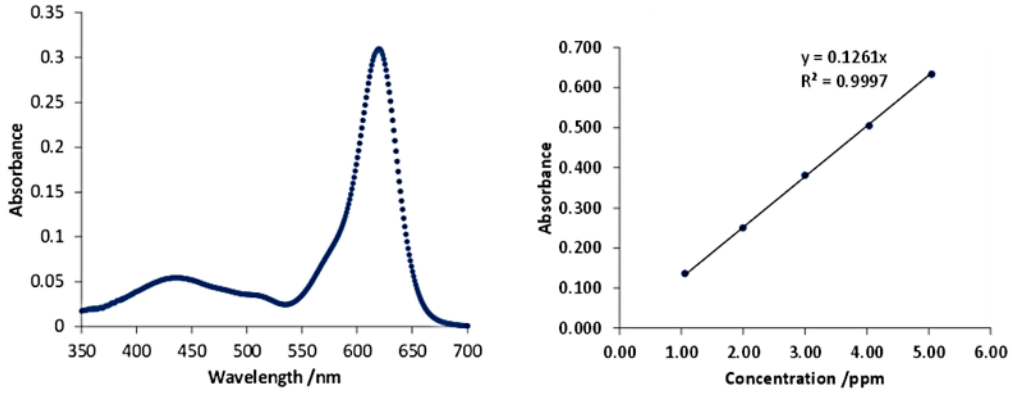

Figure 3.6 The UV-Vis spectrum for the selected sample is displayed in the graph on the left. On the right, a calibration curve has been generated from standard diluted solutions

of the sample, using a least squares linear regression equation for accurate analysis. Credit: Dr. Justin Tom

https://www.technologynetworks.com/analysis/articles/uv-vis-spectroscopy-principle-strengths-and-limitations-and-applications-349865

Chapter 4. Electroactivity of weak electricigen *Bacillus subtilis* biofilms in solution containing deep eutectic solvent components

This chapter is adapted from my following research paper:

Eghtesadi, N., Olaifa, K., Perna, F. M., Capriati, V., Trotta, M., Ajunwa, O., & Marsili, E. (2022). Electroactivity of weak electricigen Bacillus subtilis biofilms in solution containing deep eutectic solvent components. Bioelectrochemistry, 147, 108207. (Scopus Percentile: 88%, Q1)

This chapter mainly focuses on using deep Eutectic Solvents as biocompatible nutrient additives in boosting the electroactive performance of *Bacillus Subtilis* biofilms, referenced as a weakly electricigen bacterium. The experiments aimed to define the most effective DES as well as its conditions of use and then to identify the parameters explaining the improvement in electroactive performance. Thus, planktonic growth, biofilm concentration, charge output, and redox profiles were measured and compared at different solvent concentrations. For variations in solvent component concentrations, the components of DES are then used alone rather than together. Several eutectic mixtures were studied and compared, and the aqueous choline chloride glycerol (ChCl: Gly 1:2 mol mol^{-1}) showed the best results in terms of electroactivity. It appears in conclusion that the choline chloride component stands out on its own because it makes it possible to improve planktonic growth, biofilm growth, and electroactivity. The authors propose several hypotheses to explain this significant increase in performance and its role in the EET process. However, further investigations are required to validate them. The complementary research is presented in the following chapters.

4.1 Introduction

Bacteria capable of extracellular electron transfer (EET) are often termed electricigens (Schröder et al. 2015) and their electron transfer phenomena have been investigated for bioenergy production and biosensor applications. Strong electricians, such as Geobacter sp., grown on graphite electrodes produce high current density at strong oxidizing potentials via electrically conductive protein nanowires(Bruce E Logan et al. 2019). Most microorganisms show low current output under the same conditions (~0.1 Am^{-2}) and are weak electricigen as they require exogenous redox mediators to facilitate EET(Doyle and Marsili 2018b). Weak electricigens have been observed in river sediments, beach sand, compost, water samples, and hydrothermal ecosystems. Thus, it is interesting to investigate the relationship between electroactivity and the production of essential metabolites and how biofilm-driven bioprocesses can be optimized by applying electrical current or potential. (Markraphael Ajunwa et al. 2021)(Aiyer and Doyle 2022).

Improved electroactivity can be obtained through genetic alterations, such as the induction of redox mediators and reprogramming of the extracellular electron transfer (EET) pathway. However, these genetic modifications can be time-intensive and may lead to changes in the final product. Alternatively, optimizing growth media and intensifying processes have been suggested as more efficient approaches to enhance EET in organisms with weak electrochemical activity.(Astorga et al. 2019)(Jing et al. 2019).

Bacillus species are Gram-positive, spore-forming microorganisms with weak electroactivity, known for their role in producing alkaline proteases, biopolymers, biosurfactants, and antimicrobial peptides. The electroactivity of B. subtilis is closely associated with its growth and metabolic processes, with studies suggesting a link between electroactivity and its ability to survive extreme temperature and pH conditions. Integrating extracellular electron transfer (EET) with biosynthetic pathways in Bacillus species holds potential for enhancing bioprocess efficiency.(Su et al. 2020)Here, we investigate for the first time the use of Deep Eutectic Solvents (DESs) added to the bacterial growth medium at sub-toxic concentrations to boost *B. subtilis* electroactivity.

Deep Eutectic Solvents (DESs) represent a novel category of sustainable solvents characterized by their composition of two or three benign and cost-effective components, typically involving Brønsted or Lewis acids and bases. When these components are combined in specific molar ratios, they form hydrogen bonds, creating eutectic mixtures.(Hansen et al. 2021). Typical DES components (e.g., choline chloride (ChCl), lactic acid, urea (U), glycerol (Gly), amino acids, vitamins, and polyalcohols) are biodegradable and show low toxicity(Cicco et al. 2021)(Milano et al. 2017). Due to their small ecological footprint, ease of preparation, the ability to act as solvents, catalysts, and even reagents, and amenable physicochemical properties, DESs are progressively replacing toxic and volatile organic compounds (VOCs) in catalysis, dissolution, and extraction processes, and electrochemistry(Milano et al. 2017)(Maria Perna et al. 2021).

The use of DES as a minor component of a solution was recently explored in the crystallization of the lysozyme, a small hydrophilic protein(Belviso et al. 2021). DESs were found to reduce significantly solvent evaporation during the crystallization process, favoring the increase of the dissolution time of the protein crystals, playing a sort of protective role(Belviso et al. 2021)(Karimi et al. 2020)Similarly, the toxicity of DES used as a minor component of a bacterial nutrient broth was also recently investigated to assess its effect on the environment.

This study explores the impact of specific Deep Eutectic Solvents (DESs) on the electroactivity of *B. subtilis*. At non-toxic concentrations, a solution of the eutectic mixture ChCl enhances planktonic cell growth, biofilm development, and electroactivity of *B. subtilis*. These findings suggest that such DESs could potentially boost the production of crucial metabolites in electrofermentation processes involving *B. subtilis*.

4.2 Materials and Methods

4.2.1 Materials

The Deep Eutectic Solvent (DES) formulations used in this study are detailed in Table 4.1: DES1: ChCl/U (1:2 mol/mol); DES2: ChCl/LA (1:2 mol/mol); and DES3: ChCl/Gly (1:2 mol/mol). The experiments employed two types of media: a nutrient broth (NB) composed of 3 g/L beef extract and 5 g/L peptone, and a chemically defined medium (CDM) containing 10 g/L glucose, 5 g/L NH_4Cl, 0.5 g/L K_2HPO_4, 0.15 g/L $FeCl_3$, 0.5 g/L

MgSO4, 0.7 g/L CaCl2, 0.5 g/L NaCl, and 0.104 g/L MnSO4, all adjusted to pH 6.5. All media were prepared using deionized water and sterilized by autoclaving at 121°C and 109 kPa for 15 minutes. The 2-hydroxy-1,4-naphthoquinone (2-HNQ) redox mediator was sourced from Sigma Aldrich, Kazakhstan.

All commercial chemicals and reagents used were of analytical grade and prepared according to the manufacturer's specifications. The bacterial strain *Bacillus subtilis* ATCC 6051 was cultured and maintained on nutrient broth (NB) throughout the study. Electrochemical measurements were conducted using Screen-Printed Carbon Electrodes (SPE Ref. C110) from Metrohm DropSens, Spain, which included a graphite counter electrode, an Ag pseudo-reference electrode, and a graphite working electrode (WE) with a 4 mm diameter and a surface area of 0.126 cm^2. Potentials are referenced against the Ag pseudo-reference electrode. The electrochemical cells employed in the experiments had a total capacity of 10 mL and a working volume of 8 mL.

Table 4.1: Composition and Characteristics of the DESs evaluated in this study

#	C1	C2	Molar ratio C1:C2	Density
1	Urea	Choline chloride	2:1	1.19
2	Lactic acid	Choline chloride	2:1	1.17
3	Glycerol	Choline chloride	2:1	1.18

4.2.2 Methods

4.2.2.1 Bacterial growth studies

The growth curves of *Bacillus subtilis* at various concentrations of DESs and DES components were determined in both NB and CDM using 48-well plates and Gen5TM Microplate Reader and Imager Software (BioTek Instruments).

The experiments were carried out in quadruplicates, and the absorbance was measured at the wavelength of 600 nm. The results were presented as mean ± standard deviation (SD). Different DES concentrations and DES component concentrations, from about 15 mM to about 1 M, were prepared, filtered through sterile 0.2 µm filters, and then added to the final volume of 1000 µL per well.

The conditions for the incubation were 37 °C and 48 hours, respectively. To generate the inoculum, fresh cultures were grown for 24 hours at 37 °C with continuous agitation (180 rpm) and adjusted to an optical density of 0.1 (OD_{600}), which was previously calculated to represent the approximate number of colony-forming units (CFU) per milliliter.The redox mediator 2-HNQ (50 µM) was added in selected experiments.

4.2.2.2 Bioelectrochemical analyses

With a computer-controlled VSP multichannel potentiostat (Bio-Logic, France), the following measurements were made in order: chronoamperometry (CA), differential pulse voltammetry (DPV), and cyclic voltammetry (CV) right after the inoculum and at the conclusion of the experiments.

In order to reduce the impact of planktonic bacterial growth on current output, an inoculum size of 0.5 OD600 (or roughly 5 x 106 CFU mL-1) was employed. In this condition, the planktonic cell concentration remains relatively constant, and the current output is mostly due to the viable cells in the biofilm. SPEs were air dried, surface sterilized in 70% v/v ethanol, and then cleaned in sterile deionized water three times before the experiments began. The following parameters were established for Differential Pulse Voltammetry (DPV): initial potential (Ei) of -0.4 V, final potential (Ef) of 0.4 V, pulse height of 50 mV, and pulse duration of 200 ms. DPV measurements were conducted immediately after inoculation and again after 48 hours. For Chronoamperometry (CA), the working electrode

was maintained at 0.4 V for 48 hours. Each experiment's electrical charge output (measured in milliCoulombs) was calculated using EC Lab® software (Biologic, France). During incubation, the electrochemical cells were kept at a consistent temperature of 37 °C using dry baths containing steel beads. Following the assessment of Deep Eutectic Solvents (DES) effects on the electroactivity of Bacillus subtilis, additional bioelectrochemical analyses were conducted to evaluate the impact of the individual components of the eutectic mixtures on the bacterium's electroactivity. Both DPV and CA analyses were performed using molar concentrations of the individual components equivalent to those present in the DES mixtures.

4.2.2.3 Biofilm assay

Biofilms that developed on the carbon Screen-Printed Electrodes (SPEs) following electrochemical analyses were quantified using the crystal violet staining method. After each experiment, electrodes were removed from the electrochemical cells at the 48-hour mark and immersed in sterile deionized water to eliminate planktonic cells and media residues. The electrodes were then air-dried and exposed to a 0.5% (w/v) crystal violet solution for 10 minutes. Subsequently, the stained biofilms were washed and solubilized by placing the electrodes into wells of a sterile 48-well microtiter plate, each containing 1000 µL of 33% (w/v) glacial acetic acid. The absorbance of the solubilized dye was measured at 570 nm using a SmartSpec™ 3000 Spectrophotometer (Bio-Rad Laboratory, Helsinki, Finland). Each experimental condition was evaluated with four independent biological replicates.

4.2.2.4 HPLC analysis

An UltiMate 3000 HPLC system (Thermo Fisher Scientific) was used to detect and analyze riboflavin and menadione peaks in cell-free supernatants. Electrochemical cells medium was collected immediately after 48h and centrifuged at 5000 rpm for 10 minutes, followed by filtration through 0.22 µm microporous membrane to obtain cell-free supernatant.

The reference standard samples Riboflavin (Vitamin B2) and Menadione (Vitamin K3), which are commercially available, were prepared as described. A standard stock solution

for Vitamin B2 (riboflavin) was prepared by dissolving 6.9 mg of riboflavin in 100 mg of extraction. The extraction solution was made by mixing 25 mL of acetonitrile with 5 mL of acetic acid, and the volume was adjusted to 500 mL using double-distilled water. The standard stock solution for Vitamin K3 (Menadione) was prepared by dissolving 9.5 mg of menadione in 10 mL of 96% ethanol. Both standard stock solutions were filtered through a 0.22µm microporous membrane before injection in the chromatography column.

Following separation in the HPLC column, riboflavin and menadione peaks were detected spectrophotometrically at 270 and 245 nm wavelengths, respectively. All samples were analyzed with a C18 column (Hypersil Gold, 150×250mm,1.9 µm) at a flow rate of 0.2 mL min^{-1}. The mobile phase was a solution of methanol (chromatographic grade, Phase A, 65%) and a mixture of water and acetic acid 1% (chromatographic grade, phase B,35%).

4.3 Results

4.3.1 Growth experiments

In NB, *B. subtilis* cells grow quickly, reaching a peak concentration of 12–14 hours based on OD_{600} measurements. The OD_{600} did not plateau in 48 hours, and cell growth in CDM was slower (Figure 4.1). Therefore, NB was selected for additional experiments. The cell concentration in NB was higher for DES3 at concentrations lower than ~1 M (Figure 4.2).

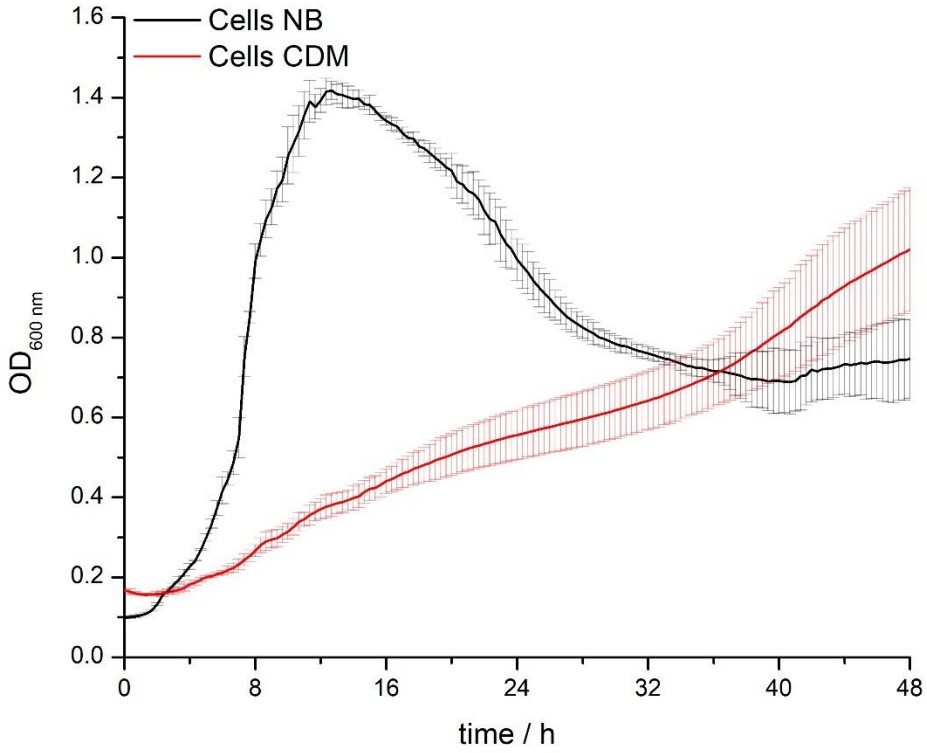

Figure 4.1 The growth curves of *Bacillus subtilis* in nutrient broth (NB) and chemically defined medium (CDM) demonstrate that the nitrogen sources in NB are more readily accessible compared to NH4Cl in CDM. This enhanced bioavailability in NB leads to faster microbial growth.

On the other hand, DES1 showed the highest cell concentration in CDM (Figure 4.3). Inhibited growth was observed in DES2, most likely due to lactic acid's low pH, which damages cell membranes and reduces viability. According to Hou et al., organic acid-based DESs inhibit bacterial growth (Hou et al. 2013).

B. subtilis growth in CDM was more significant than in NB in the presence of DES1. Increased growth in CDM could result from the additional urea supplied by DES1 as a nitrogen source in nitrogen-limited CDM. Additional studies were carried out with DES3 and NB, as these factors best facilitated *B. subtilis* growth. According to previous studies, DESs demonstrate low microbial toxicity, with little effect on microbial growth in Mueller-Hinton broth at concentrations below 200 mM (LC50 approximately 400-500 mM).

However, studies based on antibiograms might not be adequate to ascertain long-term DES toxicity.

According to a 48-h study, no toxicity was found on the DES acetylcholine chloride (AcChCl): acetamide (1:2) below 300 mM, partial inhibition was observed between 300 and 450 mM, and complete inhibition of growth was detected above 600 mM. Our findings confirm earlier studies demonstrating that ChCl-based DESs may function as supplemental nutrients and are non-toxic at concentrations below 200 mM. Higher DES concentrations inhibit cell development and extracellular respiration, suggesting that the DES formulation should be modified for improved biocompatibility.

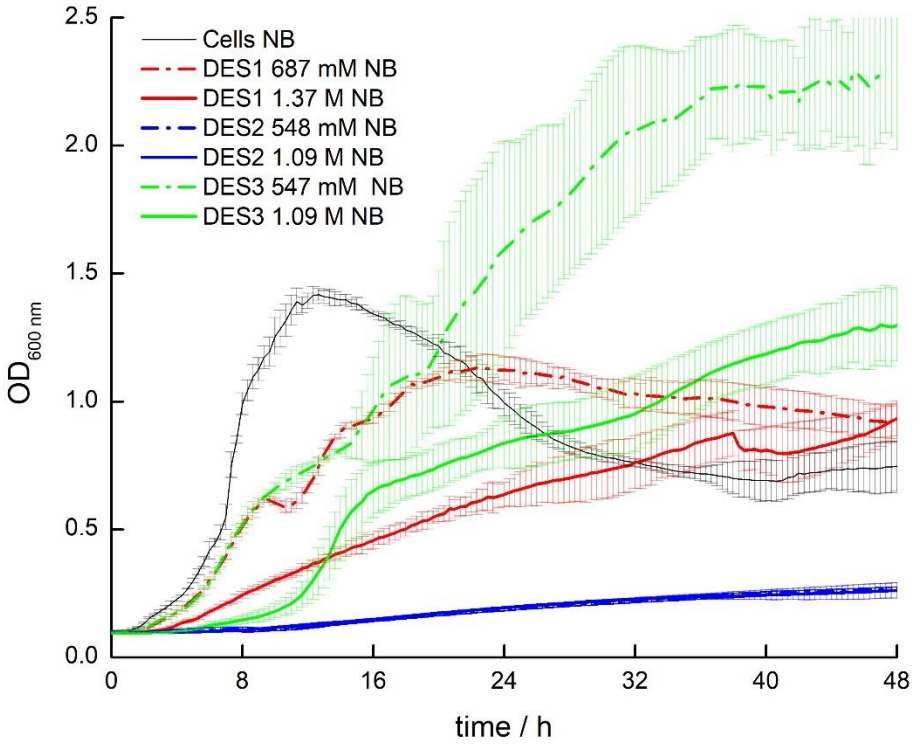

Figure 4.2 Growth curves of *Bacillus subtilis* in nutrient broth (NB) medium were assessed at two concentrations for each of the three deep eutectic solvents (DESs): ChCl/U (1:2) (red), ChCl/LA (1:2) (blue), and ChCl/Gly (1:2) (green), with a control in unmodified NB (black). Of the DESs tested, ChCl/Gly (1:2) exhibited the most pronounced effect on growth over 48 hours, followed by ChCl/U (1:2), while ChCl/LA (1:2) demonstrated inhibitory effects on growth at both concentrations.

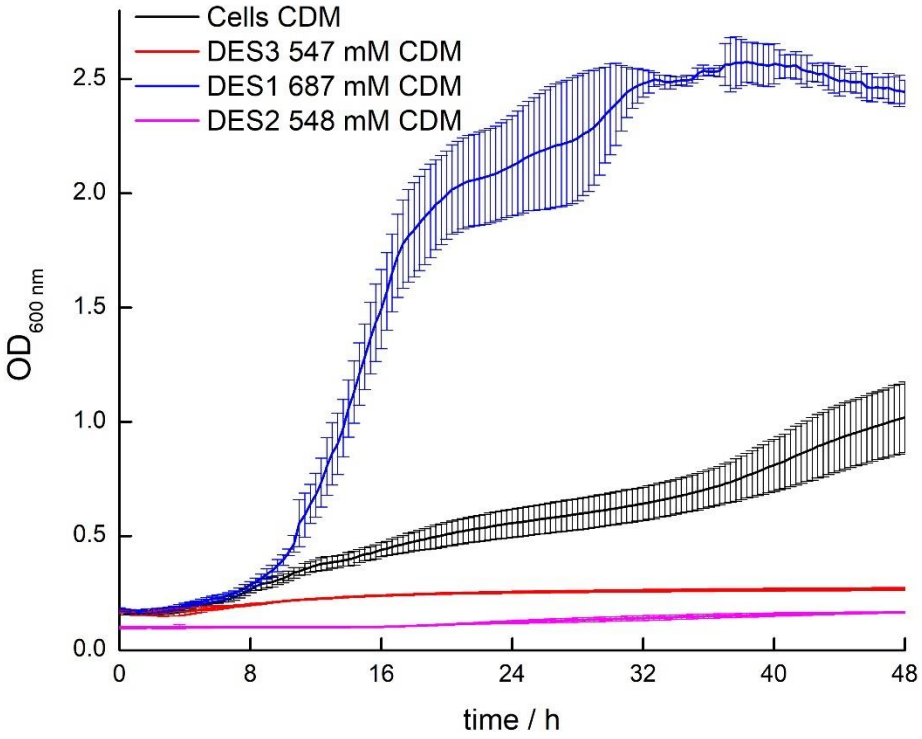

Figure 4.3 The growth curves of *B. subtilis* in a chemically defined medium (CDM) modified with the three tested DESs reveal that DES1 had the most significant impact on microbial growth.

At a concentration of 55 mM, DES3 promotes planktonic cell growth without altering its growth pattern(Figure 4.4A). However, concentrations exceeding 110 mM result in a pseudo-diauxic growth pattern, similar to the growth observed with ChCl alone (Figure 4.4 C). In contrast, Gly alone does not affect the cell growth over 48 hours or modify the growth pattern (Figure 4.4 B). Diauxic growth refers to a biphasic bacterial growth response where two distinct carbon sources, typically carbohydrates, are utilized sequentially, as indicated by the inflection point on the growth curve. (Chu and Barnes 2016). ChCl seems to function as a nutrient undergoing metabolism similar to that of amino acids. It it unlikely to be utilized as an alternative carbon source. However, earlier research has shown that bacteria may use ChCl as their only carbon source (Wargo 2013).

We hypothesize that ChCl may act as a nutritional supplement or trigger transcriptional regulators that modify carbohydrate metabolism, enhancing growth. The increase in growth was more pronounced when DES3 was present at concentrations exceeding 110 mM (Figure 4.4A). These findings suggest a synergistic interaction between ChCl and Gly, even when diluted significantly. However, additional experiments using different Gly and ChCl molar ratios, such as 1:1 or 1:3, may be required to determine the optimal medium composition. Control tests using 50 µM 2-HNQ, a standard redox mediator concentration in bioelectrochemical studies (Figure 4.4 D), had no observable impact on bacterial growth. Gly has previously been examined as a medium additive for *B. subtilis* in microbial fuel cells (Nimje et al. 2011) However, combining ChCl and Gly as bacterial media additives remains challenging. Various studies (Wen et al. 2015)(Hou et al. 2013) have shown that DESs, such as DES3 (see Table 4.1), can inhibit microbial growth in Escherichia coli and Listeria monocytogenes at high concentrations, consistent with the findings reported here. At the lower concentrations applied in this study, the impact on planktonic growth is not attributed to the solvent properties of DESs. The hydrogen-bonding structure of DES forms at concentrations above 50% w/w, which corresponds to around 4-5 M DES, depending on the specific DES used(Ferreira et al. 2021). Therefore, a DES3 concentration range of 55-547 mM was selected for bioelectrochemical experiments.

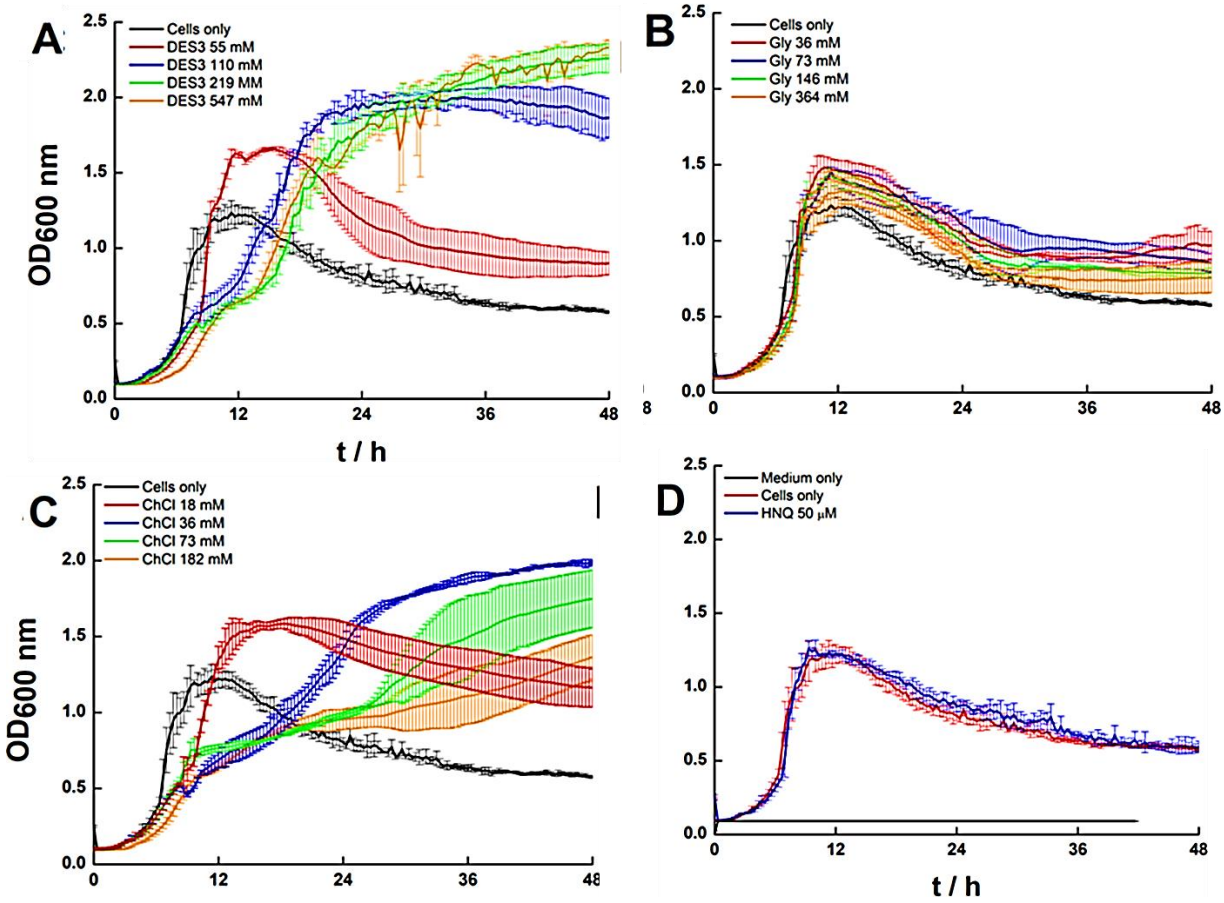

Figure 4.4 The growth behavior of B. subtilis was monitored over 48 hours at different mass concentrations of DES (A), ChCl (B), Glycerol (C). While Gly alone had little effect on growth, its combination with ChCl significantly promoted growth. Control tests conducted with 50 µM 2-HNQ demonstrated no influence on cell growth (D).

4.3.2 Biofilm analysis-crystal violet

Since electroactivity relates closely to biofilm concentration(Koch and Harnisch 2016) (Viti et al. 2014)(Paquete et al. 2022a)(Naradasu et al. 2020)After 48 hours of growth, the biofilm was quantified using crystal violet. Whereas DES3 has a negative or slightly positive effect on biofilm concentration at all investigated concentrations, ChCl at concentrations more than 36 mM considerably increases biofilm biomass, whereas Gly has a smaller effect (Figure 4.5).

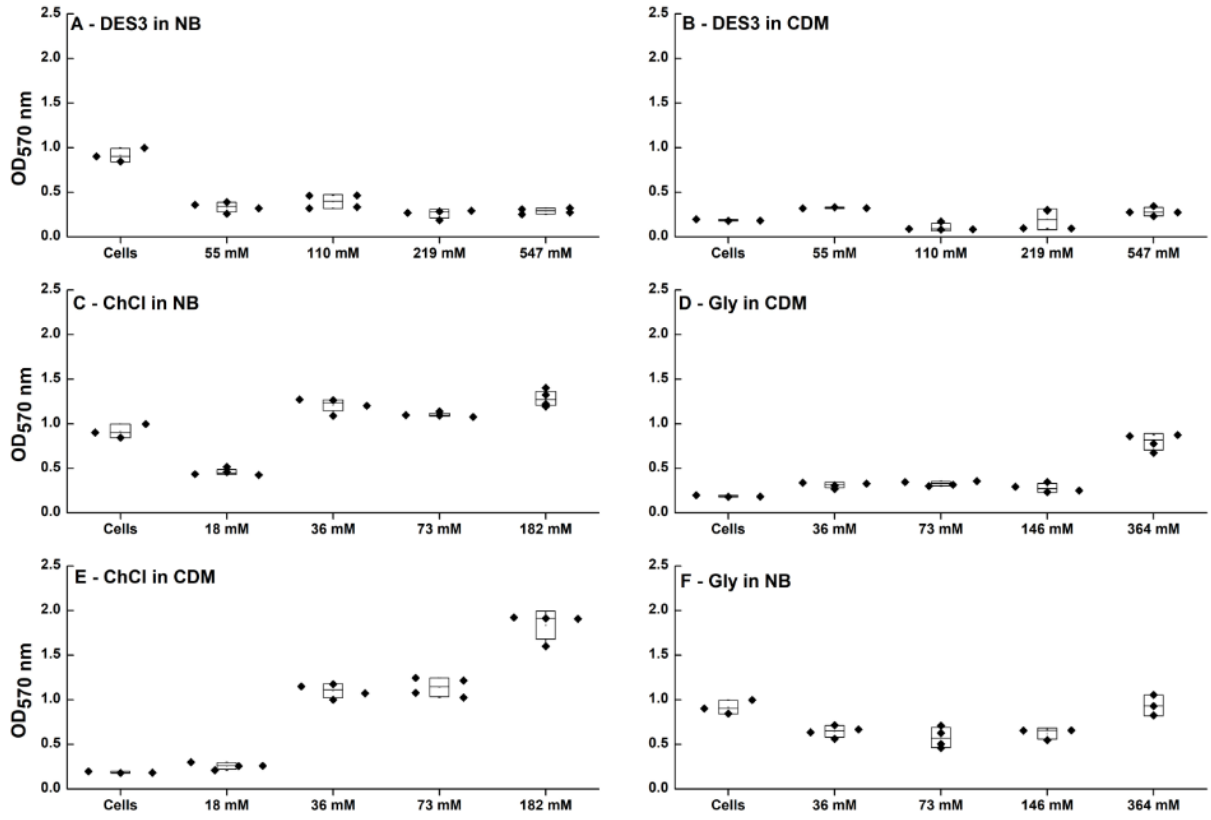

Figure 4.5 Concentration of Biofilm at varying concentrations of DES3 and DES3 components in CDM and NB nutrient mediums. ChCl elevates biofilm concentration by 50% in NB and nearly 500% in CDM.

Overall, biofilm quantification shows that ChCl increases both planktonic growth and *B. subtilis* attachment on graphite electrodes.

4.3.3 Bioelectrochemical analysis

Bioelectrochemical analysis conducted with *B. subtilis* cells at an optical density of 0.5 (OD600) cultured at 37 °C under an oxidative potential of 0.4 V (vs. Ag/AgCl) showed that the introduction of DES3 delays the onset of current but increases the peak current (Figure 4.7). The highest charge output (Figure 4.6) was observed with the addition of ChCl at concentrations of 36 and 73 mM, followed by Gly at 73 and 146 mM, and DES3 at 110 and 219 mM. The charge output produced by ChCl was notably higher than that

achieved with 50 µM of 2-HNQ, suggesting that ChCl has a distinct role in the extracellular electron transfer (EET) process. The charge output of *B. subtilis* grown in NB with DES3 and its components (Gly and ChCl) did not show a significant difference when mixed into NB without heating at equivalent concentrations (Figure 4.8). Differential pulse voltammetry (DPV) analysis of the cell-free supernatant showed prominent peaks at E = 0 V. The addition of standard menadione solutions increased in peak intensity, indicating that these peaks are likely linked to the presence of extracellular menadione (Figure 4.10). Further research is needed to elucidate the distinct roles of menadione and riboflavin in *B. subtilis* electroactivity when exposed to choline and choline-based deep eutectic solvents (DESs). In studies supplemented with 55,110, and 547 mM DES3, a significantly lower charge output of 3.73±0.74, 3.11±1.42, and 2.27±2.18 mC was reported, indicating that a bioavailable nitrogen supply is required to induce electroactivity under the challenging situations that result from the presence of Gly and ChCl. As noted earlier, adding DES at high dilutions (less than 1 M) is unlikely to result in any significant changes to the hydrogen-bonding structure of the solvents. A control experiment with pure ChCl and Gly mixed in the NB medium at the same concentration as DES3 showed no substantial difference in charge output, confirming that the solvents had minimal influence on electroactivity within the tested concentration range (Figure 4.9).

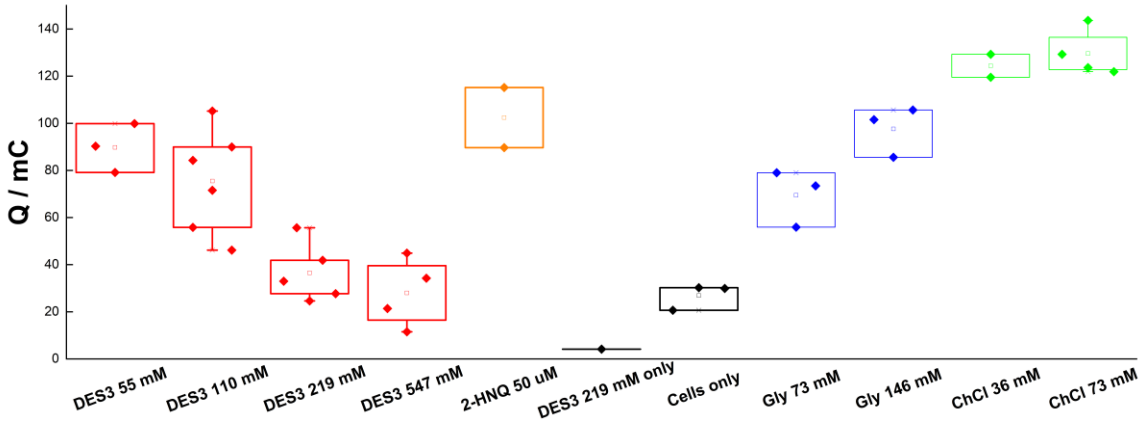

Figure 4.6 Electrochemical charge outputs of *B. subtilis* after 48 hours of cultivation in NB medium modified with DES3 and its individual components.

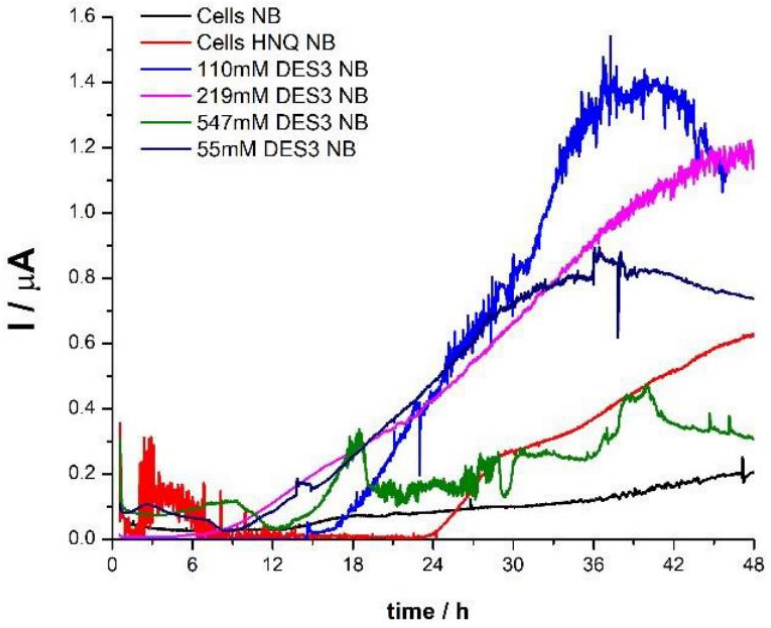

Figure 4.7 Chronoamperometric results in the presence of various concentrations of DES3 and the HNQ mediator.

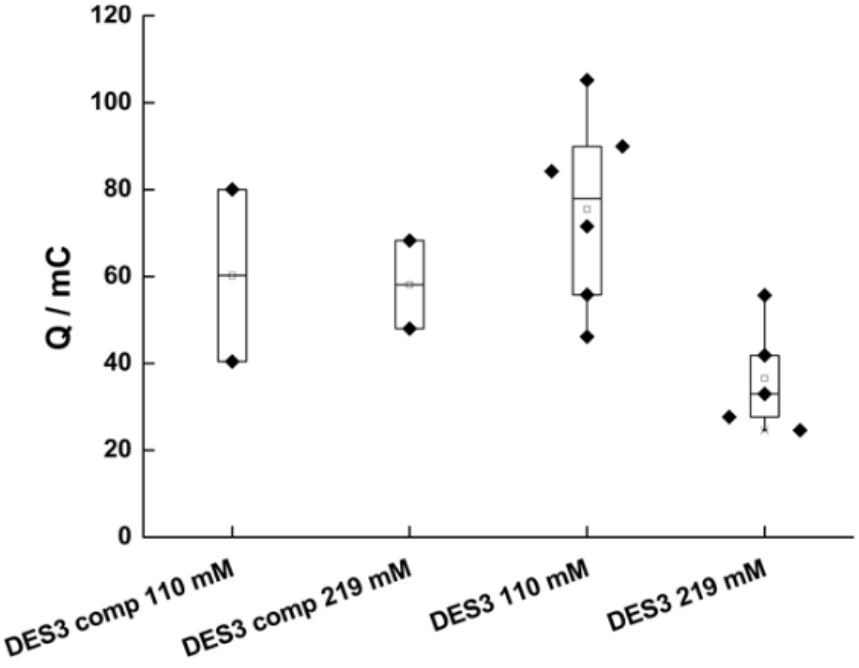

Figure 4.8 The charge output of *B. subtilis* grown in NB with DES3 and its components (Gly and ChCl) did not show a significant difference when mixed into NB without heating at equivalent concentrations.

After 48 hours of growth, differential pulse voltammetry (DPV) was employed to assess the redox-active species within the bioelectrochemical system (Figure 4.9). The analysis revealed two prominent peaks: a lower potential peak at 0.1 V, which likely corresponds to cell biomass and remained unaffected by the addition of Gly, and a higher potential peak at 0.2 V, which is probably associated with the metabolism of ChCl. Additionally, a smaller peak at -0.1 V was observed in experiments with 219 and 547 mM of DES3 (Figure 4.9), potentially indicating the toxicity of DES3 at these concentrations. This peak could be linked to partial cell lysis and the release of intracellular enzymes or other redox-active compounds. It is also possible that the low-potential peak is due to a redox mediator generated by DES3. However, chronoamperometry (CA) measurements at 0 V showed no current or charge output, suggesting that electron transfer processes were not feasible at this potential (Figure 4.11). Consequently, it can be inferred that the peak observed at -0.1 V, which appeared infrequently at 219 mM and more frequently at 547 mM DES3, likely results from partial cell lysis or cellular damage rather than indicating electron transfer at low potential. This interpretation is corroborated by the observed decrease in charge output at 219 mM, particularly at 547 mM DES3. Overall, the DPV data (Figure 4.9) indicate that while both ChCl and Gly enhance the electroactivity of *B. subtilis*, their combined effect diminishes, particularly at higher concentrations such as 547 mM. The position and intensity of the peak at 0.1 V suggest that the addition of Gly enhances electroactivity, likely due to increased cell electroactivity rather than the presence of additional redox-active species. Gly does not significantly affect biofilm biomass or planktonic cell concentration. Therefore, Gly appears to enhance the electroactivity of *B. subtilis* cells specifically. Conversely, the increase in electroactivity with ChCl addition results from a combination of planktonic and biofilm growth as well as specific electroactivity, as indicated by the peak at 0.2 V. This peak is similar to that observed with 2-HNQ, suggesting the formation of quinone or hydroquinone during the metabolism of ChCl and Gly.

The electrochemical signature of the supernatant is radically different from that of the biofilm (Figure 4.10). No peak was observed at a potential higher than 0 V, indicating that the EET process is due to redox active species in the biofilm and not in the supernatant.

Initial experiments were carried out to identify the redox-active species in the supernatant. The addition of 10 µM menadione (2-Methyl-1,4-naphthoquinone) to cell-free supernatant increased the baseline current and the main peak height in DES3 219 mM. However, the peak potential shifts to a more negative value (Table 4.2). Thus, it cannot be concluded that menadione is responsible for increased EET in *B. subtilis* added with a small concentration of DES3. However, further research is needed to determine the nature of the hypothesized redox mediator(s). Selected DPV curves of supernatants after 48 h of growth at 0.4 V vs. Ag. Also presented in Appendix 4.5:

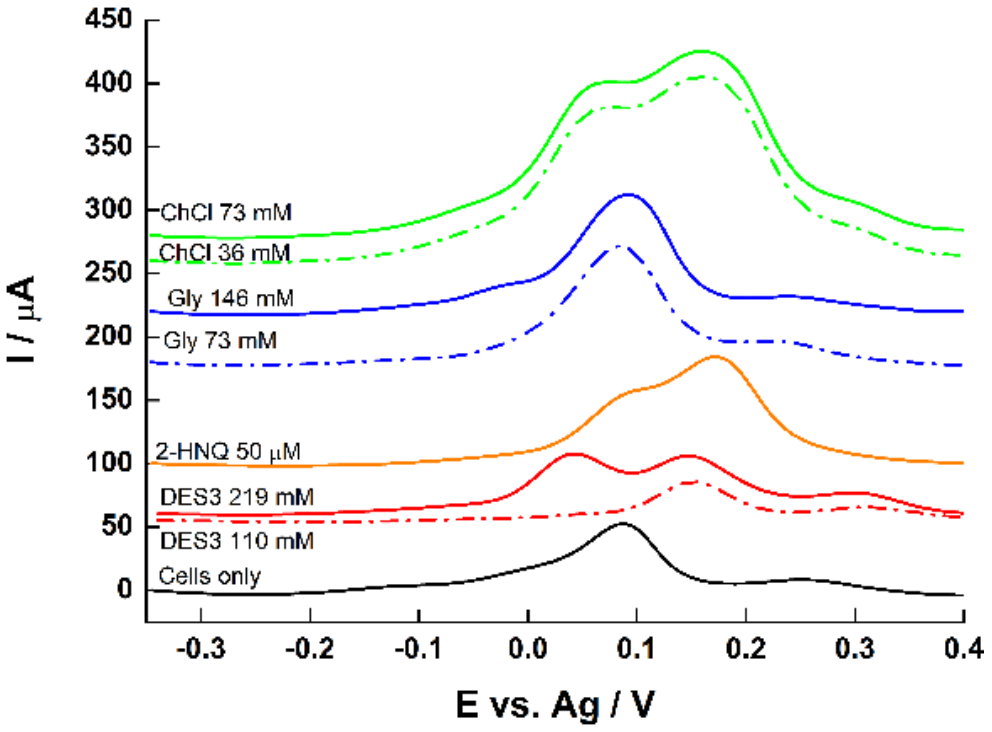

Figure 4.9 presents Representative differential pulse voltammetry (DPV) curves of B. subtilis after 48 hours of growth at 0.4 V. The curves have been adjusted for clarity and readability

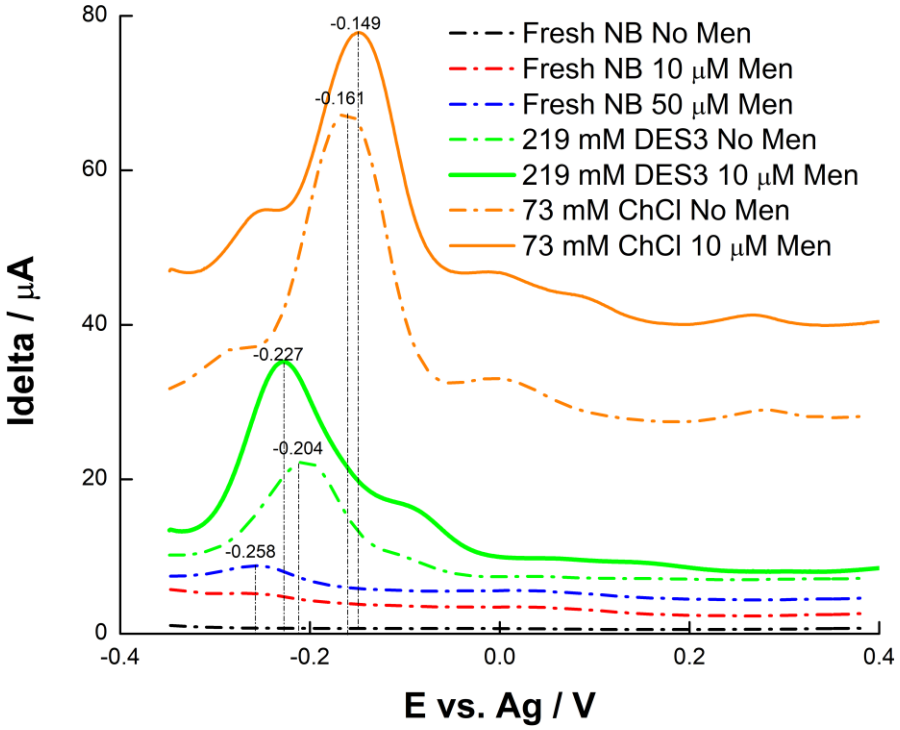

Figure 4.10 Selected DPV curves of supernatants after 48 h of growth at 0.4 V vs. Ag. Baselines are translated along the y-axis to increase readability.

Table 4.2: Potential and height of the main peak in the cell-free supernatant.

Menadione (µM)	**DES3 219 mM**		**ChCl 73 mM**	
	Peak potential (V)	Peak height (µA)	Peak potential (V)	Peak height (µA)
0	-0.204	13.3	-0.161	35.2
10	-0.227	23.0	-0.149	31.1

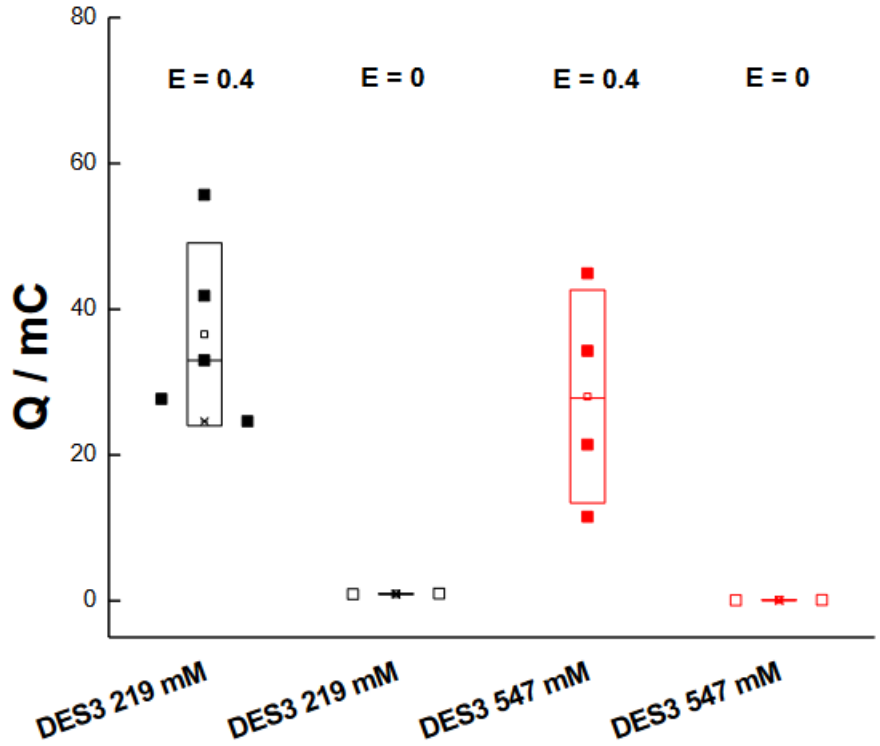

Figure 4.11 Charge output from *B. subtilis* cultured in DES3 and NB was measured on electrodes maintained at 0.4 V and 0 V over 48 hours. Negligible charge output was observed at 0 V.

4.3.4 HPLC analysis

The cell-free supernatant was characterized through HPLC (Figure 4.12, Figure 4.13). A peak near the elution time of standard riboflavin was detected in the supernatant of *B. subtilis* grown with 219 mM DES (Figure 4.12), and a peak near the elution time of standard menadione was detected in the supernatant of *B. subtilis* grown with 36 mM ChCl (Figure 4.13). Results confirmed the presence of these components in the cell-free supernatant, most likely secreted by *B. subtilis*. The retention time for riboflavin and menadione was 3.5 and 10.75 minutes, respectively. While this preliminary characterization shows the presence of putative redox mediators in the cell-free

supernatant, it is unclear whether these redox mediators contribute to the increased current output observed in the DES3-amended and ChCl-amended NB growth medium of *B. subtilis*.

In general, HPLC analysis confirmed that Menadione and riboflavin were found in the cell-free supernatant of *B. subtilis* cultured for 48 hours in electrochemical cells with 36 mM ChCl and 219 mM DES3 (Figure 4.12, 4.13). Appendix 4.6 also shows the Menadione peak in the sample containing 36mM ChCl

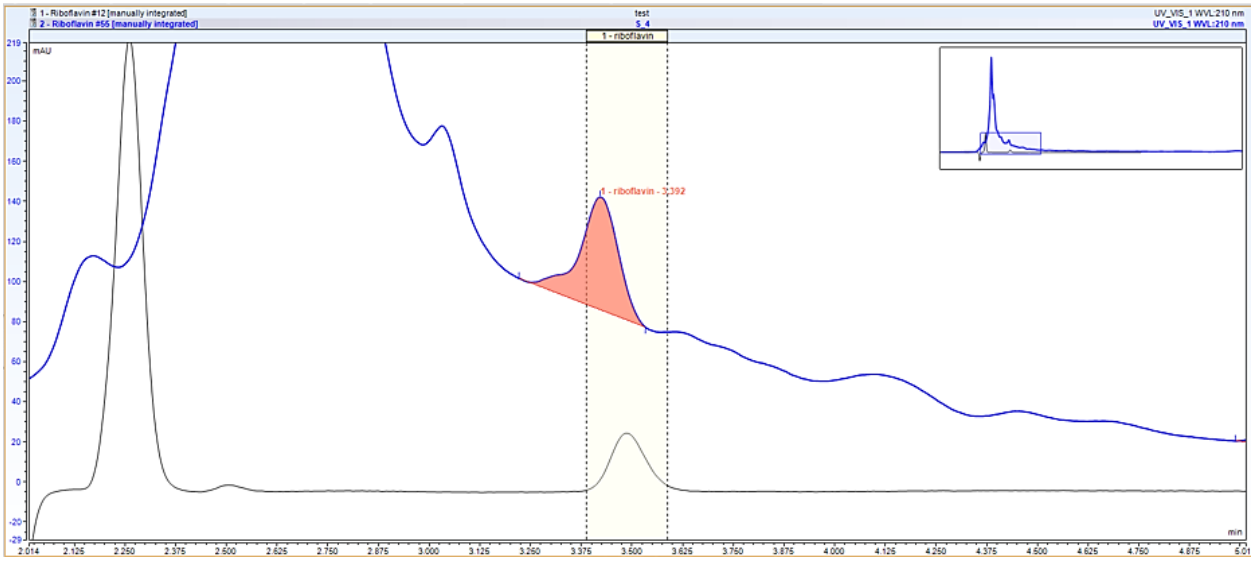

Figure 4.12 Riboflavin peak detection in the sample with 219 mM DES3 (blue trace). The black trace represents a standard riboflavin sample solution with 183 µM concentration.

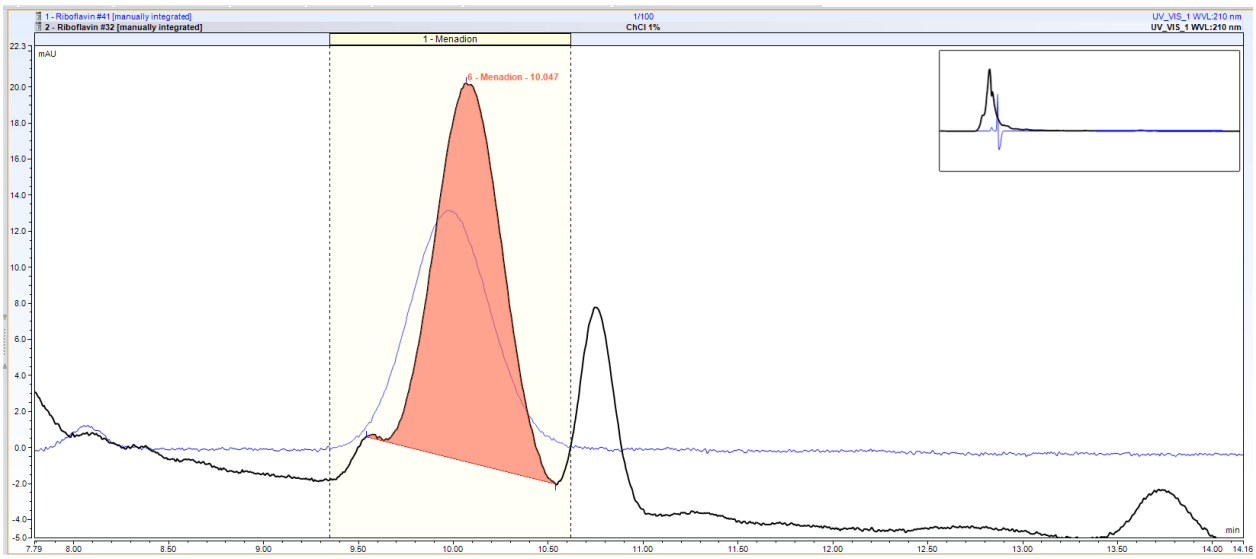

Figure 4.13 Menadione peak detection in the sample with 36 mM ChCl (blue trace). The black trace represents a standard menadione sample solution with a 55µm concentration.

4.4 Discussion

Regarding DES growth, Gly might be used as a supplementary carbon source by bacterial cells in a booster or diauxic mode, particularly at the outset of nutrient depletion in the NB medium(Martínez-Gómez et al. 2012). However, this may not be the primary cause of the unusual growth pattern, as Gly alone did not display the pseudo-diauxic impact on *B. subtilis* development.

The growth trend observed in DES3 (110-219 mM) exhibited an initial exponential increase in biomass for 7-12 hours, followed by a pseudo-diauxic transition to a brief lag phase, which extended the logarithmic growth phase and led to overall enhanced growth (Figure 4.4A). The accumulation of Gly within bacterial cells is concentration-dependent, with concentrations exceeding 0.05 mM potentially inducing bacteriostatic effects due to intracellular saturation(Schlievert et al. 1992). The high cell growth over time suggests a synergistic effect of the two DES3 components (Gly and ChCl).

The medium's osmolarity drops as the media's nutrients are consumed. This could increase turgor pressure on bacterial cells, limiting cell reproduction and possibly increasing cell death. Bacteria have devised several strategies to manage osmolarity and avoid osmotic shock (Rojas, Theriot, and Huang 2014). Bacteria may balance osmolarity by synthesizing

compatible solutes such as proline and glycine betaine, which operate as fine osmo regulators(Kempf and Bremer 1998)(Cesar et al. 2020).

ChCl serves as a precursor to glycine betaine, which B. subtilis uses to regulate cytoplasmic osmolarity(Kappes et al. 1999). As the nutrients in NB become depleted, extracellular osmolarity increases, leading to reduced growth of *B. subtilis* and necessitating an intracellular osmoregulatory response for survival. Gly acts both as a humectant and as a carbon source. Its humectant properties help retain water within cells, preventing dehydration. As a carbon source, Gly is taken up by the cell via facilitated diffusion. However, its utilization is inhibited in the presence of more preferred carbon sources, such as glucose, due to the action of the phosphoenolpyruvate phosphotransferase system (Deutscher, Francke, and Postma 2006).

Depleting primary nutrients in the medium leads to a gradual increase in cell density and the utilization of Gly as a secondary carbon source, converted into metabolic products to facilitate ATP production. (Murarka et al. 2008).

The ATP produced through this mechanism may be used by specific ATP-binding cassette (ABC) transporters to facilitate the uptake of choline into the cytoplasm, thus maintaining cellular osmolarity (Kappes et al. 1999). For extracellular electron transfer (EET), *B. subtilis* utilizes cytochromes and the NAD^+/NADH pathway. (L. Chen et al. 2019). Participation of Flavians as a redox mediator has been hypothesized (Higashitsuji et al. 2007). The ability of DESs to alter membranes or boost mediator-based electroactivity has yet to be investigated.

Differential pulse voltammetry (DPV) results indicate the involvement of metabolites from ChCl degradation in extracellular electron transfer (EET), while Gly enhances the specific electroactivity of Bacillus subtilis biofilms. This observation aligns with previous studies that demonstrated improved EET in the presence of low concentrations of Gly. (Nimje et al. 2011). However, the influence of ChCl on biofilm electroactivity has not been investigated previously.

Glycine betaine is a choline metabolite that can raise the concentration and activity of cytochrome oxidase, particularly under stress circumstances (Lee 2021), resulting in

increased electroactivity. glycine betaine acts as an osmoprotectant and modulates membrane ionic flow in B. subtilis(Cesar et al. 2020). This might explain the observed electroactivity.

Nicotinamide Adenine Dinucleotide (NAD)(Chini, Tarragó, and Chini 2017) is a signaling molecule for EET in *B. subtilis*, whereas acetylcholine(Stanaszek, Snell, and O'Neill 1977)(Yamada et al. 2005) is thought to have a similar role in other species. These signaling molecules can be generated extracellularly through choline metabolization. However, further research is required to verify this strategy. The observed increase in charge production is most likely due to variations in EET as *B. subtilis* biofilms adjust to osmotic shifts in the environment.

4.5 Conclusion

At low concentrations (55 mM), the DES combination choline chloride/glycerol (1:2 mol mol^{-1}) promoted planktonic growth of *B. subtilis* in NB without affecting its pattern; at higher concentrations (>110 mM), a pseudo-diauxic growth is observed.

These findings were consistent with choline chloride metabolization when added alone at 18 and 36mM, respectively. Glycerol alone did not affect cell development over 48 hours or influence the growth curve's shape. The growth curves showed a switching point when DES and choline chloride were introduced as secondary carbon sources to the system. This supports the idea that choline chloride might operate as a substitute nutrient or stimulate the transcription of cell growth regulators.

The DES mixture of choline chloride/glycerol (1:2 mol mol^{-1}) had little impact on biofilm concentration, whereas the independent addition of choline chloride at concentrations >36 mM significantly enhanced biofilm biomass.

Also, glycerol had little influence on biofilm biomass in NB but enhanced it at concentrations of more than 364 mM in CDM. Overall, choline chloride promotes both growth and attachment of *B. subtilis* under the tested electrochemical conditions.

The charge output data demonstrate that *B. subtilis* electroactivity increases in the presence of the DES mixture choline chloride/glycerol (1:2 mol mol^{-1}) in the concentration range

55-547mM. The highest charge output was reported when choline chloride was added at 36 and 73 mM.

After adding choline chloride, the charge output was much larger than that of 2-HNQ, indicating that ChCl plays a unique role in the EET process.

In summary, DESs like choline chloride/glycerol (1:2 mol mol^{-1}) can be introduced into growth media at non-toxic levels to enhance the electroactivity of the weak electricigen *B. subtilis*.

Although the observed impact is attributed to the components of DES rather than their solvent characteristics, non-toxic DES formulations could likely be employed at higher concentrations to enhance extracellular electron transfer (EET) between biofilms and electrodes.

Chapter 5. Osmoregulation by Choline-based deep Eutectic Solve (DES) induces electroactivity in *Bacillus subtilis* biofilms

This chapter is adapted from my following research paper:

Eghtesadi, N., Olaifa, K., Pham, T. T., Capriati, V., Ajunwa, O. M., & Marsili, E. (2024). Osmoregulation by choline-based deep eutectic solvent induces electroactivity in Bacillus subtilis biofilms. Enzyme and Microbial Technology, 180, 110485. **(Scopus Percentile: 79%, Q1)**

https://doi.org/10.1016/j.enzmictec.2024.110485

The previous chapter demonstrated that incorporating compatible solute precursors, such as choline chloride (ChCl), into the growth medium enhances current output and biofilm formation in Bacillus subtilis. In this study, a low-carbon tryptone-yeast extract medium supplemented with salts was used to subject B. subtilis to salt stress and investigate the osmoregulatory and nutritional effects of a D-sorbitol/choline chloride (ChCl) (1:1 mol mol^{-1}) deep eutectic solvent on biofilm electroactivity. The results indicate that the presence of ChCl and D-sorbitol alleviates osmotic stress caused by NaH_2PO_4 and KH_2PO_4 salts while significantly promoting biofilm production. This is likely attributed to ChCl's osmoprotective function, as it serves as a precursor to the osmoprotectant glycine betaine, and its role in stimulating the production of electroactive exopolymeric substances within the *B. subtilis* biofilm. Given that high ionic strength media are frequently utilized in microbial biotechnology, the combination of ChCl-containing deep eutectic solvents with salt stress could enhance biofilm-based electrofermentation processes, offering significant advantages for biotechnological applications.

5.1 Introduction

Extracellular electron transfer (EET) refers to the transfer of electrons between microorganisms and an externally charged surface or material. Electroactive substances can serve as electron acceptors or donors for metabolic processes affecting the transport of nutrients and other molecules across the bacterial cell membrane. Electron transfer pathways can occur via (i) a direct pathway, which involves utilizing protein structures that

are attached to the surface, such as bacterial nanowires, pili, filaments, and multiheme cytochromes, or (ii) an indirect pathway, which involves the use of redox mediators that can either be soluble or membrane-bound. Weak electricians are likely more adapted to the use of soluble electron acceptors(Kato 2016)(T. H. Lan et al. 2018)(Chai et al. 2018)(Sasaki et al. 2014).

Microbial Electrochemical Technology (MET) is one of the areas that uses electricigens for energy recovery and bioelectrosynthesis(Rabaey et al. 2009)(Schröder et al. 2015). MET aims to manipulate the metabolism of electricigens by applying electrochemical potential or current at electrodes that serve as electron acceptors or donors, thereby increasing the production of platform chemicals(Rabaey and Rozendal 2010), active pharmaceutical(Cantillo 2022) ingredients, and biopolymers(Bajracharya et al. 2016).

Bacillus subtilis is a Gram-positive spore-forming bacterium with versatile and adaptable bioprocess applications due to its ability to produce industrial interests, including extracellular enzymes, proteins, and secondary metabolites. The unique features of *B. subtilis,* such as the ability to grow in harsh environments and its well-developed protein secretion system potential for secreting large amounts of proteins such as enzymes and antimicrobial peptides, make it an attractive host for biotechnological applications like drug discovery, food processing, agricultural and pharmaceutical production(Duanis-Assaf, Steinberg, and Shemesh 2020)(L. Chen et al. 2019).

Recent investigations on potentiostat-controlled electrochemical cells have revealed that B. *subtilis* has weak electricigen characteristics, producing just a small current when exposed to oxidizing potential(L. Chen et al. 2019)(Doyle and Marsili 2018a). *B. subtilis* can also secrete outer membrane cytochromes (Omc) and membrane-bound flavins, known as redox-active molecules in EET mechanisms(Bruce E. Logan et al. 2019b)(Yin et al. 2019).

The growth of *B. subtilis* at set electrochemical potential can affect the metabolic activity of *B. subtilis* and increase the yield of high-value metabolites, such as alkaline proteases, biopolymers, biosurfactants, and antimicrobial peptides under electrofermentative conditions(Eric M Conners et al. 2022)(Gu et al. 2018)(Su et al. 2020). However, a close interaction between the microorganisms and the electrodes is required to boost the EET

rate and get an effective MET process(Xiao and Zhao 2017). For this purpose, the immobilized microorganisms should be used(Viti et al. 2014). Cells can be immobilized using a coating incorporating living microorganisms in a biocompatible, conductive polymeric matrix(Mehrotra et al. 2021).

By Immobilization, it is possible to control the concentration of microorganisms and coating thickness. (Berillo, Al-Jwaid, and Caplin 2021). However, it requires careful optimization and is susceptible to the biodegradation of the polymer(Flemming et al. 2016), which leads to lower activity and mechanical detachment of the coating(Sultana, Babauta, and Beyenal 2015).

Biofilm production is an inherent process that could be facilitated by adjusting the medium composition, nutrient content, and temperature. However, because biofilms are complex and dynamic systems, achieving consistent coating thickness and function over time is challenging(Angelini et al. 2009)(Nguyen et al. 2020).

Biofilms are aggregations of microorganisms that adhere to a surface and are enveloped within a self-produced matrix (EPS). Extracellular polymeric Substances (EPS), the main component of biofilm structure, play a pivotal role in the extracellular electroactivity mechanism. (Fathollahi and Coupe 2021)The EPS layer, as a main product of bioelectrochemical systems, is not only a shielding for the cells from the surrounding environment, which serves carbon and energy sources for biofilm, but also many components of the EPS matrix, such as polysaccharides, proteins, nucleic acids, and lipids, are redox active or electrochemically active and could possess semiconductive properties that facilitate the transfer of solutes in the defined extracellular, and stabilize protein complexes which may act as electron conduits through the biofilm (Kostakioti, Hadjifrangiskou, and Hultgren 2013)(Xie et al. 2023)(Isaac et al. 2017)(Luo et al. 2015).

Biofilms are exposed to local-scale dispersal in the presence of specific physicochemical stress or under flow conditions and in continuous processes(Kostakioti et al. 2013)(Angelini et al. 2009).

Several studies have determined the effect of contaminants and pollution, such as heavy metals (Fathollahi and Coupe 2021) and organic compounds at sub-inhibitory

concentrations, on biofilm development and dispersal (Zhou et al. 2022)(Tuck et al. 2021). In electro-fermentation (EF) procedures, stimulating biofilm formation is predicted to boost EET and, as a result, enhance the rate of biosynthesis of high-added value compounds(Eghtesadi et al. 2022). EET rate has been enhanced through several strategies, including physical and chemical pretreatment of the inoculum source, amendment of the growth medium with specific nutrients, media optimization, and biofilm engineering(Luo et al. 2015)(S. Chen et al. 2019)(Chiranjeevi and Patil 2020). EET rate can also be improved by increasing the conductivity of the growth medium, for example, by adding salts. Salts, on the other hand, can influence the membrane potential of microorganisms and decrease metabolic activity(Rath et al. 2016). Therefore, novel media formulations that protect biofilms from osmotic stress are worth investigating.

Deep eutectic solvents (DESs) are a new emerging class of solvents comprised of a mixture of hydrogen bond acceptors (HBAs) and hydrogen bond donors (HBDs). Many DES compositions with various applications are available due to their feasibility for customized design(Abbasi et al. 2022)(Pandey et al. 2017). DESs are broadly substituted by toxic and volatile organic compounds (VOCs) in many biotechnological and biomedical processes(Pandey et al. 2017), such as photosynthesis reactions and bioelectrochemistry(Belviso et al. 2021). Besides several other characteristics, high biodegradability, non-toxicity, low cost, low volatility, and eco-friendliness make them an attractive candidate to replace them with conventional ionic solvents(Hansen et al. 2021)(Mbous et al. 2016).

The ability of choline chloride: glycerol (1:2 mol mol^{-1}) DES composition to boost the electroactive performance of *B. Subtilis* biofilms was studied in our previous work(Eghtesadi et al. 2022). The DES mixture was found to increase the planktonic growth, biofilm formation, and electroactivity of the *B. subtilis* at specific concentrations. The increase in planktonic growth was most likely due to the nutritional effect of Choline Chloride (ChCl) as a substitute carbon source. Biofilm biomass enhancement was most likely due to ChCl being a precursor of glycine betaine(Boch et al. 1996)(Kapfhammer et al. 2005). This compatible osmolyte likely plays an essential role in osmoregulation and

also seems to enhance the electroactivity through ionic flow and induce transmembrane potential(Wargo 2013)(Venkova et al. 2017)(Kay 2017).

Environmental salinity is an effective parameter in biofilm development. Under salt-stress situations, EPS production may be boosted as a protective strategy for bacterial cells, helping them to survive osmotic stress(Yin et al. 2019)(Gregory and Boyd 2021). Glycine betaine synthesis is one the initial responses of *B. subtilis* to osmotic stress. In high salinity conditions, synthesizing glycine betaine osmoprotectant might control the ionic membrane flow of B. *subtilis* and boost its cytochrome oxidase activity, resulting in enhanced electroactivity(Lee 2021)(Wargo 2013)(Bremer and Krämer 2019)(Strøm 1998).

In the current study, planktonic growth, biofilm formation, and the improvement in electroactive performance were studied in the presence of a deep eutectic mixture (DES) of D-sorbitol/ChCl (1:1 mol mol^{-1}) and its components) at non-toxic concentrations.

It was found that the presence of DES as a mixture and its components could enhance biofilm formation. EPS, as the main structure of the biofilm in *B. subtilis,* is capable of producing membrane-bound cytochrome- c and flavin and facilitating and boosting the extracellular Electron Transfer process (EET)(Li et al. 2016)(Olar, Badea, and Chifiriuc 2022)(Epstein 2003). This, in turn, could enhance the electroactivity of the *B. subtilis.*

To find the optimum condition for electroactivity enhancement, planktonic growth, and biofilm formation were studied in the presence of two selected salts at low concentrations (less than 5%) and Glycine betaine as an osmoprotectant that *B. subtilis* could synthesize in the presence of ChCl. Salinity conditions up to a certain level could enhance biofilm formation to protect the cell from the lysis. Redox-active components of EPS structure in the biofilm could enhance the electroactivity. Also, adding glycine betaine to the system or its synthesis in the presence of ChCl in the environment could regulate the ionic exchange activity of the membrane and enhance the electroactivity of the *B. subtilis.* Results confirmed that the direct addition of Glycine betaine to electroactivity enhancement is higher than when it is synthesized due to its precursor ChCl.

5.2 Materials and Methods

5.2.1 Materials

A chemically defined Tryptone-Yeast (TY) medium (Tryptone 20 g/L, Yeast extract 6.7 g/L) with a pH adjusted to 6.5 was employed as a nutrient medium. This medium was then modified with a biocompatible deep eutectic solvent (D-sorbitol/ChCl (1:1 mol/mol)), its components (choline chloride (ChCl) and D-sorbitol), two inorganic salts (NaH_2PO_4 and KH_2PO_4), and a compatible solute (anhydrous betaine ($(CH_3)_3NCH_2CO_2$)). All media were prepared using deionized water and sterilized at 121 °C and 104 kPa for 20 minutes.

The chemicals used were of analytical grade and sourced from Sigma Aldrich and Thermo Fisher Scientific, Kazakhstan, following the manufacturers' guidelines. *B. subtilis* ATCC 6051 was sub-cultured and maintained on TY medium at 37 °C throughout the experiments. Electrochemical studies employed Screen-Printed Carbon Electrodes (SPE) with a 4 mm diameter graphite working electrode (WE), graphite counter electrodes (CE), and Ag pseudo-reference electrodes (Metrohm-Dropsens SPE Ref. C110). All electrochemical potentials are reported relative to the Ag pseudo-reference electrodes. The electrochemical experiments were conducted in 10 mL methacrylate cells with an 8 mL working volume.

5.2.2 Bacterial growth curves

The growth curves of Bacillus subtilis at varying concentrations of choline chloride (ChCl), D-sorbitol, their eutectic mixture (DES), and their simple combination in response to different concentrations of monosodium phosphate (NaH_2PO_4) and monopotassium phosphate (KH_2PO_4) salts in TY medium, were measured using 48-well flat-bottom plates and analyzed with a Gen5™ Microplate Reader and Imager Software (BioTek Instruments).

Absorbance was measured at 570 nm (OD_{570}), and experiments were performed in three dependent biological replicates, with results presented as the mean ± standard deviation (SD). The concentrations of ChCl, D-sorbitol, and their eutectic mixture varied from 5 mM to 6210 mM. The components were dissolved in the prepared TY medium for each

experiment and then sterilized using a 0.2 μm filter. Each well in the 48-well plate was filled with 1 mL of the solution. The incubation temperature and time were 37 °C and 48 h, respectively. For inoculum, 10 mL of fresh overnight culture were grown in 50 mL volume sterilized tubes with caps closed for 16 h at 37 °C, under constant agitation (180 rpm), and the resulting bacterial suspension was used as inoculum. The wells were inoculated with OD_{570} = 0.1, which was earlier determined to be approximately 10^6 colonies forming units (CFU) per mL. Four dependent biological replicates (i.e., four wells) were analyzed for each experimental condition

5.2.3 Biofilm assay

The crystal violet assay was employed for semi-quantitative biofilm detection formed in the microtiter plate wells at the end of the growth curve determination described in Section 3.3.

Following the 48-hour incubation period, the wells were gently emptied of unattached cells and media, and the microtiter plates were air-dried for 15-20 minutes at room temperature. Next, 1000 μL of 0.1% crystal violet solution (Crystal Violet, ACROS organics) was added to each well, and the plates were incubated at room temperature for 15 min. Next, 1000 μL of 33% acetic acid in water was added to each microtiter plate well and incubated at room temperature for 10-15 minutes to solubilize the biofilm-bound crystal violet dye. Subsequently, the solubilized crystal violet was transferred to a new microtiter plate, and the OD_{570} was measured using a Gen5TM Microplate Reader and Imager Software (BioTek Instruments). Four dependent biological replicates (i.e., four wells) were analyzed for each experimental condition.

5.2.4 Microscopy analysis

At the conclusion of the experiment, biofilms formed on selected screen-printed electrodes (SPEs) were visualized using an Axio Zoom.V16 microscope (Carl Zeiss). After 48 hours, the electrodes were extracted from the electrochemical cells and immersed in a 0.1% (w/v) crystal violet solution for 1 hour. The SPEs were then rinsed by immersing in deionized water to remove excess stains and allowed to air dry. The stained biofilms were examined

under 25x magnification, and the biofilm coverage on the SPE surface was quantitatively analyzed using MATLAB code developed by our research team.

5.2.5 HPLC analyses (Riboflavin detection in the supernatant)

The riboflavin concentration in the supernatant was collected immediately after bioelectrochemical experiments. Cell-free supernatants were collected, sterile filtered, and subsequently injected into the HPLC system (Accela 600, Thermo Scientific, USA). All the preparation steps and equipment settings were identical to those described in Chapter Four (section 4.2). The riboflavin concentration was then quantified from the peak at 3.7 min. Four independent biological replicates (i.e., four electrochemical cells) were analyzed for each experimental condition.

5.2.6 Determination of riboflavin in the supernatant using UV-vis spectrophotometry

After electrochemical experiments, the riboflavin concentration in the supernatant was determined through UV-visible spectrophotometry. The supernatants were collected and centrifuged in ultra-clear tubes at 20000 rpm for 30 min at 4 °C. The samples were then filtered using sterile 0.22 μm filters to obtain cell-free supernatant. The absorbance of the collected sample was then measured at 440 nm sing SmartSpec™ 3000 Spectrophotometer (Bio-Rad Laboratory automated Multiscan EX reader Lab systems)(Chu et al. 2022)(Bartzatt and Wol 2014). Four dependent biological replicates (i.e., four electrochemical cells) were analyzed for each experimental condition.

5.2.7 Bioelectrochemical analysis

In all electrochemical experiments, screen-printed carbon electrodes (SPEs) with a 4 mm diameter and a 0.126 cm^2 carbon working electrode (WE), carbon counter electrode (CE), and Ag pseudo-reference electrode (Metrohm-Dropsens SPE Ref. C110) were employed. All reported potentials are relative to the Ag/AgCl pseudo-reference electrode. The electrochemical experiments utilized 10 mL polymethacrylate electrochemical cells with a working volume of 8 mL. Chronoamperometry (CA) and differential pulse voltammetry

(DPV) were conducted sequentially to investigate the electrochemical activity of Bacillus subtilis in the presence of the chemicals outlined in Section 2.1, using a VSP multichannel potentiostat (Bio-Logic, France). Prior to each experiment, the SPEs were surface-sterilized with 70% (v/v) ethanol, rinsed twice with sterile deionized water, and air-dried in a sterile Petri dish within a fume hood. The electrochemical cells were maintained at 37 °C using a dry steel bead bath throughout the experiments.

For the CA, the WE were set at 0.4 V for 48 h. For DPV, parameters were set as follows: Ei = - 0.4 V and Ef = 0.4 V, pulse height 50 mV, and pulse time 200 ms. Each experiment's cumulative charge output (mC) was also calculated by integrating the current output with time using EC Lab® software (Biologic, France).

5.2.8 Statistical Data Analysis

The statistical significance of biofilm formation for each treatment (n=4) under varying experimental conditions was assessed using one-way ANOVA, followed by Tukey's post hoc test. Prior to conducting the post hoc analysis, the normality of the data distribution was evaluated using the Prism Normality and Lognormality test. Results were expressed as mean values ± standard deviation (SD), and all statistical analyses were conducted at a significance level of 0.05. Data analysis was performed using Prism and Origin 8.5 software.

5.3 Results

5.3.1 Planktonic Growth Results

The addition of D-sorbitol/ChCl (1:1 mol mol^{-1}) DES in the range of 20-200 mM increased maximum growth and prolonged the growth phase of planktonic cells. The effect was not considerable. At lower concentrations (< 20 mM), while at higher concentrations (>200 mM), the DES has a toxic impact on planktonic growth (**Figure 5.1)**

B. subtilis rapidly metabolizes sorbitol with the help of sorbitol dehydrogenase (SDH), which transforms sorbitol to fructose in cellular metabolism by utilizing NAD^+ as a coenzyme. As DES comprises both a carbon source (D-sorbitol) and an Osmo protective

agent precursor (ChCl) (Brill et al. 2011), experiments were conducted with the separate DES components at the same quantities to deconvolute their influence on planktonic development **(Figure 5.2** and **5.3)**. The addition of ChCl to the TY medium slightly boosted maximum growth and delayed the death phase **(Figure 5.2)**.

Tryptone is a nutrient source lacking in carbohydrates, and introducing ChCl or ChCl-containing compounds into the medium could help compensate this deficiency while promoting carbohydrate metabolism.(Eghtesadi et al. 2022).

This subsequently promotes additional growth. Interestingly, there was little to no difference in the maximum OD570 at all concentrations tested up to 200 mM. However, at ChCl concentrations of 200 mM and higher, a prolonged stationary phase and a decrease in maximum OD_{570} were observed. The impact of D-sorbitol was minimal at concentrations below 200 mM.At higher concentrations, the maximum OD_{570} declined without significantly affecting the exponential phase of the growth curve. (**Figure 5.3**).

The addition of D-sorbitol and ChCl in the same proportions (**Figure 5.4**) did not substantially boost the growth rate or maximum growth compared to DES. These results support a synergistic impact of the components in the form of DES.

When using whole cells of Arthrobacter simplex, the ChCl-urea DES displayed a similar effect on bacterial viability, membrane integrity, retention of metabolic activity, and the efficiency of 1,2-dehydrogenation of cortisone acetate.(Mao et al. 2018) Figure 5.1 includes only the selected concentration for clarity. See Appendix 5.1 (a to d) for all the concentrations tested.

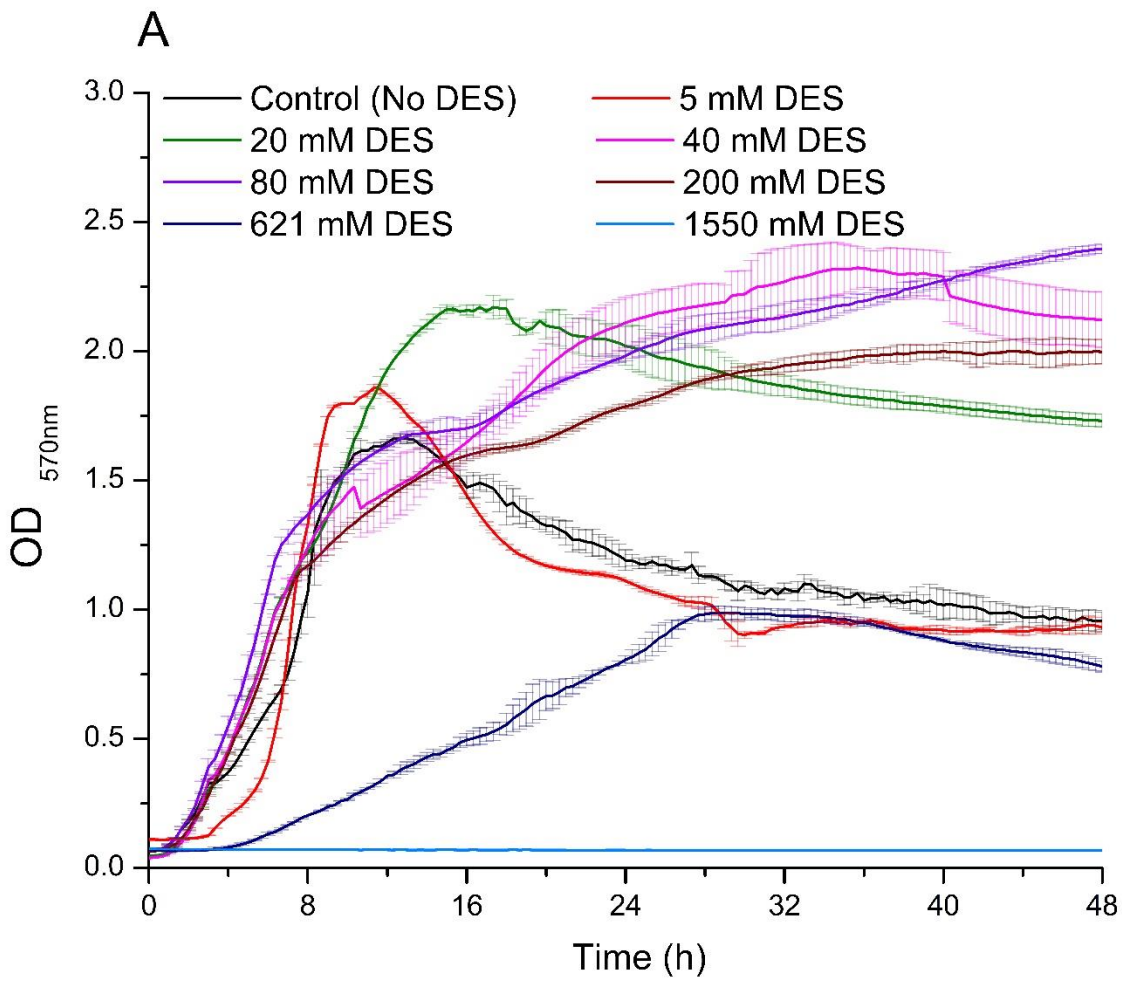

Figure 5.1 *B. subtilis* Planktonic growth was monitored over 48 hours at varying molar concentrations of the DES composed of D-sorbitol and ChCl (1:1 mol/mol).. Number of independent biological replicates = 4.

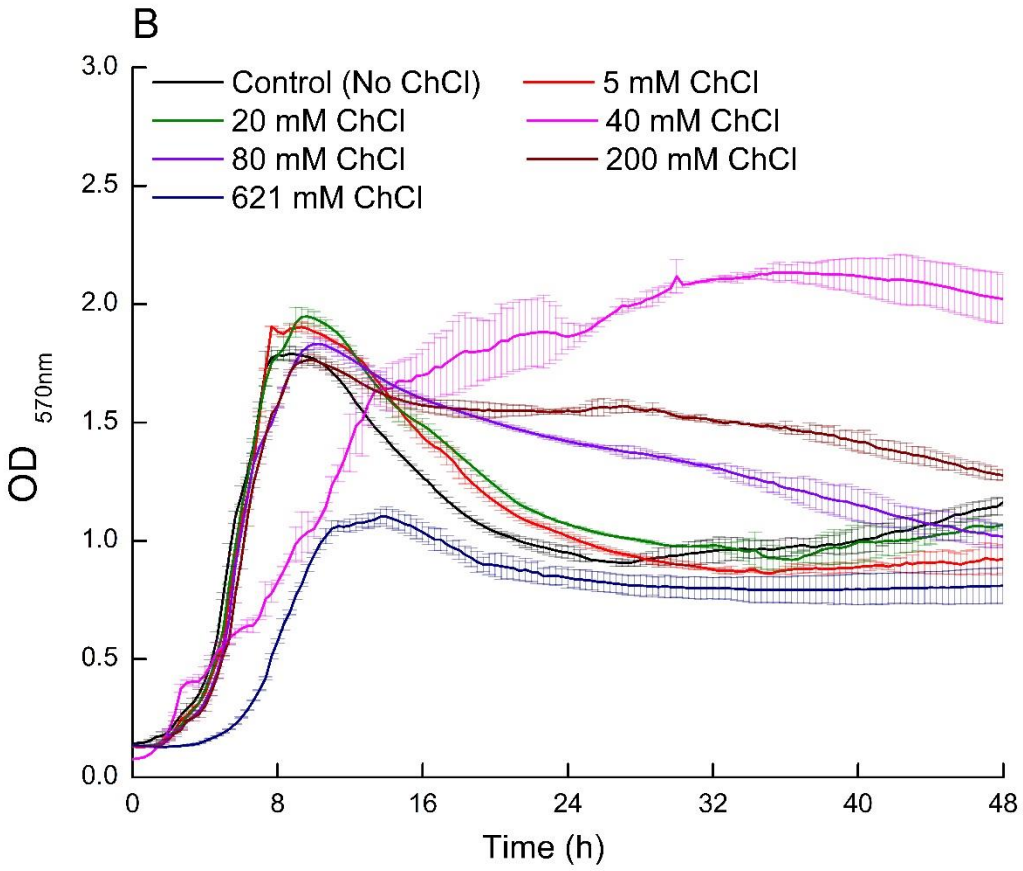

Figure 5.2 *B. subtilis* planktonic growth was monitored over a 48-hour at various molar concentrations of ChCl. Number of independent biological replicates = 4.

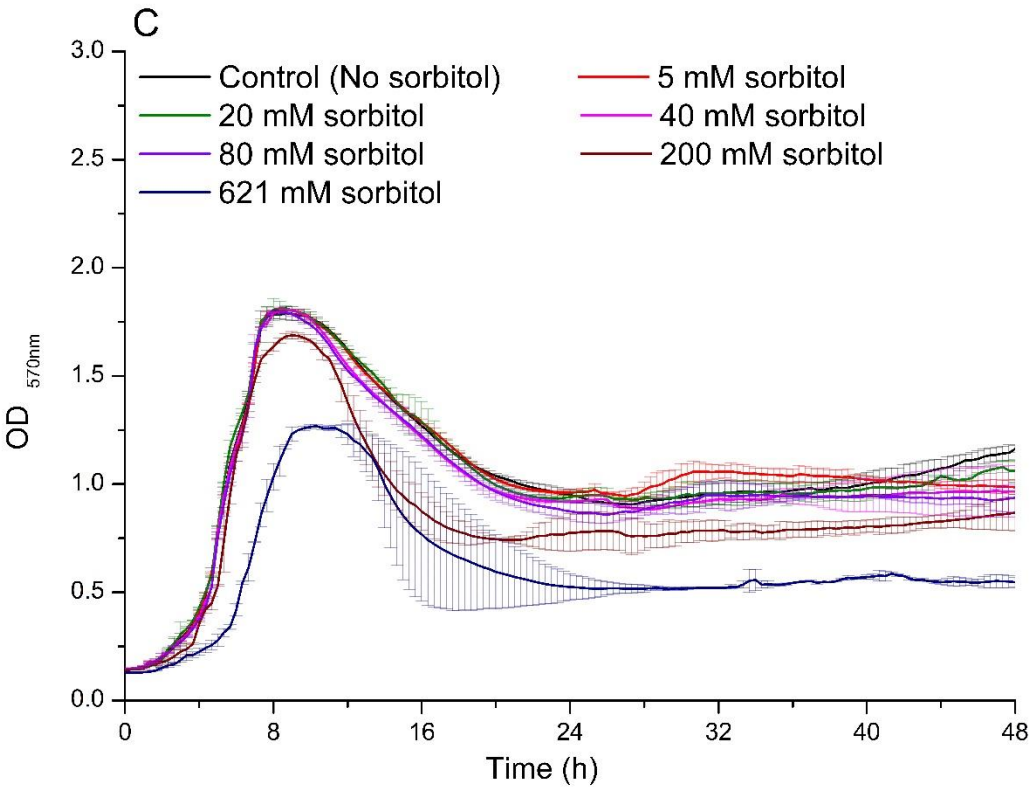

Figure 5.3 *B. subtilis* planktonic growth was monitored over a 48-hour at various molar concentrations of D-sorbitol. Number of independent biological replicates = 4.

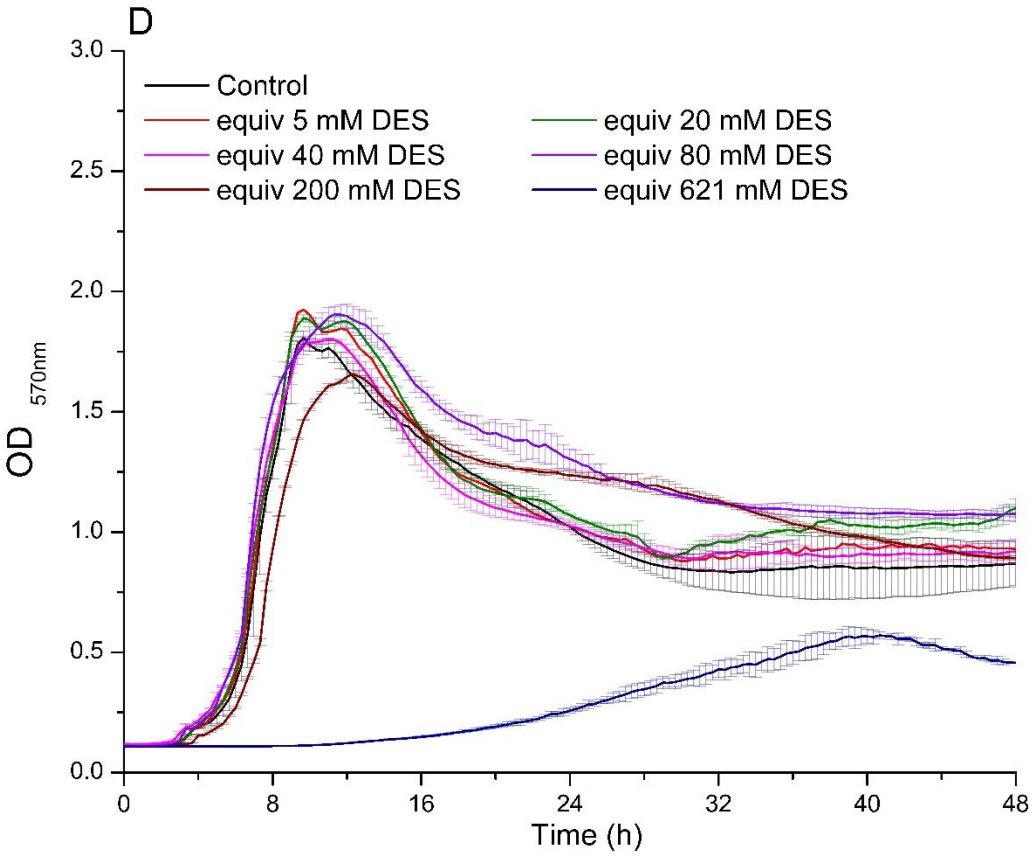

Figure 5.4 *B. subtilis* planktonic growth was monitored over a 48-hour at an equivalent concentration of (D-sorbitol + ChCl). Number of independent biological replicates = 4.

B. subtilis is widely considered a halotolerant bacterium, with some strains tolerating salt concentrations up to 30% wt/wt (Yin et al. 2019) (Santos and Da Costa 2002; Ji et al. 2022). Furthermore, the addition of a small amount of salt may serve as a source of ions that are beneficial to many cellular activities (Strathmann 2004).

For NaH_2PO_4 or KH_2PO_4, concentrations lower than 5% wt/wt enhance the maximum growth and slow the death rate. However, the lag phase was extended at higher concentrations, and at 10% wt/wt, the planktonic growth was completely inhibited

(**Figures 5.5** and **5.6**). The effects of sub-toxic concentration of DES were tested at two selected concentrations of NaH_2PO_4 and KH_2PO_4, one below the maximum tolerance (2% wt/wt) and one above the maximum tolerance (5% wt/wt) to verify if the additions of DES could increase *B. subtilis* growth (**Figure 5.7** and **Figure 5.8**). The results reveal that the addition of 40 mM DES induces a second growth phase at 11-12 h and delays the onset of the death phase at 2% wt/wt salt concentrations for both salts but has no considerable impact at 5% wt/wt salt concentrations **(Figure 5.6)**. (Thayalakumaran, Bethune, and McMahon 2007).**Error! Hyperlink reference not valid.** This is consistent with the osmoprotective effect of ChCl contained in the DES. Results for the wider range of the salt concentration are presented in Appendix 5.2.

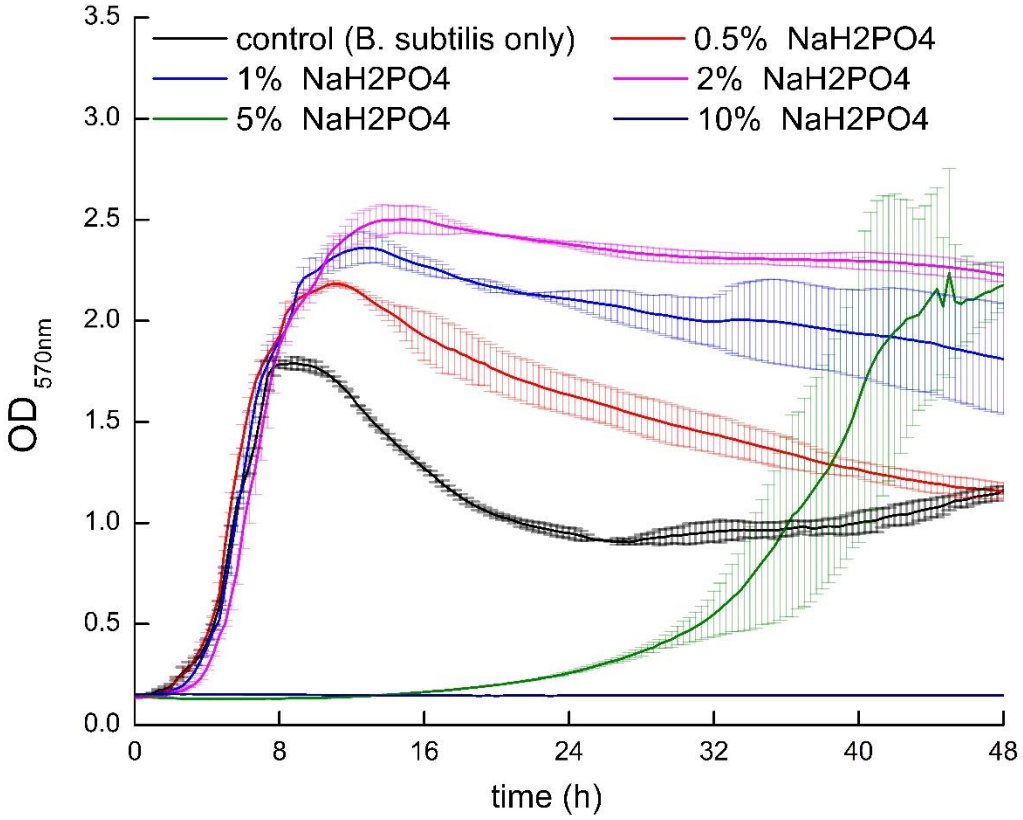

Figure 5.5 *B. subtilis* planktonic growth in the presence of A) increasing concentrations of NaH2PO4 (wt/wt). Number of independent biological replicates = 4.

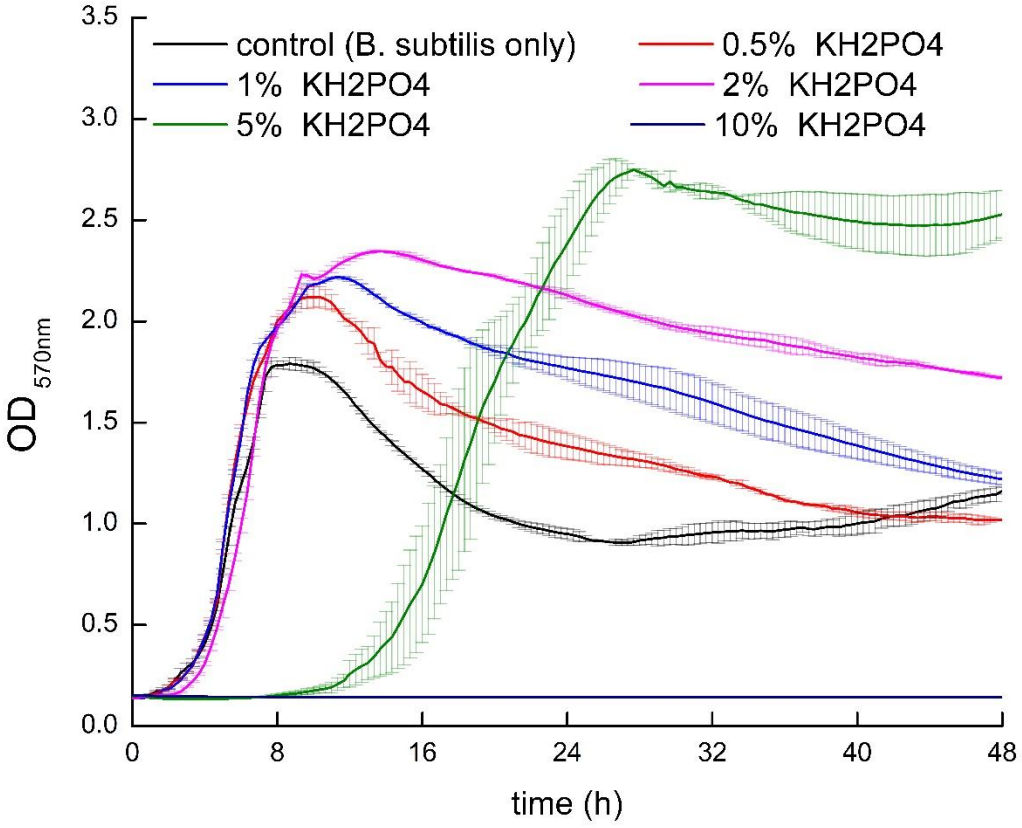

Figure 5.6 *B. subtilis* planktonic growth in the presence of increasing concentrations of KH2PO4 (wt/wt). Number of independent biological replicates = 4.

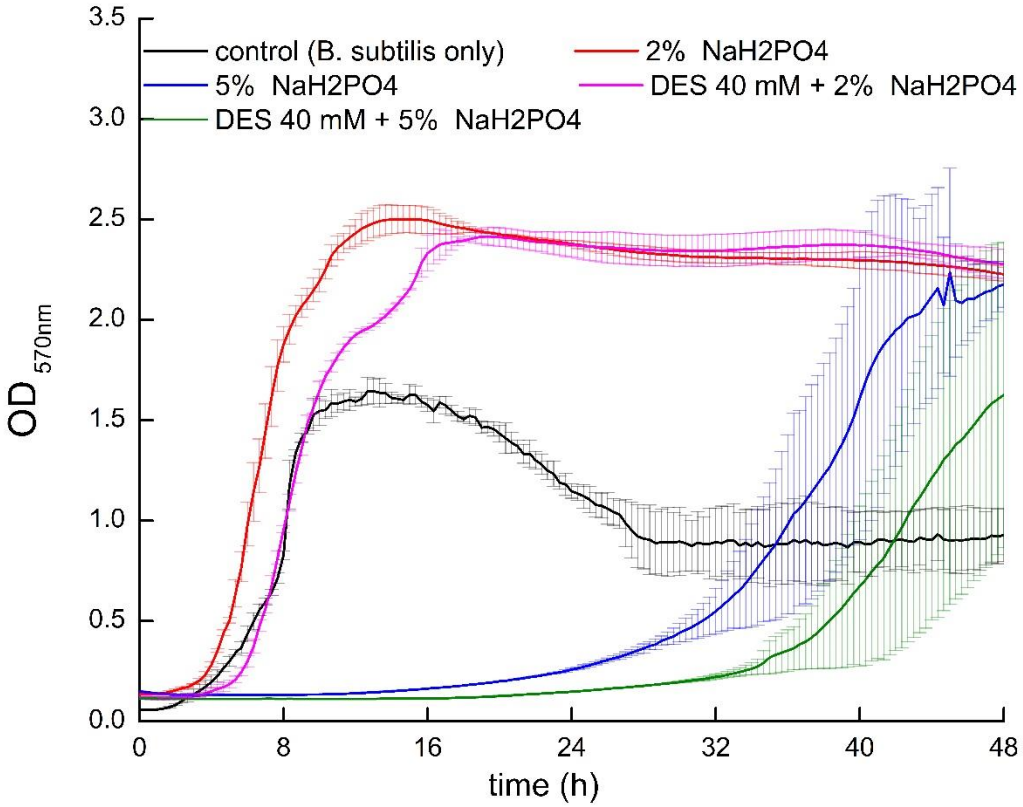

Figure 5.7 Planktonic growth of *B. subtilis* in the presence of A) increasing concentrations 2 and 5 % wt/wt NaH2PO4 with 40 mM DES. Number of independent biological replicates = 4.

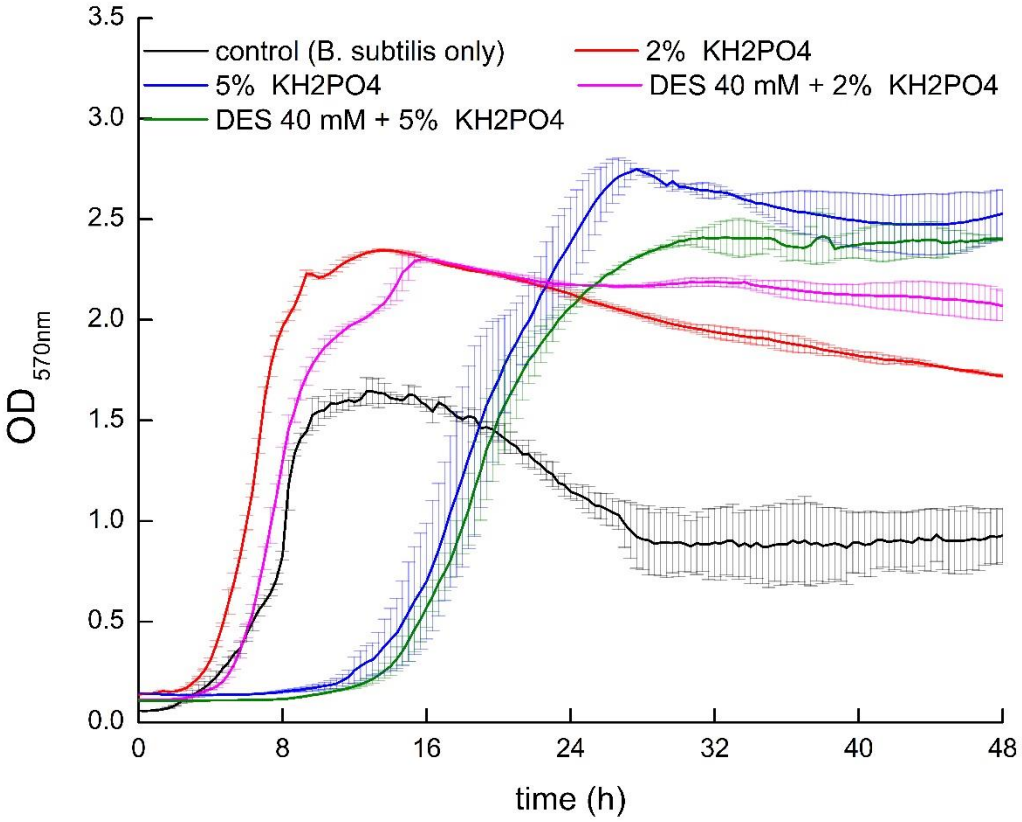

Figure 5.8 Planktonic growth of *B. subtilis* in the presence of 2 and 5 % wt/wt KH2PO4 with 40 mM DES. Number of independent biological replicates = 4.

5.3.2 biofilms results

Increasing the DES concentration in the range tested (5-100 mM) increased biofilm formation (**Figure 5.9)**. Interestingly, the addition of ChCl had no impact on biofilm development (Figure **5.10**), but D-sorbitol had a favorable effect on biofilm formation only at concentrations less than 60 mM, with 10 mM demonstrating the highest optical density value **(Figure 5.11)**.

Although lower concentrations of D-sorbitol (≤60 mM) showed an able effect on biofilm formation, the higher concentrations of D-sorbitol (100 mM) are expected to enhance osmolarity and reduce nutritional medium water activity (a_w) (Schultz 2016; Cesar et al. 2020).

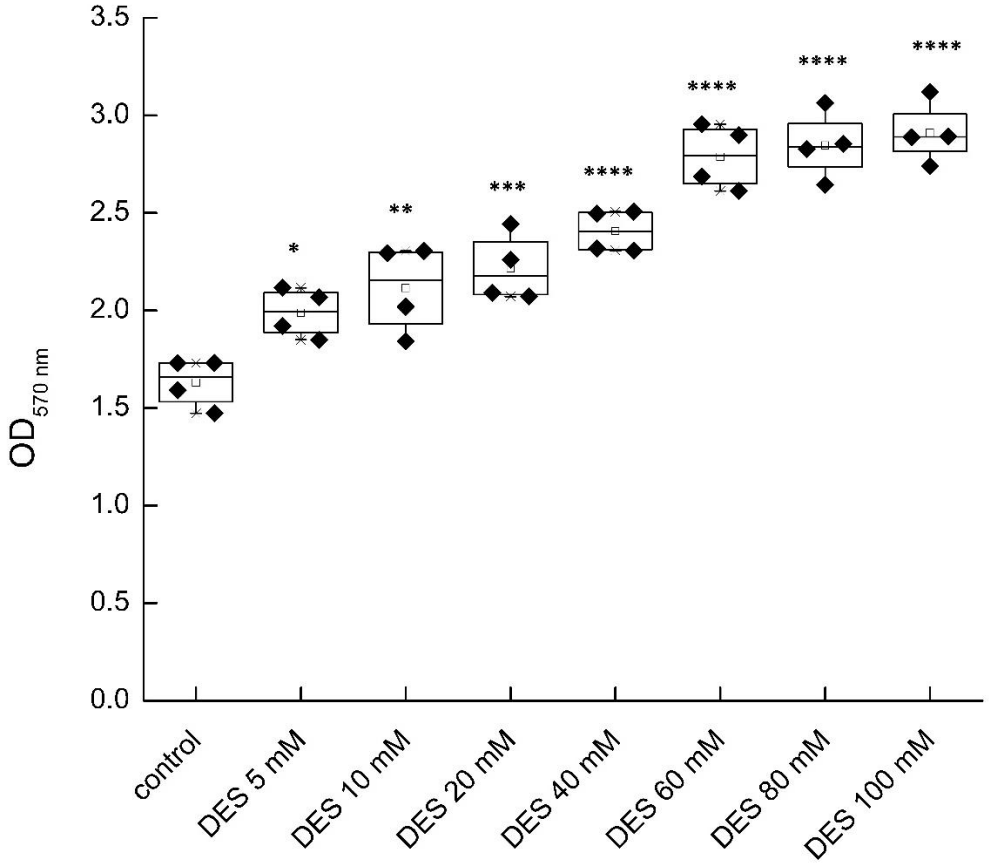

Figure 5.9 Biofilm formation in the presence of increasing concentrations of DES. Number of independent biological replicates = 4. ***, **, ***, ****** indicate statistically significant difference between treated cells and control cells at $p<0.05$, $0.01<p<0.05$, $0.001<p<0.01$, *and* $0.0001<p<0.001$, respectively, following to Tukey's test from ANOVA.

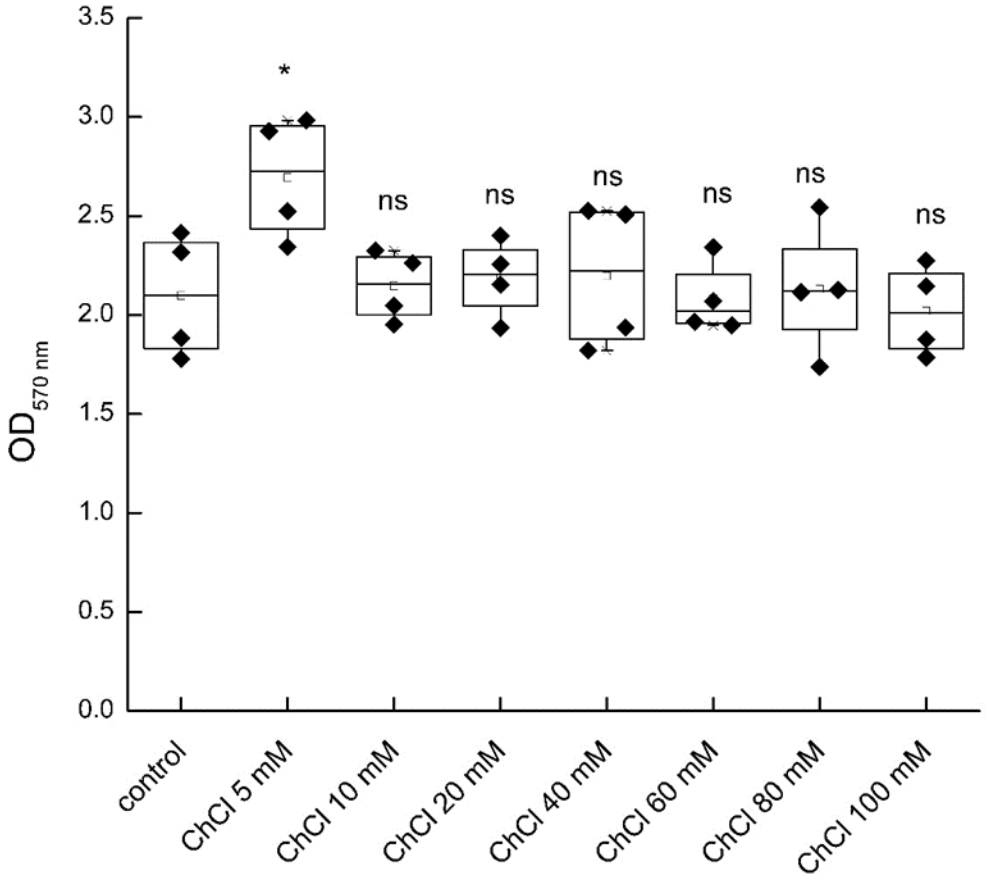

Figure 5.10 Biofilm formation in the presence of increasing concentrations of ChCl. Number of independent biological replicates = 4. ***, **, ***, ****** indicate statistically significant difference between treated cells and control cells at $p<0.05$, $0.01<p<0.05$, $0.001<p<0.01$, *and* $0.0001<p<0.001$, respectively, following to Tukey's test from ANOVA.

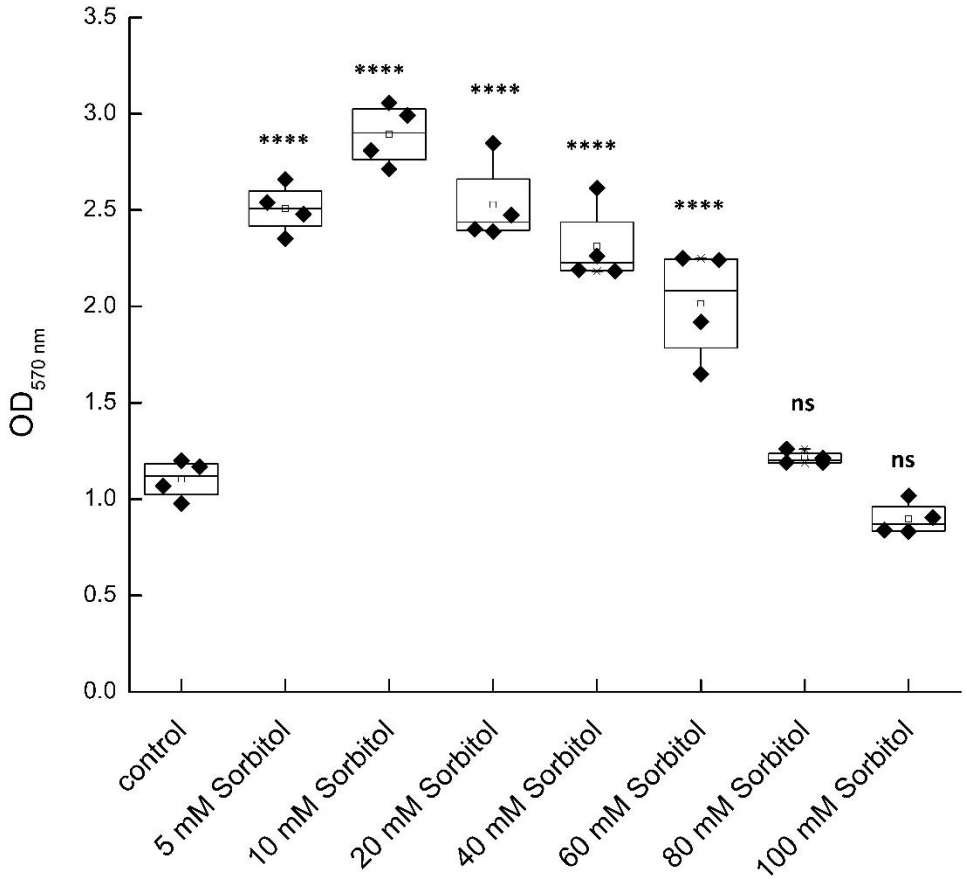

Figure 5.11 Biofilm formation in the presence of increasing concentrations of D-sorbitol. Number of independent biological replicates = 4. ***, **, ***, ****** indicate statistically significant difference between treated cells and control cells at $p<0.05$, $0.01<p<0.05$, $0.001<p<0.01$, *and* $0.0001<p<0.001$, respectively, following to Tukey's test from ANOVA.

While the presence of NaH2PO4 and KH2PO4 reduces biofilm development at concentrations of more than 1% wt/wt **(Figure 5.12)**, the addition of betaine alone had no effect on biofilm formation at concentrations ranging from 5 to 200 mM **(Appendix 5.3)**. Subsequently, when salt stress was applied under a specific concentration of betaine (40 mM), betaine stabilized biofilm biomass with increased concentrations of 1-2% (wt/wt) of NaH_2PO_4 and KH_2PO_4 salts.

Furthermore, the addition of 40 mM betaine to a medium containing 2% KH2PO4 (wt/wt) could increase biofilm development **(Figure 5.13)**. This increase, however, was not detected for 2% NaH2PO4 (wt/wt). This indicates that betaine treatment has an ion-dependent (Na vs. K ions) effect on biofilm formation.

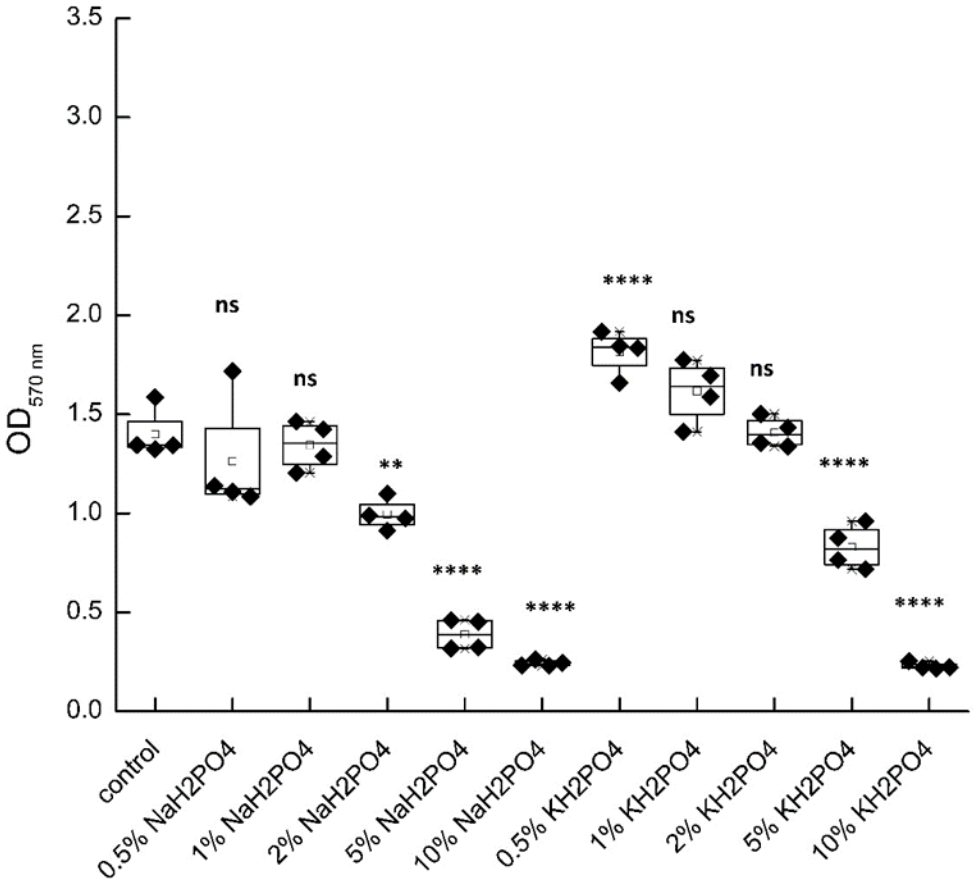

Figure 5.12 Biofilm formation in the presence of NaH_2PO_4 and KH_2PO_4.Number of independent biological replicates = 4. ***, **, ***, ****** indicate statistically significant difference between treated cells and control cells at *p<0.05, 0.01<p<0.05, 0.001<p<0.01, and 0.0001<p<0.001,* respectively, following to Tukey's test from ANOVA.

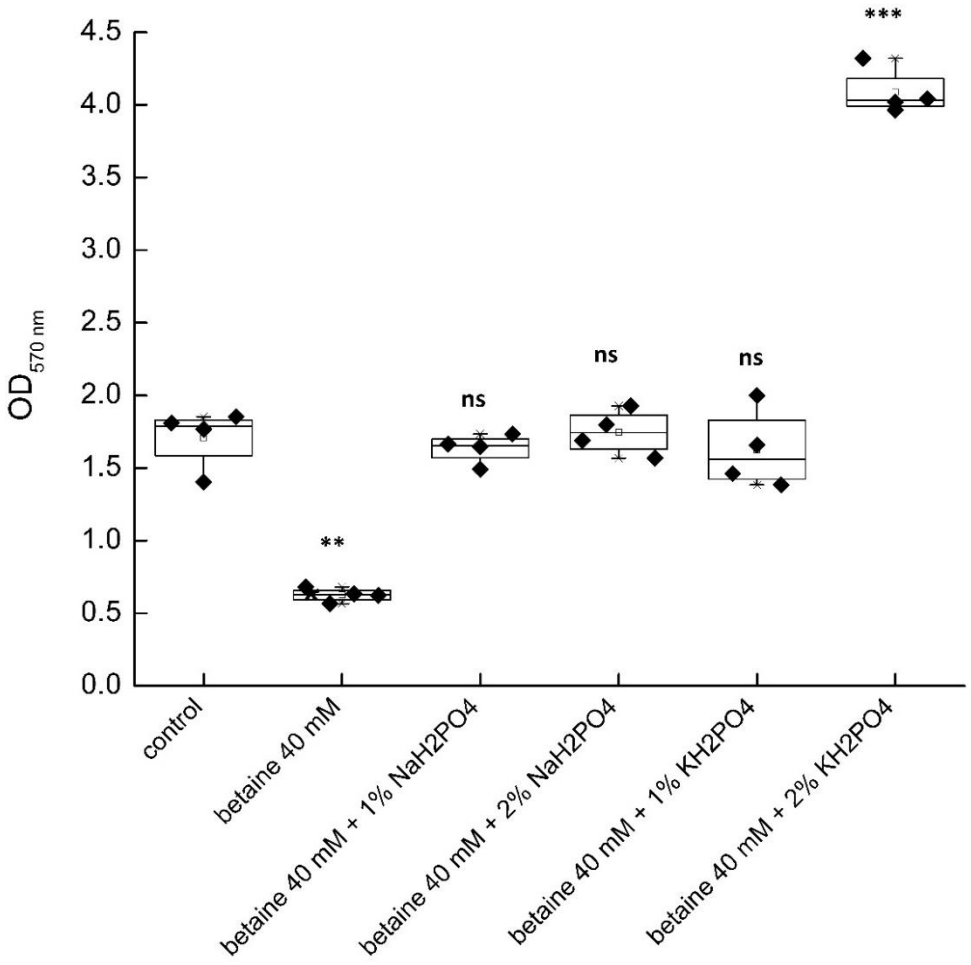

Figure 5.13 the effect of betaine and salts on biofilm formation. Number of independent biological replicates = 4. ***, **, ***, ****** indicate statistically significant difference between treated cells and control cells at *p<0.05, 0.01<p<0.05, 0.001<p<0.01, and 0.0001<p<0.001,* respectively, following to Tukey's test from ANOVA.

The effect of DES and its components at 40 mM concentration on *B. subtilis* biofilm formation in the presence and absence of NaH_2PO_4 and KH_2PO_4 salts differ **(Figure 5.14** to **Figure 5.16).** DES and ChCl increase slightly the biofilm formation in the presence of salts at 1 and 2% (wt/wt), while the effect of sorbitol is much stronger, although it does not change between 1 and 2% (wt/wt) of salt.

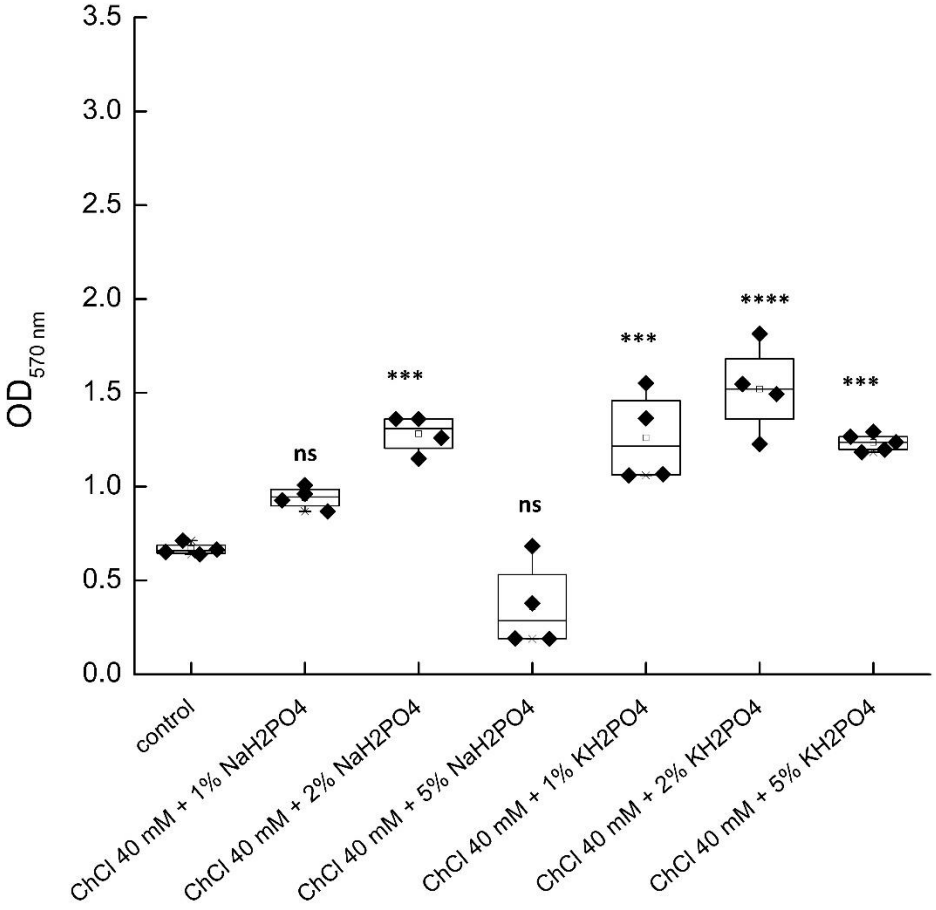

Figure 5.14 Effect on biofilm formation of ChCl and salts. The number of independent biological replicates = 4. ***, **, ***, ****** indicate a statistically significant difference between treated cells and control cells at $p<0.05$, $0.01<p<0.05$, $0.001<p<0.01$, *and* $0.0001<p<0.001$, respectively, following to Tukey's test from ANOVA

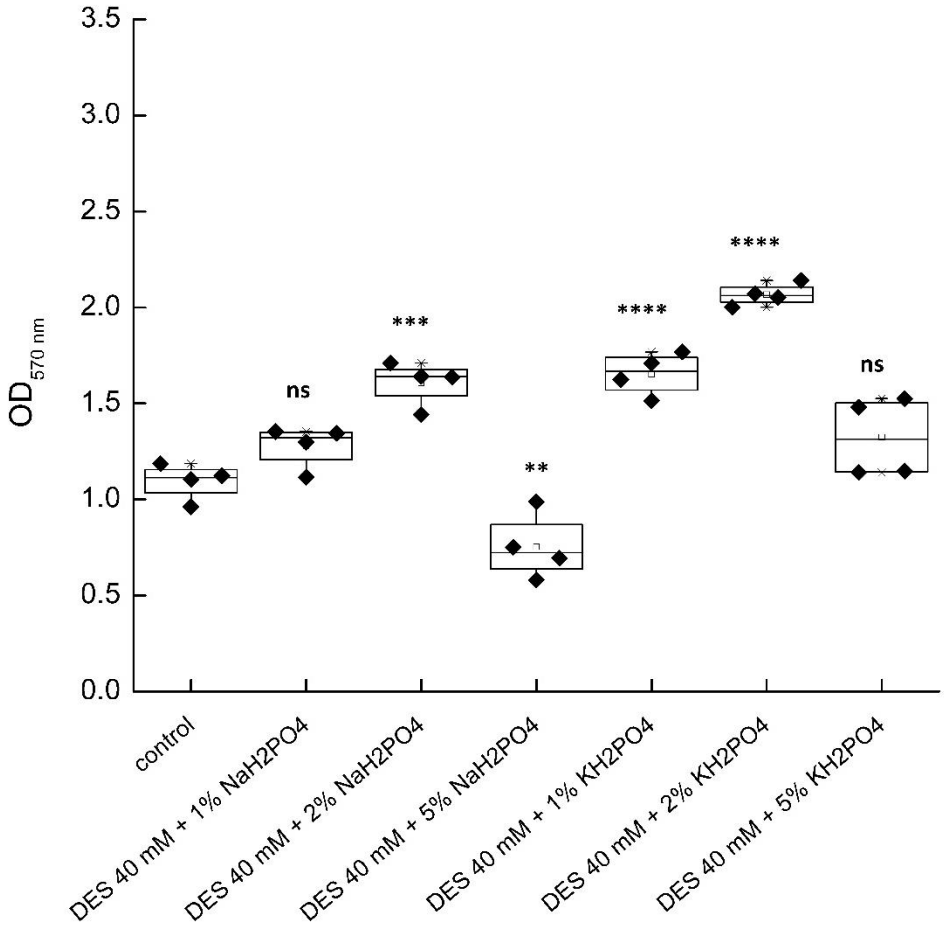

Figure 5.15 Effect on biofilm formation of DES and salts. The number of independent biological replicates = 4. ***, **, ***, ****** indicate a statistically significant difference between treated cells and control cells at $p<0.05$, $0.01<p<0.05$, $0.001<p<0.01$, *and* $0.0001<p<0.001$, respectively, following to Tukey's test from ANOVA

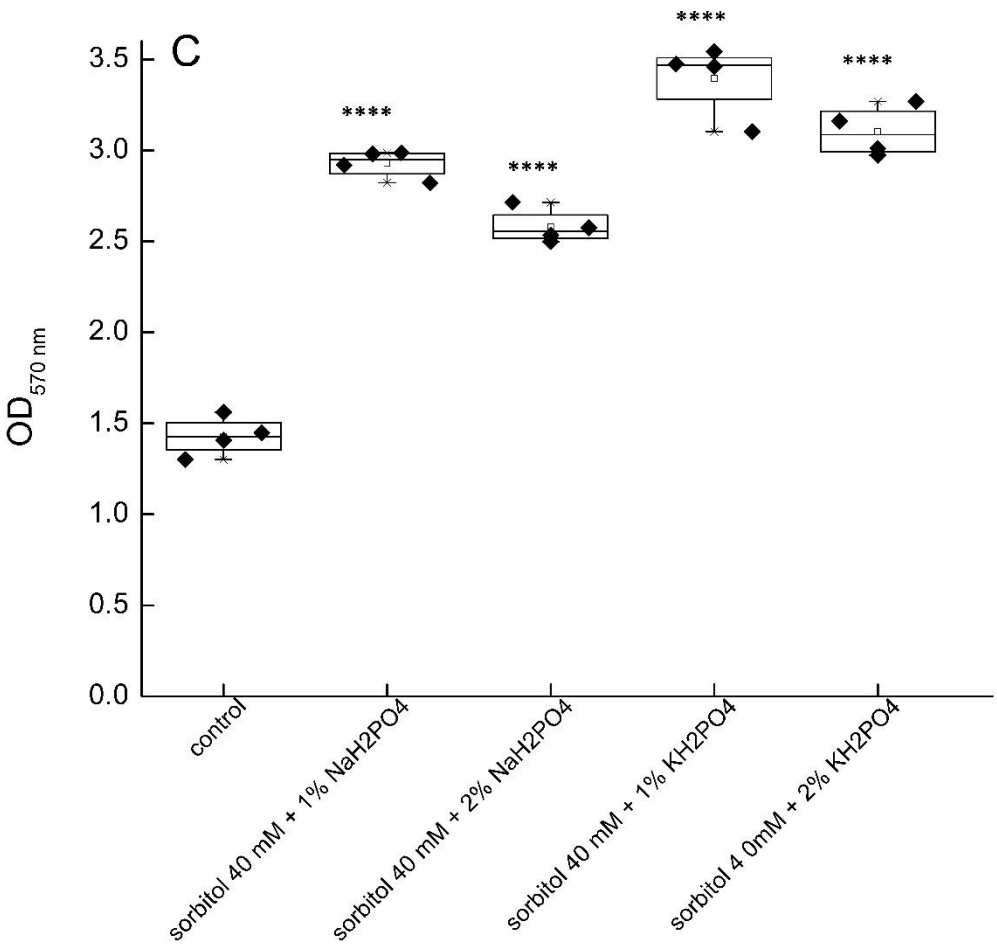

Figure 5.16 Effect on biofilm formation of sorbitol and salts. The number of independent biological replicates = 4. ***, **, ***, ****** indicates a statistically significant difference between treated cells and control cells at $p<0.05$, $0.01<p<0.05$, $0.001<p<0.01$, *and* $0.0001<p<0.001$, respectively, following to Tukey's test from ANOVA.

5.3.3 Bioelectrochemical results

DPV was conducted to investigate the redox-active species produced in bioelectrochemical experiments (**Appendix 5.5**). The highest peaks were observed at the potential between 0.03 and 0.1 V, and the peak current increased at 48 h due to the accumulation of redox-active species in the biofilm grown on the SPE surface (**Figure 5.22**). However, in samples

containing 40 mM ChCl and above, the peak potential shifted to a more positive potential (**Appendix 5.5A**).

Overall, the DPV results show that adding a pure organic Choline Chloride (ChCl) compound, either independently or in the form of ChCl-containing Deep Eutectic Solvents (DES), to *B. subtilis* increases the biofilm's electroactivity. This is likely due to the increased production of biofilm EPS. (Li, Kong, and Wu 2021) Or the involvement of metabolites from ChCl degradation in EET. Electrical stimulation at 0.4 V vs. Ag/AgCl could enhance ionic flux, transmembrane potentials, and electroactive EPS production at high salinity conditions.

The results of the bioelectrochemical experiments at 0.4 V confirm that adding DES and NaH2PO4 salts can delay the onset of current and increase the maximum current produced (**Figure 5.17**). The highest charge output (**Figure 5.18**) was observed upon the addition of DES 40 mM and ChCl 40 mM + NaH_2PO_4 2% (wt/wt), respectively, which is consistent with the biofilm amount detected on the working electrode of the SPE.

The highest peaks were identified at the potential between 0.03 and 0.1 V, and the peak current increased at 48 h, most probably due to the accumulation of redox-active species in the biofilm grown on the SPE surface (**Appendix 5.6**). However, in samples containing 40 mM ChCl and above, the peak potential shifted to a more positive potential (**Appendix 5.7).** Electrical stimulation at 0.4 V vs. Ag/AgCl might increase ionic flow, transmembrane potentials, and electroactive EPS production at high salinity conditions.

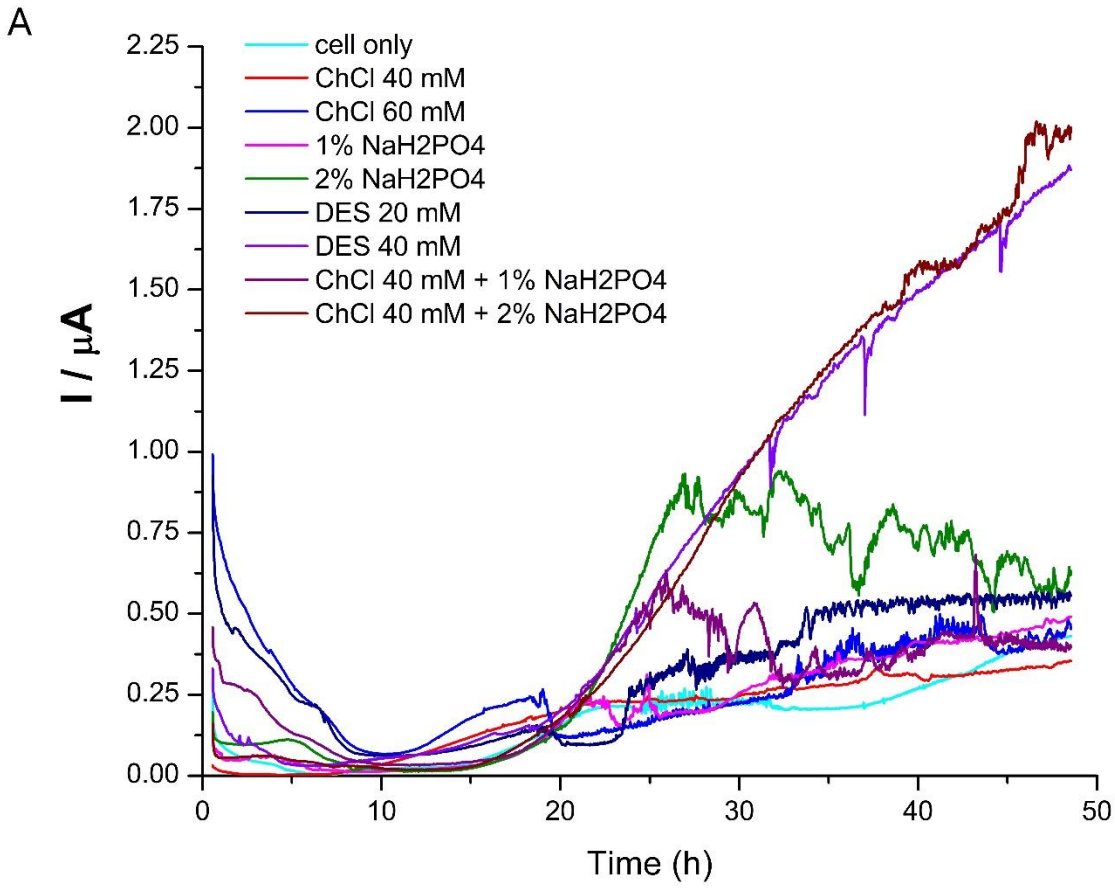

Figure 5.17 Chronoamprometry (CA) output for *B. subtilis* after 48 h growth at 400 mV in TY medium.

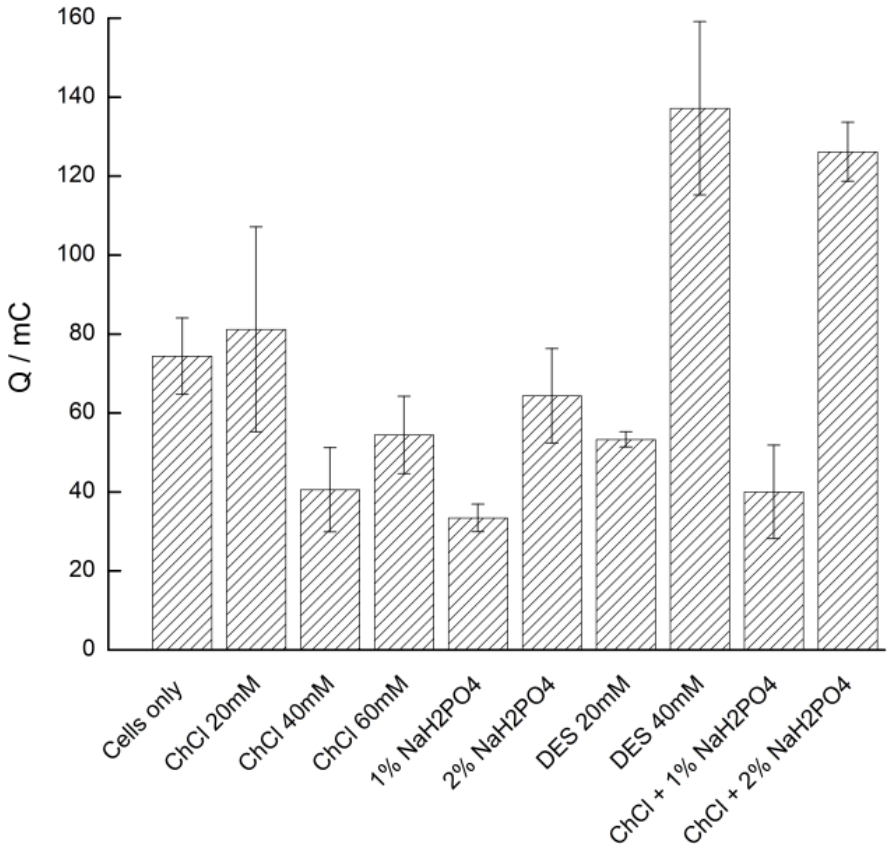

Figure 5.18: cumulative charge output for *B. subtilis* after 48 h growth at 400 mV in TY medium.

5.3.4 UV-VIS spectroscopy analysis

Riboflavin concentration in selected supernatants was assayed by UV/*VIS* spectrophotometer as a fast and broadly applicable approach due to the aqueous solubility of riboflavin. The standard curve was obtained using riboflavin detection with spectrophotometry protocols (Bartzatt and Wol 2014)(Chu et al. 2022) . The absorbance of the collected and filtered sample was measured at 440 nm (OD_{440}). Table 5.1 shows the standard Calibration data for riboflavin determination by UV-*VIS* spectroscopy.

The average value of the four independent biological replicates was fitted to the standard curve, as presented in **Table 5.2 and Figure 5.19** .Comparison of calculated concentrations from supernatants to those obtained from the standard curve shows a very high statistic accuracy of R2= 0.997. The concentration of secreted riboflavin into the supernatant shows a higher value for the DES 40mM condition.

We could not track a clear relationship between riboflavin concentration and electroactivity. This implies that other electron transfer processes within the biofilm are mediated by the observed EET in the presence of ChCl, DES, and DES components, as well as concurrent salt stress.

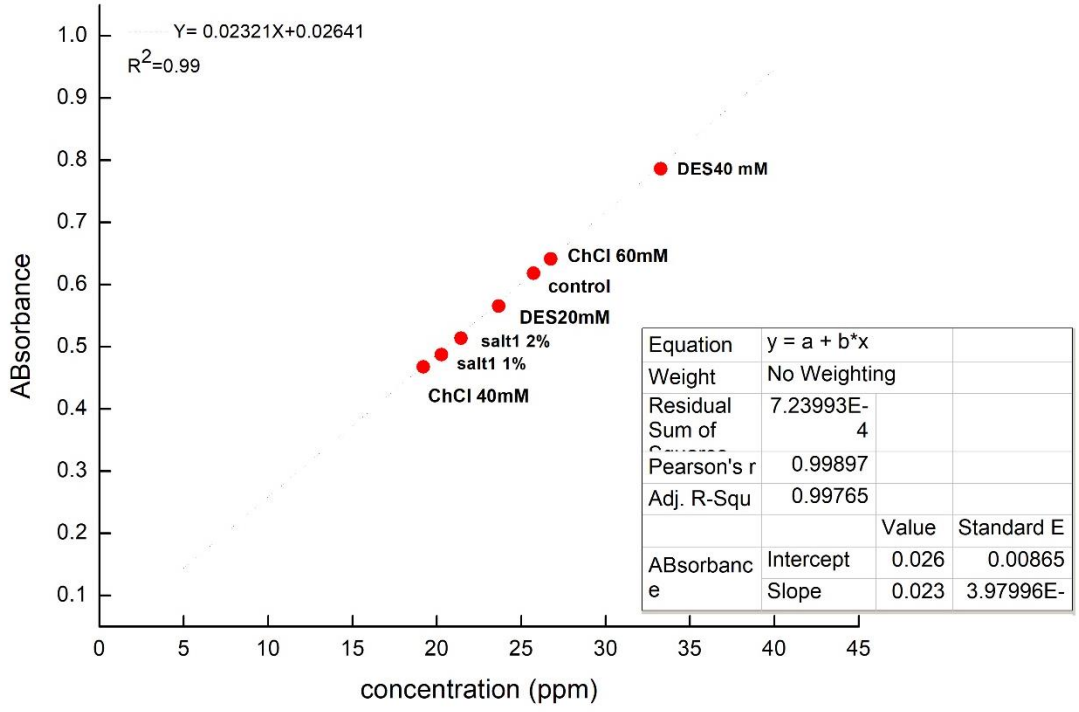

Figure 5.19 Spectrometric estimation of riboflavin concentration in supernatants

Table 5.1: Calibration data for riboflavin determination by UV-*VIS* spectroscopy.

No.	Concentration (ppm)	Absorbance Mean S.D (n=3)
1	5	0.144±0.001
2	10	0.255±0.002
3	15	0.380±0.001
4	20	0.493±0.002
5	25	0.619±0.004
6	30	0.736±0.005

Table 5.2: Determination of riboflavin concentration in selected supernatant.

Sample	Absorbance Mean S.D (n=4)	Concentration (ppm)
Control	0.641±0.001	26.49±0.04
NaH_2PO_4 1%	0.487±0.001	19.84±0.06
NaH_2PO_4 2%	0.513±0.001	20.96±0.05
KH_2PO_4 1%	0.665±0.002	27.51±0.09
KH_2PO_4 2%	0.513±0.006	20.96±0.26
DES 20 mM	0.565±0.002	23.22±0.09
DES 40 mM	0.786±0.002	33.73±0.09
ChCl 40 mM	0.467±0.001	18.98±0.05
ChCl 60 mM	0.689±0.002	28.55±0.09

5.3.5 Microscopy results

Following a 48-hour electrochemical experiment, fluorescence microscopy was employed to assess biofilm growth on the WE surface (**Figure 5.20**), with biofilm coverage quantified using MATLAB (**Figure 5.21**).

As fluorescence microscopy is a two-dimensional imaging method, biofilm coverage does not directly correspond to the total biomass on the electrode and is presented here for qualitative comparison. A significant increase in biofilm coverage is observed with rising concentrations of DES and ChCl, particularly in the presence of NaH2PO4. This is consistent with enhanced biofilm formation detected via crystal violet staining on SPE selected results are presented as **Figure 5.22** and with the wider range of data presented in **Appendix 5.8**. The results suggest that exopolysaccharides (EPS) are produced to alleviate osmotic stress.

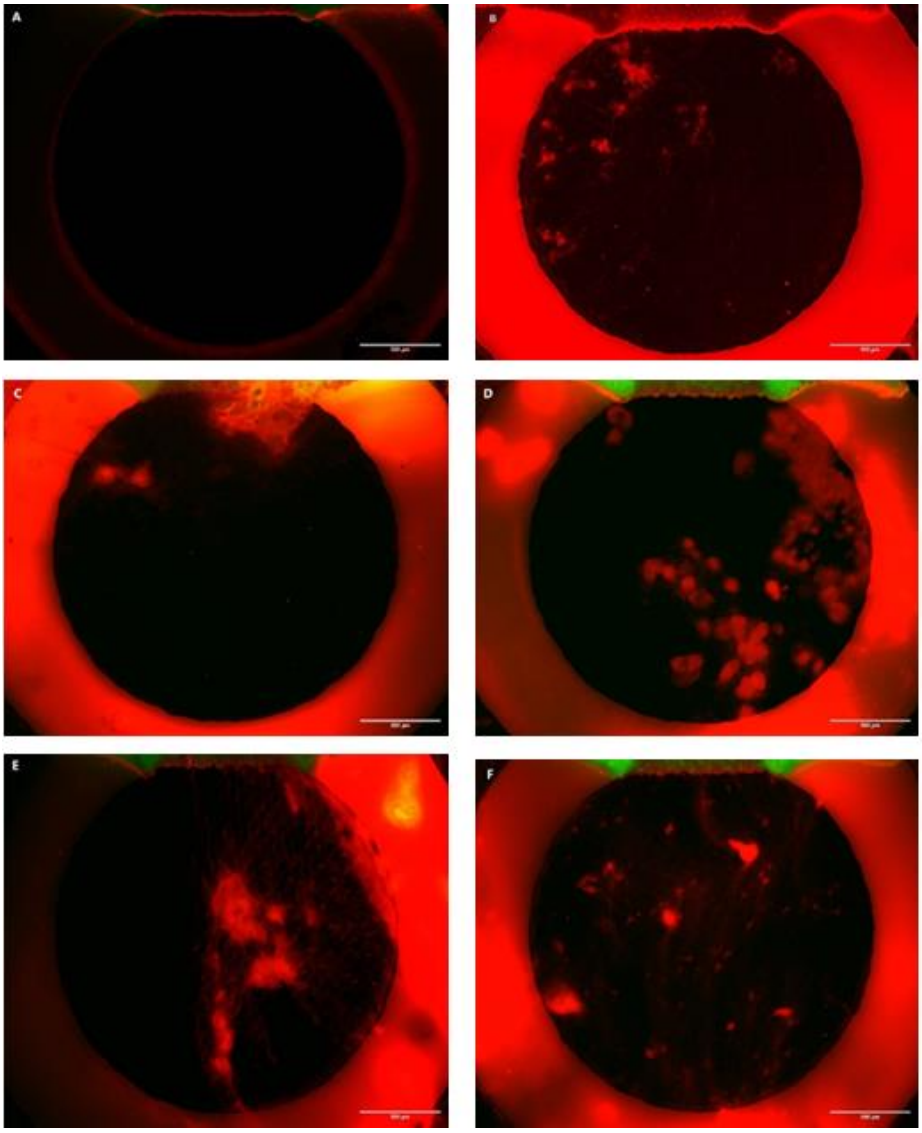

Figure 5.20 Biofilm formation on the SPE WE after 48 h CA at 0.4 V in various conditions. (A) Bare electrode (B) *B. subtilis* biofilm only (C) *B. subtilis* biofilm with 20 mM DES (D) *B. subtilis* biofilm with 40 mM DES (E) *B. subtilis* biofilm with 40 mM ChCl and 1% wt/wt NaH2PO4 (F) *B. subtilis* biofilm with 40 mM ChCl and 2% wt/wt NaH2PO4. All the electrodes were observed under the same condition with a 25x10 lens.

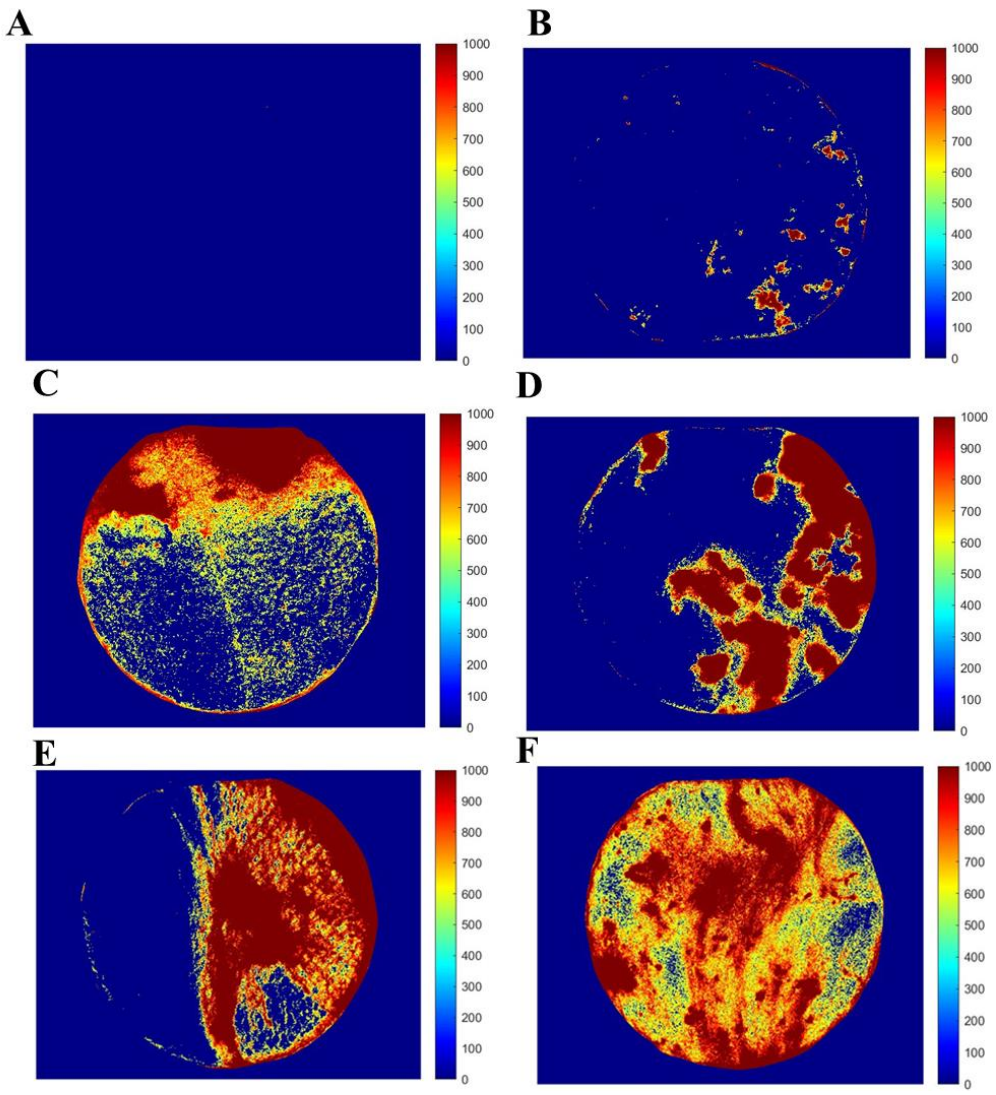

Figure 5.21 Heat map of biofilm intensity formed on the SPE WE after 48 h CA at 0.4 V in the presence of various conditions. (A) Bare electrode (B) B. subtilis biofilm only (C) B. subtilis biofilm with 20 mM DES (D) B. subtilis biofilm with 40 mM DES (E) B. subtilis biofilm with 40 mM ChCl and 1% wt/wt NaH2PO4 (F) B. subtilis biofilm with 40 mM ChCl and 2% wt/wt NaH2PO4. All the electrodes were observed under the same condition with 25x10 lens.

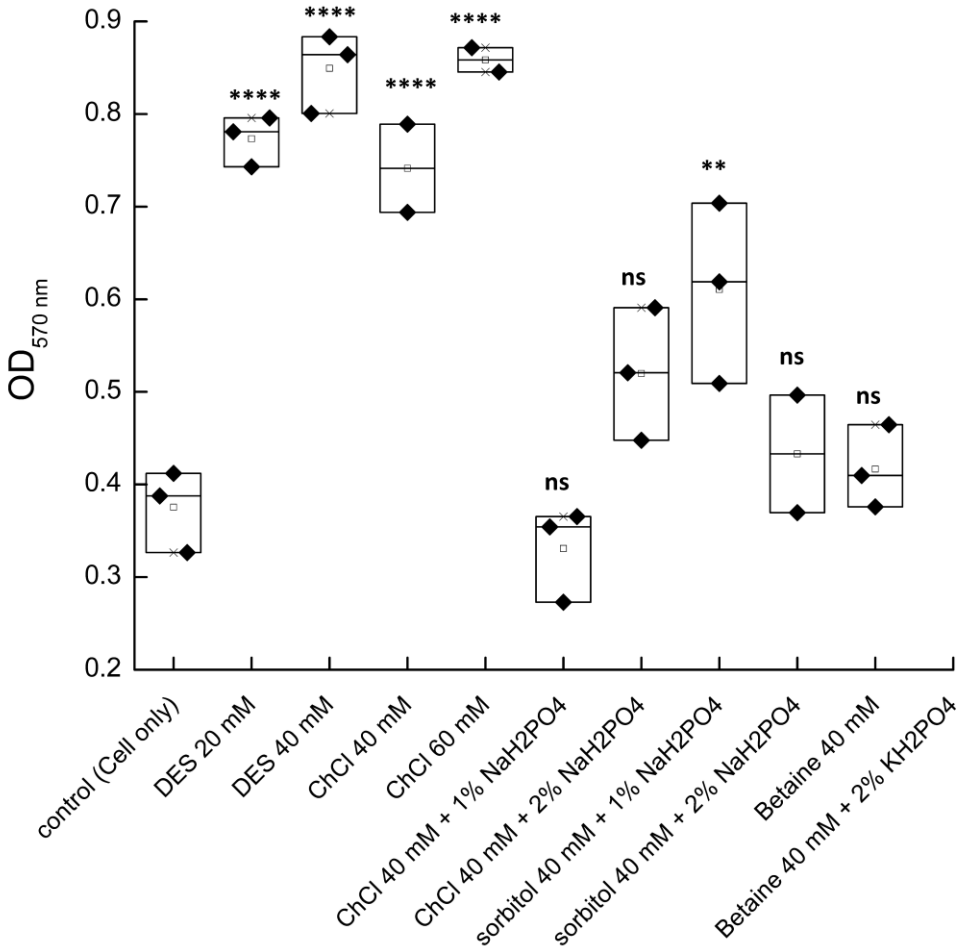

Figure 5.22 Biofilm on SPE for selected conditions. Number of independent biological replicates =3.

5.4 Discussion

According to the growth curves ((**Figure 5.1 to 5.4**), the presence of the DES at a range of 20–200 mM accelerated growth by delaying the start of the stationary phase, particularly during the transition from exponential to stationary phases. However, both 40 mM and 80 mM DES had the most significant effects on growth because the addition of DES at these doses resulted in continuous growth throughout a 24-hour period. On the other hand, Figure 5.1 compares 40 mM and 80 mM concentrations and reveals that 40 mM results in the higher individual OD570nm. This finding agreed with the previous work result that showed ChCl at a concentration of almost 40mM, which showed the optimum growth and biofilm

formation. The impact was not noticeable at lower concentrations (< 20 mM), and higher concentrations (> 200 mM) of DES showed toxicity to planktonic growth and inhibited the growth (Figure 5.1). Adding Sorbitol dehydrogenase (SDH) to the growth medium, which uses NAD^+ as a cofactor in cellular metabolism to convert sorbitol to fructose, helps *B. subtilis* quickly metabolize sorbitol. The observed pattern for DESs in the range of 20 to 200mM was not observed when individual components of the DES were used (**figures 5.2 and 5.3**).

Growth in the presence of DES was primarily seen during the transition from the exponential phase to the stationary phase by delaying the onset of the stationary phase. This pattern was not observed with the individual DES components, where growth rapidly declined and the stationary phase transitioned more quickly. This suggests a distinct benefit of eutectic solvents for bacterial growth compared to simple mixtures of the same individual components, as the eutectic mixtures are combined at specific ratios and temperatures below the melting points of the individual components. Since tryptone is a nutrient source lacking in carbohydrates, adding ChCl or ChCl-containing agents to the medium may compensate for this deficiency, boosting carbohydrate metabolism and leading to an overall increase in maximum growth (**Figure 5.2**). The slight variation in results observed in this study compared to the findings in the previous work (Chapter 4) is likely due to differences in growth response to the media used. In the earlier study, tryptone-yeast extract medium and nutrient broth were utilized. Although both media are complex, the mineral content may differ, which could account for the minor differences in how B. subtilis metabolizes ChCl at similar concentrations. The impact of D-sorbitol alone was minimal at concentrations below 200mM. However, when D-sorbitol and ChCl were combined in the same proportions as in DES (**figure 5.4)**, the behavior did not replicate that of DES, suggesting that the synergistic effect of DES components differs from that of the individual compounds.

On the other hand, the addition of 40 mM DES as the optimum DES concentration induces a second growth phase at 11-12 h and delays the onset of the death phase at 2% wt/wt salt concentrations for both salts but does not show any considerable impact at higher (5% wt/wt) salt concentrations. (Thayalakumaran, Bethune, and McMahon 2007). This is consistent with the osmoprotective effect of ChCl contained in the DES compound. The enhancement of biofilm biomass formation by DES may be linked to the presence of sorbitol, which acts as a supplementary carbon source and an accessible carbon reserve for EPS synthesis. In contrast, ChCl helps alleviate osmotic stress in the presence of salts (1-2% wt/wt), likely due to its role as a precursor for the osmoprotectant glycine betaine. Additionally, introducing 40 mM betaine into a medium with 2% KH2PO4 (wt/wt) can further promote biofilm growth **(Figure 5.13)**. This increase, however, was not detected for 2% NaH2PO4 (wt/wt). This indicates that betaine treatment has an ion-dependent (Na *vs.* K ions) effect on biofilm formation.

For NaH2PO4 or KH2PO4, concentrations lower than 5% wt/wt enhance the maximum growth and slow down the death rate. However, the lag phase was extended at higher concentrations, and at 10% wt/wt, the planktonic growth was inhibited entirely (**Figures 5.5 and 5.6**). The combination of NaH2PO4 and KH2PO4 salts and 40 mM DES (D-sorbitol/ChCl, 1:1 mol mol^{-1}) enhances biofilm production in *B. subtilis* grown under static anoxic conditions. Also, when salt stress was applied under a specific concentration of betaine (40 mM), betaine stabilized biofilm biomass with increased concentrations of 1-2% (wt/wt) of NaH2PO4 and KH2PO4 salts (**Figures 5.7 and 5.8**).

The results of biofilm formation in the presence of DES were consistent with the planktonic growth results, which implies the synergy between D-sorbitol and ChCl in promoting biofilm formation. However, ChCl promoted planktonic growth without causing a significant effect on biofilms. This may be due to the sensitivity and vulnerability of planktonic cells to the osmotic variation compared to the cells protected within a biofilm shield. This effect can occur even in a medium lacking added salt. The osmoprotection provided by ChCl predominantly affects individual cells subjected to osmotic stress, potentially due to changes in cell size resulting from water accumulation and ion flux across the membrane. These processes are regulated by the activity of osmolytes (Dai and Zhu 2018).

D-sorbitol promotes biofilm formation without notably influencing planktonic growth, making it a suitable additional carbon source for biofilm production. Once absorbed, D-sorbitol is swiftly converted into sorbitol-6-phosphate by the phosphoenolpyruvate-dependent phosphotransferase (PTS) sorbitol system. This modified sorbitol is then integrated into the sugar structure of the extracellular polymeric substance (EPS) within the biofilm, thereby boosting biofilm production.(Venkova et al. 2017). The combination of D-sorbitol as an additional carbon source and ChCl as an osmoprotectant precursor seems ideal for bioprocess application. It is effective in both planktonic growth and biofilm formation enhancement(Arce-Cordero et al. 2021)(Gregg et al. 2022). D-sorbitol can also influence the water activity (a_w) of the medium by interacting with water molecules through its ions(Venkova et al. 2017). This interaction may trigger the release of exopolysaccharides in the extracellular polymeric substance (EPS), serving as the primary cellular response to unfavorable and stressful environmental conditions. As a result, this enhances the adhesion of B. subtilis cells to each other and the surface of the substrate.(Cesar et al. 2020)(Arce-Cordero et al. 2021)(Gregg et al. 2022). Also, EPS composition shows semiconductive properties and higher production of EPS can improve the EET rate and electrochemical response(Kapfhammer et al. 2005) (Roychoudhury, Haussinger, and Oesterhelt 2012). EPS plays an important role in regulating proline-compatible solute and ion uptake. A direct correlation exists between cytoplasmic activity and the microbial content of extracellular polymeric substances (EPS), with EPS overproduction serving as the primary microbial response to water scarcity. The negatively charged groups in the EPS structure can bind to the cations and prevent the entrance of positive ions through the membrane(Kapfhammer et al. 2005)(Kapfhammer et al. 2005). Unlike ChCl, a precursor for betaine, betaine is a basic compatible solute employed by most bacteria. It primarily affects transmembrane ion flow and membrane potential through ion-specific regulatory mechanisms that can modulate intracellular pH levels. The addition of betaine did not alter biofilm formation in the concentration range of 5 to 200 (**Appendix 5.3**). This is most probably due to the role of betaine as a compatible solute osmoregulator, which controls the osmotic stress and avoids significant osmotic changes in the system. The consistent biofilm results, even in the presence of higher concentrations of Betaine, could be attributed to this characteristic. Following the introduction of salt stress, betaine

at a concentration of 40 mM helped stabilize biofilm biomass in the presence of increased levels (1-2% wt/wt) of NaH2PO4 and KH2PO4 salts. Furthermore, adding 40 mM betaine to a medium containing 2% KH2PO4 (wt/wt) enhanced biofilm formation **(Figure 5.13)**. However, this increase was not observed for 2% NaH_2PO_4 (wt/wt). This signifies an ion-dependent (Na vs. K ions) influence on biofilm production with betaine treatment.

The impact of DES and its components at a 40 mM concentration on *B. subtilis* biofilm formation varies depending on the presence or absence of NaH2PO4 and KH2PO4 salts. **(Figure 5.15).**

In the presence of salts at 1% and 2% (wt/wt), DES and ChCl moderately enhance biofilm formation, whereas sorbitol shows a more pronounced effect. However, its impact remains consistent between the two salt concentrations. However, the charge output data indicate that the influence of ChCl on biofilm formation does not directly align with that of betaine when both are used alongside salts to induce osmotic stress. This discrepancy likely arises from glycine betaine synthesis from choline in *B. subtilis*, catalyzed by the GbsB and GbsA dehydrogenases. Additionally, the presence of betaine in the medium may affect gene expression, leading to variations in biomass accumulation as part of the osmotic stress response.

5.5 conclusion

The influence of DES on planktonic growth, particularly at lower concentrations, was attributed mainly to the pronounced effects of its individual components, sorbitol and choline chloride (ChCl), when added either separately or together in a solution. While this suggests that DES's hydrogen bonding could impact planktonic growth, concentrations above 200 mM inhibited growth. Notably, DES did not alleviate osmotic stress in planktonic growths. At concentrations above 2% wt. for salts and 200 mM for DES, both DES and salts inhibit planktonic growth. Bioelectrochemical studies show a slight positive impact of ChCl on charge output when salts are present. In summary, the findings indicate that adding ChCl or ChCl-based DES at low levels boosts biofilm formation and reduces

osmotic stress. This insight may improve bioelectrochemical processes like electro-fermentation, especially in media with high electrolyte concentrations.

The combination of inorganic salts, specifically NaH2PO4 and KH2PO4, with 40 mM DES (D-sorbitol/ChCl, 1:1 mol/mol) promotes biofilm production in B. subtilis under static anoxic conditions. The beneficial effect of DES on biofilm formation is linked to sorbitol, which serves as an additional carbon source and a readily available carbon pool for EPS synthesis. In the presence of salts (1-2% w/w), ChCl helps reduce osmotic stress, likely due to its role as a precursor for the osmoprotectant glycine betaine. However, in the presence of salts (1-2 % w/w), ChCl mitigates osmotic stress, likely because ChCl is the precursor of the osmoprotective agent glycine betaine. The effect of ChCl on biofilm formation is lower than betaine, likely because the synthesis of glycine betaine from choline in *B. subtilis* is mediated by the GbsB and GbsA dehydrogenases. In the 20-80 mM concentration range, DES significantly impacts planktonic growth, an effect only partially mirrored when its components, sorbitol and ChCl, are added individually or together in an aqueous solution. This suggests a possible role of DES's hydrogen bonding in influencing planktonic growth. However, DES concentrations above 200 mM inhibited growth and did not alleviate osmotic stress in planktonic cells. Both DES and salts hinder planktonic growth at concentrations above 2% wt. for salts and 200 mM for DES. Bioelectrochemical studies show a slight increase in charge output due to ChCl in the presence of salts. Overall, low concentrations of DES promote biofilm formation and reduce osmotic stress, providing insights for improving bioelectrochemical processes like electrofermentation in high-electrolyte media.

5.6 Outcome

Osmoregulation by Choline-based deep Eutectic Solve (DES) induces electroactivity in Bacillus subtilis biofilms

Neda Eghtesadi, Kayode Olaifa, Tri T. Pham, Vito Capriati, Obinna M. Ajunwa, Enrico Marsili

Chapter 6. Antibacterial Action of Zn2+ Ions Driven by the In Vivo Formed ZnO Nanoparticles

This chapter is adapted from my following research paper:

Vitasovic T, Caniglia G, **Eghtesadi N**, Ceccato M, Bojesen ED, Gosewinkel U, Neusser G, Rupp U, Walther P, Kranz C, Ferapontova EE (2024). Antibacterial action of Zn2+ ions driven by the in vivo formed ZnO nanoparticles. ACS Applied Materials & Interfaces. 10;16(24):30847-59. **(Scopus Percentile: 95%, Q1)**

This chapter has mainly investigated the effect of different concentrations of ZnO Nanoparticles and Zn ions on *E-coli* viability. What is going to be present in the following pages is a part of the main work that aimed to find an alternative for ZnO as a widely used antibiotic with unpleasant environmental effects. Here, we found out that Zn^{2+} in its ionic form is an eco-friendlier antibacterial, and its biocidal action is comparable with ZnO NPs (<100 nm size), with a minimal biocidal concentration being 41 μg ml^{-1} vs. 5 μg ml^{-1} of ZnO NPs, as determined for 10^3CFU ml^{-1} *E. coli*.

Through complementary experiments, we discovered that the antimicrobial effect of Zn^{2+} ions is primarily linked to their absorption by *E. coli* and subsequent transformation into insoluble ZnO nanocomposites within the bacterial cells at an internal pH of 7.7. These *in vivo*-formed nanocomposites then compromise *E. coli* membranes and intracellular structures by generating insoluble bio-composites, which may initiate characteristic ZnO reactions harmful to the cells, such as producing reactive oxygen species. This study reveals a distinct mechanism by which Zn^{2+} ions lead to bacterial cell death. This process could also apply to other metal ions capable of forming semiconductor oxides and insoluble hydroxides at the slightly alkaline intracellular pH of certain bacteria.

6.1 Introduction

The use of antibiotics as antibacterial supplements in livestock presents notable risks and can result in the spread of antibiotic-resistant bacteria to human health(Ventola 2015). Moreover, it can disrupt environmental ecology by changing the microbial makeup of the environment. Over 90% of the antibiotics given to animals can be excreted and end up in the environment, promoting the buildup of antibiotic-resistant microorganisms.(Bartlett, Gilbert, and Spellberg 2013)(Bartlett et al. 2013).

Zinc Oxide nanomaterials are good alternatives to antibiotics due to their strong antimicrobial activity stability and being categorized as safe compounds by the US Food and Drug Administration (FDA)(Ma et al. 2021)(Youn and Choi 2022). The antibacterial property of ZnO NPs is mostly associated with their capability to produce Reactive Oxygen Species (ROS) such as hydroxyl radical (·OH)and Hydrogen Peroxide (H2O2), which are capable of oxidative damaging the cellular membrane, DNA/RNA, and proteins(Djurišić et al. 2015)(Qi et al. 2017)(Gold et al. 2018).

Despite their good antibacterial properties, concerns regarding the unpleasant environmental effect of ZnO NPs and their accumulation in the environment have caused some legal limitations in the allowed dosage of NPs in animal food(Gold et al. 2018)(Kim et al. 2022). Zn^{2+} salts, known for their antibacterial activity for almost a century, can be considered a safer replacement for ZnO NPs in animal nutrition. Antibacterial formulations composed of Zn^{2+} salts show lower ecotoxicity effects than ZnO NPs(Babich and Stotzky 1978)(Winslow and Haywood 1931).

The following pages investigate the biocidal efficiency of ZnO NPs and $ZnCl_2$ against the Gram-negative bacterium *E. coli* under identical conditions, avoiding the formation of third Zn compounds with ions of buffered media, which may obstruct mechanistic interpretation.

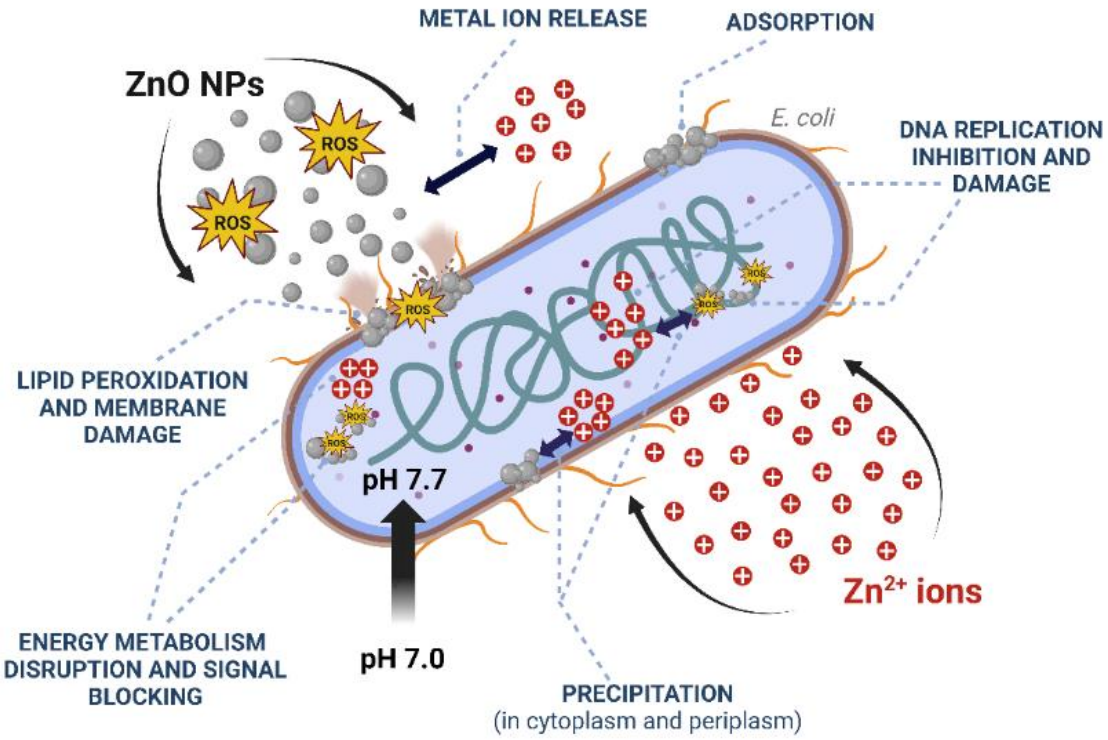

Figure 6.1 Schematic representation of antibacterial action of Zn^{2+} and ZnO nanoparticles at the environmental pH 7.0.

6.2 Material and Methods

6.2.1 Materials

Anhydrous 3-(N-morpholino) propanesulfonic acid (MOPS-free acid; ≥99.5%), the components of Luria- Bertani broth (LB), ZnCl2 (99.999%), and ZnO nanopowder (<100 nm particle size; ≤100%) were used as received from Sigma-Aldrich, Denmark. The pH of MOPS buffer was adjusted by adding 1 M NaOH. LB broth used for *E. coli* cultivation was prepared by mixing tryptone (10 g l–1), yeast extract (5 g l–1), and NaCl (10 g l–1), giving the final pH of 7.0, followed by sterilization in a high-pressure steam chamber at 121°C for 30 min. The agar plates, used for antibacterial testing, were prepared using the standard protocol by dissolving 12.5-1.50 g of agar powder (Scharlab S.L., ESP) in one liter of a sterilized LB medium. The initial freeze-dried E. coli culture, reference strain DH5α (catalogue no. DSM 6897), was purchased from DSMZ, Germany. All solutions were prepared using Bio-Cell Milli-Q water (resistivity ≥18 MΩ cm at 25°C, Millipore, Bedford, USA).

6.2.2 Bacterial strain

The strain used in this experiment was *E. coli* ATCC 25955. It was chosen as a model because it is a recognized biomarker of environmental contamination and infections, yet it exists in non-pathogenic forms suitable for safe studies using numerous techniques.

6.2.3 Bacteria cultivation

A culture of *E. coli* was grown in LB broth for 18 h at 37°C, under shaking at 80 rpm in a shaking incubator Innova 4000 Shaker (New Brunswick Scientific, UK). The overnight culture was centrifuged for 5 min at 5000 rpm using Eppendorf Mini Spin 5452 centrifuge (Eppendorf AG, Germany), at room temperature (rt) of 23±1°C. The obtained pellet was then repeatedly washed and re-suspended in a sterile 20 mM MOPS buffer, pH 7.0, followed by centrifugation at 5000 rpm for 5 min. Finally, the concentration of bacteria in the washed suspension was estimated by optical density (OD) measurements at 600 nm using a UV Mini-1240 UV-VIS spectrophotometer (Shimadzu Co., Japan). For the repeats, the OD600 was adjusted to 0.2-0.4.

6.2.4 Preparation of the test compound for biocidal activity

ZnCl2: 100 mM ZnCl2 stock solution was prepared by dissolving 68.2 mg of the ZnCl2 a compound in 5 mL of Distilled water (DI), sonicated for 30 minutes to ensure complete solubility, and thereafter filter-sterilized. Different concentrations ranging from (0.1 mM to 1 mM) were made from the stock solution and used immediately.

ZnO: 5mg of ZnO nano-powder was weighted and dissolved in 5 ml of 20 mM MOPS (pH 7.0), sonicated for 30 minutes to ensure complete solubility, and thereafter filter-sterilized to obtain 1000µg/ml ZnO stock solution. Different concentrations (1 µg/ml to 50 µg/ml) were made from the stock solution and used immediately. When not used, the stock solution was kept at room temperature and devoid of sunlight.

Then 0.9 mL of different concentrations of ZnCl2 and ZnO were mixed with 100 µL of certain cell dilution (approximately 10 6 colonies forming units per mL of *E-coli*) in 1.5 mL Eppendorf tubes in quadruplicate. Each well of the 48-well plate was filled with 800µL

of the aforementioned Eppendorf tube content. The incubation temperature and time were 37 °C and 24 h, respectively, with intervals of 1 h.

6.2.5 Antibacterial activity test of ZnO NPs and ZnCl2 by microbiological culturing

The washed bacterial suspensions were diluted at rt to a concentration of either 10^4 CFU ml^{-1} or 10^7 CFU ml^{-1} using 20 mM MOPS buffer, pH 7.0. Then, 100 µL of the 10^4 or 10^7 CFU m–1 bacterial suspension was added to 900 µl of either the ZnO NP suspension or $ZnCl_2$ solution in the same buffer.

To escape ZnO-linked photocatalytic reactions, the resulting *E. coli* suspensions were incubated in the dark, at room temperature for 1.5 h, under shaking at 85 rpm. All incubated bacterial suspensions were ten-fold diluted. Finally, 100 µl of the suspensions were uniformly spread on the LB agar plates to determine the cell viability. The number of viable bacterial colonies was counted after 24 h incubation at 37°C, followed by the additional check after 48 h. Each set of experiments was repeated three times. The cell viability was expressed as a ratio (%) of colony-forming units (CFU) detected on the plates inoculated with treated and untreated (control) bacterial suspensions. **Figure 6.2** shows the schematic of the antibacterial activity test.

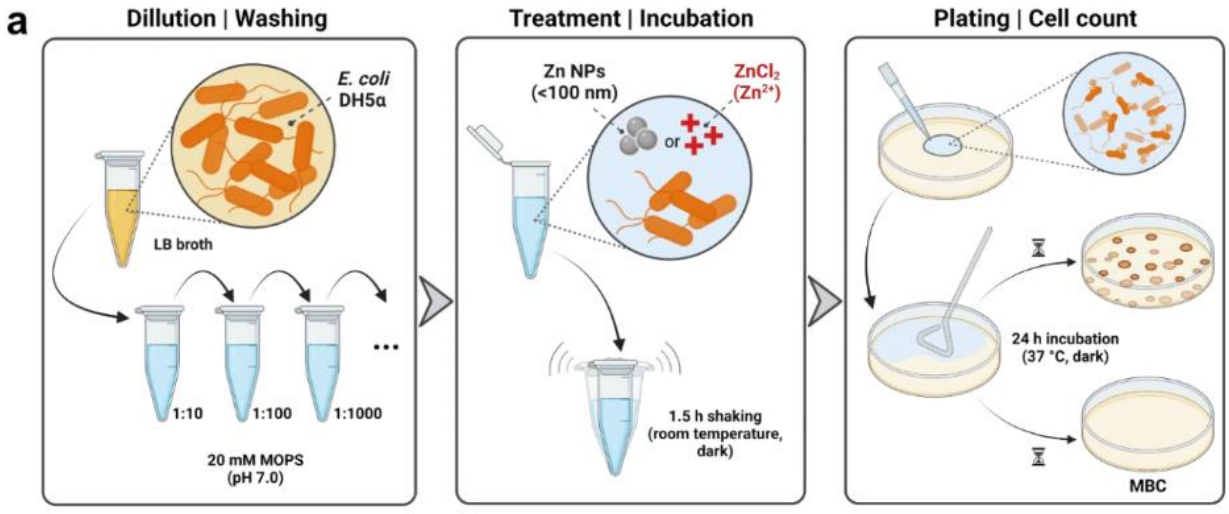

Figure 6.2 (a) Schematic presentation of the antibacterial activity test(Vitasovic et al. 2024).

6.3 Result

The growth curves of E-Coli treated with different concentrations of ZnO and ZnCl2 were determined in 48-flat-bottomed well plates using CLARIOstar Microplate Reader Pred Plus Microplate Reader, Germany and (MARS) Data Analysis Software, **Figure 6.3 A and B** . All the bacterial growth experiments were performed using a Luria–Bertani (LB) medium. The bacteria cultivation procedure was exactly the same as what was already explained in the experimental section. For inoculation, fresh overnight cultures were prepared in 50 mL sterilized tubes with closed caps at 37°C under constant shaking at 180 rpm and used as the inoculum. The wells were inoculated with an initial OD 600 = 0.1, which corresponded to roughly 10^6 colony-forming units (CFU) per mL. Absorbance was measured at 600 nm (OD 600), and the experiments were performed in four independent biological replicates, with the results presented as mean ± standard deviation (SD).

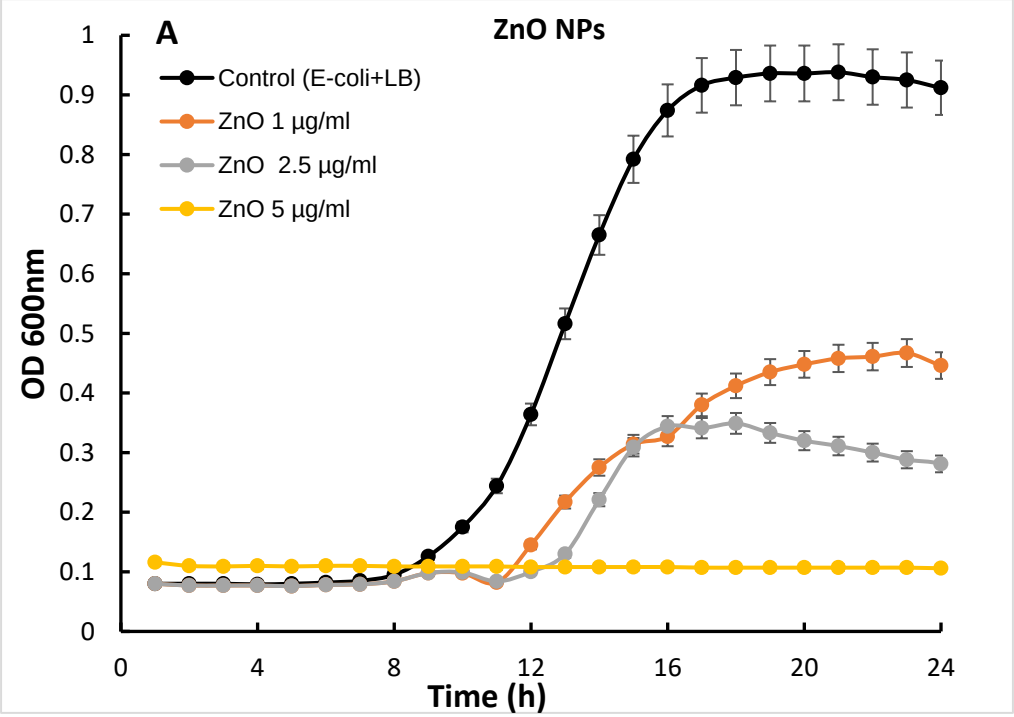

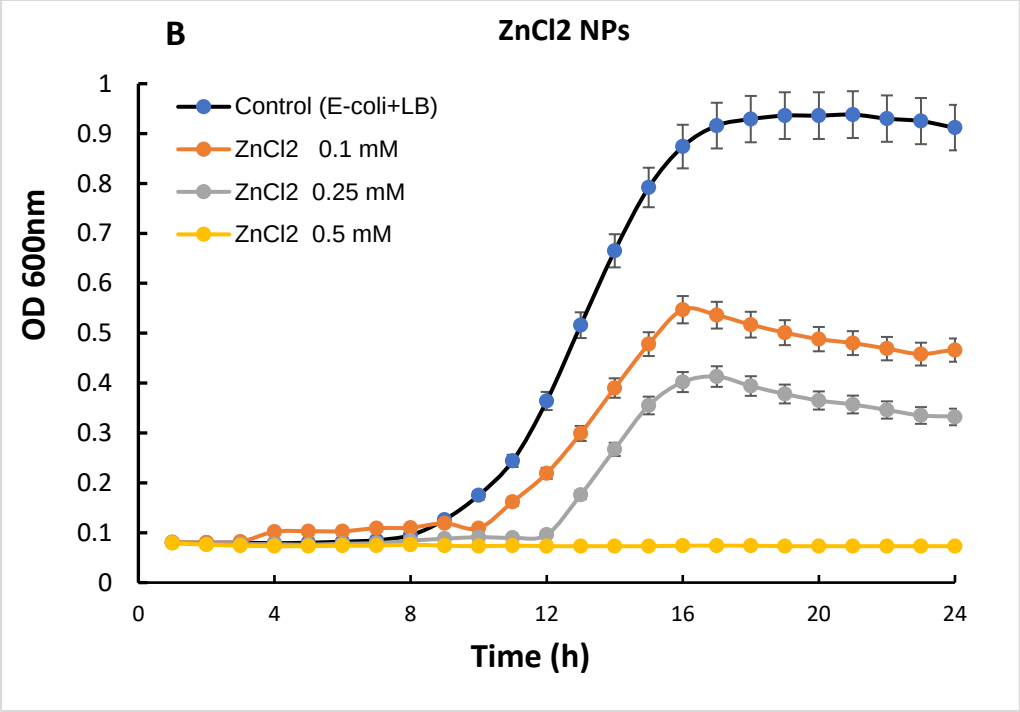

Figure 6.3 Planktonic growth of *E-coli* over 24 h at different concentrations of **A**) ZnO NPs **B**) ZnCl2. Number of independent biological replicates = 4.

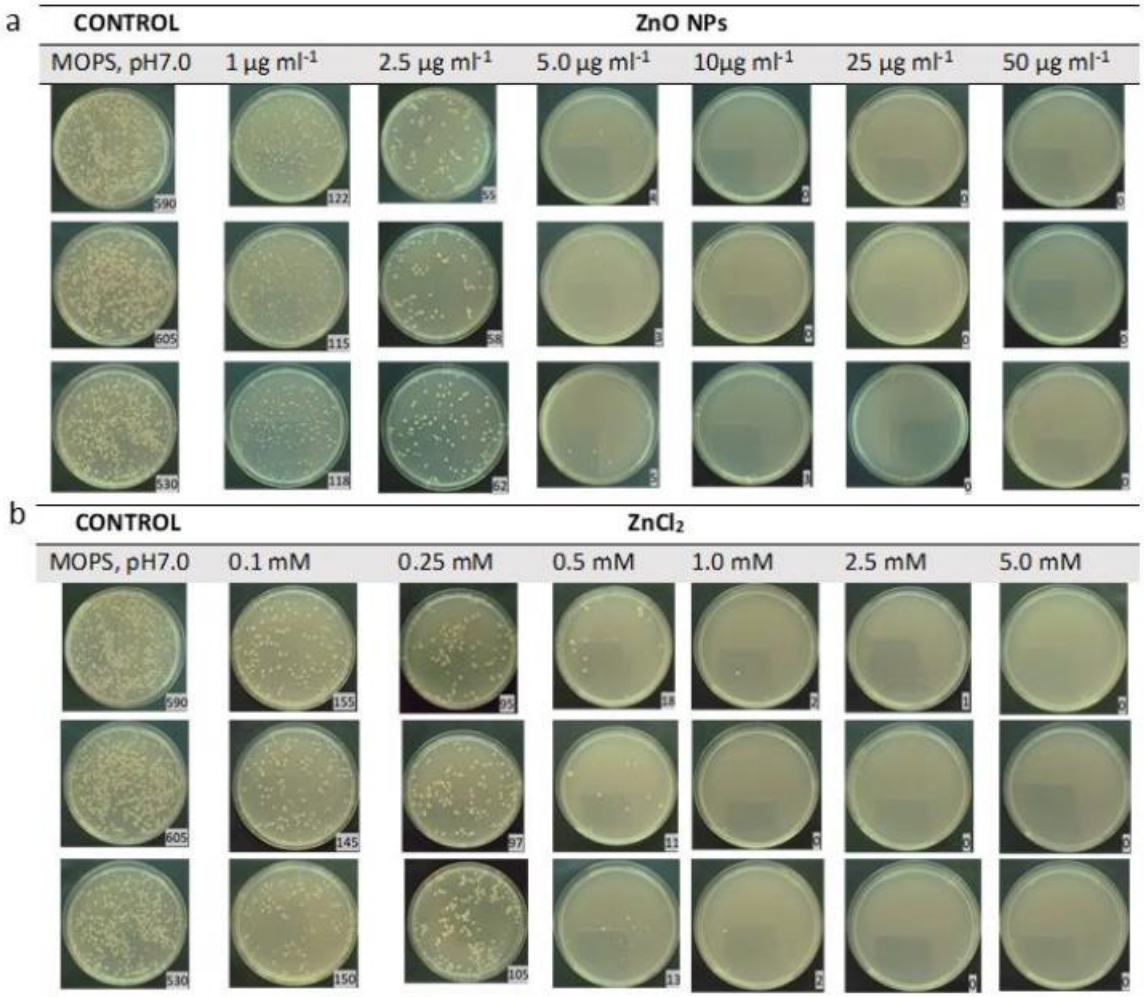
a
CONTROL
ZnO NPs
MOPS, pH7.0
1 µg ml-1
2.5 µg ml-1
5.0 µg ml-1
10µg ml-1
25 µg ml-1
50 µg ml-1
b
CONTROL
ZnCl2
MOPS, pH7.0
0.1 mM
0.25 mM
0.5 mM
1.0 mM
2.5 mM
5.0 mM

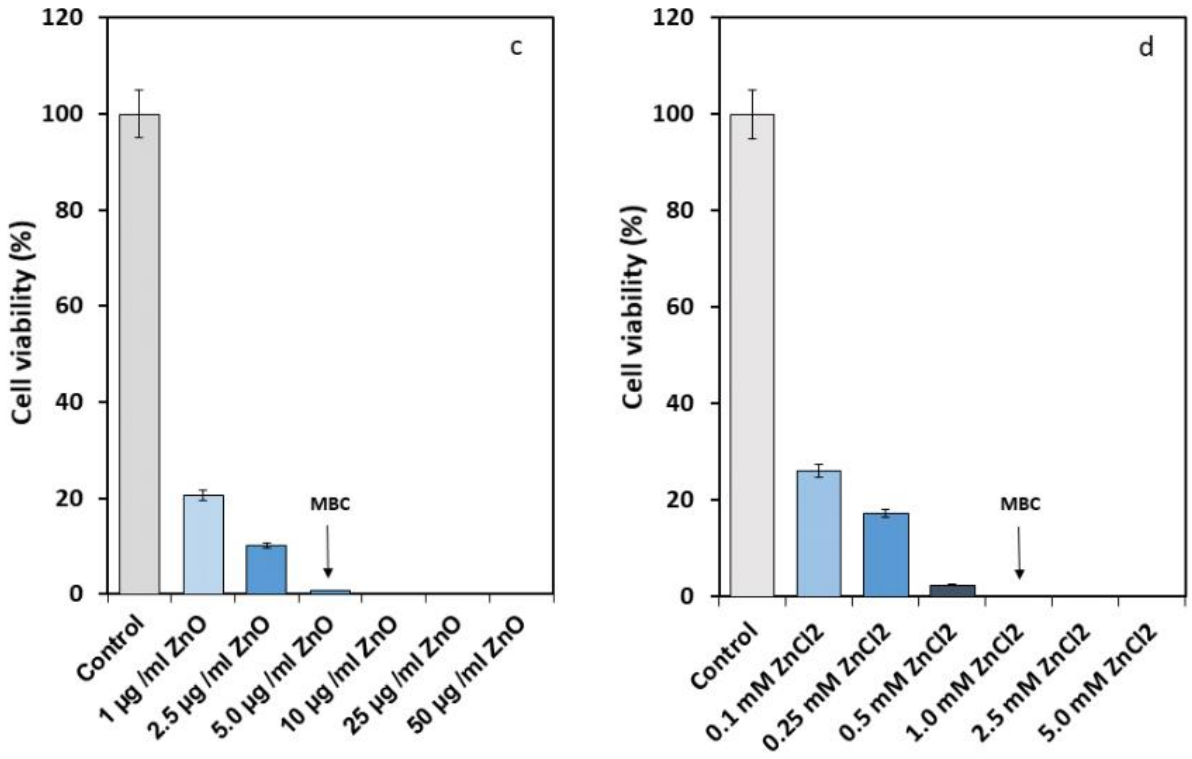

Figure 6.4 Biocidal action of (a, c) ZnO NPs (≤100 nm) and (b, d) ZnCl2 against E. coli. Prior to plate inoculation, (1.1 ± 0.2) ×106 CFU ml−1 bacterial samples were incubated with different concentrations of ZnCl2 for 1.5 h, at rt, in the dark and under shaking at 85 rpm. After inoculation, bacterial samples were incubated for 24 h on LB agar plates at 37°C. NB: No further change in the CFU count was observed after 48 h. (c, d) Data on cell viability are shown as mean values, and standard deviations are for triplicate samples (n = 3). MBC: the minimal biocidal concentration. Due to the high concentration of bacteria (~106), all biocide-treated samples were diluted 10 times prior to incubation on an agar plate.

6.4 Conclusion

The biocidal response of ZnO NPs and Zn^{2+} ion towards *E. coli* was investigated under identical conditions, excluding their non-specific interactions with media, by microbiological culturing in the dark. The minimal biocidal concentration of both agents was lower than previously reported, 5 µg ml^{-1} (or 0.06 mM if totally dissolved) ZnO NPs

(<100 nm) and 0.5 mM (or 41 µg ml^{-1} if transformed to ZnO) ZnCl2 and comparable with the internal cellular content of Zn^{2+}. It seems that the Antimicrobial action of Zn^{2+} ions correlated with the formation of amorphous ZnO/Zn(OH)x nanocomposites inside the bacterial cells, triggered by the pH change from pH 7.0 (the external media) to pH 7.7 (the internal pH of *E.coli*). This hypothesis was supported by *in vitro* studies and analysis of in vivo formed precipitates and their composition, which was done later in this research.

6.5 Outcome

Antibacterial Action of Zn2+ Ions Driven by the In Vivo Formed ZnO Nanoparticles

Toni Vitasovic, Giada Caniglia, Neda Eghtesadi, Marcel Ceccato, Espen Drath Bojesen, Ulrich Gosewinkel, Gregor Neusser, Ulrich Rupp, Paul Walther, Christine Kranz, and Elena E. Ferapontova* https://doi.org/10.1021/acsami.4c04682

Chapter 7. General Conclusions, limitations, and future plan

7.1 General conclusion

This research focused on studying the impact of a selected deep eutectic solvent (DES) mixture on the growth, biofilm formation, and electroactivity of *Bacillus subtilis* under various conditions. Results of the first part of this study showed that at low concentrations (55 mM) of DES composition containing ChCl compound (choline chloride/glycerol (1:2 mol/mol), this DES mixture enhances planktonic growth without altering the growth pattern. In contrast, higher concentrations (>110 mM) induce pseudo-diauxic growth. This behavior was consistent with the choline chloride metabolization that was shown at 18 and 36 mM when the choline chloride was administered alone. On the other hand, neither the growth curve pattern nor cell growth over a period of 48 hours are significantly altered by glycerol alone. Interestingly, the DES mixture exhibits negligible effects on biofilm concentration, while choline chloride independently increases biofilm biomass at

concentrations exceeding 36 mM. Similarly, glycerol has a minimal impact on biofilm biomass in a nutrient broth medium.

The study further reveals choline chloride's role in promoting electroactivity within the DES concentration range of 55-547 mM. Notably, the highest charge output was achieved with choline chloride additions at 36 and 73 mM, even higher than the effects of 2-HNQ, implying a unique role of choline chloride in the extracellular electron transfer (EET) process. These findings suggest that DES formulations, such as choline chloride/glycerol (1:2 mol/mol), can be incorporated at non-toxic concentrations to bolster the electroactivity of weak electricigens like *B. subtilis*.

Based on the findings of the first part of the study, the second part of this research was mainly focused on the role of ChCl as a precursor of glycine betaine, which is a compatible osmolyte in osmoregulation and enhancing electroactivity through regulating ionic flow and inducing transmembrane potential. Moreover, the Osmoprotective effect of ChCl-based DESs and glycine betaine on *B. subtilis* was studied. The combined presence of inorganic salts (NaH2PO4 and KH2PO4) and 40 mM DES (D-sorbitol/ChCl, 1:1 mol/mol) enhances biofilm production under static anoxic conditions. The positive impact is attributed to sorbitol acting as a secondary carbon source and a carbon pool for extracellular polymeric substance synthesis. Additionally, choline chloride, as a precursor to the osmoprotective agent glycine betaine, mitigates osmotic stress in the presence of salts.

Bioelectrochemical experiments indicate that choline chloride has a small positive effect on charge output when salts are present. However, at higher concentrations (above 200 mM for DES and 2% wt/wt for salts), both DES and salts inhibit planktonic growth, suggesting that DES does not alleviate osmotic stress on planktonic growth.

In conclusion, the addition of choline chloride or choline chloride-containing DES at low concentrations enhances biofilm formation and mitigates osmotic stress, offering potential improvements for bioelectrochemical processes such as electro-fermentation, particularly in media with concentrated electrolytes. These findings underscore the multifaceted role of DES in microbial growth and electroactivity, presenting new avenues for optimizing bioelectrochemical systems.

The outcomes of this thesis provide an optimistic approach to enhancing *B. subtilis* electroactivity and bioproduction of its high-added-value metabolites under electrofermentative conditions. The addition of DESs to the electrolyte medium as biocatalysis has a good potential to provide a suitable environment for the enzyme/substrate reaction, likely due to complex hydrogen bonding.

DESs show promising effects as biocatalysis and provide a suitable environment for the enzyme/substrate reaction, mostly due to the complex hydrogen bonding of their structure.

7.2 Limitations and recommendations for future work

- Although this research investigated several DESs and their components, future studies on different DESs and configuration designs could enhance the applicability and comprehensiveness of this study. Moreover, designing a large-scale electrochemical system can examine the real-world application of DESs in the biosynthesis process through whole-cell catalysts.
- Despite the high sensitivity of SPEs in the detection and monitoring of biofilm, their small surface area may affect the result of biofilm formation and its comparability with large-scale
- Biofilm microstructure could exhibit significant variations between smooth and porous electrodes, potentially influencing the production of biopolymers and metabolites. In future work, the effect of electrode surface on the biofilm formation and electroactivity can be studied.
- A larger surface area is likely to promote greater biofilm formation, consequently enhancing electrochemical output. Therefore, the current densities of a typical three-electrode system and an SPE could differ significantly due to variations in surface area and structural design. The correlation between surface area and electroactivity enhancement can be investigated in future work.

- **Experimental Conditions**: The conditions under which the DESs were studied could be modified. Future studies can explore variations in temperature, pH, and other environmental factors that could influence their efficacy.

- **The molecular mechanisms** through which DESs, particularly choline chloride, enhance electroactivity remain insufficiently characterized. The hypotheses proposed need further validation through more detailed biochemical and molecular analyses.

- **Incorporating in-situ analytical techniques** into our research will enable us to observe the immediate effects of DESs on *B. subtilis* biofilms, capturing dynamic processes and transient states that would otherwise be overlooked by ex-situ methods. This real-time monitoring is crucial for gaining a deeper understanding of the mechanisms by which DESs enhance electroactivity and for optimizing their application in biofilm-based electro-fermentation processes. By leveraging the strengths of both single-entity electrochemical techniques and in-situ analytical methods, we can achieve a more precise and comprehensive understanding of the electrochemical and biochemical interactions within *B. subtilis* biofilms.

- **Applying a biohybrid electrochemical system setup** to immobilize electro-active microbes within polymer matrices. This method suggests the formation of homogeneous and robust biofilm on the electrode surface, which is critical in EF systems. The biofilm can be readily engineered to maintain a thin structure, maximizing the surface-to-volume ratio. The biofilm formation of *B. subtilis* can be enhanced through the application of a biohybrid model. The suggested biohybrid electrochemical system shows high resistance to oxygen exposure. This system exhibits a distinctive anoxic zone near the electrode surface, even under rigorous air sparging conditions, making it particularly advantageous for industrial and large-scale applications.

- **Strain engineering of Bacillus subtilis to enhance biofilm formation** can be another promising approach to improve biofilm formation and, consequently, Electroactivity enhancement. As biofilms could facilitate better electron transfer and metabolic activity. Genetic modifications can be employed to upregulate genes involved in biofilm formation, such as those encoding extracellular matrix components like polysaccharides, proteins, and DNA. Additionally, pathways

regulating cell adhesion and communication can be optimized to promote robust biofilm development. The engineered *B. subtilis* strains can subsequently be utilized in our system to investigate their potential impact on enhancing performance outcomes.

Appendixes

Appendix A

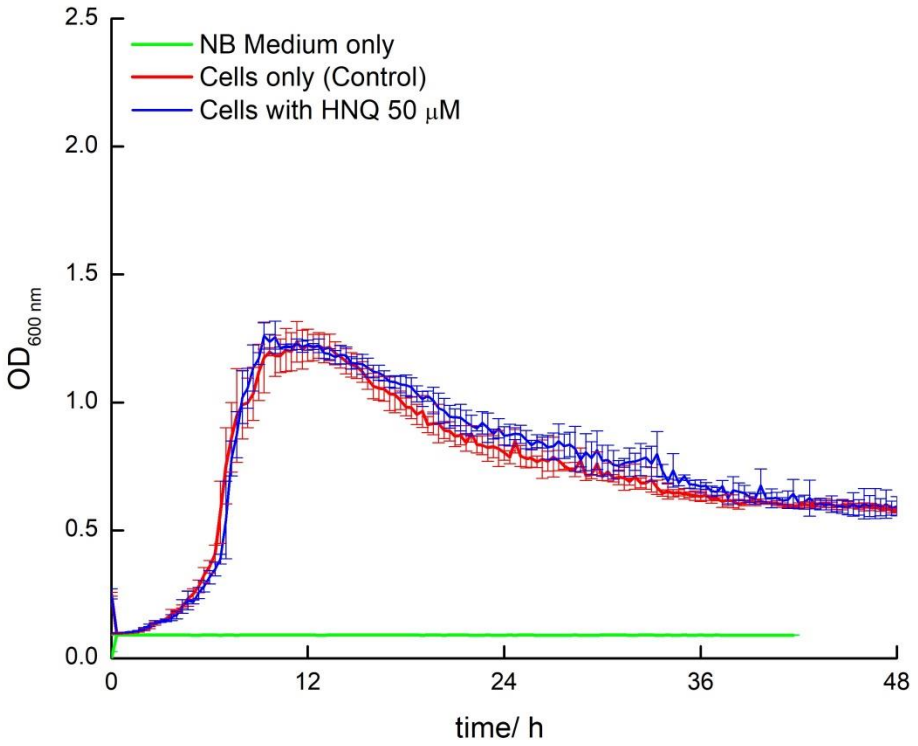

Appendix 4.1 Comparison between planktonic growth of B. subtilis over 48 h in presence and absence of 50μM 2-hydroxy-1,4-naphthoquinone (HNQ) as mediator. NB medium (without bacteria) was used as a negative control. Number of independent biological replicates = 4.

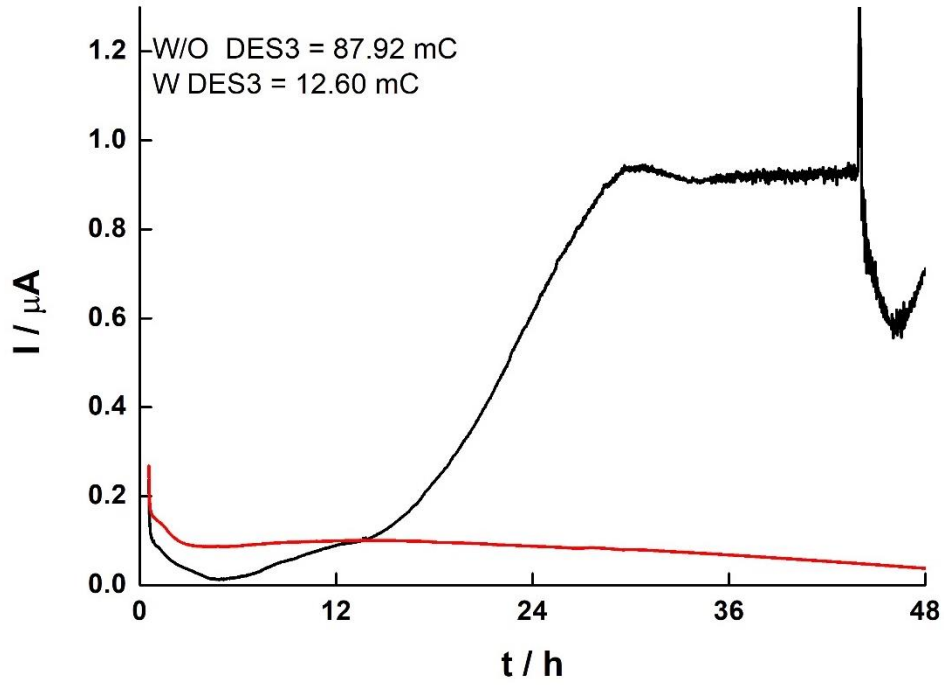

Appendix 4.2 Chronoamperometric traces of *B. subtilis* in the presence of 50% w/w (red trace) and without DES3 (black trace). Both experiments were inoculated to a final OD_{600} = 1 (approximately 10^7 cfu mL^{-1}). Both growth and extracellular respiration are negatively impacted at 50% w/w DES3 (red trace).

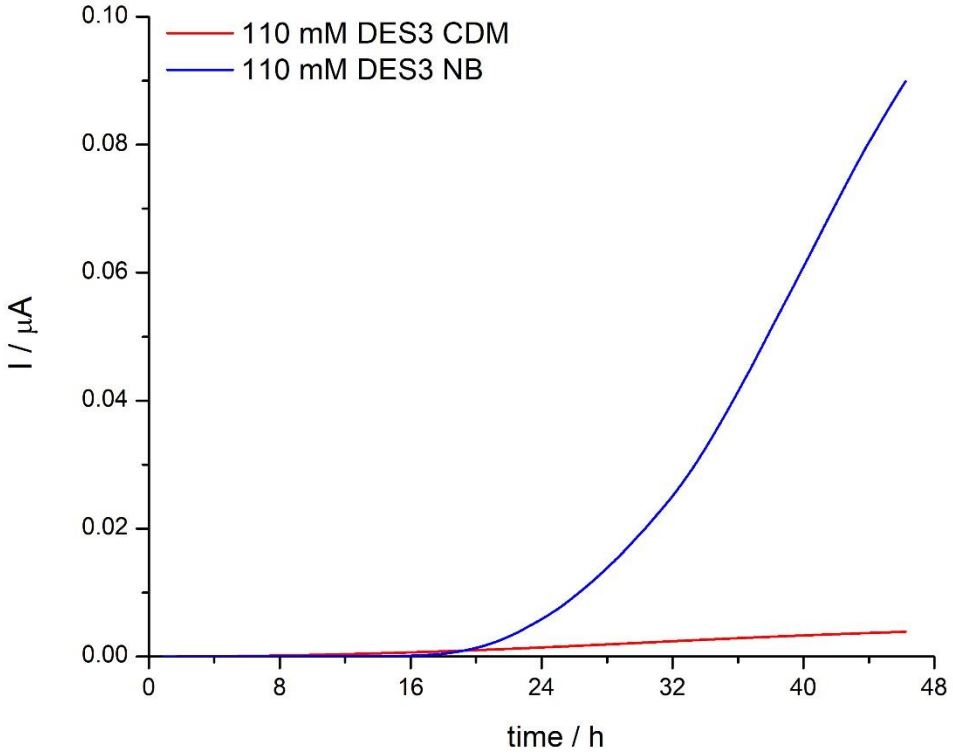

Appendix 4.3 Chronoamperometric traces of *B. subtilis in* NB and CDM medium in the presence of 110 mM DES3. Current production in the NB was much higher.

Cyclic voltammetry plots of DES 3 treated *B. subtilis* (110 and 219 mM DES in NB) showed a pattern of oxidation and reduction cycles that clearly define an electroactive system. CV plots are good indicators of electroactivity in bacteria as they determine the various redox peaks from oxidation and reduction cycles. Peak intensity and position are vital in determining specific electroactivity profile of the organism. The CV plots (Appendix 4.4) showed a marked increase in cycle width from 0h to 48h, indicating a rise in electroactivity with increased proliferation of cells. The CV of control experiments without cells showed no current production as a near zero current output was observed (purple dashed line). As cells grew, current production increased as subsequently indicated

in the increased width of the curves. There were also noticeable differences between the CV plots of 110 mM and 219 mM DES treatments. The varied positions of voltage peaks were indicative of differences in electroactive signatures resulting from inducements of different electroactive mechanisms elicited by the varied concentrations of DES.

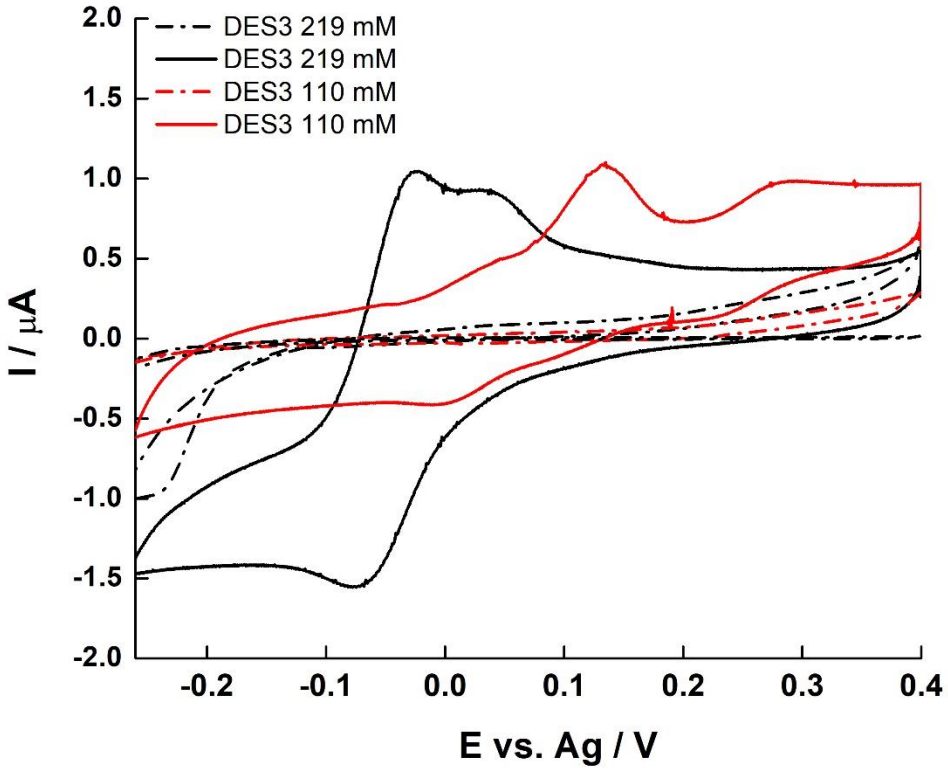

Appendix 4.4 Cyclic voltammograms of NB-grown *B.subtilis* with 110 mM and 219 mM DES3. Purple dashed lines represent control; red and black dashed lines represent CV plots at 0h; and continuous lines represent CV plots at 48 h.

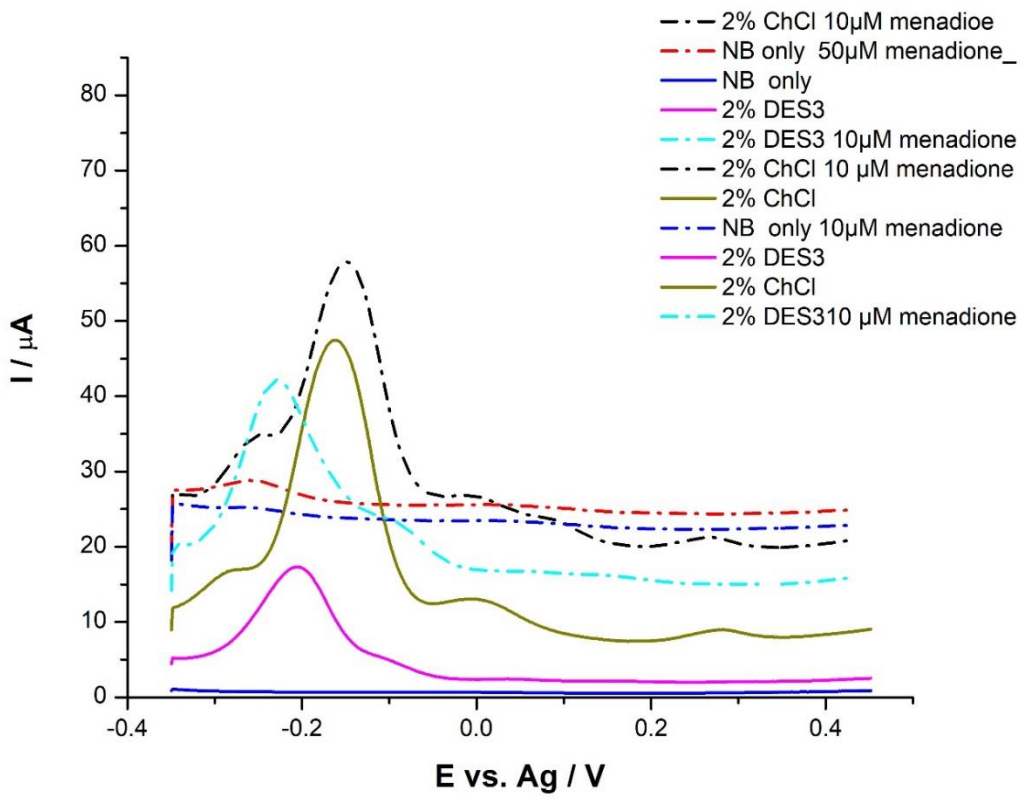

Appendix 4.5: Selected DPV curves of supernatants after 48 h of growth at 0.4 V vs. Ag.

Almost all peaks belong to the 2%ChCl and 2% DES3 supernatants, are negatively charged, and are in the range of -0.4 to 0. The current output after the addition of 10µM Menadione increased significantly. This could be due to the formation of quinone in the metabolization of ChCl and DES3. Also, the addition of 50µM menadione to the medium increased the electron activity.

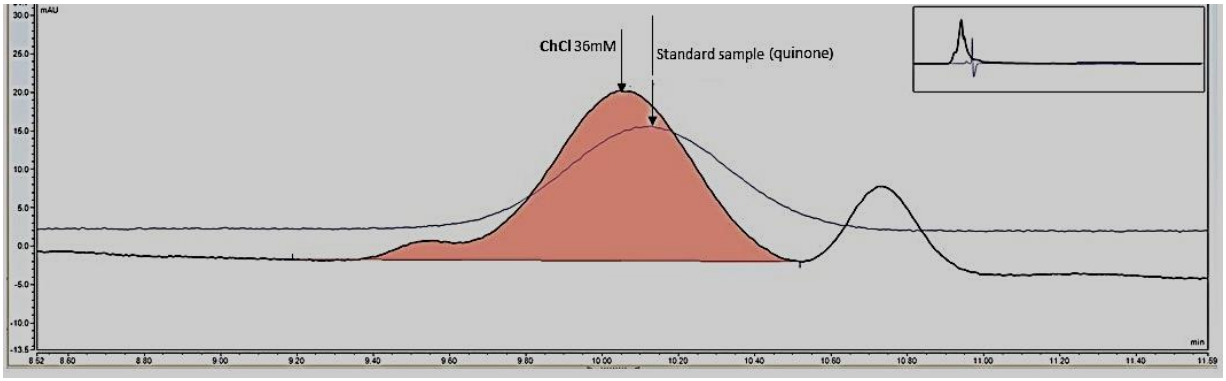

Appendix 4.6: Menadione peak in the sample containing 36mM ChCl

Appendix B

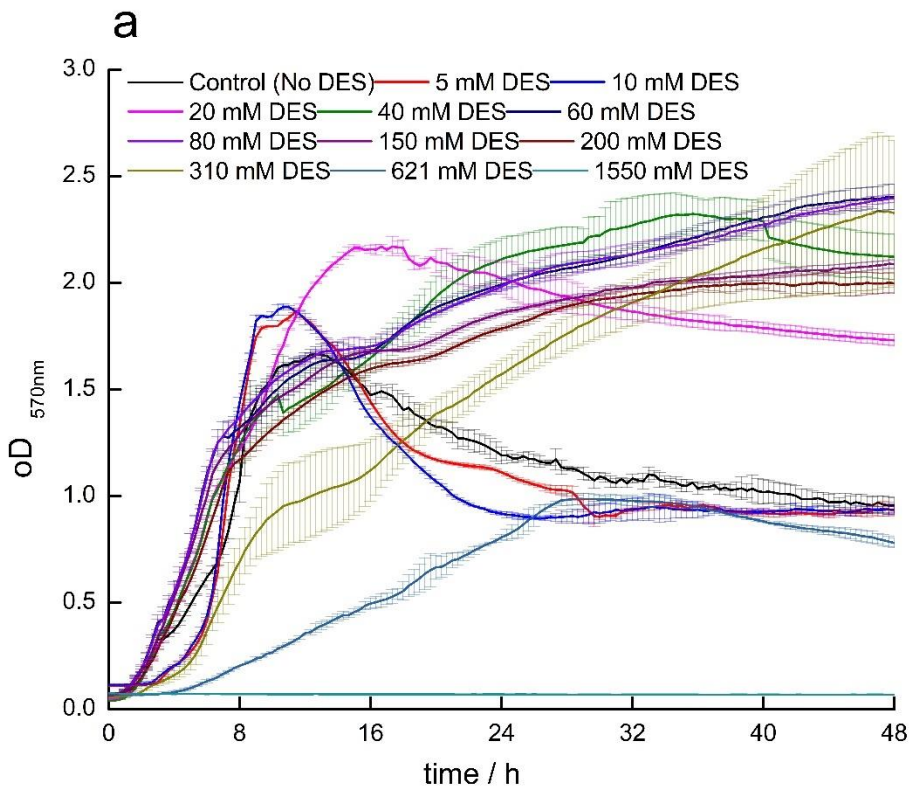
a
Control (No DES)
5 mM DES
10 mM DES
20 mM DES
40 mM DES
60 mM DES
80 mM DES
150 mM DES
200 mM DES
310 mM DES
621 mM DES
1550 mM DES
oD 570nm
time / h
0.0
0.5
1.0
1.5
2.0
2.5
3.0
0
8
16
24
32
40
48

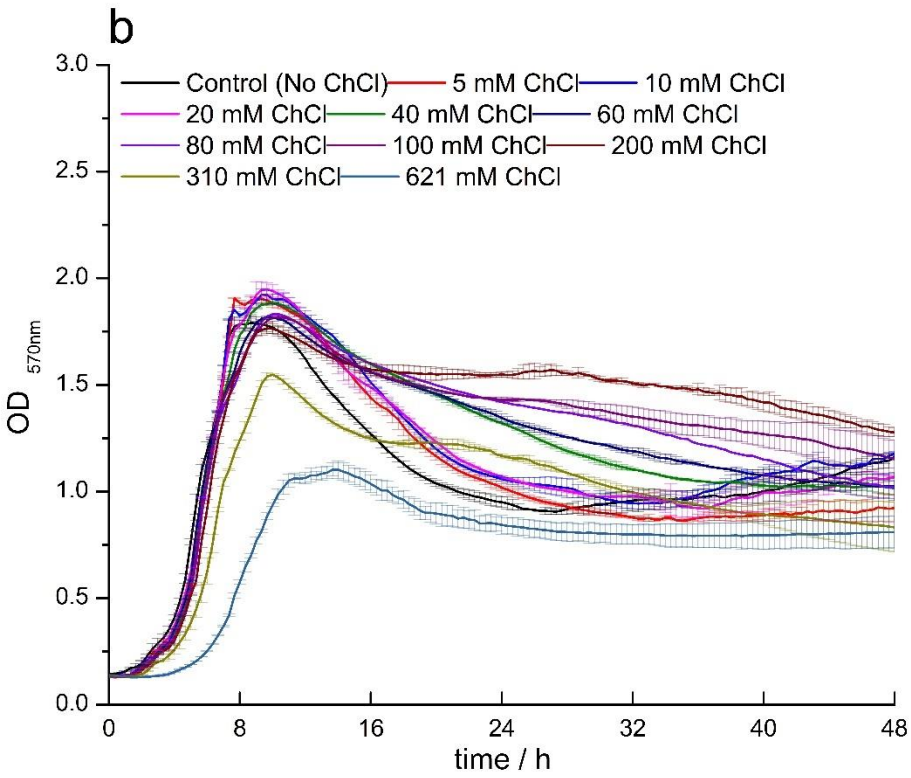
b
Control (No ChCl)
5 mM ChCl
10 mM ChCl
20 mM ChCl
40 mM ChCl
60 mM ChCl
80 mM ChCl
100 mM ChCl
200 mM ChCl
310 mM ChCl
621 mM ChCl
OD 570nm
3.0
2.5
2.0
1.5
1.0
0.5
0.0
0
8
16
24
32
40
48
time / h

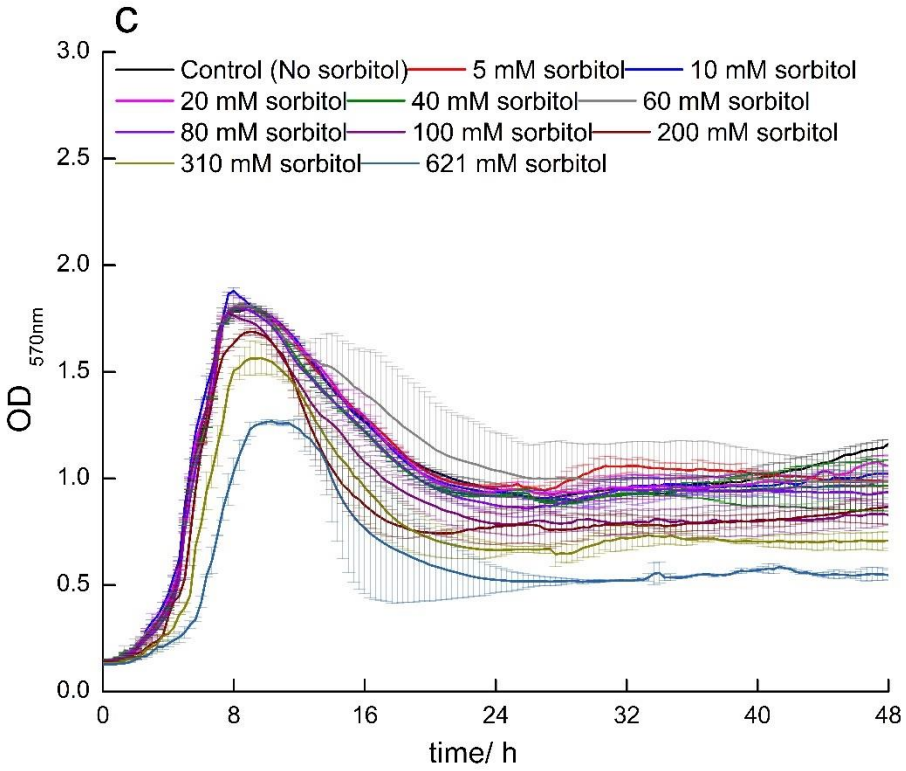
C
Control (No sorbitol)
5 mM sorbitol
10 mM sorbitol
20 mM sorbitol
40 mM sorbitol
60 mM sorbitol
80 mM sorbitol
100 mM sorbitol
200 mM sorbitol
310 mM sorbitol
621 mM sorbitol
OD 570nm
3.0
2.5
2.0
1.5
1.0
0.5
0.0
0
8
16
24
32
40
48
time/ h

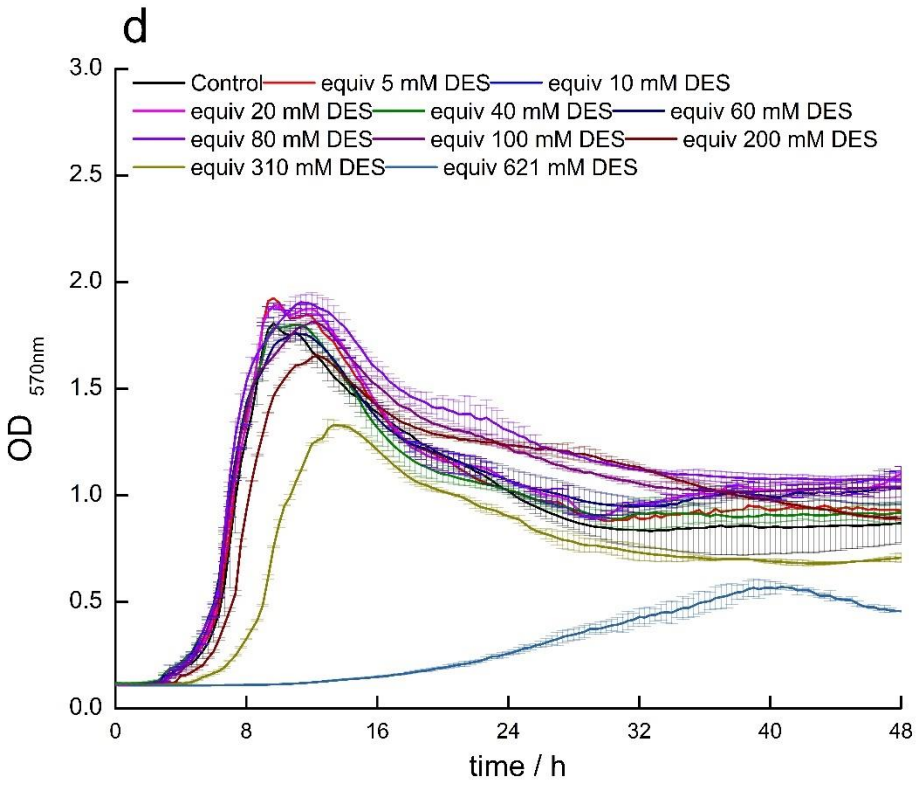

Appendix 5.1: Planktonic growth of *B. subtilis* over 48 h at different molar concentrations of a) DES (D-sorbitol/ChCl 1:1 mol mol−1); b) ChCl; c) D-sorbitol; d) equivalent concentration of (D-sorbitol + ChCl). Number of independent biological replicates = 4.

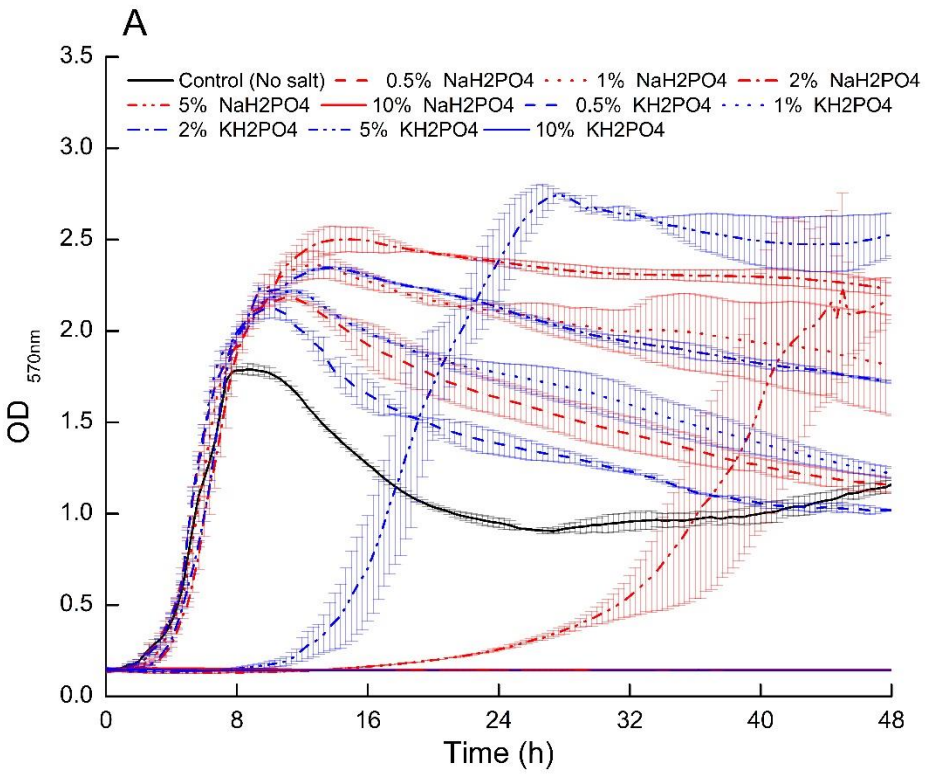
A
Control (No salt)
0.5% NaH2PO4
1% NaH2PO4
2% NaH2PO4
5% NaH2PO4
10% NaH2PO4
0.5% KH2PO4
1% KH2PO4
2% KH2PO4
5% KH2PO4
10% KH2PO4
OD 570nm
Time (h)
0.0
0.5
1.0
1.5
2.0
2.5
3.0
3.5
0
8
16
24
32
40
48

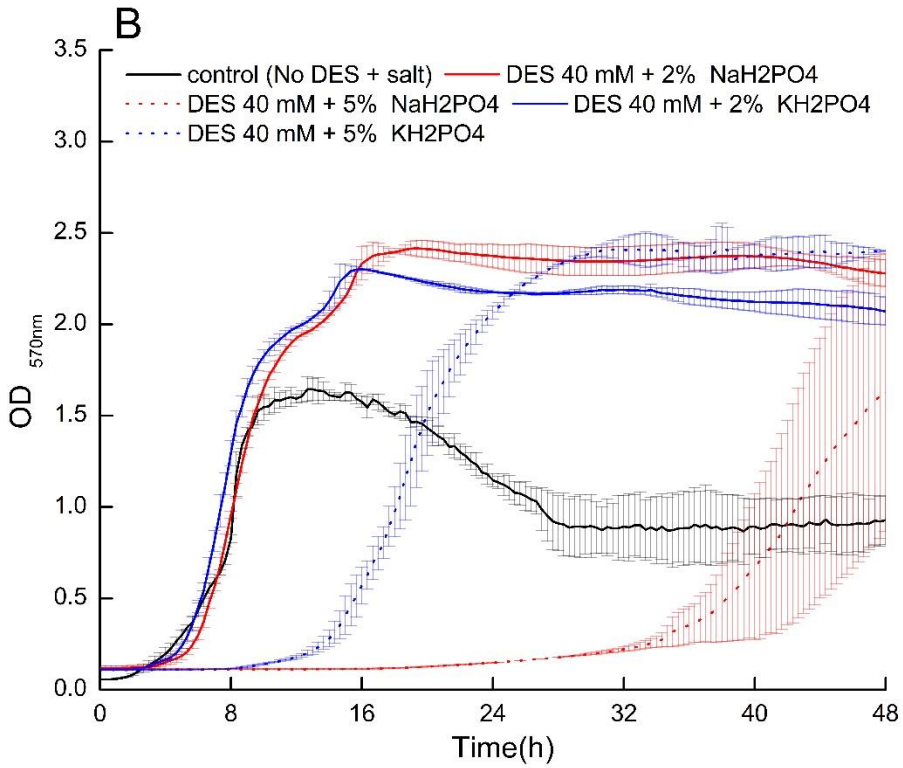

Appendix 5.2: Planktonic growth of *B. subtilis* in the presence of A) increasing concentrations of NaH_2PO_4 and KH_2PO_4 (wt/wt); B) 2 and 5 % wt/wt of NaH_2PO_4 and KH_2PO_4 with 40 mM DES. Number of independent biological replicates = 4.

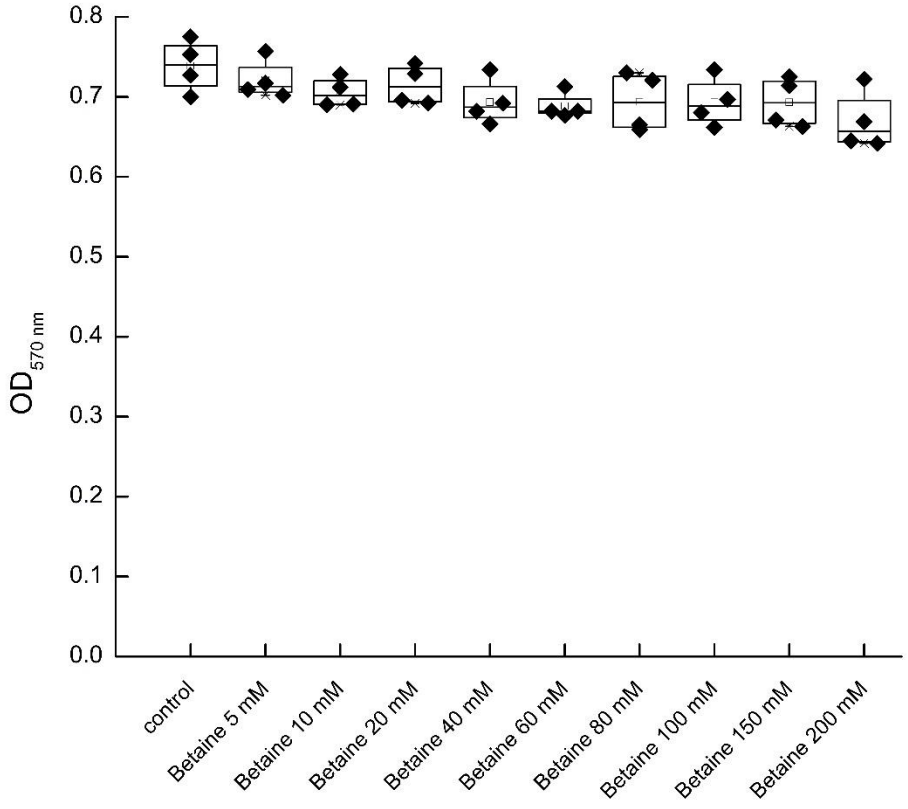

Appendix 5.3: *B. subtilis* biofilm formation in the presence of various concentrations of betaine anhydrous.

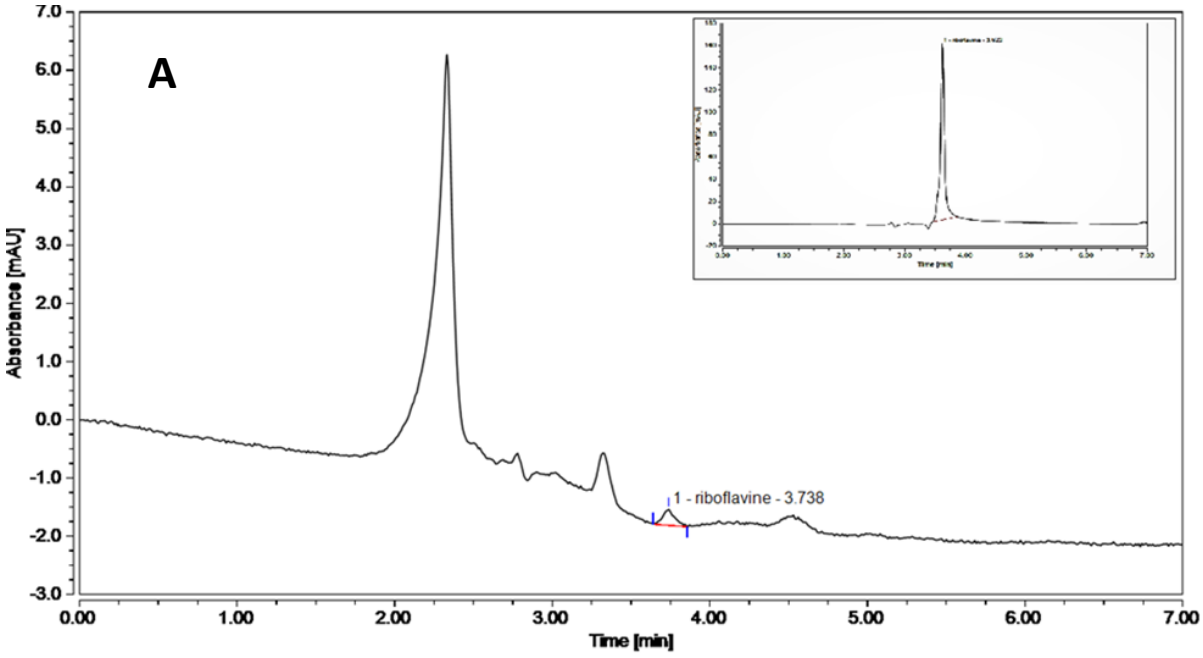
A
Absorbance [mAU]
Time [min]
1 - riboflavine - 3.738

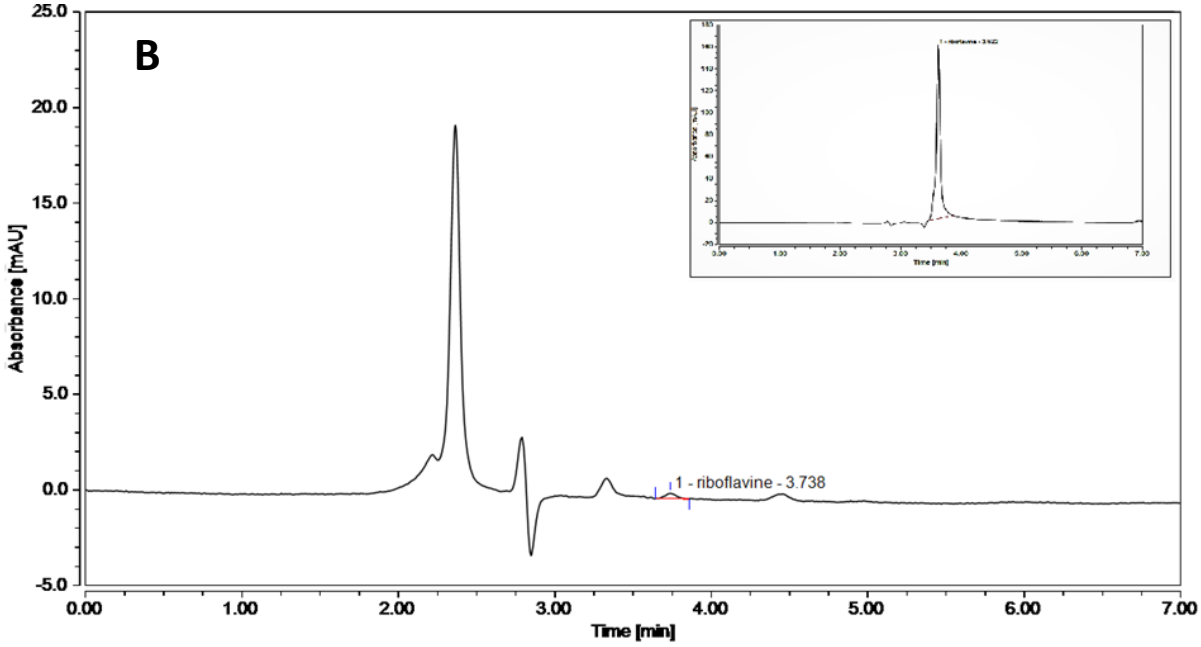
B
Absorbance [mAU]
Time [min]
1 - riboflavine - 3.738

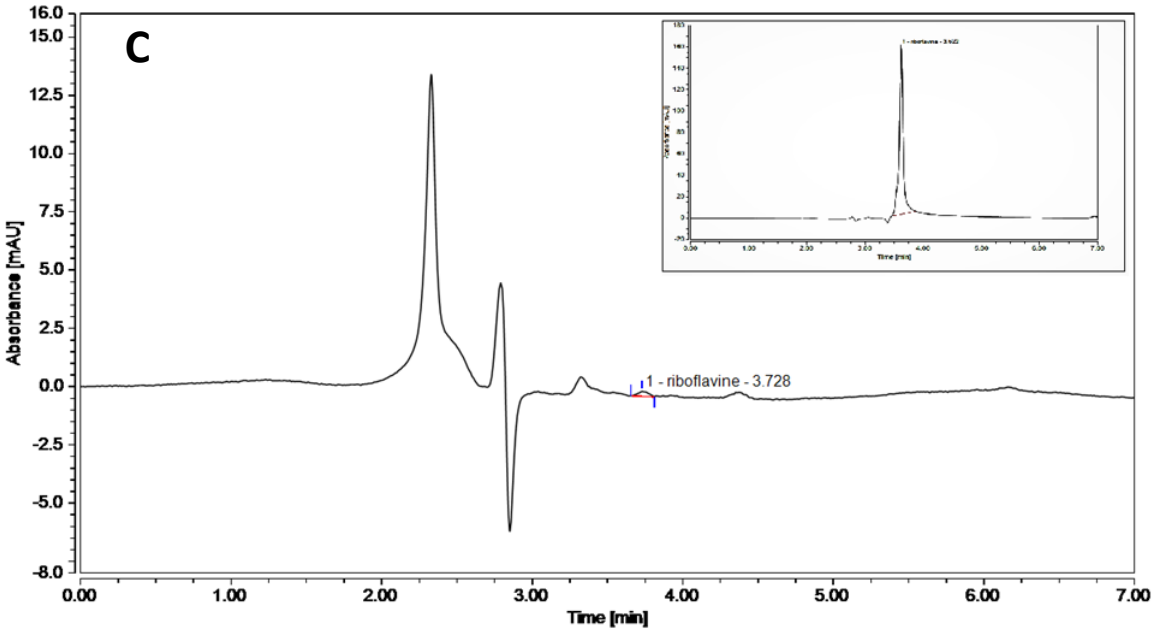

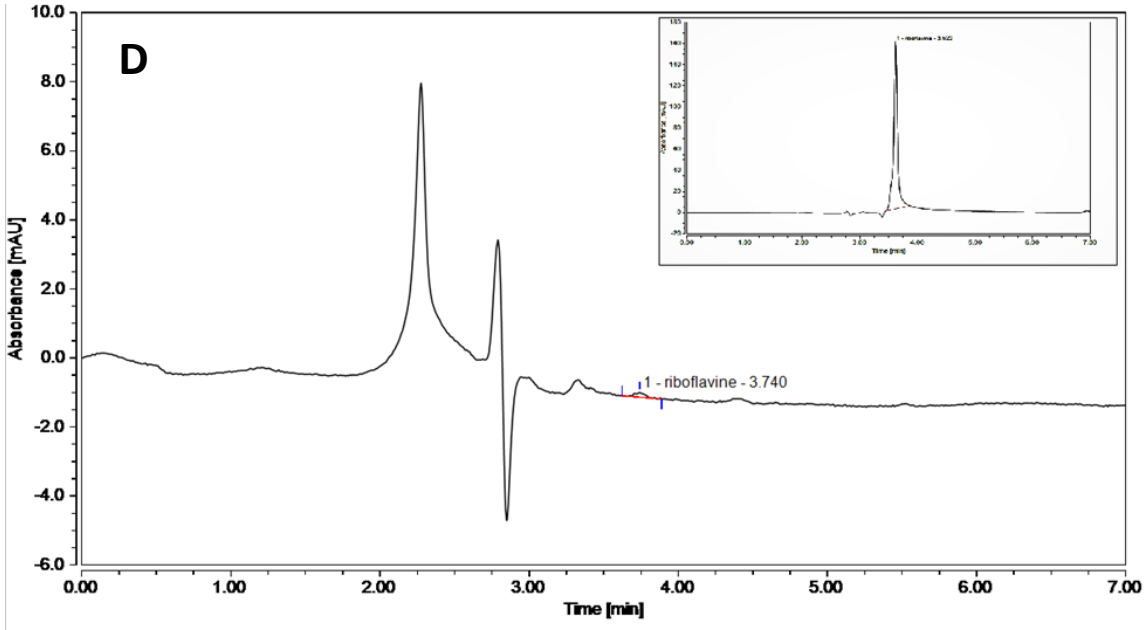

Appendix 5.4: Riboflavin peak detection in the supernatants (A) cell only (B)DES 40 mM (C) ChCl 40Mm (D) ChCh 40mM+2%NaH2PO4. The standard peak for riboflavin is presented in the inset.

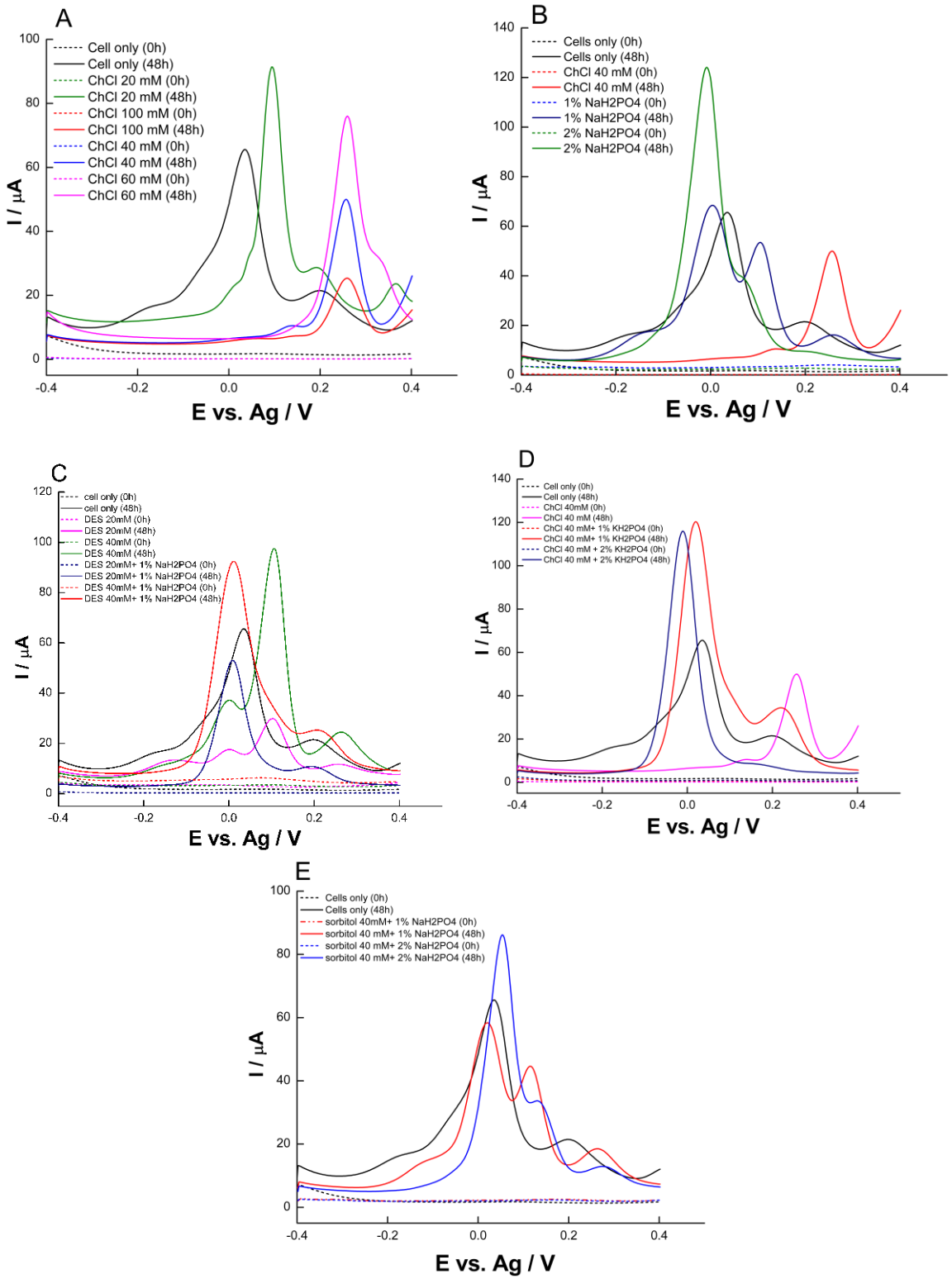

Appendix 5.5: DPV analysis of the selected condition at 0 h and after 48 h of growth at 0.4 V for various treatment conditions.

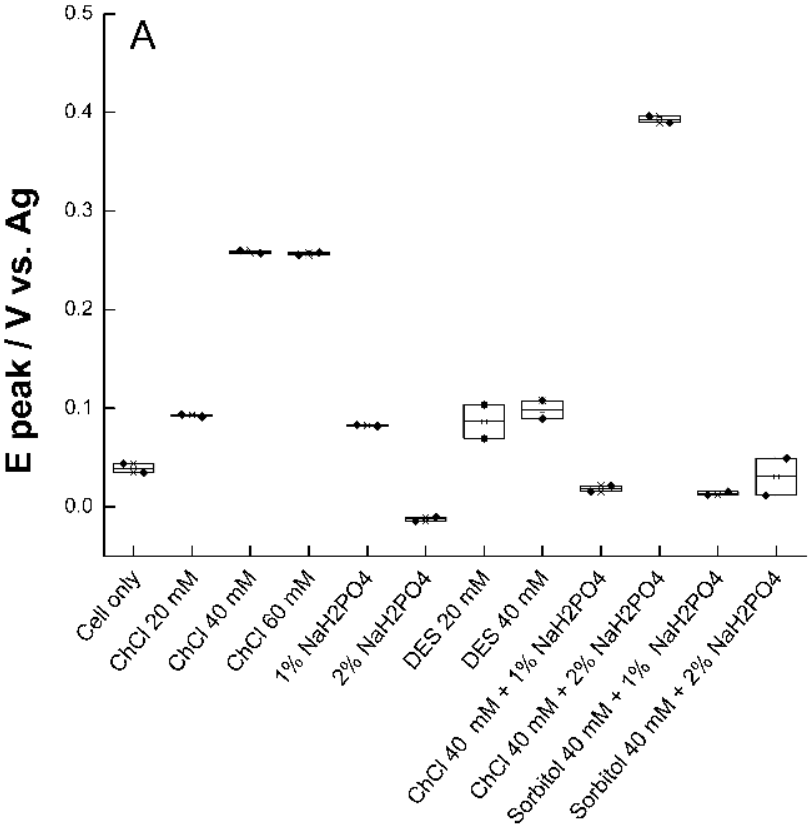

Appendix 5.6: Peak position of DPV at E = 0.4 vs. Ag. for treated *B. subtilis* samples

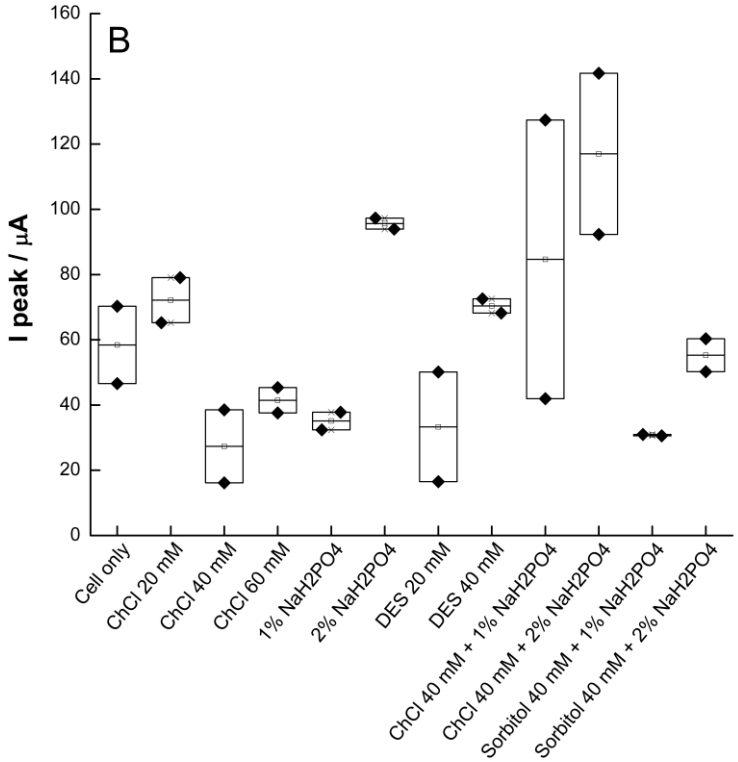

Appendix 5.7: Peak intensity (B) of DPV at E = 0.4 vs. Ag. for treated B. subtilis samples

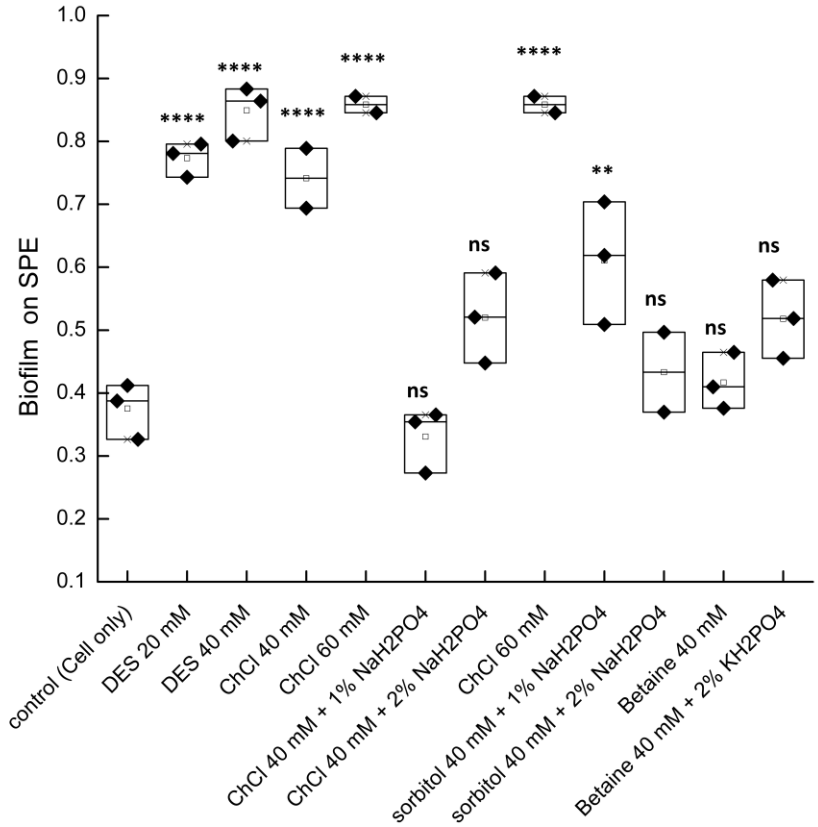

Appendix 5.8 Biofilm on SPE coverage obtained from crystal violet staining immediately after electrochemical experiments. Number of independent biological replicates =3

Appendix 5.9 One-way ANOVA followed by Tukey's test on effect of the test compound on biofilm formation of *B. subtilis*.

Descriptive statistics

	Sample Size	*Mean*	*Standard Deviation*	*SE of Mean*
control	*4*	*1.63115*	*0.12422*	*0.06211*
DES 5mM	*4*	*1.989*	*0.12459*	*0.0623*
DES 10mM	*4*	*2.11475*	*0.22541*	*0.11271*
DES 20mM	*4*	*2.217*	*0.17356*	*0.08678*
DES 40mM	*4*	*2.407*	*0.10927*	*0.05464*
DES 60mM	*4*	*2.7885*	*0.16478*	*0.08239*
DES 80mM	*4*	*2.84725*	*0.17118*	*0.08559*
DES 100mM	*4*	*2.91075*	*0.15689*	*0.07845*

Overall ANOVA

	DF	*Sum of Squares*	*Mean Square*	*F Value*	*Prob>F*
Model	*7*	*5.90375*	*0.84339*	*32.92933*	*8.2844E-11*
Error	*24*	*0.61469*	*0.02561*		

Total	*31*	*6.51845*

Null Hypothesis: The means of all levels are equal.

Alternative Hypothesis: The means of one or more levels are different.

At the 0.05 level, the population means are significantly different.

Tukey's post hoc test for comparison of means

	MeanDiff	*SEM*	*q Value*	*Prob*	*Alpha*	*Sig*	*LCL*	*UCL*
DES 5mM vs. control	*0.35785*	*0.11316*	*4.47206*	*0.06873*	*0.05*	*0*	*-0.01694*	*0.73264*
DES 10 mM vs. control	*0.4836*	*0.11316*	*6.04356*	*0.00546*	*0.05*	*1*	*0.10881*	*0.85839*
DES 20 mM vs. control	*0.58585*	*0.11316*	*7.32138*	*6.04306E-4*	*0.05*	*1*	*0.21106*	*0.96064*
DES 40 mM vs. control	*0.77585*	*0.11316*	*9.69581*	*1.05816E-5*	*0.05*	*1*	*0.40106*	*1.15064*
DES 60 mM vs. control	*1.15735*	*0.11316*	*14.46342*	*0*	*0.05*	*1*	*0.78256*	*1.53214*
DES 80 mM vs. control	*1.2161*	*0.11316*	*15.19762*	*0*	*0.05*	*1*	*0.84131*	*1.59089*
DES 100 mM vs. control	*1.2796*	*0.11316*	*15.99118*	*0*	*0.05*	*1*	*0.90481*	*1.65439*

*Sig = 1 indicates that the difference of the means is significant at the 0.05 level; Sig = 0 indicates that the difference of the means is not significant at the 0.05 level.

Appendix 5.10: One-way ANOVA followed by Tukey's test on effect of the test compound on biofilm formation of *B. subtilis*

Descriptive statistics

	Sample Size	*Mean*	*Standard Deviation*	*SE of Mean*
control	*4*	*2.09875*	*0.31412*	*0.15706*
ChCl 5 mM	*4*	*2.69475*	*0.31074*	*0.15537*
ChCl 10 mM	*4*	*2.147*	*0.17586*	*0.08793*
ChCl 20 mM	*4*	*2.18675*	*0.19603*	*0.09802*
ChCl 40 mM	*4*	*2.19825*	*0.37175*	*0.18587*
ChCl 60 mM	*4*	*2.0815*	*0.1818*	*0.0909*
ChCl 80 mM	*4*	*2.13075*	*0.32929*	*0.16465*
ChCl 100 mM	*4*	*2.021*	*0.22811*	*0.11405*

Overall ANOVA

	DF	*Sum of Squares*	*Mean Square*	*F Value*	*Prob>F*
Model	*7*	*1.23473*	*0.17639*	*2.36647*	*0.05458*
Error	*24*	*1.78889*	*0.07454*		
Total	*31*	*3.02362*			

Null Hypothesis: The means of all levels are equal.

Alternative Hypothesis: The means of one or more levels are different.

At the 0.05 level, the population means are significantly different.

Tukey's post hoc test for comparison of means

	MeanDiff	*SEM*	*q Value*	*Prob*	*Alpha*	*Sig*	*LCL*	*UCL*
ChCl 5 mM vs. control	*0.596*	*0.19305*	*4.36606*	*0.08029*	*0.05*	*0*	*-0.04337*	*1.23537*
ChCl 10 mM vs. control	*0.04825*	*0.19305*	*0.35346*	*1*	*0.05*	*0*	*-0.59112*	*0.68762*
ChCl 20 mM vs. control	*0.088*	*0.19305*	*0.64465*	*0.99976*	*0.05*	*0*	*-0.55137*	*0.72737*
ChCl 40 mM vs. control	*0.0995*	*0.19305*	*0.7289*	*0.99945*	*0.05*	*0*	*-0.53987*	*0.73887*

ChCl 60 mM vs. control	*-0.01725*	*0.19305*	*0.12637*	*1*	*0.05*	*0*	*-0.65662*	*0.62212*
ChCl 80 mM vs. control	*0.032*	*0.19305*	*0.23442*	*1*	*0.05*	*0*	*-0.60737*	*0.67137*
ChCl 100 mM vs. control	*-0.07775*	*0.19305*	*0.56957*	*0.99989*	*0.05*	*0*	*-0.71712*	*0.56162*

Appendix 5.11 One-way ANOVA followed by Tukey's test on effect of the test compound on biofilm formation of *B. subtilis*

Descriptive statistics

	Sample Size	*Mean*	*Standard Deviation*	*SE of Mean*
control	*4*	*1.10375*	*0.10102*	*0.05051*
5 mM D-sorbitol	*4*	*2.50775*	*0.1274*	*0.0637*
10 mM D-sorbitol	*4*	*2.8925*	*0.15912*	*0.07956*
20 mM D-sorbitol	*4*	*2.528*	*0.21604*	*0.10802*
40 mM D-sorbitol	*4*	*2.31225*	*0.20374*	*0.10187*
60 mM D-sorbitol	*4*	*2.015*	*0.28826*	*0.14413*
80 mM D-sorbitol	*4*	*1.21275*	*0.03348*	*0.01674*

100 mM D-sorbitol	*4*	*0.89775*	*0.08524*	*0.04262*

Overall ANOVA

	DF	*Sum of Squares*	*Mean Square*	*F Value*	*Prob>F*
Model	*7*	*16.13485*	*2.30498*	*79.68272*	*4.66294E-15*
Error	*24*	*0.69425*	*0.02893*		
Total	*31*	*16.82909*			

Null Hypothesis: The means of all levels are equal.

Alternative Hypothesis: The means of one or more levels are different; at the 0.05 level, the population means are significantly different.

Tukey's post hoc test for comparison of means

	MeanDiff	*SEM*	*q Value*	*Prob*	*Alpha*	*Sig*	*LCL*	*UCL*
D-sorbitol 5mM vs. control	*1.404*	*0.12026*	*16.50995*	*0*	*0.05*	*1*	*1.0057*	*1.8023*
D-sorbitol 10mM vs. control	*1.78875*	*0.12026*	*21.03431*	*4.44118E-8*	*0.05*	*1*	*1.39045*	*2.18705*

D-sorbitol 20mM vs. control	*1.42425*	*0.12026*	*16.74808*	*4.79332E-8*	*0.05*	*1*	*1.02595*	*1.82255*
D-sorbitol 40mM vs. control	*1.2085*	*0.12026*	*14.21102*	*0*	*0.05*	*1*	*0.8102*	*1.6068*
D-sorbitol 60mM vs. control	*0.91125*	*0.12026*	*10.71559*	*1.98241E-6*	*0.05*	*1*	*0.51295*	*1.30955*
D-sorbitol 80mM vs. control	*0.109*	*0.12026*	*1.28176*	*0.98252*	*0.05*	*0*	*-0.2893*	*0.5073*
D-sorbitol 100mM vs. control	*-0.206*	*0.12026*	*2.4224*	*0.67945*	*0.05*	*0*	*-0.6043*	*0.1923*

Appendix 5.12 One-way ANOVA followed by Tukey's test on effect of the test compound on biofilm formation of *B. subtilis*

Descriptive statistics

	Sample Size	*Mean*	*Standard Deviation*	*SE of Mean*
control	*4*	*1.4*	*0.12504*	*0.06252*
0.5% NaH_2PO_4	*4*	*1.26275*	*0.3043*	*0.15215*

1% NaH_2PO_4	*4*	*1.34525*	*0.12007*	*0.06004*
2% NaH_2PO_4	*4*	*0.99425*	*0.07738*	*0.03869*
5% NaH_2PO_4	*4*	*0.3885*	*0.0792*	*0.0396*
10% NaH_2PO_4	*4*	*0.2425*	*0.01448*	*0.00724*
0.5%KH_2PO_4	*4*	*1.8145*	*0.10998*	*0.05499*
1% KH_2PO_4	*4*	*1.6175*	*0.15657*	*0.07828*
2% KH_2PO_4	*4*	*1.40775*	*0.07531*	*0.03765*
5% KH_2PO_4	*4*	*0.83*	*0.10961*	*0.05481*
10% KH_2PO_4	*4*	*0.22875*	*0.01711*	*0.00856*

Overall ANOVA

	DF	*Sum of Squares*	*Mean Square*	*F Value*	*Prob>F*
Model	*10*	*12.42002*	*1.242*	*72.01506*	*0*
Error	*33*	*0.56913*	*0.01725*		
Total	*43*	*12.98915*			

Null Hypothesis: The means of all levels are equal.

Alternative Hypothesis: The means of one or more levels are different.

At the 0.05 level, the population means are significantly different.

Tukey's post hoc test for comparison of means

	MeanDiff	*SEM*	*q Value*	*Prob*	*Alpha*	*Sig*	*LCL*	*UCL*
0.5% NaH_2PO_4 vs. control	*-0.13725*	*0.09286*	*2.09022*	*0.91688*	*0.05*	*0*	*-0.45788*	*0.18338*
1% NaH_2PO_4 vs. control	*-0.05475*	*0.09286*	*0.83381*	*0.99994*	*0.05*	*0*	*-0.37538*	*0.26588*
2% NaH_2PO_4 vs. control	*-0.40575*	*0.09286*	*6.1793*	*0.00476*	*0.05*	*1*	*-0.72638*	*-0.08512*
5% NaH_2PO_4vs. control	*-1.0115*	*0.09286*	*15.40446*	*8.18933E-8*	*0.05*	*1*	*-1.33213*	*-0.69087*
10% NaH_2PO_4 vs. control	*-1.1575*	*0.09286*	*17.62794*	*2.63457E-8*	*0.05*	*1*	*-1.47813*	*-0.83687*
0.5% KH_2PO_4 vs. control	*0.4145*	*0.09286*	*6.31255*	*0.00368*	*0.05*	*1*	*0.09387*	*0.73513*
1% KH_2PO_4 vs. control	*0.2175*	*0.09286*	*3.31238*	*0.43111*	*0.05*	*0*	*-0.10313*	*0.53813*

2% KH_2PO_4 vs. control	*0.00775*	*0.09286*	*0.11803*	*1*	*0.05*	*0*	*-0.31288*	*0.32838*
5% KH_2PO_4 vs. control	*-0.57*	*0.09286*	*8.68071*	*3.1156E-5*	*0.05*	*1*	*-0.89063*	*-0.24937*
10% KH_2PO_4 vs. control	*-1.17125*	*0.09286*	*17.83734*	*2.68941E-8*	*0.05*	*1*	*-1.49188*	*-0.85062*

Appendix 5.13: One-way ANOVA followed by Tukey's test on effect of the test compound on biofilm formation of *B. subtilis*

Descriptive statistics

	Sample Size	*Mean*	*Standard Deviation*	*SE of Mean*
control	*4*	*1.708*	*0.20634*	*0.10317*
betaine 40mM	*4*	*0.626*	*0.04767*	*0.02383*
betaine 40 mM + 1% NaH_2PO_4	*4*	*1.634*	*0.1025*	*0.05125*

betaine 40 mM + 2% NaH_2PO_4	*4*	*1.746*	*0.15369*	*0.07685*
betaine 40 mM + 1% KH_2PO_4	*4*	*1.62575*	*0.27489*	*0.13744*
betaine 40 mM + 2% KH_2PO_4	*4*	*4.08675*	*0.15942*	*0.07971*

Overall ANOVA

	DF	*Sum of Squares*	*Mean Square*	*F Value*	*Prob>F*
Model	*5*	*26.44553*	*5.28911*	*176.34749*	*1.23235E-14*
Error	*18*	*0.53987*	*0.02999*		
Total	*23*	*26.9854*			

Null Hypothesis: The means of all levels are equal.

Alternative Hypothesis: The means of one or more levels are different.

At the 0.05 level, the population means are significantly different.

Tukey's post hoc test for comparison of means

	MeanDiff	*SEM*	*q Value*	*Prob*	*Alpha*	*Sig*	*LCL*	*UCL*
betaine 40 mM vs. control	*-1.082*	*0.12246*	*12.49542*	*7.3772E-7*	*0.05*	*1*	*-1.47118*	*-0.69282*
betaine 40 mM + 1% NaH_2PO_4 vs. control	*-0.074*	*0.12246*	*0.85458*	*0.98935*	*0.05*	*0*	*-0.46318*	*0.31518*
betaine 40 mM + 2% NaH_2PO_4 vs. control	*0.038*	*0.12246*	*0.43884*	*0.99954*	*0.05*	*0*	*-0.35118*	*0.42718*
betaine 40 mM +1% KH_2PO_4 vs. control	*-0.08225*	*0.12246*	*0.94986*	*0.98294*	*0.05*	*0*	*-0.47143*	*0.30693*
betaine 40 mM + 2% KH_2PO_4 vs. control	*2.37875*	*0.12246*	*27.47086*	*0*	*0.05*	*1*	*1.98957*	*2.76793*

Appendix 5.14 One-way ANOVA followed by Tukey's test on effect of the test compound on biofilm formation of *B. subtilis*

Descriptive statistics

	Sample Size	*Mean*	*Standard Deviation*	*SE of Mean*
control	*4*	*0.667*	*0.03182*	*0.01591*
ChCl40 mM + 1% NaH_2PO_4	*4*	*0.94125*	*0.05884*	*0.02942*
ChCl 40 mM + 2% NaH_2PO_4	*4*	*1.28275*	*0.10108*	*0.05054*
ChCl 40 mM + 5% NaH_2PO_4	*4*	*0.3605*	*0.23273*	*0.11637*
ChCl 40 mM + 1% KH2PO4	*4*	*1.26075*	*0.24078*	*0.12039*

ChCl 40 mM + 2% KH_2PO_4	*4*	*1.5205*	*0.24025*	*0.12012*
ChCl 40 mM + 5% KH_2PO_4	*4*	*1.2354*	*0.04523*	*0.02023*

Overall ANOVA

	DF	*Sum of Squares*	*Mean Square*	*F Value*	*Prob>F*
Model	*6*	*3.98671*	*0.66445*	*26.01835*	*6.26391E-9*
Error	*22*	*0.56183*	*0.02554*		
Total	*28*	*4.54854*			

Null Hypothesis: The means of all levels are equal.

Alternative Hypothesis: The means of one or more levels are different.

At the 0.05 level, the population means are significantly different.

Tukey's post hoc test for comparison of means

	MeanDiff	*SEM*	*q Value*	*Prob*	*Alpha*	*Sig*	*LCL*	*UCL*

ChCl 40 mM + 1% NaH_2PO_4 vs. control	*0.27425*	*0.113*	*3.4323*	*0.23422*	*0.05*	*0*	*-0.09145*	*0.63995*
ChCl 40 mM + 2% NaH_2PO_4 vs. Control	*0.61575*	*0.113*	*7.70624*	*3.12843E-4*	*0.05*	*1*	*0.25005*	*0.98145*
ChCl 40 mM + 5% NaH2PO4 vs. control	*-0.3065*	*0.113*	*3.83591*	*0.14168*	*0.05*	*0*	*-0.6722*	*0.0592*
ChCl 40 mM + 1% KH_2PO_4 vs. control	*0.59375*	*0.113*	*7.43091*	*4.92997E-4*	*0.05*	*1*	*0.22805*	*0.95945*
ChCl 40 mM + 2% KH_2PO_4 vs. control	*0.8535*	*0.113*	*10.68174*	*2.81513E-6*	*0.05*	*1*	*0.4878*	*1.2192*
ChCl 40 mM + 5% KH_2PO_4 vs. control	*0.5684*	*0.1072*	*7.49844*	*4.40881E-4*	*0.05*	*1*	*0.22146*	*0.91534*

Appendix 5.15 One-way ANOVA followed by Tukey's test on effect of the test compound on biofilm formation of *B. subtilis*

Descriptive statistics

	Sample Size	*Mean*	*Standard Deviation*	*SE of Mean*
control	*4*	*1.09425*	*0.09493*	*0.04746*
DES 40mM+1% NaH_2PO_4	*4*	*1.278*	*0.11069*	*0.05535*
DES 40mM+2% NaH_2PO_4	*4*	*1.608*	*0.11569*	*0.05785*
DES 40mM+5% NaH_2PO_4	*4*	*0.7535*	*0.1711*	*0.08555*
DES 40 mM + 1% KH_2PO_4	*4*	*1.6545*	*0.11076*	*0.05538*

DES 40 mM + 2% KH_2PO_4	*4*	*2.06675*	*0.05759*	*0.0288*
DES 40 mM + 5% KH_2PO_4	*4*	*1.3235*	*0.20753*	*0.10376*

Overall ANOVA

	DF	*Sum of Squares*	*Mean Square*	*F Value*	*Prob>F*
Model	*6*	*4.33882*	*0.72314*	*41.29733*	*1.46853E-10*
Error	*21*	*0.36772*	*0.01751*		
Total	*27*	*4.70654*			

Null Hypothesis: The means of all levels are equal.

Alternative Hypothesis: The means of one or more levels are different; at the 0.05 level, the population means are significantly different.

Tukey's post hoc test for comparison of means

	MeanDiff	*SEM*	*q Value*	*Prob*	*Alpha*	*Sig*	*LCL*	*UCL*
DES 40 mM + 1% NaH_2PO_4 vs. control	*0.18375*	*0.09357*	*2.77721*	*0.46413*	*0.05*	*0*	*-0.12042*	*0.48792*

DES 40 mM + 2% NaH_2PO_4 vs. control	*0.51375*	*0.09357*	*7.76484*	*3.29077E-4*	*0.05*	*1*	*0.20958*	*0.81792*
DES 40 mM + 5% NaH_2PO_4 vs. control	*-0.34075*	*0.09357*	*5.15011*	*0.02173*	*0.05*	*1*	*-0.64492*	*-0.03658*
DES 40 mM + 1% KH_2PO_4 vs. control	*0.56025*	*0.09357*	*8.46764*	*1.07781E-4*	*0.05*	*1*	*0.25608*	*0.86442*
DES 40 mM + 2% KH_2PO_4 vs. control	*0.9725*	*0.09357*	*14.69841*	*7.18972E-8*	*0.05*	*1*	*0.66833*	*1.27667*
DES 40 mM + 5% KH_2PO_4 vs. control	*0.22925*	*0.09357*	*3.46489*	*0.22739*	*0.05*	*0*	*-0.07492*	*0.53342*

Appendix 5.16: One-way ANOVA followed by Tukey's test on effect of the test compound on biofilm formation of *B. subtilis*

Descriptive statistics

	Sample Size	*Mean*	*Standard Deviation*	*SE of Mean*
control	*4*	*1.429*	*0.10742*	*0.05371*
D-sorbitol 40 mM +1% NaH_2PO_4	*4*	*2.92725*	*0.0766*	*0.0383*
D-sorbitol 40 mM + 2% NaH_2PO_4	*4*	*2.58*	*0.09472*	*0.04736*
D-sorbitol 40mM+1% KH_2PO_4	*4*	*3.3945*	*0.1984*	*0.0992*
D-sorbitol 40mM+2% KH_2PO_4	*4*	*3.10325*	*0.13657*	*0.06828*

Overall ANOVA

	DF	*Sum of Squares*	*Mean Square*	*F Value*	*Prob>F*
Model	*4*	*9.30221*	*2.32555*	*137.78253*	*1.23868E-11*

Error	*15*	*0.25318*	*0.01688*
Total	*19*	*9.55539*	

Null Hypothesis: The means of all levels are equal.

Alternative Hypothesis: The means of one or more levels are different.

At the 0.05 level, the population means are significantly different.

Tukey's post hoc test for comparison of means

	MeanDiff	*SEM*	*q Value*	*Prob*	*Alpha*	*Sig*	*LCL*	*UCL*
D-sorbitol 40 mM + 1% NaH_2PO_4 vs. control	*1.49825*	*0.09187*	*23.06472*	*0*	*0.05*	*1*	*1.21458*	*1.78192*
D-sorbitol 40 mM + 2% NaH_2PO_4 vs. control	*1.151*	*0.09187*	*17.719*	*7.70898E-8*	*0.05*	*1*	*0.86733*	*1.43467*
D-sorbitol 40 mM + 1% KH_2PO_4 vs. control	*1.9655*	*0.09187*	*30.25777*	*0*	*0.05*	*1*	*1.68183*	*2.24917*

D-sorbitol 40 mM + 2% KH_2PO_4 vs. control	*1.67425*	*0.09187*	*25.77414*	*0*	*0.05*	*1*	*1.39058*	*1.95792*

Appendix 5.17 Biofilm fraction on SPE electrode obtained by microscopy. One-way ANOVA followed by Tukey's test on effect of the test compound on biofilm formation of *B. subtilis*.

Descriptive statistics

	Sample Size	*Mean*	*Standard Deviation*	*SE of Mean*
bare electrode	*3*	*0.00425*	*6.90541E-4*	*3.98684E-4*
Cell only	*3*	*0.05267*	*0.00651*	*0.00376*
DES 40 mM	*3*	*0.757*	*0.01819*	*0.0105*
DES 20 mM	*3*	*0.585*	*0.04124*	*0.02381*

ChCl 40 mM + 1% NaH_2PO_4	*3*	*0.70167*	*0.08203*	*0.04736*
ChCl 40 mM + 2% NaH_2PO_4	*3*	*0.89683*	*0.02924*	*0.01688*
ChCl 60 mM	*3*	*0.29*	*0.02*	*0.01155*
ChCl 40 mM	*3*	*0.175*	*0.03291*	*0.019*
	Sample Size	*Mean*	*Standard Deviation*	*SE of Mean*

Overall ANOVA

	DF	*Sum of Squares*	*Mean Square*	*F Value*	*Prob>F*
Model	*7*	*2.49267*	*0.3561*	*255.67905*	*3.33067E-15*
Error	*16*	*0.02228*	*0.00139*		
Total	*23*	*2.51496*			

Null Hypothesis: The means of all levels are equal.

Alternative Hypothesis: The means of one or more levels are different.

At the 0.05 level, the population means are significantly different.

Tukey's post hoc test for comparison of means

	MeanDiff	*SEM*	*q Value*	*Prob*	*Alpha*	*Sig*	*LCL*	*UCL*
cell only vs. bare electrode	*0.04841*	*0.03047*	*2.24697*	*0.75022*	*0.05*	*0*	*-0.05708*	*0.15391*
DES 40 mM vs. bare electrode	*0.75275*	*0.03047*	*34.93607*	*0*	*0.05*	*1*	*0.64725*	*0.85824*
DES 20 mM vs. bare electrode	*0.58075*	*0.03047*	*26.95331*	*3.67711E-8*	*0.05*	*1*	*0.47525*	*0.68624*
ChCl 40 mM+ 1% NaH_2PO_4 vs. bare electrode	*0.69741*	*0.03047*	*32.36797*	*0*	*0.05*	*1*	*0.59192*	*0.80291*

ChCl 40 mM+ 2% NaH_2PO_4 vs. bare electrode	*0.89258*	*0.03047*	*41.42577*	*0*	*0.05*	*1*	*0.78708*	*0.99807*
ChCl 60 mM vs. bare electrode	*0.28575*	*0.03047*	*13.26195*	*1.43352E-6*	*0.05*	*1*	*0.18025*	*0.39124*

References

Abbasi, Nabeel Mujtaba, Muhammad Qamar Farooq, and Jared L. Anderson. 2022. “Investigating the Effect of Systematically Modifying the Molar Ratio of Hydrogen Bond Donor and Acceptor on Solvation Characteristics of Deep Eutectic Solvents Formed Using Choline Chloride Salt and Polyalcohols.” *Journal of Chromatography A* 1667:462871. doi: 10.1016/J.CHROMA.2022.462871.

Achinas, Spyridon, Nikolaos Charalampogiannis, and Gerrit Jan Willem Euverink. 2019. “A Brief Recap of Microbial Adhesion and Biofilms.” *Applied Sciences 2019, Vol. 9, Page 2801* 9(14):2801. doi: 10.3390/APP9142801.

Adilkhanova, Alina, Anar Ormantayeva, Aisholpan Kaziullayeva, Kayode Olaifa, Neda Eghtesadi, Azza H. Abbas, Cinzia Calvio, Tri T. Pham, Obinna M. Ajunwa, and Enrico Marsili. 2024. “Electrofermentation Increases Concentration of Poly γ-Glutamic Acid in Bacillus Subtilis Biofilms.” *Microbial Biotechnology* 17(3). doi: 10.1111/1751-7915.14426.

Aelterman, Peter, Mathias Versichele, Massimo Marzorati, Nico Boon, and Willy Verstraete. 2008. “Loading Rate and External Resistance Control the Electricity Generation of Microbial Fuel Cells with Different Three-Dimensional Anodes.” *Bioresource Technology* 99(18):8895–8902. doi: 10.1016/j.biortech.2008.04.061.

Aiyer, Kartik, and Lucinda E. Doyle. 2022. “Capturing the Signal of Weak Electricigens: A Worthy Endeavour.” *Trends in Biotechnology* 40(5):564–75. doi: 10.1016/J.TIBTECH.2021.10.002.

Aliane, Samia, and Amina Meliani. 2021. “Bacterial Biofilms: Formation, Advantages for Community Members, Clinical

Implications, and Antibiotic Resistance." *Environmental and Experimental Biology* 19(3). doi: 10.22364/eeb.19.12.

Alonso-Lomillo, M. A., O. Domínguez-Renedo, and M. J. Arcos-Martínez. 2010. "Screen-Printed Biosensors in Microbiology; A Review." *Talanta* 82(5):1629–36. doi: 10.1016/j.talanta.2010.08.033.

Alvarez-Ordóñez, Avelino, Laura M. Coughlan, Romain Briandet, and Paul D. Cotter. 2019. "Biofilms in Food Processing Environments: Challenges and Opportunities." *Annual Review of Food Science and Technology* 10:173–95. doi: 10.1146/annurev-food-032818-121805.

Angelini, Thomas E., Marcus Roper, Roberto Kolter, David A. Weitz, and Michael P. Brenner. 2009. "Bacillus Subtilis Spreads by Surfing on Waves of Surfactant." *Proceedings of the National Academy of Sciences of the United States of America* 106(43):18109–13. doi: 10.1073/PNAS.0905890106.

de Araújo, Lívia Caroline Alexandre, and Maria Betânia Melo de Oliveira. 2020. "Effect of Heavy Metals on the Biofilm Formed by Microorganisms from Impacted Aquatic Environments." *Bacterial Biofilms* 19.

Arce-Cordero, J. A., H. F. Monteiro, H. Phillips, K. Estes, and A. P. Faciola. 2021. "Effects of Unprotected Choline Chloride on Microbial Fermentation in a Dual-Flow Continuous Culture Depend on Dietary Neutral Detergent Fiber Concentration." *Journal of Dairy Science* 104(3):2966–78.

Aryal, Nabin, Fariza Ammam, Sunil A. Patil, and Deepak Pant. 2017. "An Overview of Cathode Materials for Microbial Electrosynthesis of Chemicals from Carbon Dioxide." *Green Chemistry* 19(24):5748–60. doi: 10.1039/c7gc01801k.

Astorga, Solange E., Liang Xing Hu, Enrico Marsili, and Yizhong Huang. 2019. “Electrochemical Signature of Escherichia Coli on Nickel Micropillar Array Electrode for Early Biofilm Characterization.” *ChemElectroChem* 6(17):4674–80. doi: 10.1002/CELC.201901063.

Babauta, Jerome, Ryan Renslow, Zbigniew Lewandowski, and Haluk Beyenal. 2012. “Electrochemically Active Biofilms: Facts and Fiction. A Review.” *Biofouling* 28(8):789–812. doi: 10.1080/08927014.2012.710324.

Babich, H., and G. Stotzky. 1978. “Toxicity of Zinc to Fungi, Bacteria, and Coliphages: Influence of Chloride Ions.” *Applied and Environmental Microbiology* 36(6):906–14. doi: 10.1128/AEM.36.6.906-914.1978.

Bajracharya, Suman, Mohita Sharma, Gunda Mohanakrishna, Xochitl Dominguez Benneton, David P. B. T. B. Strik, Priyangshu M. Sarma, and Deepak Pant. 2016. “An Overview on Emerging Bioelectrochemical Systems (BESs): Technology for Sustainable Electricity, Waste Remediation, Resource Recovery, Chemical Production and Beyond.” doi: 10.1016/j.renene.2016.03.002.

Baluta, Sylwia, Francesca Meloni, Kinga Halicka, Adam Szyszka, Antonio Zucca, Maria Itria Pilo, and Joanna Cabaj. 2022. “Differential Pulse Voltammetry and Chronoamperometry as Analytical Tools for Epinephrine Detection Using a Tyrosinase-Based Electrochemical Biosensor.” doi: 10.1039/d2ra04045j.

Bartlett, John G., David N. Gilbert, and Brad Spellberg. 2013. “Seven Ways to Preserve the Miracle of Antibiotics.” *Clinical Infectious Diseases* 56(10):1445–50. doi: 10.1093/CID/CIT070.

Bartzatt, Ronald, and Tasloach Wol. 2014. “Detection and Assay of Vitamin B-2 (Riboflavin) in Alkaline Borate Buffer with

UV/Visible Spectrophotometry.” doi: 10.1155/2014/453085.

Behera, Manaswini, Partha S. Jana, and M. M. Ghangrekar. 2009. “Performance Evaluation of Low Cost Microbial Fuel Cell Fabricated Using Earthen Pot with Biotic and Abiotic Cathode.” doi: 10.1016/j.biortech.2009.07.089.

Belviso, Benny Danilo, Filippo Maria Perna, Benedetta Carrozzini, Massimo Trotta, Vito Capriati, and Rocco Caliandro. 2021. “Introducing Protein Crystallization in Hydrated Deep Eutectic Solvents.” *ACS Sustainable Chemistry and Engineering*. doi: 10.1021/ACSSUSCHEMENG.1C01230/SUPPL_FILE/SC1C01230_SI_001.PDF.

Berillo, Dmitriy, Areej Al-Jwaid, and Jonathan Caplin. 2021. “Polymeric Materials Used for Immobilisation of Bacteria for the Bioremediation of Contaminants in Water.” doi: 10.3390/polym.

Boch, J., B. Kempf, and E. Bremer. 1994. “Osmoregulation in Bacillus Subtilis: Synthesis of the Osmoprotectant Glycine Betaine from Exogenously Provided Choline.” *Journal of Bacteriology* 176(17):5364–71. doi: 10.1128/JB.176.17.5364-5371.1994.

Boch, Jens, Bettina Kempf, Roland Schmid, and Erhard Bremer. 1996. “Synthesis of the Osmoprotectant Glycine Betaine in Bacillus Subtilis: Characterization of the GbsAB Genes.” *Journal of Bacteriology* 178(17):5121–29. doi: 10.1128/JB.178.17.5121-5129.1996.

Bond, Daniel R., and Derek R. Lovley. 2003. “Electricity Production by Geobacter Sulfurreducens Attached to Electrodes.” *Applied and Environmental Microbiology* 69(3):1548–55. doi: 10.1128/AEM.69.3.1548-1555.2003/ASSET/F4A7F315-959D-4605-A43B-3B7D1386F8C7/ASSETS/GRAPHIC/AM0331568007.JPEG.

Borole, Abhijeet P., Gemma Reguera, Bradley Ringeisen, Zhi Wu Wang, Yujie Feng, and Byung Hong Kim. 2011. “Electroactive Biofilms: Current Status and Future Research Needs.” *Energy and Environmental Science* 4(12):4813–34. doi: 10.1039/c1ee02511b.

Bremer, Erhard, and Reinhard Krämer. 2019. “Responses of Microorganisms to Osmotic Stress.” *Annual Review of Microbiology* 73:313–34. doi: 10.1146/ANNUREV-MICRO-020518-115504.

Von Canstein, Harald, Jun Ogawa, Sakayu Shimizu, and Jonathan R. Lloyd. 2008. “Secretion of Flavins by Shewanella Species and Their Role in Extracellular Electron Transfer.” *Applied and Environmental Microbiology* 74(3):615–23. doi: 10.1128/AEM.01387-07.

Cantillo, David. 2022. “Synthesis of Active Pharmaceutical Ingredients Using Electrochemical Methods: Keys to Improve Sustainability.” *Chem. Commun* 58:619. doi: 10.1039/d1cc06296d.

Cesar, Spencer, Maya Anjur-Dietrich, Brian Yu, Ethan Li, Enrique Rojas, Norma Neff, Tim F. Cooper, and Kerwyn Casey Huang. 2020. “Bacterial Evolution in High-Osmolarity Environments.” *MBio* 11(4):1–17. doi: 10.1128/MBIO.01191-20/SUPPL_FILE/MBIO.01191-20-SM001.AVI.

Chai, Yunrong, Peng Cai, Osnat Gillor, Eiko E. Kuramae, Ohana Y. A Costa, and Jos M. Raaijmakers. 2018. “Microbial Extracellular Polymeric Substances: Ecological Function and Impact on Soil Aggregation.” doi: 10.3389/fmicb.2018.01636.

Chen, Lixiang, Changli Cao, Shuhua Wang, John R. Varcoe, Robert C. T. Slade, Claudio Avignone-Rossa, and Feng Zhao. 2019.

"Electron Communication of Bacillus Subtilis in Harsh Environments." *IScience* 12:260–69. doi: 10.1016/J.ISCI.2019.01.020.

Chen, Shuiliang, Sunil A. Patil, Robert Keith Brown, and Uwe Schröder. 2019. "Strategies for Optimizing the Power Output of Microbial Fuel Cells: Transitioning from Fundamental Studies to Practical Implementation." *Applied Energy* 233–234:15–28. doi: 10.1016/J.APENERGY.2018.10.015.

Chini, Claudia C. S., Mariana G. Tarragó, and Eduardo N. Chini. 2017. "NAD and the Aging Process: Role in Life, Death and Everything in Between." *Molecular and Cellular Endocrinology* 455:62–74. doi: 10.1016/J.MCE.2016.11.003.

Chiranjeevi, P., and Sunil A. Patil. 2020. "Strategies for Improving the Electroactivity and Specific Metabolic Functionality of Microorganisms for Various Microbial Electrochemical Technologies." *Biotechnology Advances* 39. doi: 10.1016/J.BIOTECHADV.2019.107468.

Choi, Serah, Bongkyu Kim, and In Seop Chang. 2018. "Tracking of Shewanella Oneidensis MR-1 Biofilm Formation of a Microbial Electrochemical System via Differential Pulse Voltammetry." *Bioresource Technology* 254(January):357–61. doi: 10.1016/j.biortech.2018.01.047.

Chu, Dominique, and David J. Barnes. 2016. "The Lag-Phase during Diauxic Growth Is a Trade-off between Fast Adaptation and High Growth Rate." *Scientific Reports* 6(December 2015):1–15. doi: 10.1038/srep25191.

Chu, Ronghao, Rui Li, Chen Wang, and Rui Ban. 2022. "Production of Vitamin B2 (Riboflavin) by Bacillus Subtilis." *Journal of Chemical Technology & Biotechnology* 97(8):1941–49. doi: 10.1002/JCTB.7017.

Cicco, Luciana, Giuseppe Dilauro, Filippo Maria Perna, Paola Vitale, and Vito Capriati. 2021. “Advances in Deep Eutectic Solvents and Water: Applications in Metal- And Biocatalyzed Processes, in the Synthesis of APIs, and Other Biologically Active Compounds.” *Organic and Biomolecular Chemistry* 19(12):2558–77. doi: 10.1039/d0ob02491k.

Conners, Eric M, Karthikeyan Rengasamy, and Arpita Bose. 2022. “Biotechnology Methods Mini-Review Electroactive Biofilms: How Microbial Electron Transfer Enables Bioelectrochemical Applications.” *Journal of Industrial Microbiology and Biotechnology* 49:12. doi: 10.1093/jimb/kuac012.

Conners, Eric M., Karthikeyan Rengasamy, and Arpita Bose. 2022. “Electroactive Biofilms: How Microbial Electron Transfer Enables Bioelectrochemical Applications.” *Journal of Industrial Microbiology and Biotechnology* 49(4). doi: 10.1093/jimb/kuac012.

Costerton, J. W., G. G. Geesey, and K. J. Cheng. 1978. “How Bacteria Stick.” *Scientific American* 238(1):86–95. doi: 10.1038/SCIENTIFICAMERICAN0178-86.

Cournet, Amandine, Marie Line Délia, Alain Bergel, Christine Roques, and Mathieu Bergé. 2010. “Electrochemical Reduction of Oxygen Catalyzed by a Wide Range of Bacteria Including Gram-Positive.” *Electrochemistry Communications* 12(4):505–8. doi: 10.1016/j.elecom.2010.01.026.

Dai, Xiongfeng, and Manlu Zhu. 2018. “High Osmolarity Modulates Bacterial Cell Size through Reducing Initiation Volume in Escherichia Coli Downloaded From.” *Molecular Biology and Physiology* 3:430–48. doi: 10.1128/mSphere.

Deutscher, Josef, Christof Francke, and Pieter W. Postma. 2006. “How Phosphotransferase System-Related Protein Phosphorylation Regulates Carbohydrate Metabolism in Bacteria.” *Microbiology and Molecular Biology Reviews* 70(4):939–1031. doi: 10.1128/mmbr.00024-06.

Djurišić, Aleksandra B., Yu Hang Leung, Alan M. C. Ng, Xiao Ying Xu, Patrick K. H. Lee, Natalie Degger, and R. S. S. Wu. 2015. “Toxicity of Metal Oxide Nanoparticles: Mechanisms, Characterization, and Avoiding Experimental Artefacts.” *Small (Weinheim an Der Bergstrasse, Germany)* 11(1):26–44. doi: 10.1002/SMLL.201303947.

Doyle, Lucinda E., and Enrico Marsili. 2018a. “Weak Electricigens: A New Avenue for Bioelectrochemical Research.” *Bioresource Technology* 258(December 2017):354–64. doi: 10.1016/j.biortech.2018.02.073.

Doyle, Lucinda E., and Enrico Marsili. 2018b. “Weak Electricigens: A New Avenue for Bioelectrochemical Research.” *Bioresource Technology* 258:354–64. doi: 10.1016/J.BIORTECH.2018.02.073.

Duanis-Assaf, Danielle, Doron Steinberg, and Moshe Shemesh. 2020. “Efficiency of Bacillus Subtilis Metabolism of Sugar Alcohols Governs Its Probiotic Effect against Cariogenic Streptococcus Mutans.” *Artificial Cells, Nanomedicine and Biotechnology* 48(1):1222–30. doi: 10.1080/21691401.2020.1822855.

Dulon, Sophie, Sandrine Parot, Marie Line Delia, and Alain Bergel. 2007. “Electroactive Biofilms: New Means for Electrochemistry.” *Journal of Applied Electrochemistry* 37(1):173–79. doi: 10.1007/s10800-006-9250-8.

Eghtesadi, Neda, Kayode Olaifa, Filippo Maria Perna, Vito Capriati, Massimo Trotta, Obinna Ajunwa, and Enrico Marsili. 2022.

"Electroactivity of Weak Electricigen Bacillus Subtilis Biofilms in Solution Containing Deep Eutectic Solvent Components." *Bioelectrochemistry* 147:108207. doi: 10.1016/J.BIOELECHEM.2022.108207.

Epstein, Wolfgang. 2003. "The Roles and Regulation of Potassium in Bacteria." *Progress in Nucleic Acid Research and Molecular Biology* 75:293–320. doi: 10.1016/S0079-6603(03)75008-9.

Erable, Benjamin, Narcis M. Duţeanua, M. M. Ghangrekar, Claire Dumas, and Keith Scott. 2010. "Application of Electro-Active Biofilms." *Biofouling* 26(1):57–71. doi: 10.1080/08927010903161281.

Esar, C. ´., I. Torres, Andrew Kato Marcus, Hyung-Sool Lee, Prathap Parameswaran, Rosa Krajmalnik-Brown, and Bruce E. Rittmann. 2009. "A Kinetic Perspective on Extracellular Electron Transfer by Anode-Respiring Bacteria." doi: 10.1111/j.1574-6976.2009.00191.x.

Fathollahi, Alireza, and Stephen J. Coupe. 2021. "Effect of Environmental and Nutritional Conditions on the Formation of Single and Mixed-Species Biofilms and Their Efficiency in Cadmium Removal." doi: 10.1016/j.chemosphere.2021.131152.

Ferreira, Ana S. D., Rita Craveiro, Ana Rita Duarte, Susana Barreiros, Eurico J. Cabrita, and Alexandre Paiva. 2021. "Effect of Water on the Structure and Dynamics of Choline Chloride/Glycerol Eutectic Systems." *Journal of Molecular Liquids* 342:117463. doi: 10.1016/j.molliq.2021.117463.

Finkenstadt, Victoria L. 2005. "Natural Polysaccharides as Electroactive Polymers." *Applied Microbiology and Biotechnology* 67(6):735–45. doi: 10.1007/S00253-005-1931-4/METRICS.

Flemming, Hans-Curt, Jost Wingender, Ulrich Szewzyk, Peter Steinberg, Scott A. Rice, and Staffan Kjelleberg. 2016. “Biofilms: An Emergent Form of Bacterial Life.” *Nature Publishing Group*. doi: 10.1038/nrmicro.2016.94.

Flemming, Hans Curt, and Jost Wingender. 2010. “The Biofilm Matrix.” *Nature Reviews Microbiology* 8(9):623–33. doi: 10.1038/nrmicro2415.

Furst, Ariel L., and Matthew B. Francis. 2019. “Impedance-Based Detection of Bacteria.” *Chemical Reviews* 119(1):700–726. doi: 10.1021/ACS.CHEMREV.8B00381/ASSET/IMAGES/LARGE/CR-2018-00381F_0012.JPEG.

García, Alejandro, Miranda Ferrari, Samuel J. Rowley-Neale, and Craig E. Banks. 2021. “Screen-Printed Electrodes: Transitioning the Laboratory in-to-the Field.” *Talanta Open* 3:100032. doi: 10.1016/j.talo.2021.100032.

Ghosh, Anirban, Narayansaswamy Jayaraman, and Dipankar Chatterji. 2020. “Small-Molecule Inhibition of Bacterial Biofilm.” *ACS Omega* 5(7):3108–15. doi: 10.1021/ACSOMEGA.9B03695.

Godbole, Vaanie, Simranjeet Singh, Praveen C. Ramamurthy, Nadeem A. Khan, Manisha Bisht, Manoj Kumar Pal, Joginder Singh, Gaurav Kumar, Ali Esrafili, and Mahmood Yousefi. 2023. “Electroactive Microbe Communication: A Crucial Aspect for Energy Generation in Bio-Electrochemical Systems.” *Journal of Environmental Chemical Engineering* 11(5):110646. doi: 10.1016/j.jece.2023.110646.

Gold, Karli, Buford Slay, Mark Knackstedt, and Akhilesh K. Gaharwar. 2018. “Antimicrobial Activity of Metal and Metal-Oxide Based Nanoparticles.” *Advances in Therapy* 1(3). doi: 10.1002/ADTP.201700033.

Gong, Ziying, Huan Yu, Junqi Zhang, Feng Li, and Hao Song. 2020. “Microbial Electro-Fermentation for Synthesis of Chemicals and Biofuels Driven by Bi-Directional Extracellular Electron Transfer.” *Synthetic and Systems Biotechnology* 5(4):304–13. doi: 10.1016/J.SYNBIO.2020.08.004.

Gregg, Caroline R., Oscar J. Tejeda, Lindsey F. Spencer, Allan J. Calderon, Dianna V Bourassa, Jessica D. Starkey, and Charles W. Starkey. 2022. “Impacts of Increasing Additions of Choline Chloride on Growth Performance and Carcass Characteristics of Broiler Chickens Reared to 66 Days of Age.” *Animals* 12(14):1808.

Gregory, Gwendolyn J., and E. Fidelma Boyd. 2021. “Stressed out: Bacterial Response to High Salinity Using Compatible Solute Biosynthesis and Uptake Systems, Lessons from Vibrionaceae.” *Computational and Structural Biotechnology Journal* 19:1014–27. doi: 10.1016/J.CSBJ.2021.01.030.

Gu, Yang, Xianhao Xu, Yaokang Wu, Tengfei Niu, Yanfeng Liu, Jianghua Li, Guocheng Du, and Long Liu. 2018. “Advances and Prospects of Bacillus Subtilis Cellular Factories: From Rational Design to Industrial Applications.” *Metabolic Engineering* 50:109–21. doi: 10.1016/J.YMBEN.2018.05.006.

Hansen, Benworth B., Stephanie Spittle, Brian Chen, Derrick Poe, Yong Zhang, Jeffrey M. Klein, Alexandre Horton, Laxmi Adhikari, Tamar Zelovich, Brian W. Doherty, Burcu Gurkan, Edward J. Maginn, Arthur Ragauskas, Mark Dadmun, Thomas A. Zawodzinski, Gary A. Baker, Mark E. Tuckerman, Robert F. Savinell, and Joshua R. Sangoro. 2021. “Deep Eutectic Solvents: A Review of Fundamentals and Applications.” *Chemical Reviews* 121(3):1232–85. doi: 10.1021/acs.chemrev.0c00385.

Haslett, Nicholas. 2012. “Development of a Eukaryotic Microbial Fuel Cell Using Arxula Adeninivorans.”

ter Heijne, A., M. A. Pereira, J. Pereira, and T. Sleutels. 2021. “Electron Storage in Electroactive Biofilms.” *Trends in Biotechnology* 39(1):34–42. doi: 10.1016/j.tibtech.2020.06.006.

Hernández-Fernández, F. J., A. Pérez De Los Ríos, M. J. Salar-García, V. M. Ortiz-Martínez, L. J. Lozano-Blanco, C. Godínez, F. Tomás-Alonso, and J. Quesada-Medina. 2015. “Recent Progress and Perspectives in Microbial Fuel Cells for Bioenergy Generation and Wastewater Treatment.” *Fuel Processing Technology* 138:284–97. doi: 10.1016/J.FUPROC.2015.05.022.

Higashitsuji, Yuhei, Annemarie Angerer, Sabine Berghaus, Birgit Hobl, and Matthias Mack. 2007. “RibR, a Possible Regulator of the Bacillus Subtilis Riboflavin Biosynthetic Operon, in Vivo Interacts with the 5′-Untranslated Leader of Rib MRNA.” *FEMS Microbiology Letters* 274(1):48–54. doi: 10.1111/J.1574-6968.2007.00817.X.

Hou, Xue Dan, Qiu Ping Liu, Thomas J. Smith, Ning Li, and Min Hua Zong. 2013. “Evaluation of Toxicity and Biodegradability of Cholinium Amino Acids Ionic Liquids.” *PLoS ONE* 8(3). doi: 10.1371/JOURNAL.PONE.0059145.

Huang, Jun, Bo Tong, Zhe Li, Tao Zhou, Jianbo Zhang, and Zhangquan Peng. 2018. “Probing the Reaction Interface in Li-Oxygen Batteries Using Dynamic Electrochemical Impedance Spectroscopy: Discharge-Charge Asymmetry in Reaction Sites and Electronic Conductivity.” *Journal of Physical Chemistry Letters* 9(12):3403–8. doi: 10.1021/ACS.JPCLETT.8B01351/SUPPL_FILE/JZ8B01351_SI_001.PDF.

Isaac, Paula, Mauricio Javier Alessandrello, Alexandre José Macedo, Cristina Esté Vez, and Marcela Alejandra Ferrero. 2017. “Pre-

Exposition to Polycyclic Aromatic Hydrocarbons (PAHs) Enhance Biofilm Formation and Hydrocarbon Removal by Native Multi-Species Consortium." *Journal of Environmental Chemical Engineering* 5:1372–78. doi: 10.1016/j.jece.2017.02.031.

Jasu, Amrita, and Rina Rani Ray. 2021. "Biofilm Mediated Strategies to Mitigate Heavy Metal Pollution: A Critical Review in Metal Bioremediation." *Biocatalysis and Agricultural Biotechnology* 37(September):102183. doi: 10.1016/j.bcab.2021.102183.

Ji, Chao, Huimei Tian, Xiaohui Wang, Xin Song, Ruicheng Ju, Huying Li, Qixiong Gao, Chaohui Li, Pengcheng Zhang, Jintai Li, Liping Hao, Changdong Wang, Yanyan Zhou, Ruiping Xu, Yue Liu, Jianfeng Du, and Xunli Liu. 2022. "Bacillus Subtilis HG-15, a Halotolerant Rhizoplane Bacterium, Promotes Growth and Salinity Tolerance in Wheat (Triticum Aestivum)." *BioMed Research International* 2022. doi: 10.1155/2022/9506227.

Jiang, Yujia, Yansong Liu, Xiaoyu Zhang, Hao Gao, Lu Mou, Mengdi Wu, Wenming Zhang, Fengxue Xin, and Min Jiang. 2021. "Biofilm Application in the Microbial Biochemicals Production Process." *Biotechnology Advances* 48(December 2020):107724. doi: 10.1016/j.biotechadv.2021.107724.

Jing, Xianyue, Xing Liu, Chengsheng Deng, Shanshan Chen, and Shungui Zhou. 2019. "Chemical Signals Stimulate Geobacter Soli Biofilm Formation and Electroactivity." *Biosensors and Bioelectronics* 127:1–9. doi: 10.1016/J.BIOS.2018.11.051.

Joo, Hwang Soo, and Michael Otto. 2012. "Molecular Basis of in Vivo Biofilm Formation by Bacterial Pathogens." *Chemistry and Biology* 19(12):1503–13. doi: 10.1016/j.chembiol.2012.10.022.

Kapfhammer, Dagmar, Ece Karatan, Kathryn J. Pflughoeft, and Paula I. Watnick. 2005. "Role for Glycine Betaine Transport in Vibrio

Cholerae Osmoadaptation and Biofilm Formation within Microbial Communities." *APPLIED AND ENVIRONMENTAL MICROBIOLOGY* 71(7):3840–47. doi: 10.1128/AEM.71.7.3840.

Kappes, Rainer M., Bettina Kempf, Susanne Kneip, Jens Boch, Jutta Gade, Jana Meier-Wagner, and Erhard Bremer. 1999. "Two Evolutionarily Closely Related ABC Transporters Mediate the Uptake of Choline for Synthesis of the Osmoprotectant Glycine Betaine in Bacillus Subtilis." *Molecular Microbiology* 32(1):203–16. doi: 10.1046/j.1365-2958.1999.01354.x.

Karimi, Mohammad Bagher, Fereidoon Mohammadi, and Khadijeh Hooshyari. 2020. "Potential Use of Deep Eutectic Solvents (DESs) to Enhance Anhydrous Proton Conductivity of Nafion 115® Membrane for Fuel Cell Applications." *Journal of Membrane Science* 611:118217. doi: 10.1016/j.memsci.2020.118217.

Kato, Souichiro. 2016. "Microbial Extracellular Electron Transfer and Its Relevance to Iron Corrosion." *Microbial Biotechnology* 9(2):141–48. doi: 10.1111/1751-7915.12340.

Kay, Alan R. 2017. "How Cells Can Control Their Size by Pumping Ions." *Frontiers in Cell and Developmental Biology* 5(MAY):41. doi: 10.3389/FCELL.2017.00041/BIBTEX.

Kempf, Bettina, and Erhard Bremer. 1998. "Uptake and Synthesis of Compatible Solutes as Microbial Stress Responses to High-Osmolality Environments." *Archives of Microbiology* 170(5):319–30. doi: 10.1007/s002030050649.

Khan, Mohammad Mansoob, Sajid A. Ansari, D. Pradhan, M. Omaish Ansari, Do Hung Han, Jintae Lee, and Moo Hwan Cho. 2013. "Band Gap Engineered TiO2 Nanoparticles for Visible Light Induced Photoelectrochemical and Photocatalytic Studies." *Journal*

of Materials Chemistry A 2(3):637–44. doi: 10.1039/C3TA14052K.

Khater, Dena Z., K. M. El-khatib, and Rabeay Y. A. Hassan. 2018. "Exploring the Bioelectrochemical Characteristics of Activated Sludge Using Cyclic Voltammetry." *Applied Biochemistry and Biotechnology* 184(1):92–101. doi: 10.1007/S12010-017-2528-Y/FIGURES/7.

Kim, Insoo, Karthika Viswanathan, Gopinath Kasi, Sarinthip Thanakkasaranee, Kambiz Sadeghi, and Jongchul Seo. 2022. "ZnO Nanostructures in Active Antibacterial Food Packaging: Preparation Methods, Antimicrobial Mechanisms, Safety Issues, Future Prospects, and Challenges." *Food Reviews International* 38(4):537–65. doi: 10.1080/87559129.2020.1737709.

Kim, Sung Hee, Saerom Park, Hyejeong Yu, Ji Hyun Kim, Hyung Joo Kim, Yung Hun Yang, Yong Hwan Kim, Kwang Jin Kim, Eunsung Kan, and Sang Hyun Lee. 2016. "Effect of Deep Eutectic Solvent Mixtures on Lipase Activity and Stability." *Journal of Molecular Catalysis B: Enzymatic* 128:65–72. doi: 10.1016/J.MOLCATB.2016.03.012.

Koch, Christin, and Falk Harnisch. 2016. "What Is the Essence of Microbial Electroactivity?" *Frontiers in Microbiology* 7(NOV). doi: 10.3389/FMICB.2016.01890/FULL.

Kohlstedt, Michael, Praveen K. Sappa, Hanna Meyer, Sandra Maaß, Adrienne Zaprasis, Tamara Hoffmann, Judith Becker, Leif Steil, Michael Hecker, Jan Maarten van Dijl, Michael Lalk, Ulrike Mäder, Jörg Stülke, Erhard Bremer, Uwe Völker, and Christoph Wittmann. 2014. "Adaptation of Bacillus Subtilis Carbon Core Metabolism to Simultaneous Nutrient Limitation and Osmotic Challenge: A Multi-Omics Perspective." *Environmental Microbiology* 16(6):1898–1917. doi: 10.1111/1462-2920.12438.

Kostakioti, Maria, Maria Hadjifrangiskou, and Scott J. Hultgren. 2013. “Bacterial Biofilms: Development, Dispersal, and Therapeutic Strategies in the Dawn of the Postantibiotic Era.” *Cold Spring Harbor Perspective in Medicine*. doi: 10.1101/cshperspect.a010306.

Kouzuma, Atsushi, Xian Ying Meng, Nobutada Kimura, Kazuhito Hashimoto, and Kazuya Watanabe. 2010. “Disruption of the Putative Cell Surface Polysaccharide Biosynthesis Gene SO3177 in Shewanella Oneidensis MR-1 Enhances Adhesion to Electrodes and Current Generation in Microbial Fuel Cells.” *Applied and Environmental Microbiology* 76(13):4151–57. doi: 10.1128/AEM.00117-10.

Kuehn, Martin, Martina Hausner, Hans Joachim Bungartz, Michael Wagner, Peter A. Wilderer, and Stefan Wuertz. 1998. “Automated Confocal Laser Scanning Microscopy and Semiautomated Image Processing for Analysis of Biofilms.” *Applied and Environmental Microbiology* 64(11):4115–27. doi: 10.1128/AEM.64.11.4115-4127.1998/FORMAT/EPUB.

Kumar, Smita S., Vivek Kumar, and Suddhasatwa Basu. 2019. “Electroanalytical Techniques for Investigating Biofilms in Microbial Fuel Cells.” *Bioelectrochemical Interface Engineering* 149–63. doi: 10.1002/9781119611103.ch9.

Kumar, Y., P. Singh, P. Pramanik, and D. Das. 2019. “Electrochemical Determination of Guanine and Uric Acid Using NdFeO3 Nps Modified Graphite Paste Electrode.”

Lahiri, Dibyajit, Moupriya Nag, Sougata Ghosh, Ankita Dey, and Rina Rani Ray. 2022. *Electroactive Biofilm and Electron Transfer in MES*. Elsevier Inc.

Lan, Tzu-Hsuan, Chin-Tsan Wang, Thangavel Sangeetha, Yung-Chin Yang, and Akhil Garg. 2018. “Constructed Mathematical Model for Nanowire Electron Transfer in Microbial Fuel Cells.” doi: 10.1016/j.jpowsour.2018.09.074.

Lan, Tzu Hsuan, Chin Tsan Wang, Thangavel Sangeetha, Yung Chin Yang, and Akhil Garg. 2018. “Constructed Mathematical Model for Nanowire Electron Transfer in Microbial Fuel Cells.” *Journal of Power Sources* 402:483–88. doi: 10.1016/J.JPOWSOUR.2018.09.074.

Lee, Icksoo. 2021. “Regulation of Cytochrome c Oxidase by Natural Compounds Resveratrol, (–)-Epicatechin, and Betaine.” *Cells* 10(6). doi: 10.3390/cells10061346.

Lefebvre, O., A. Al-Mamun, and H. Y. Ng. 2008. “A Microbial Fuel Cell Equipped with a Biocathode for Organic Removal and Denitrification.” *Water Science and Technology* 58(4):881–85. doi: 10.2166/wst.2008.343.

Li, Pu Sheng, Wei Liang Kong, and Xiao Qin Wu. 2021. “Salt Tolerance Mechanism of the Rhizosphere Bacterium JZ-GX1 and Its Effects on Tomato Seed Germination and Seedling Growth.” *Frontiers in Microbiology* 12. doi: 10.3389/FMICB.2021.657238/FULL.

Li, Shan-Wei, Guo-Ping Sheng, Yuan-Yuan Cheng, and Han-Qing Yu. 2016. “Redox Properties of Extracellular Polymeric Substances (EPS) from Electroactive Bacteria OPEN.” *Nature Publishing Group*. doi: 10.1038/srep39098.

Li, Zhong, Xinyu Wang, Jie Wang, Xinyi Yuan, Xiaoyu Jiang, Yanyi Wang, Chao Zhong, Dake Xu, Tingyue Gu, and Fuhui Wang. 2022. “Bacterial Biofilms as Platforms Engineered for Diverse Applications.” *Biotechnology Advances* 57(October

2021):107932. doi: 10.1016/j.biotechadv.2022.107932.

Limoli, Dominique H., Christopher J. Jones, and Daniel J. Wozniak. 2015. “Bacterial Extracellular Polysaccharides in Biofilm Formation and Function.” *Microbiology Spectrum* 3(3). doi: 10.1128/MICROBIOLSPEC.MB-0011-2014/ASSET/A068B798-75CF-42E4-8A39-04F4EFBE3269/ASSETS/GRAPHIC/MB-0011-2014-FIG2.GIF.

Liu, Qiaoling, Xinhui Zhao, Dongkun Yu, Haitao Yu, Yibin Zhang, Zhimin Xue, and Tiancheng Mu. 2019. “Novel Deep Eutectic Solvents with Different Functional Groups towards Highly Efficient Dissolution of Lignin.” *Green Chemistry* 21(19):5291–97. doi: 10.1039/C9GC02306B.

Logan, Bruce E., Ruggero Rossi, Ala’a Ragab, and Pascal E. Saikaly. 2019a. “Electroactive Microorganisms in Bioel Ectrochemical Systems.” *Nature Reviews Microbiology* 17(5):307–19. doi: 10.1038/s41579-019-0173-x.

Logan, Bruce E., Ruggero Rossi, Ala’a Ragab, and Pascal E. Saikaly. 2019b. “Electroactive Microorganisms in Bioelectrochemical Systems.” *Nature Reviews Microbiology 2019 17:5* 17(5):307–19. doi: 10.1038/s41579-019-0173-x.

Logan, Bruce E, Ruggero Rossi, Alaa Ragab, and Pascal E. Saikaly. 2019. “Electroactive Microorganisms in Bioelectrochemical Systems.” *Nature Reviews Microbiology* 307–319. doi: 10.1038/s41579-019-0173-x.

Lovley, Derek R. 2012. “Electromicrobiology.” *Annual Review of Microbiology* 66:391–409. doi: 10.1146/annurev-micro-092611-150104.

Luo, Jianmei, Ming Li, Minghua Zhou, and Youshuang Hu. 2015. “Characterization of a Novel Strain Phylogenetically Related to

Kocuria Rhizophila and Its Chemical Modification to Improve Performance of Microbial Fuel Cells." *Biosensors and Bioelectronics* 69:113–20. doi: 10.1016/J.BIOS.2015.02.025.

Ma, Xin, Mengqi Qian, Zhiren Yang, Tingting Xu, and Xinyan Han. 2021. "Effects of Zinc Sources and Levels on Growth Performance, Zinc Status, Expressions of Zinc Transporters, and Zinc Bioavailability in Weaned Piglets." *Animals* 11(9). doi: 10.3390/ANI11092515/S1.

Mao, Shuhong, Kang Li, Yali Hou, Yanna Liu, Shaoxian Ji, Huimin Qin, and Fuping Lu. 2018. "Synergistic Effects of Components in Deep Eutectic Solvents Relieve Toxicity and Improve the Performance of Steroid Biotransformation Catalyzed by Arthrobacter Simplex." doi: 10.1002/jctb.5629.

Maria Perna, Filippo, Paola Vitale, Vito Capriati, Luciana Cicco, and Giuseppe Dilauro. 2021. "Organic & Biomolecular Chemistry Organic & Biomolecular Chemistry Advances in Deep Eutectic Solvents and Water: Applications in Metal-and Biocatalyzed Processes, in the Synthesis of APIs, and Other Biologically Active Compounds." *Org. Biomol. Chem* 19:2558. doi: 10.1039/d0ob02491k.

Markraphael Ajunwa, Obinna, Olubusola Ayoola Odeniyi, Emmanuel Oluwaseun Garuba, Enrico Marsili, and Abiodun Anthony Onilude. 2021. "Influence of Enhanced Electrogenicity on Anodic Biofilm and Bioelectricity Production by a Novel Microbial Consortium." *Process Biochemistry* 104. doi: 10.1016/j.procbio.2021.01.003.

Marsili, Enrico, Daniel B. Baron, Indraneel D. Shikhare, Dan Coursolle, Jeffrey A. Gralnick, and Daniel R. Bond. 2008a. "Shewanella

Secretes Flavins That Mediate Extracellular Electron Transfer." *Proceedings of the National Academy of Sciences of the United States of America* 105(10):3968–73. doi: 10.1073/PNAS.0710525105/SUPPL_FILE/10525TABLE2.PDF.

Marsili, Enrico, Daniel B. Baron, Indraneel D. Shikhare, Dan Coursolle, Jeffrey A. Gralnick, and Daniel R. Bond. 2008b. "Shewanella Secretes Flavins That Mediate Extracellular Electron Transfer." *Proceedings of the National Academy of Sciences of the United States of America* 105(10):3968–73. doi: 10.1073/PNAS.0710525105.

Marsili, Enrico, Daniel B. Baron, Indraneel D. Shikhare, Dan Coursolle, Jeffrey A. Gralnick, and Daniel R. Bond. 2008c. "Shewanella Secretes Flavins That Mediate Extracellular Electron Transfer." *Proceedings of the National Academy of Sciences of the United States of America* 105(10):3968–73. doi: 10.1073/PNAS.0710525105.

Marsili, Enrico, Jian Sun, and Daniel R. Bond. 2010. "Voltammetry and Growth Physiology of Geobacter Sulfurreducens Biofilms as a Function of Growth Stage and Imposed Electrode Potential." *Electroanalysis* 22(7–8):865–74. doi: 10.1002/elan.200800007.

Martínez-Gómez, Karla, Noemí Flores, Héctor M. Castañeda, Gabriel Martínez-Batallar, Georgina Hernández-Chávez, Octavio T. Ramírez, Guillermo Gosset, Sergio Encarnación, and Francisco Bolivar. 2012. "New Insights into Escherichia Coli Metabolism: Carbon Scavenging, Acetate Metabolism and Carbon Recycling Responses during Growth on Glycerol." *Microbial Cell Factories* 11:1–21. doi: 10.1186/1475-2859-11-46.

Mbous, Yves Paul, Maan Hayyan, Adeeb Hayyan, Won Fen Wong, Ali Hashim, and Chung Yeng Looi. 2016. "Research Review Paper Applications of Deep Eutectic Solvents in Biotechnology and Bioengineering-Promises and Challenges." doi:

10.1016/j.biotechadv.2016.11.006.

Méhes, Gábor, Arghyamalya Roy, Xenofon Strakosas, Magnus Berggren, Eleni Stavrinidou, and Daniel T. Simon. 2020. "Organic Microbial Electrochemical Transistor Monitoring Extracellular Electron Transfer." *Advanced Science (Weinheim, Baden-Wurttemberg, Germany)* 7(15). doi: 10.1002/ADVS.202000641.

Mehrotra, Tithi, Subhabrata Dev, Aditi Banerjee, Abhijit Chatterjee, Rachana Singh, and Srijan Aggarwal. 2021. "Use of Immobilized Bacteria for Environmental Bioremediation: A Review." doi: 10.1016/j.jece.2021.105920.

Meireles, Ana, Ana L. Gonçalves, Inês B. Gomes, Lúcia Chaves Simões, and Manuel Simões. 2015. "Methods to Study Microbial Adhesion on Abiotic Surfaces." *AIMS Bioengineering* 2(4):297–309. doi: 10.3934/bioeng.2015.4.297.

Milano, Francesco, Livia Giotta, Maria Rachele Guascito, Angela Agostiano, Stefania Sblendorio, Ludovico Valli, Filippo M. Perna, Luciana Cicco, Massimo Trotta, and Vito Capriati. 2017. "Functional Enzymes in Nonaqueous Environment: The Case of Photosynthetic Reaction Centers in Deep Eutectic Solvents." *ACS Sustainable Chemistry and Engineering* 5(9):7768–76. doi: 10.1021/ACSSUSCHEMENG.7B01270/SUPPL_FILE/SC7B01270_SI_001.PDF.

Monhemi, Hassan, Mohammad Reza Housaindokht, Ali Akbar Moosavi-Movahedi, and Mohammad Reza Bozorgmehr. 2014. "How a Protein Can Remain Stable in a Solvent with High Content of Urea: Insights from Molecular Dynamics Simulation of Candida Antarctica Lipase B in Urea : Choline Chloride Deep Eutectic Solvent." *Physical Chemistry Chemical Physics : PCCP* 16(28):14882–93. doi: 10.1039/C4CP00503A.

Mukhi, Mayur. 2022. “Bene Fi Cial Bio Fi Lms : A Minireview of Strategies To Enhance Bio Fi Lm Formation for Biotechnological Applications.” (December 2021).

Munteanu, Florentina Daniela, Ana Maria Titoiu, Jean Louis Marty, and Alina Vasilescu. 2018. “Detection of Antibiotics and Evaluation of Antibacterial Activity with Screen-Printed Electrodes.” *Sensors 2018, Vol. 18, Page 901* 18(3):901. doi: 10.3390/S18030901.

Murarka, Abhishek, Yandi Dharmadi, Syed Shams Yazdani, and Ramon Gonzalez. 2008. “Fermentative Utilization of Glycerol by Escherichia Coli and Its Implications for the Production of Fuels and Chemicals.” *Applied and Environmental Microbiology* 74(4):1124–35. doi: 10.1128/AEM.02192-07.

Naradasu, Divya, Alexis Guionet, Waheed Miran, and Akihiro Okamoto. 2020. “Microbial Current Production from Streptococcus Mutans Correlates with Biofilm Metabolic Activity.” *Biosensors and Bioelectronics* 162:112236. doi: 10.1016/J.BIOS.2020.112236.

Narenkumar, Jayaraman, Kuppusamy Sathishkumar, Raja Kumaresan Sarankumar, Kadarkarai Murugan, and Aruliah Rajasekar. 2017. “An Anticorrosive Study on Potential Bioactive Compound Produced by Pseudomonas Aeruginosa TBH2 against the Biocorrosive Bacterial Biofilm on Copper Metal.” *Journal of Molecular Liquids* 243:706–13. doi: 10.1016/J.MOLLIQ.2017.08.075.

Nevin, K. P., H. Richter, S. F. Covalla, J. P. Johnson, T. L. Woodard, A. L. Orloff, H. Jia, M. Zhang, and D. R. Lovley. 2008. “Power

Output and Columbic Efficiencies from Biofilms of Geobacter Sulfurreducens Comparable to Mixed Community Microbial Fuel Cells." *Environmental Microbiology* 10(10):2505–14. doi: 10.1111/J.1462-2920.2008.01675.X.

Nguyen, Phu-Tho, Tho-Thi Nguyen, Duc-Cuong Bui, Phuoc-Toan Hong, Quoc-Khanh Hoang, Huu-Thanh Nguyen, and Ho Chi Minh City. 2020. "Exopolysaccharide Production by Lactic Acid Bacteria: The Manipulation of Environmental Stresses for Industrial Applications." *AIMS Microbiology* 6(4):451–69. doi: 10.3934/microbiol.2020027.

Nimje, Vanita Roshan, Chien Yen Chen, Chien Cheng Chen, Hau Ren Chen, Min Jen Tseng, Jiin Shuh Jean, and Young Fo Chang. 2011. "Glycerol Degradation in Single-Chamber Microbial Fuel Cells." *Bioresource Technology* 102(3):2629–34. doi: 10.1016/j.biortech.2010.10.062.

Obileke, Ke Christ, Helen Onyeaka, Edson L. Meyer, and Nwabunwanne Nwokolo. 2021. "Microbial Fuel Cells, a Renewable Energy Technology for Bio-Electricity Generation: A Mini-Review." *Electrochemistry Communications* 125:107003.

Olar, Rodica, Mihaela Badea, and Mariana Carmen Chifiriuc. 2022. "Metal Complexes—A Promising Approach to Target Biofilm Associated Infections." *Molecules 2022, Vol. 27, Page 758* 27(3):758. doi: 10.3390/MOLECULES27030758.

Oliot, M., L. Etcheverry, A. Mosdale, R. Basseguy, M. L. Délia, and A. Bergel. 2017. "Separator Electrode Assembly (SEA) with 3-Dimensional Bioanode and Removable Air-Cathode Boosts Microbial Fuel Cell Performance." *Journal of Power Sources* 356:389–99. doi: 10.1016/J.JPOWSOUR.2017.03.016.

Pandey, Ashish, Bhawna, Divya Dhingra, and Siddharth Pandey. 2017. "Hydrogen Bond Donor/Acceptor Cosolvent-Modified

Choline Chloride-Based Deep Eutectic Solvents." *Journal of Physical Chemistry B* 121(16):4202–12. doi: 10.1021/ACS.JPCB.7B01724/SUPPL_FILE/JP7B01724_SI_001.PDF.

Pankratova, Galina, Dmitry Pankratov, Ross D. Milton, Shelley D. Minteer, and Lo Gorton. 2019. "Following Nature: Bioinspired Mediation Strategy for Gram-Positive Bacterial Cells." *Advanced Energy Materials* 9(16):1–6. doi: 10.1002/aenm.201900215.

Paquete, Catarina M., Miriam A. Rosenbaum, Lluís Bañeras, Amelia Elena Rotaru, and Sebastià Puig. 2022a. "Let's Chat: Communication between Electroactive Microorganisms." *Bioresource Technology* 347:126705. doi: 10.1016/J.BIORTECH.2022.126705.

Paquete, Catarina M., Miriam A. Rosenbaum, Lluís Bañeras, Amelia Elena Rotaru, and Sebastià Puig. 2022b. "Let's Chat: Communication between Electroactive Microorganisms." *Bioresource Technology* 347(November 2021). doi: 10.1016/j.biortech.2022.126705.

Park, Heechul, Alan F. Schwartzman, Tzu Chieh Tang, Lei Wang, and Timothy K. Lu. 2023. "Ultra-Lightweight Living Structural Material for Enhanced Stiffness and Environmental Sensing." *Materials Today Bio* 18:6–8. doi: 10.1016/j.mtbio.2022.100504.

Perna, Filippo Maria, Paola Vitale, and Vito Capriati. 2020. "Deep Eutectic Solvents and Their Applications as Green Solvents." *Current Opinion in Green and Sustainable Chemistry* 21:27–33. doi: 10.1016/J.COGSC.2019.09.004.

Popescu, Dorin-Mirel. 2016. "An Investigation of Bacterial Composition and Biofilm Structure in Mixed-Community Bioanodes."

Qi, Kezhen, Bei Cheng, Jiaguo Yu, and Wingkei Ho. 2017. "Review on the Improvement of the Photocatalytic and Antibacterial

Activities of ZnO." *Journal of Alloys and Compounds* 727:792–820. doi: 10.1016/J.JALLCOM.2017.08.142.

Rabaey, Korneel, Lars Angenent, Uwe Schroder, and Jurg Keller. 2009. *Bioelectrochemical Systems*. IWA publishing.

Rabaey, Korneel, Nico Boon, Monica Höfte, and Willy Verstraete. 2005. "Microbial Phenazine Production Enhances Electron Transfer in Biofuel Cells." *Environmental Science and Technology* 39(9):3401–8. doi: 10.1021/ES048563O/ASSET/IMAGES/LARGE/ES048563OF00005.JPEG.

Rabaey, Korneel, Suzanne T. Read, Peter Clauwaert, Stefano Freguia, Philip L. Bond, Linda L. Blackall, and Jurg Keller. 2008. "Cathodic Oxygen Reduction Catalyzed by Bacteria in Microbial Fuel Cells." *The ISME Journal 2008 2:5* 2(5):519–27. doi: 10.1038/ismej.2008.1.

Rabaey, Korneel, and René A. Rozendal. 2010. "Microbial Electrosynthesis — Revisiting the Electrical Route for Microbial Production." *Nature Publishing Group* 8. doi: 10.1038/nrmicro2422.

Rafiee, Mohammad, Dylan J. Abrams, Luana Cardinale, Zachary Goss, Antonio Romero-Arenas, and Shannon S. Stahl. 2024. "Cyclic Voltammetry and Chronoamperometry: Mechanistic Tools for Organic Electrosynthesis." *This Journal Is Cite This: Chem. Soc. Rev* 566:566. doi: 10.1039/d2cs00706a.

Rath, Kristin M., Arpita Maheshwari, Per Bengtson, and Johannes Rousk. 2016. "Comparative Toxicities of Salts on Microbial Processes in Soil." *Applied and Environmental Microbiology* 82(7):2012–20. doi: 10.1128/AEM.04052-15.

Reimers, Clare E., Leonard M. Tender, Stephanie Fertig, and Wei Wang. 2001. "Harvesting Energy from the Marine Sediment -

Water Interface." *Environmental Science and Technology* 35(1):192–95. doi: 10.1021/ES001223S/ASSET/IMAGES/LARGE/ES001223SF00004.JPEG.

Richter, Hanno, Kelly P. Nevin, Hongfei Jia, Daniel A. Lowy, Derek R. Lovley, and Leonard M. Tender. 2009. "Cyclic Voltammetry of Biofilms of Wild Type and Mutant Geobacter Sulfurreducens on Fuel Cell Anodes Indicates Possible Roles of OmcB, OmcZ, Type IV Pili, and Protons in Extracellular Electron Transfer." *Energy & Environmental Science* 2(5):506–16. doi: 10.1039/B816647A.

Rojas, Enrique, Julie A. Theriot, and Kerwyn Casey Huang. 2014. "Response of Escherichia Coli Growth Rate to Osmotic Shock." *Proceedings of the National Academy of Sciences of the United States of America* 111(21):7807–12. doi: 10.1073/pnas.1402591111.

Roychoudhury, Arpita, Dieter Haussinger, and Filipp Oesterhelt. 2012. "Effect of the Compatible Solute Ectoine on the Stability of the Membrane Proteins." *Protein & Peptide Letters* 19(8):791–94. doi: 10.2174/092986612801619570.

Saleem Khan, M., Dake Xu, Dan Liu, Yassir Lekbach, Ke Yang, and Chunguang Yang. 2019. "Corrosion Inhibition of X80 Steel in Simulated Marine Environment with Marinobacter Aquaeolei." *Acta Metallurgica Sinica (English Letters)* 32(11):1373–84. doi: 10.1007/S40195-019-00912-4.

Sánchez, Carlos, Paolo Dessì, Maeve Duffy, and Piet N. L. Lens. 2020. "Microbial Electrochemical Technologies: Electronic Circuitry and Characterization Tools." *Biosensors and Bioelectronics* 150:111884. doi: 10.1016/J.BIOS.2019.111884.

Santos, Helena, and Milton S. Da Costa. 2002. “Compatible Solutes of Organisms That Live in Hot Saline Environments.” *Environmental Microbiology* 4(9):501–9. doi: 10.1046/J.1462-2920.2002.00335.X.

Saratale, Ganesh Dattatraya, Rijuta Ganesh Saratale, Muhammad Kashif Shahid, Guangyin Zhen, Gopalakrishnan Kumar, Han Seung Shin, Young Gyun Choi, and Sang Hyoun Kim. 2017. “A Comprehensive Overview on Electro-Active Biofilms, Role of Exo-Electrogens and Their Microbial Niches in Microbial Fuel Cells (MFCs).” *Chemosphere* 178:534–47. doi: 10.1016/j.chemosphere.2017.03.066.

Sasaki, Kengo, Yota Tsuge, Daisuke Sasaki, and Akihiko Kondo. 2014. “Increase in Lactate Yield by Growing Corynebacterium Glutamicum in a Bioelectrochemical Reactor.” *Journal of Bioscience and Bioengineering* 117(5):598–601. doi: 10.1016/J.JBIOSC.2013.10.026.

Schievano, Andrea, Tommy Pepé Sciarria, Karolien Vanbroekhoven, Heleen De Wever, Sebastià Puig, Stephen J. Andersen, Korneel Rabaey, and Deepak Pant. 2016. “Focus on Bioelectrochemistry Electro-Fermentation-Merging Electrochemistry with Fermentation in Industrial Applications.” doi: 10.1016/j.tibtech.2016.04.007.

Schlievert, P. M., J. R. Deringer, M. H. Kim, S. J. Projan, and R. P. Novick. 1992. “Effect of Glycerol Monolaurate on Bacterial Growth and Toxin Production.” *Antimicrobial Agents and Chemotherapy* 36(3):626–31. doi: 10.1128/AAC.36.3.626.

Schröder, Uwe, Falk Harnisch, and Largus T. Angenent. 2015. “Microbial Electrochemistry and Technology: Terminology and Classification.” *Energy & Environmental Science* 8(2):513–19. doi: 10.1039/C4EE03359K.

Seker, Urartu Ozgur Safak, Allen Y. Chen, Robert J. Citorik, and Timothy K. Lu. 2017. “Synthetic Biogenesis of Bacterial Amyloid Nanomaterials with Tunable Inorganic-Organic Interfaces and Electrical Conductivity.” *ACS Synthetic Biology* 6(2):266–75. doi: 10.1021/ACSSYNBIO.6B00166/ASSET/IMAGES/LARGE/SB-2016-00166A_0006.JPEG.

Socas-Rodríguez, Bárbara, M. Vanessa Torres-Cornejo, Gerardo Álvarez-Rivera, and Jose A. Mendiola. 2021. “Deep Eutectic Solvents for the Extraction of Bioactive Compounds from Natural Sources and Agricultural By-Products.” *Applied Sciences (Switzerland)* 11(11). doi: 10.3390/APP11114897.

Song, Hai Liang, Ying Zhu, and Jie Li. 2019. “Electron Transfer Mechanisms, Characteristics and Applications of Biological Cathode Microbial Fuel Cells – A Mini Review.” *Arabian Journal of Chemistry* 12(8):2236–43. doi: 10.1016/J.ARABJC.2015.01.008.

Song, Young-Chae, Dae-Sup Kim, Jung-Hui Woo, Bakthavachallam Subha, Seong-Ho Jang, and Subpiramaniyam Sivakumar. 2015. “Effect of Surface Modification of Anode with Surfactant on the Performance of Microbial Fuel Cell.” doi: 10.1002/er.3284.

Stanaszek, P. M., J. F. Snell, and J. J. O’Neill. 1977. “Isolation, Extraction, and Measurement of Acetylcholine from Lactobacillus Plantarum.” *Applied and Environmental Microbiology* 34(2):237–39. doi: 10.1128/aem.34.2.237-239.1977.

Strøm, Arne R. 1998. “Osmoregulation in the Model Organism Escherichia Coli: Genes Governing the Synthesis of Glycine Betaine and Trehalose and Their Use in Metabolic Engineering of Stress Tolerance.” *Journal of Biosciences* 23(4):437–45. doi: 10.1007/BF02936137/METRICS.

Su, Yuan, Chuan Liu, Huan Fang, and Dawei Zhang. 2020. “Bacillus Subtilis: A Universal Cell Factory for Industry, Agriculture,

Biomaterials and Medicine." *Microbial Cell Factories* 19(1):1–12. doi: 10.1186/s12934-020-01436-8.

Sultana, Sujala T., Jerome T. Babauta, and Haluk Beyenal. 2015. "Biofouling The Journal of Bioadhesion and Biofilm Research Electrochemical Biofilm Control: A Review." doi: 10.1080/08927014.2015.1105222.

Sun, Yaxu, Xiaoyan Jia, Ru Yang, Xiaojie Qin, Xiaoxue Zhou, Hui Zhang, Weibao Kong, Ji Zhang, and Junlong Wang. 2022. "Deep Eutectic Solvents Boosting Solubilization and Se-Functionalization of Heteropolysaccharide: Multiple Hydrogen Bonds Modulation." *Carbohydrate Polymers* 284:119159. doi: 10.1016/J.CARBPOL.2022.119159.

Tapia, J. M., J. A. Muñoz, F. González, M. L. Blázquez, and A. Ballester. 2011. "Mechanism of Adsorption of Ferric Iron by Extracellular Polymeric Substances (EPS) from a Bacterium Acidiphilium Sp." *Water Science and Technology : A Journal of the International Association on Water Pollution Research* 64(8):1716–22. doi: 10.2166/WST.2011.649.

Thayalakumaran, T., M. G. Bethune, and T. A. McMahon. 2007. "Achieving a Salt Balance—Should It Be a Management Objective?" *Agricultural Water Management* 92(1–2):1–12. doi: 10.1016/J.AGWAT.2007.05.004.

Torregrosa-Crespo, Javier, Xavier Marset, Gabriela Guillena, Diego J. Ramón, and Rosa María Martínez-Espinosa. 2020. "New Guidelines for Testing 'Deep Eutectic Solvents' Toxicity and Their Effects on the Environment and Living Beings." *Science of the Total Environment* 704. doi: 10.1016/J.SCITOTENV.2019.135382.

Trivinho-Strixino, F., J. S. Santos, and M. Souza Sikora. 2017. "Electrochemical Synthesis of Nanostructured Materials." *Nanostructures* 53–103. doi: 10.1016/B978-0-323-49782-4.00003-6.

Tuck, Benjamin, Elizabeth Watkin, Maria Forsyth, Anthony Somers, Mahdi Ghorbani, and Laura L. Machuca. 2021. “Evaluation of a Novel, Multi-Functional Inhibitor Compound for Prevention of Biofilm Formation on Carbon Steel in Marine Environments.” *Scientific Reports* | 11:15697. doi: 10.1038/s41598-021-94827-9.

Ucar, Deniz, Yifeng Zhang, and Irini Angelidaki. 2017. “An Overview of Electron Acceptors in Microbial Fuel Cells.” *Frontiers in Microbiology* 8(APR):1–14. doi: 10.3389/fmicb.2017.00643.

Venkova, Tatiana, Maria Jesus Yebra, Bopda Waffo Alain, Antonius Suwanto, Paloma López, Adrian Pérez-Ramos, Maria L. Werning, Alicia Prieto, Pasquale Russo, Giuseppe Spano, and Mari L. Mohedano. 2017. “Characterization of the Sorbitol Utilization Cluster of the Probiotic Pediococcus Parvulus 2.6: Genetic, Functional and Complementation Studies in Heterologous Hosts.” doi: 10.3389/fmicb.2017.02393.

Ventola, C. Lee. 2015. “The Antibiotic Resistance Crisis: Part 1: Causes and Threats.” *Pharmacy and Therapeutics* 40(4):277. doi: Article.

Verma, Jyoti, Deepak Kumar, Nimmi Singh, Sanjeev S. Katti, and Yatish T. Shah. 2021. *Electricigens and Microbial Fuel Cells for Bioremediation and Bioenergy Production: A Review*. Vol. 19. Springer International Publishing.

Vijay, Ankisha, Jayesh M. Sonawane, and Prakash C. Ghosh. 2022. *Electroactive Biofilm and Electron Transfer in the Microbial Electrochemical System*. Elsevier Inc.

Vitasovic, Toni, Giada Caniglia, Neda Eghtesadi, Marcel Ceccato, Espen Drath, Bo✓Jesen, Ulrich Gosewinkel, Gregor Neusser, Ulrich

Rupp, Paul Walther, Christine Kranz, and Elena E. Ferapontova. 2024. “Antibacterial Action of Zn 2+ Ions Driven by the In Vivo Formed ZnO Nanoparticles.” *Applied Material and Interfaces (ACS)*. doi: 10.1021/acsami.4c04682.

Viti, Carlo, Elisa Masi, Marzena Ciszak, Luisa Santopolo, Arcangela Frascella, Luciana Giovannetti, Emmanuela Marchi, and Stefano Mancuso. 2014. “Electrical Spiking in Bacterial Biofilms.” doi: 10.1098/rsif.2014.1036.

Wang, Yan, Yucui Hou, Weize Wu, Dongdong Liu, Youan Ji, and Shuhang Ren. 2016. “Roles of a Hydrogen Bond Donor and a Hydrogen Bond Acceptor in the Extraction of Toluene from N-Heptane Using Deep Eutectic Solvents.” *Green Chemistry* 18(10):3089–97. doi: 10.1039/C5GC02909K.

Wargo, Matthew J. 2013. “Homeostasis and Catabolism of Choline and Glycine Betaine: Lessons from Pseudomonas Aeruginosa.” *Applied and Environmental Microbiology* 79(7):2112–20. doi: 10.1128/AEM.03565-12.

Wei, Jincheng, Peng Liang, and Xia Huang. 2011. “Recent Progress in Electrodes for Microbial Fuel Cells.” *Bioresource Technology* 102(20):9335–44. doi: 10.1016/j.biortech.2011.07.019.

Wen, Qing, Jing Xin Chen, Yu Lin Tang, Juan Wang, and Zhen Yang. 2015. “Assessing the Toxicity and Biodegradability of Deep Eutectic Solvents.” *Chemosphere* 132:63–69. doi: 10.1016/J.CHEMOSPHERE.2015.02.061.

Wikene, Kristine Opsvik, Håkon Valen Rukke, Ellen Bruzell, and Hanne Hjorth Tønnesen. 2017. “Investigation of the Antimicrobial Effect of Natural Deep Eutectic Solvents (NADES) as Solvents in Antimicrobial Photodynamic Therapy.” *Journal of Photochemistry and Photobiology B: Biology* 171:27–33. doi: 10.1016/J.JPHOTOBIOL.2017.04.030.

Winkelströter, Lizziane Kretli, Fernanda Barbosa dos Reis Teixeira, Eliane Pereira Silva, Virgínia Farias Alves, and Elaine Cristina Pereira De Martinis. 2014. "Unraveling Microbial Biofilms of Importance for Food Microbiology." *Microbial Ecology* 68(1):35–46. doi: 10.1007/S00248-013-0347-4.

Winslow, C. E. A., and Eloise T. Haywood. 1931. "The Specific Potency of Certain Cations with Reference to Their Effect on Bacterial Viability." *Journal of Bacteriology* 22(1):49–69. doi: 10.1128/JB.22.1.49-69.1931.

Wright, Jennifer, Polly Moreland, Anil Wipat, Meng Zhang, and Martyn Dade-Robertson. 2020. "Engineered Ureolytic Bacillus Subtilis and Its Future in Microbial Induced Calcium Carbonate Precipitation (MICCP)." *Access Microbiology* 2(7A):10–11. doi: 10.1099/acmi.ac2020.po0143.

Xavier, Karina B., and Bonnie L. Bassler. 2003. "LuxS Quorum Sensing: More than Just a Numbers Game." *Current Opinion in Microbiology* 6(2):191–97. doi: 10.1016/S1369-5274(03)00028-6.

Xiao, Yong, and Feng Zhao. 2017. "Electrochemical Roles of Extracellular Polymeric Substances in Biofilms." *Current Opinion in Electrochemistry* 4(1):206–11. doi: 10.1016/J.COELEC.2017.09.016.

Xie, Jiaying, Hongmin Zhang, Yinhui Li, Hao Li, Yingjie Pan, Yong Zhao, and Qingchao Xie. 2023. "Transcriptome Analysis of the Biofilm Formation Mechanism of Vibrio Parahaemolyticus under the Sub-Inhibitory Concentrations of Copper and Carbenicillin." *Frontiers in Microbiology* 14:1128166. doi: 10.3389/FMICB.2023.1128166/BIBTEX.

Xu, Shuai, Alexandre Barrozo, Leonard M. Tender, Anna I. Krylov, and Mohamed Y. El-Naggar. 2018. "Multiheme Cytochrome

Mediated Redox Conduction through Shewanella Oneidensis MR-1 Cells." *Journal of the American Chemical Society* 140(32):10085–89. doi: 10.1021/jacs.8b05104.

Yamada, Tomoya, Takeshi Fujii, Tamotsu Kanai, Taku Amo, Tadayuki Imanaka, Hiroshi Nishimasu, Takayoshi Wakagi, Hirofumi Shoun, Masahiro Kamekura, Yoichi Kamagata, Takeshi Kato, and Koichiro Kawashima. 2005. "Expression of Acetylcholine (ACh) and ACh-Synthesizing Activity in Archaea." *Life Sciences* 77(16):1935–44. doi: 10.1016/j.lfs.2005.01.026.

Yi, Hana, Kelly P. Nevin, Byoung Chan Kim, Ashely E. Franks, Anna Klimes, Leonard M. Tender, and Derek R. Lovley. 2009. "Selection of a Variant of Geobacter Sulfurreducens with Enhanced Capacity for Current Production in Microbial Fuel Cells." *Biosensors and Bioelectronics* 24(12):3498–3503. doi: 10.1016/J.BIOS.2009.05.004.

Yin, Wen, Yiting Wang, Lu Liu, and Jin He. 2019. "Biofilms: The Microbial 'Protective Clothing' in Extreme Environments." *International Journal of Molecular Sciences 2019, Vol. 20, Page 3423* 20(14):3423. doi: 10.3390/IJMS20143423.

You, Zixuan, Jianxun Li, Yuxuan Wang, Deguang Wu, Feng Li, and Hao Song. 2023. "Advances in Mechanisms and Engineering of Electroactive Biofilms." *Biotechnology Advances* 66(November 2022):108170. doi: 10.1016/j.biotechadv.2023.108170.

Youn, Su Min, and Soo Jin Choi. 2022. "Food Additive Zinc Oxide Nanoparticles: Dissolution, Interaction, Fate, Cytotoxicity, and Oral Toxicity." *International Journal of Molecular Sciences 2022, Vol. 23, Page 6074* 23(11):6074. doi: 10.3390/IJMS23116074.

Zhang, Wei Jun. 2011. "A Review of the Electrochemical Performance of Alloy Anodes for Lithium-Ion Batteries." *Journal of Power*

Sources 196(1):13–24. doi: 10.1016/J.JPOWSOUR.2010.07.020.

Zhou, Lean, Yongliang Wu, Shiqi Zhang, Yifu Li, Yang Gao, Wei Zhang, Liu Tian, Tian Li, Qing Du, and Shiquan Sun. 2022. "Recent Development in Microbial Electrochemical Technologies: Biofilm Formation, Regulation, and Application in Water Pollution Prevention and Control." *Journal of Water Process Engineering* 49(May):103135. doi: 10.1016/j.jwpe.2022.103135.